THE TSA DA GLISZA (REGAL RIDGE) EMERALD OCCURRENCE, SOUTHEASTERN YUKON TERRITORY, CANADA:

DESCRIPTIVE, GENETIC, AND EXPLORATION MODELS

by

HEATHER LEAH DOUGLAS NEUFELD
B.Sc., The University of British Columbia, 2002

A THESIS SUBMITTED IN PARTIAL FULFILMENT OF
THE REQUIREMENTS FOR THE DEGREE OF
MASTER OF SCIENCE

in

THE FACULTY OF GRADUATE STUDIES
Geological Sciences

THE UNIVERSITY OF BRITISH COLUMBIA
December 2004

ABSTRACT

Emerald at the Tsa da Glisza property in the Finlayson Lake district of southeastern Yukon is hosted by mid-Paleozoic mafic metavolcanic rocks which overly the shallowly dipping western edge of a 112 Ma granite pluton. The main host rocks for the mineralization are high-Ca boninites (high-magnesium basalt to andesite) with anomalously high Cr contents. Beryl occurs within quartz-tourmaline veins, and in highly altered schist zones either adjacent to the veins, or near vein terminations. Several generations of syn- to late tectonic quartz veins are present at Tsa da Glisza , and emeralds are associated mainly with the latest vein set, especially near the intersection between these and older veins. The quartz veining is related to progressive Cretaceous deformation and to the relatively late emplacement of the granite intrusions. Aplite dikes associated with the intrusion locally contain beryl within quartz-rich segregations, and these beryl-bearing aplites differ chemically from non-mineralized intrusions by having higher Be and Na and lower K, Li, and F contents. The oxygen isotopic composition of the granite is distinct from that of the chlorite schist. The extent of homogenization of the two isotopic signatures can be tracked by the changing oxygen isotopic composition, and may be used to determine whether there was sufficient reaction between the veins fluids and host schist to produce emerald. ^{39}Ar-^{40}Ar geochronology confirms that mineralization occurred synchronous with regional deformation and metamorphism related to intrusion of the granite pluton from approximately 112 to 108 Ma. A genetic model for the emerald mineralization has been formulated: vein fluids were mixtures of fluids from both magmatic and local metasomatic sources. Beryllium derived from an adjacent Cretaceous granite was transported as both hydroxide and fluoride complexes within dominantly magmatic fluids. Emerald crystallized during cooling after the magmatic fluids mixed with hydrothermal fluids that had scavenged Cr from the surrounding mafic schist. Based on this genetic model, further exploration in the Finlayson Lake region, and the northern Cordillera, should focus on areas where permeable (schist rather than serpentinized ultramafic), high-Cr host rock is in close proximity to evolved felsic intrusive rocks.

TABLE OF CONTENTS

LIST OF TABLES

LIST OF FIGURES

ACKNOWLEDGEMENTS

I would like to thank Dr. Lee Groat and Dr. Jim Mortensen for guidance, supervision, and improvements to this work, and also for instigating and supporting my love of the Yukon. Dr. Mati Raudsepp is thanked for guidance and helpful suggestions for analytical work, and for reviewing this thesis. Thank you to my fellow grads for support, and good 'discussions'. Many of the faculty in the department patiently helped me to formulate and test various hypotheses. Dawn Kellet provided excellent and entertaining field assistance. Most of all I want to thank my family and my husband Josh for support, inspiration, and encouragement. This work results from field and laboratory work that was funded by the National Sciences and Engineering Research Council (NSERC), True North Gems, Inc., and the Yukon Geological Survey.

CHAPTER 1

Introduction

1.1 OVERVIEW

The Tsa da Glisza emerald occurrence was discovered in 1998. The occurrence is hosted within rocks of the Yukon Tanana terrane in the Pelly Mountains of the Finalyson Lake district, southeastern Yukon Territory (Fig. 1.1). Tsa da Glisza hosts the only known Cr-bearing emerald in the Canadian Cordillera. Emerald is an extremely valuable gemstone, and is rare because the required elements Be and Cr (with or without vanadium) are geochemically incompatible, and therefore are rarely found together in environments in which beryl is stable.

Groat *et al.* (2002) reported on a reconnaissance study of the geology of the mineralized region at Tsa da Glisza, the mineralogy of emerald and tourmaline, initial fluid-inclusion work, and limited geochronologic and stable isotope results. Due to their limited data, a comprehensive genetic model for the formation of emerald at Tsa da Glisza was not presented. Additional fluid-inclusion studies gave further information on the pressure, temperature and fluid conditions during emerald mineralization, presented in Marshall *et al.* (2003). They suggest that no distinction can be made between a tectonic-hydrothermal (shear zone-related) versus a magmatic or hybrid origin for the deposit.

1.2 GEOCHEMISTRY OF BERYL (VAR. EMERALD)

Beryl is a cyclosilicate with the ideal chemical formula $Be_3Al_2Si_6O_{18}$. The structure of beryl is shown in Figure 1.2. Non-polar rings of Si_6O_{18} are arranged in layers. Sheets of Be and Al ions fit between these layers, with Be^{2+} in tetrahedral coordination and Al^{3+} in octahedral coordination. The silicate rings are positioned one above the other along the c-axis, such that channels occur within the rings. The channels can accommodate a wide variety of ions and molecules, most notably alkalis (e.g. Na^{+}, K^{+}) and water. The substitution of divalent and trivalent ions into the octahedral site is the exchange responsible for the coloration of beryl, producing a wide range of colours, the most notable being "emerald green". The exchange of Cr^{3+}, V^{3+}, and Fe^{3+} chromophores at the octahedral site causes a range of green, shades of

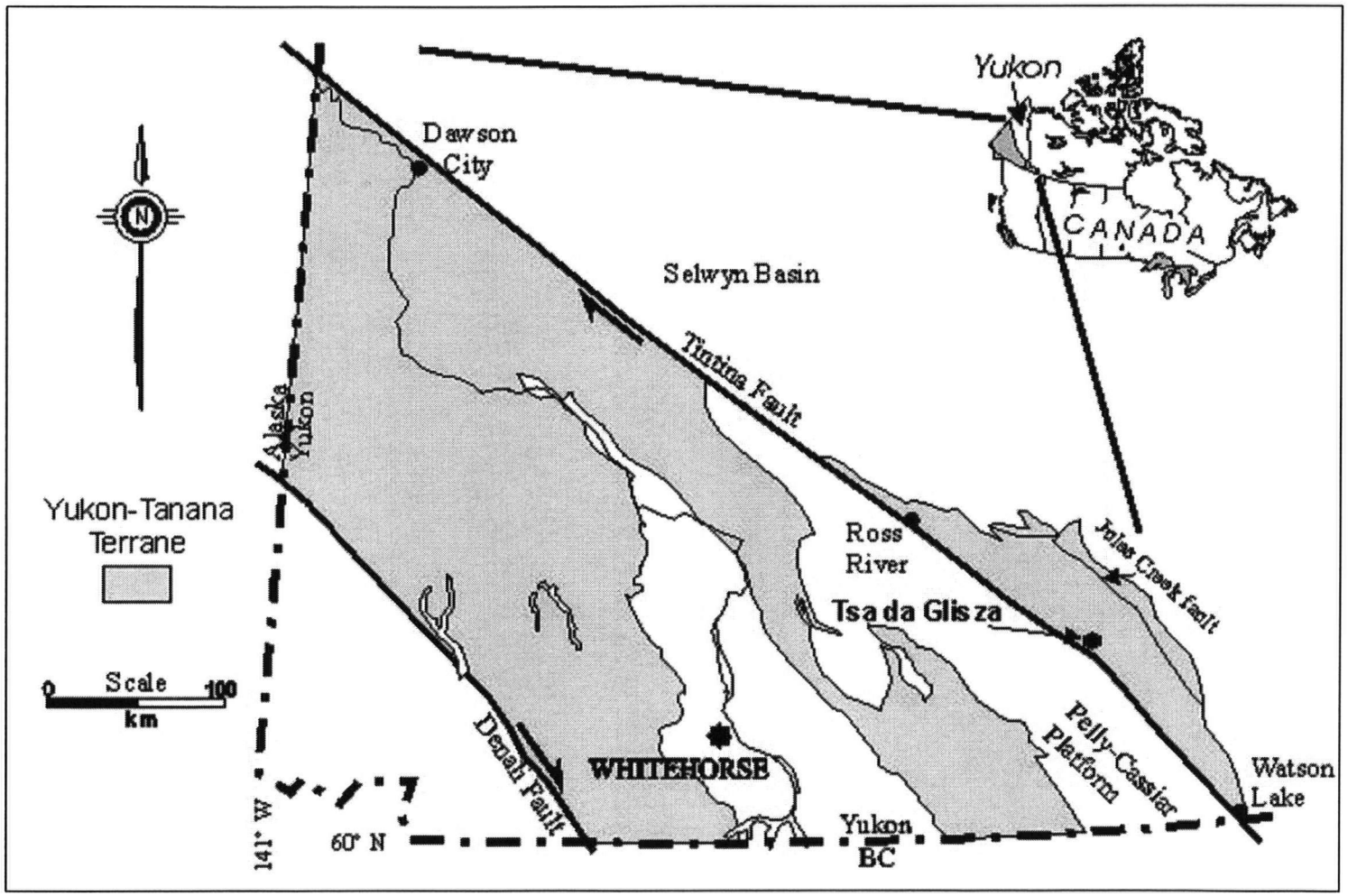

Figure 1.1. Location map of the Tsa da Glisza emerald occurrence, Yukon Territory, Canada.

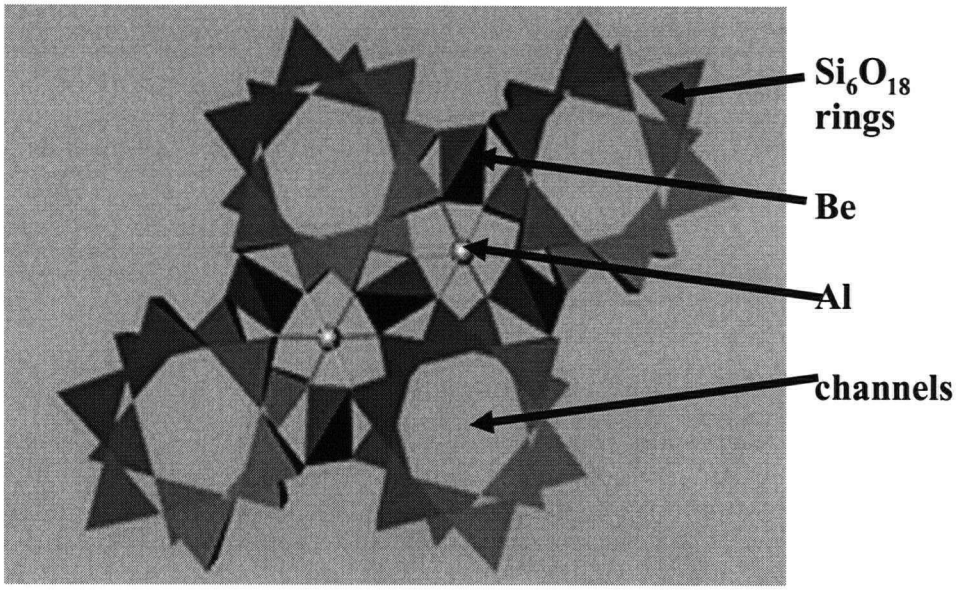

Figure 1.2. Crystallographic structure of beryl. View down the C-axis. Modified from Klein (1998).

which are observed in clear, gem-quality beryl, allowing for the qualification of the term "emerald". The definition of "emerald" is still under considerable debate (e.g. Conklin, 2002; Schwartz and Schmetzer, 2002). In this work, I define emerald as dark green, clear, gem-quality beryl, as opposed to opaque beryl crystals ranging in colour from white through dark green.

1.3 GEOLOGICAL SETTINGS OF EMERALD DEPOSITS

Emerald deposits may be related to pegmatitic, magmatic-hydrothermal, or non-magmatic processes. A recent review of Be mineralogy, petrology, and geochemistry (Grew, 2002) compiled and delineated the various genetic models proposed for emerald deposits worldwide (e.g. Cerny, 2002; Franz and Morteani, 2002; Barton and Young, 2002) . Due to discrepancies in nomenclature in the literature, the terms outlined by Barton and Young (2002) are used here.

Emerald occurring in pegmatite is usually associated with mid-level granitic pegmatites of the rare-element class (Cerny, 2002). There is a continuum from Be-enriched magmas to pegmatites to hydrothermal vein deposits (London and Evensen, 2002). Most Be-generating magmas have low CaO and high F contents.

Metasomatism driven by granitic magmatism, where pegmatites or quartz-muscovite-feldspar veins intrude ultramafic or mafic Cr-bearing rocks, is invoked to explain most emerald deposits (Kazmi and Snee, 1989; Sinkankas, 1989). Quartz-poor and biotite-rich contact-parallel metasomatic zones usually accompany the emerald-bearing dikes and veins (Barton and Young, 2002). The related intrusive rocks are usually peraluminous biotite and biotite-muscovite granites with mineralogically simple veins, although some deposits are associated with mineralogically complex pegmatites. Emerald occurs within both vein alteration envelopes and within the veins (dominantly quartz, muscovite, and plagioclase) themselves, which often show evidence of reaction with the host mafic or ultramafic rocks. Although metasomatic desilicification of pegmatites is commonly associated with emerald mineralization, it is often difficult to determine the timing of metasomatism relative to emplacement, and also to determine whether the altering fluids were dominantly hydrothermal or magmatic (Barton and Young, 2002).

Many of the world-renowned emerald deposits are hosted within ultramafic rocks, and show defined multiple metasomatic zones, known as "blackwall" assemblages (e.g. Franqueira, Spain; Reft River, Russia; Menzies, Australia; Habachtal, Austria; Carnaiba, Brazil). Emerald usually occurs in the innermost biotite-rich zone, and is commonly associated with fluorite and

F-bearing phlogopite, a coincidence which suggests that the Mg-Ca-rich host rocks triggered F precipitation, in turn precipitating Ba and Al as emerald (e.g. Soboleva et al., 1972).

Mafic-hosted emerald-bearing veins do not show multiple metasomatic zones on their selvages, but are commonly enveloped by a single biotite-rich layer, likely due to the higher Si and Ca, and lower Mg contents of mafic relative to ultramafic rocks (e.g. Khaltaro, Pakistan; Laurs et al., 1996) (Barton and Young, 2002). At Khaltaro, the formation of fluorite and biotite released the Cr and Fe necessary to form emerald at the contact of albite-quartz-muscovite veins with amphibolite (Laurs et al., 1996).

Non-magmatic origins are established for some emerald deposits. These are currently split into two groups: brine-related and metamorphic (schist-type, or shear zone) occurrences. Emerald deposits in Columbia are basinal brine-related, occurring in tension gash carbonate-quartz-albite-pyrite veins within Be-rich basinal sedimentary rocks. Franz and Morteani (2002) classify all emerald deposits formed in the context of metamorphism, as "schist-type" deposits. They argue that emerald in these deposits, being generally less than 2 cm in length, the typical size of metamorphic porphyroblasts, has grown at the contact between metamorphosed Cr-rich mafic to ultramafic rocks and Be-rich K-N-Al quartzofeldspathic rocks (including meta-pegmatites and aplites), during post-intrusive deformation and metamorphism which locally redistributed and reprecipitated Be. Franz and Morteani (2002) suggest that the intrusion of small igneous bodies cannot provide the necessary large amounts of fluid for the extensive alteration envelopes commonly associated with mineralized bodies, whereas metasomatic reactions can easily explain the envelopes. This hydrothermal-metasomatic model is referred to by Barton and Young as "shear-zone-related".

The formation of shear zone-related emerald is still under considerable debate. The importance of "blackwall" zoning and regional metamorphism in emerald formation at the Habachtal, Austria and Gravelotte, South Africa deposits was identified by Grundmann and Morteani (1989), Nwe and Grundmann (1990) and Nwe and Morteani (1993). Their model invokes a regional tectonic event to redistribute Be present in K-Na-Al silicate rocks at their intrusive or tectonic contact with ultramafic Cr- and Mg-rich rocks. Beryl, phenakite, and chrysoberyl precipitate at this contact, within multiple metasomatic "blackwall" zones. While their occurrence within biotite-rich zones in metamorphosed mafic and ultramafic rocks appears similar to many igneous-related deposits, shear-zone emeralds, grown during regional metamorphism, usually have textures demonstrating their synkinematic overgrowths of other minerals (Grundmann and Morteani, 1989). These emeralds also have higher Fe and Mg contents

than emerald from other deposit types (Barton and Young, 2002). CO_2-bearing inclusions and non-magmatic oxygen isotope ratios are common for these moderate-salinity systems with no associated igneous rocks, that form deposits in Austria, Afghanistan, Pakistan, and Brazil (Kazmi and Snee, 1989; Giuliani et al., 1990).

The distinction between magmatic-hydrothermal, and non-magmatic (hydrothermal-metasomatic, shear zone) origins is difficult in deposits where both igneous bodies and evidence for regional metamorphism occur (e.g. Franqueira, Spain; Martin-Izard et al., 1995, Franz et al., 1996 and Gravelotte, South Africa; Nwe and Morteani, 1993). The Franqueira deposit contains emerald after phenakite, and emerald after chrysoberyl, within phlogopite-tourmaline alteration zones on the edge of quartz-albite-muscovite-K-feldspar veins within dunite. The emerald overgrowths, and multiple zones of alteration within an ultramafic rocks, allow for a shear-zone metamorphic interpretation for emerald formation, but the evidence does not necessarily preclude coeval magma emplacement. Similar overgrowth of emerald on phenakite and chrysoberyl during deformation could occur with synkinematic intrusion accompanied by progressive growth of metasomatic zones (Barton and Young, 2002). Similarly, the Gravelotte deposit in South Africa contains beryl after phenakite within biotite-rich alteration zones (Grundmann and Morteani, 1989; Nwe and Morteani, 1993; Robb and Robb, 1986). Non-gem beryl occurs within both foliated and unfoliated albite-quartz-muscovite veins intruded into mafic host rocks. Franz and Morteani (2002) suggest that with detailed investigation of structural relationships between deformation features in the metamorphic rocks, beryl growth and intrusion, many deposits currently classified as magmatic-hydrothermal will fit the shear zone-related model.

1.4 PURPOSE

The objectives of the project were, (1) to more completely characterize emerald and beryl mineralization at the Tsa da Glisza occurrence; (2) to develop a genetic model for the mineralization at the occurrence; and (3) to use the data acquired to develop emerald exploration guidelines specific to the northern Canadian Cordillera. More specifically, research was aimed towards confirming the role of a nearby granite pluton in the mineralizing process, determining the source of Cr, the sequence of events and fluid chemistry during the mineralization process, and inferring the structural dynamics during the mineralization event.

Research involved the following methods:

1. Property-scale mapping, and trench mapping was completed to constrain the geology, structure and alteration assemblages associated with emerald mineralization.
2. Optical microscopy, using polished thin sections, was used to characterize mineralized zones, host rocks, and associated intrusive rocks.
3. Whole-rock geochemical analyses of mineralized and unmineralized whole rocks were obtained, and were tested for possible correlations between the composition of beryl/emerald and intrusive rocks, including element depletions that are spatially associated with beryl/emerald mineralization.
4. X-ray diffraction was used to characterize minerals from mineralized zones and host rocks.
5. Isotopic dating of selected samples, using both Ar-Ar and U-Pb methods, was used to determine the age of intrusions and mineral phases spatially associated with the beryl/emerald mineralization.
6. Stable isotope analysis of oxygen and hydrogen was used to characterize the interaction between mineralizing fluids and the host rocks.
7. Characterization of sample suites of emerald and tourmaline using the scanning electron microscope to identify mineral inclusions and chemical zoning, and use that information to develop a sequence of mineralization.
8. Electron microprobe analysis of sample suites of emerald and tourmaline, to determine the extent of chemical substitution in the minerals, and to relate the mineral chemistry to host geology and fluid chemistry.

Rock samples were collected by the author from outcrop and drill core at the Tsa da Glisza property during field research in both 2002 and 2003. Samples of emerald for the sample set were obtained from True North Gems, Inc. All geochemical data was obtained from samples collected by the author, except for that presented in Appendix 2, which is True North Gems, Inc. data from the 2003 field season.

Results are presented here in manuscript format. The manuscript is roughly based on a three-fold system of investigation, including a preliminary descriptive model, a genetic model based on results of research, and a model for further regional exploration based on the genetic model. Chapter two describes the property geology, structural interpretations, and mineralization at the Tsa da Glisza property. This descriptive model results from field research conducted in 2003. Chapter three revises the descriptive model based on further research conducted in 2003

and 2004, outlines the various genetic models that might apply to the Tsa da Glisza deposit, and suggests the most likely genetic model. Chapter four focusses on the exploration model, and specifically, its application to the Finlayson Lake district of Yukon Territory. Some overlap of information could not be avoided since these manuscripts were prepared for individual publication.

CHAPTER 2

[1]Geology and structural setting of the Tsa da Glisza emerald property, Finlayson Lake district, southeastern Yukon.

2.1 INTRODUCTION

The Tsa da Glisza property is located in the Finlayson Lake district of southeastern Yukon within the Pelly Mountains (Fig. 2.1). The property consists of 93 quartz mining claims covering a total of 18 km^2, centred at 61°16.6' north latitude, 133°5.5' west latitude on NTS map sheet 105G/7.

This paper reports on new field work by the authors during 2003. Our three-week program focussed on producing a detailed (1:2500 scale) geological map of the Tsa da Glisza property (Fig. 2.2). We also carried out structural studies to better understand the structural evolution of the area and possible structural controls on the localization of emerald mineralization.

2.2 PROPERTY EXPLORATION HISTORY

Chevron Canada first explored the area from 1978 to 1980, carrying out a regional stream sediment sampling and prospecting program on the Howdee claims, 1 km southwest of the Tsa da Glisza property (Yukon MINFILE 2002, 105G 147, Deklerk, 2002). With the discovery of the Kudz Ze Kayah volcanogenic massive sulphide(VMS) deposit in the early 1990s, the Finlayson district saw renewed exploration interest. Expatriate Resources carried out exploration targeting VMS mineralization on the Goal claims (claims now including Tsa da Glisza) in 1995 and 1996, with a program involving geological mapping, prospecting, soil sampling and hand trenching. While prospecting for Expatriate Resources in September 1998, geologist W. Wengynowski

---

[1] A version of this chapter has been published. Neufeld, H.L.D., Israel, S., Groat, L.A. and Mortensen, J.K., 2004. Geology and structural setting of the Tsa da Glisza emerald property, Finlayson Lake district, southeastern Yukon. *In:* Yukon Exploration and Geology 2003, D.S. Emond and L.L. Lewis (eds.), Yukon Geological Survey, p.281-288.

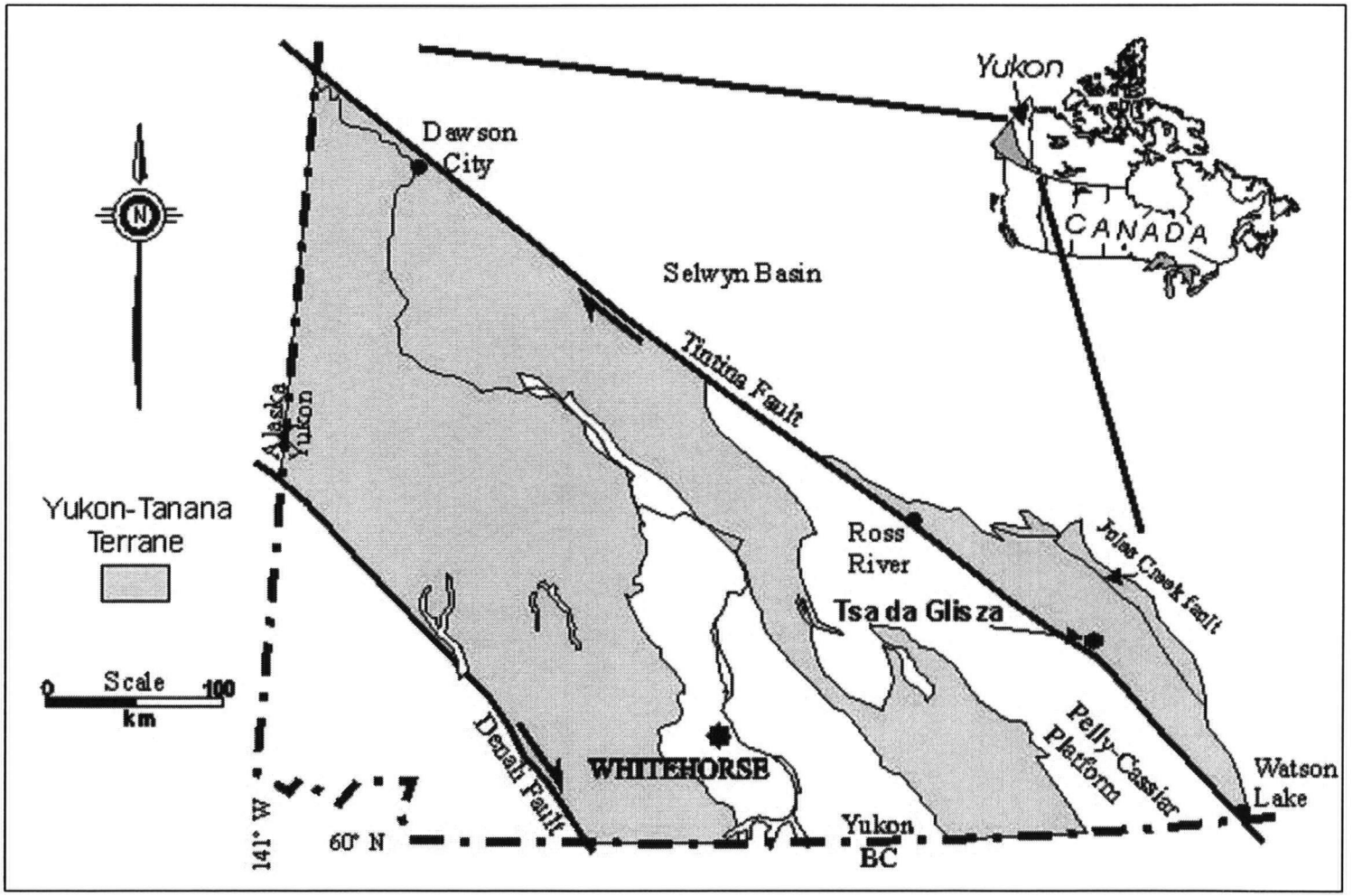

Figure 2.1. Location map of the Tsa da Glisza emerald occurrence, Yukon Territory, Canada.

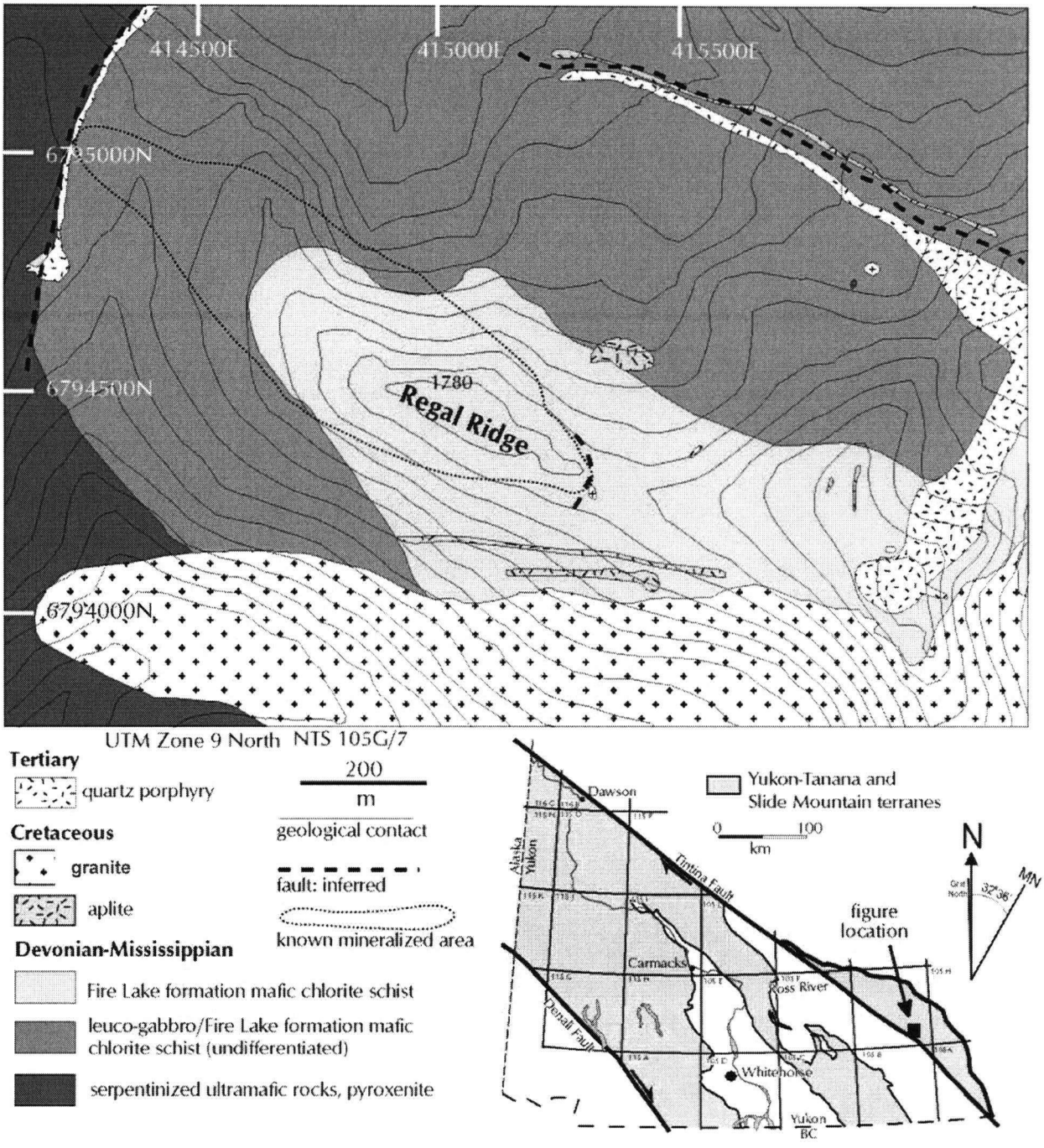

Figure 2.2. Preliminary geological map of the Tsa da Glisza property (NTS map 105G/7). Location map (inset) modified from Groat et al. (2002).

discovered green beryl and emerald on Expatriate's GoalNet property (Goal claims). Detailed work on the property began in July 1999; by late August, numerous green beryl- and emerald-bearing float trains and six main sources had been discovered in a 900 by 400 m area on both sides of the ridge (Groat et al., 2002).

In mid-2001, True North Gems, Inc. entered into an option agreement with Expatriate Resources Ltd. to acquire a 50% interest in the property. True North carried out an evaluation program in 2001, trench mapping and sampling over the property. In March of 2002, True North purchased Expatriate's remaining 50% interest in the Tsa da Glisza property and later that year carried out a more extensive field program consisting of a small drilling program which resulted in the discovery of new mineralized zones. A small processing mill was also constructed.

Results of reconnaissance investigations of the geology and emerald occurrences at Tsa da Glisza carried out by the authors during the 2002 field season were summarized in Neufeld et al. (2003).

2.3 REGIONAL GEOLOGY

The Tsa da Glisza area is located within the Yukon-Tanana terrane. Rocks in this area are composed of mainly pre-Late Devonian quartz-rich metaclastic rocks and carbonates and Late Devonian and Mississippian meta-volcanic and -plutonic rocks which are inferred to have formed in continental magmatic arc (Mortensen and Jilson,1985; Mortensen, 1992; Murphy, 1998; Murphy and Piercey, 2000) and back-arc settings (Piercey et al., 2000a, b). The oldest rocks are in the pre-Late Devonian to earliest Mississipian Grass Lakes succession. The Fire Lake formation, composed of mafic meta-volcanic rocks (mainly chloritic phyllite) (Murphy et al., 2002), is the second-oldest formation within the Grass Lakes succession. The Kudz Ze Kayah formation in the footwall of the Money Creek Thrust stratigraphically overlies the Fire Lake formation; and the Wolverine formation unconformably overlies the Kudz Ze Kayah formation (Piercey et al., 2001). The rocks were thrust onto the North American miogeocline between Late Triassic and earliest Cretaceous time.

All rocks are intruded by several ca. 112 Ma quartz-monzonite to granite intrusions of the Cassiar-Anvil suite (Mortensen, unpublished data). In the Finlayson Lake district these Cretaceous intrusions lie in a 25 km-long northerly trend, with the Tsa da Glisza property located

at the approximate mid-point. The intrusions are late- to post-kinematic with respect to the main Cretaceous deformation (D. Murphy, pers. comm., 2003).

The Tintina fault lies 14 km southwest of the Tsa da Glisza property (Fig. 2.1), and possibly related faults run through the Finlayson Lake district.

2.4 PROPERTY GEOLOGY

The main host rock for the emerald-bearing veins at Tsa da Glisza is green-grey chlorite-plagioclase schist that locally contains biotite and actinolite porphyroblasts. This schist forms part of the Upper Devonian Fire Lake mafic metavolcanic unit (Fig. 2.2; unit DF of Murphy et al., 2002). At Tsa da Glisza, the rock is invariably foliated and lineated, and in some areas has a waxy phyllitic texture. Despite the pervasive deformation that the unit has experienced, some quartz amygdules are still locally recognizable. Piercey et al. (1999) show that unit DF regionally consists of rocks with geochemical signatures ranging from boninites (high-magnesium andesite to basalt) through island arc tholeites, calc-alkaline and non-arc volcanic rocks. Geochemical analyses of the Tsa da Glisza mafic schist all fall in the range of high-Ca boninites (high-magnesium basalt to andesite; Fig. 2.3). The mafic schists on Tsa da Glisza have anomalously high Cr contents (average 960 ppm Cr), and these local host rocks are likely the source of Cr chromophore in the emerald (Table 2.1).

A actinolite-plagioclase-biotite schist (also unit DF) of possible leuco-gabbro protolith is closely interfingered with the mafic schist and could not be mapped separately at the scale of our mapping (Fig. 2.2). In hand sample, the actinolite-plagioclase schist is distinctly mottled green and white in color, with millimetre-scale actinolite and plagioclase crystals causing the mottled texture. It is a more competent rock than the chlorite schist and is generally less altered by quartz veining.

The irregular contacts between the two units likely reflect primary interlayering (the leuco-gabbro forming synvolcanic feeder dykes and/or sills to the Fire Lake unit volcanic rocks) which has been further complicated by subsequent transposition of the original contacts.

Brown-weathering, dark-green to black, variably serpentinized ultramafic rocks occur in the western and northern parts of the map area (Fig. 2.2). Murphy et al. (2002) suggest that the ultramafic bodies represent intrusive sills that fed the overlying Fire Lake volcanic rocks (DF) via gabbroic dikes (Dmi). Alteration of the ultramafic rocks where they are crosscut by younger

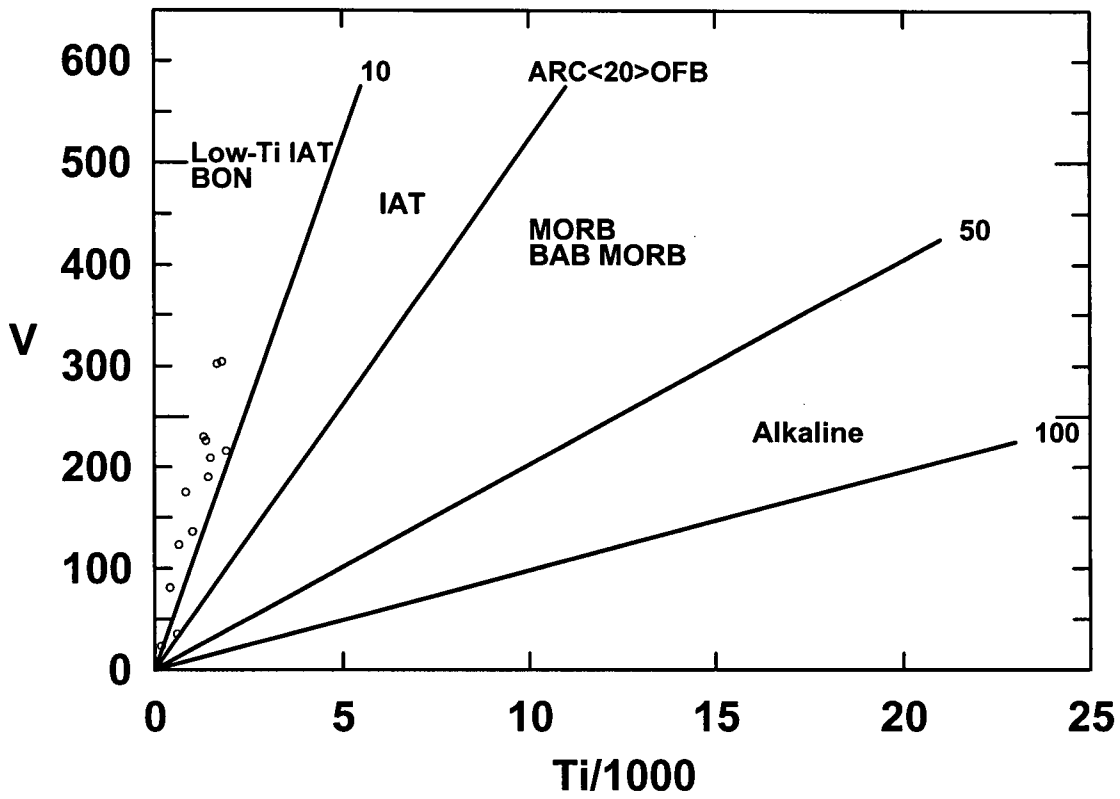

Figure 2.3. Vanadium versus titanium/1000 diagram of mafic metavolcanic schist (unit DF) at Tsa da Glisza. The schist plots as low-titanium boninite, a high-magnesium andesite-basalt. Modified from Shervais (1982). Abbreviations: BON – boninite; IAT – island arc tholeite; MORB – mid-ocean-ridge basalt; BAB – back-arc basin; ARC – arc basalt; OFB – ocean floor basalt.

Table 2.1. Whole-rock geochemistry of selected representative samples from various rock units at the Tsa da Glisza property.

	ultramafic Dum	leuco-gabbro DF	mafic schist DF	granite Kg	aplite	beryl-bearing aplite
Oxide (wt.%)						
SiO2	37.59	55.19	52.74	72.58	73.36	76.09
Al2O3	3.92	14.07	11.29	15.12	15.76	13.91
Fe2O3	13.31	5.51	8.89	1.39	0.63	0.36
CaO	0.81	8.8	7.98	0.94	0.93	2.15
MgO	32.86	9.2	12.47	0.49	0.16	0.07
Na2O	0.05	3.04	1.39	3.02	4.00	4.38
Cr2O3	0.52	0.04	0.14	0.03	0.03	0.03
K2O	0.02	0.64	0.24	4.62	3.50	1.61
FeO	8.8	4.24	7.16	0.93	0.40	0.33
H2O-	0.24	0.04	0.14	0.10	0.03	0.05
H2O+	11.45	1.64	3.22	0.72	0.63	0.30
LOI	10.25	1.33	2.68	1.19	0.98	0.72
Total	99.59	98.06	99.14	99.78	99.47	99.40
Element (ppm)						
B	40	<20	<20	30.00	30.00	20.00
Be	<0.05	0.2	0.39	11.13	30.54	114.85
Cr	3900	220	908.75	133.33	120.00	146.67
F	<20	30	83.75	1076.67	441.67	180.00
Li	1.9	25.1	62.03	157.33	58.56	33.27
Cl	<50	120	253.33	<50	100.00	<50
Cs	4.1	4.5	14.18	22.23	12.88	12.77
Cu	60	42	64.63	<5	57.00	27.00
Mo	3	3	2.71	3.33	4.00	4.00
Ni	1415	142	251.78	9.00	6.83	6.67
Pb	<5	<5	4.40	47.00	26.00	15.67
Sc	11.8	34.9	42.58	4.17	2.18	0.72
Sn	<1	<1	3.00	19.67	31.83	13.50
Ta	<0.5	<0.5	0.05	2.17	7.35	5.57
U	<0.5	<0.5	0.12	8.47	9.08	13.70
V	81	123	220.89	13.67	<5	<5
W	10	11	10.38	27.00	8.17	11.00
Zn	57	36	65.78	54.00	16.33	9.50
Zr	<0.5	<0.5	26.19	98.13	42.53	33.63

Note: Most major elements were analysed by XRF, and most trace elements by ICP-MS or ICP-ES. Li, Be, Cr, Mo were determined by AAS, B and Cl by INAA, FeO by titration.

aplitic dykes and sills is highly variable, and much less extensive than that seen in the mafic schist or leuco-gabbro units. This suggests there was a more limited interaction between the host rock and the felsic magma and intruding fluids. The ultramafic unit has not yet been found to host emerald-bearing quartz veins.

The pluton proximal to the Tsa da Glisza emerald occurrence is part of the Anvil Plutonic Suite (Mortensen et al., 2000), a 112-100 Ma suite of felsic intrusions which regionally are associated with numerous W, Mo, Au, and Bi occurrences. The 112 Ma two-mica (biotite>muscovite) granite extends to the east of Tsa da Glisza, as well as far to the north and south. It is weakly foliated to unfoliated, with shallowly dipping contacts. Tsa da Glisza is situated above the shallowly-dipping western margin of the intrusion (Fig. 2.4). Mapping during the 2003 field season confirmed that the mafic host rocks for emerald mineralization at Tsa da Glisza are underlain by Cretaceous granite at a relatively shallow depth (approximately 800 metres) and that the emerald occurrence is considerably closer to a granitic body than previously inferred by Groat et al. (2002).

Numerous aplite dykes from 40 cm to 10 m in width occur on the property. These bodies are variably strained, ranging from massive and essentially undeformed to strongly deformed in places. The extent of hydrothermal alteration surrounding the dykes is also highly variable.

2.5 STRUCTURAL SETTING

The Fire Lake mafic metavolcanic formation was initially deformed in the early Mississippian, at ca. 360 Ma, shortly after the unit was deposited (Murphy and Piercey, 2000). This early deformation resulted in contraction and folding, and the formation of foliation-parallel, centimetre-scale, non-mineralized quartz veins. Most of this mid-Paleozoic deformation was overprinted by deformation during Cretaceous time.

In the Early Cretaceous, rocks at Tsa da Glisza were subjected to non-coaxial, simple shearing as a result of major contraction related to northwest-verging, Cordillera-wide orogen-parallel deformation. Foliation related to this deformation is generally west-northwest striking in the Tsa da Glisza area and dips shallowly to the north. Quartz veins were formed and deformed during the progressive movement of the shear system. This resulted in considerable variability in the amount of deformation of individual veins or portions of veins depending on their

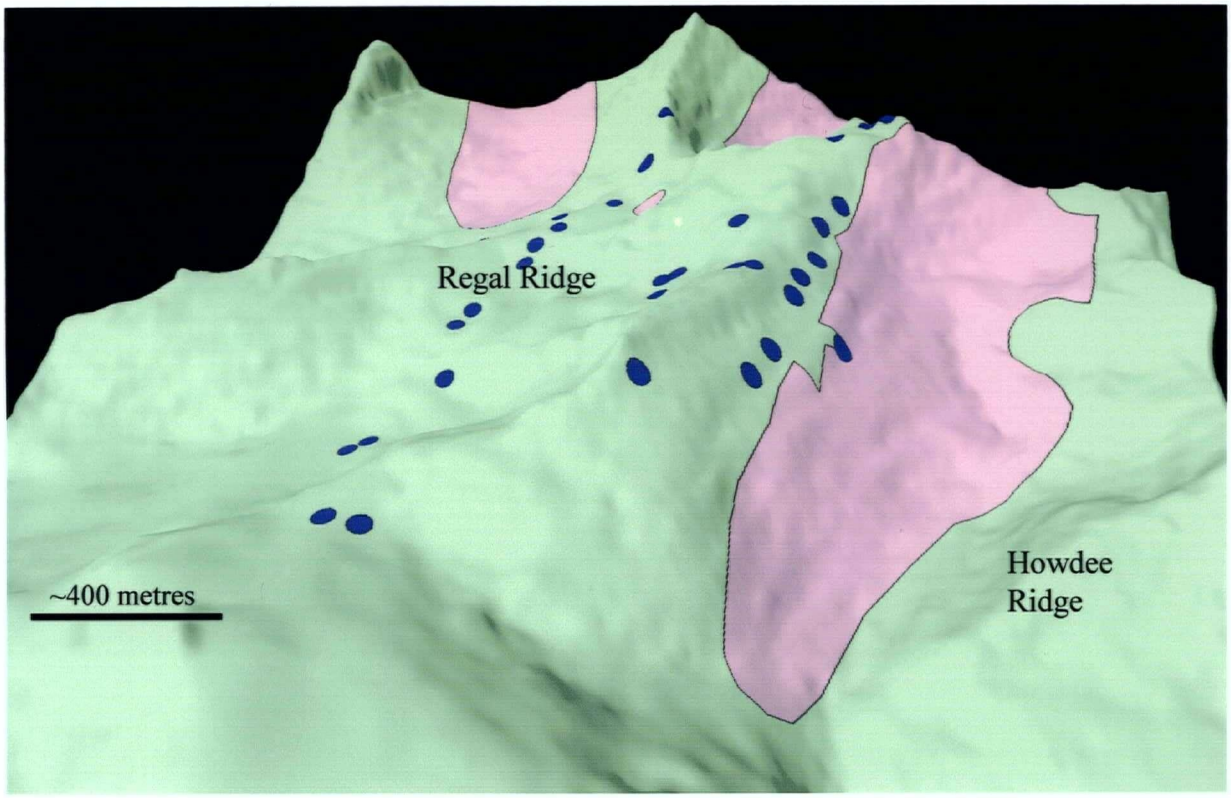

Figure 2.4. Three-dimensional map looking to the east over the Tsa da Glisza property, showing the granite intrusion (darker grey) and location of aplite dike outcrop (blue circles). The original discovery areas of mineralization sit on Regal Ridge, above and between protruding 'fingers' of the granite's western edge.

orientation within the shear system and the time when they were introduced to the system. The oldest veins in the system are typically isoclinally folded and boudinaged, while the youngest veins are generally planar or slightly folded. Emplacement of the large granite body to the southeast, and subsequent intrusion of aplite dikes, appears to have coincided with a re-orientation of the shear system and development of a new generation of veins within the system. This is shown by the presence of at least two directions of lineations that are thought to have developed within the shear system and two directions of boudinage exhibited by the most strongly deformed veins. Brittle-ductile shearing outlasted intrusion of the granite and aplite bodies, since strong ductile shear zones are present within some of the aplite dykes.

Most of the quartz veining observed at Regal Ridge is thought to be related to progressive Cretaceous deformation and the relatively late-tectonic emplacement of the granite intrusions.

Late-stage, brittle deformation, in the form of thrust and strike-slip faults and rusty-weathering alteration zones, cross-cuts much of the earlier deformation observed on the property. This deformation could be associated with regional deformation related to movement along the Tintina Fault and emplacement of Eocene dykes and sills. These dykes and brittle faults appear to follow the same zones of weakness which were exploited by the aplite bodies.

2.6 MINERALIZATION AND DISCUSSION

Quartz veins are abundant throughout the property, and by far the majority of them appear to be related to Cretaceous deformation. Early veins are typically relatively thin, foliation-parallel, relatively sulphide-rich, and contain no tourmaline. All of the other quartz veins, including those that contain beryl and emerald, are associated with at least some amount of tourmaline, either within the veins or in the immediate vein selvages. The younger veins are at least ten centimetres wide, except where they have been boudinaged. The degree of alteration surrounding the veins varies from almost no evident alteration, to metre-wide horizons of soft, rusty-weathering, jarosite-rich schist. This rustiness is likely due to weathering of finely disseminated sulphides (especially pyrrhotite) that is commonly present in the alteration envelopes on the veins. Emerald is found associated with veins of several different orientations. Mineralization appears to be particularly well developed in the area of intersection between the youngest generation of veins and older, more deformed veins. Emeralds occur along the margins of quartz veins in highly-altered schist, as well as within the quartz veins themselves. The

mineralizing event is therefore interpreted to have occurred over a considerable period of time, but was mainly syn- to late-tectonic, coinciding with the waning stages of granite intrusion. Crack-seal textures are present locally within some of the quartz veins, with tourmaline filling the cracks. Late ductile deformation has also affected some of the emerald-bearing veins, as evidenced by the presence of healed fractures in emerald and micro-boudinage of tourmaline grains within vein quartz.

Most aplites are spatially associated with abundant quartz veins which either cut the aplite bodies themselves or the schists immediately adjacent to the aplites. Some of these veins locally contain emerald. At least two of the aplites locally contain beryl or emerald, which confirms the authors' hypothesis that there is a continuum from the granitic intrusion through aplite dikes to beryl-bearing quartz veins (Neufeld et al., 2003).

Beryl-bearing aplite dikes chemically differ from non-mineralized intrusions (both aplites and the main granite body) by having lower potassium and F and higher Be contents (Figures 2.5 and 2.6; Table 2.1). This may provide a useful geochemical method for identifying intrusive phases elsewhere in the region that have a higher potential for being associated with emerald mineralization. The low F values are surprising, however, since we hypothesize that the Be was transported within intrusion-derived fluids as a F complex. Since an effort was made to avoid actual beryl mineralization when sampling (in order to avoid a nugget-effect chemical anomaly), it is possible that F that is contained as fluorite inclusions within beryl grains was also missed. This hypothesis assumes that F is intimately related to Be in the beryl-forming process, and only separates at the site of beryl crystallization, leaving the remainder of the intrusion relatively depleted in F. However, this could alternately indicate that Be was travelling also as a hydroxy and/or chloride complex, although there is little evidence for the later.

2.7 CONCLUSIONS

This most recent work has resulted in a number of important findings, as listed below:

1. The discovery of emerald and beryl mineralization in the aplite dikes is more evidence for a genetic link between the granite pluton and the emerald-bearing quartz veins.
2. The granite underlies the deposit at an estimated depth of 800 metres, with depth increasing to the west-northwest.

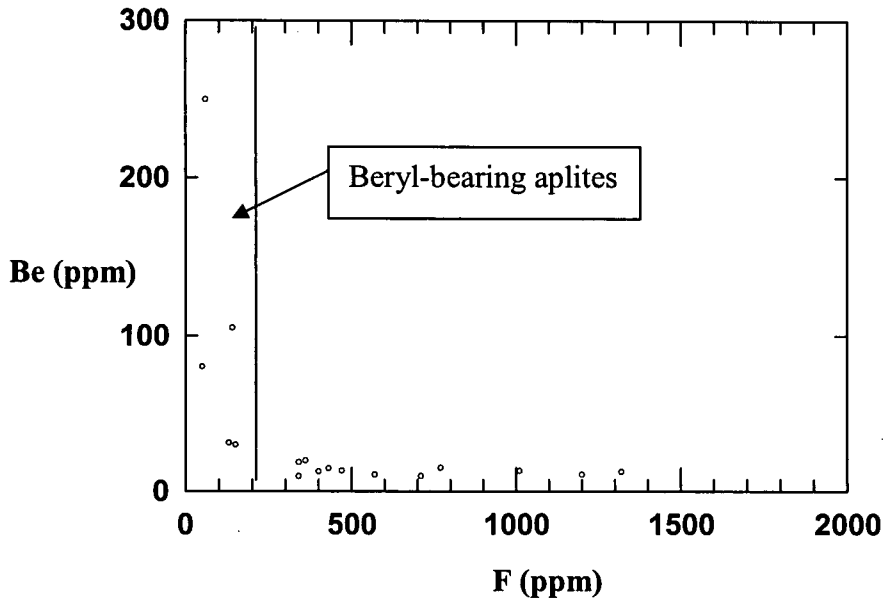

Figure 2.5. Beryllium versus fluorine diagram for all Tsa da Glisza aplite dykes. Beryl- and emerald-bearing aplite dykes have much lower fluorine contents than aplite dykes that do not contain beryl.

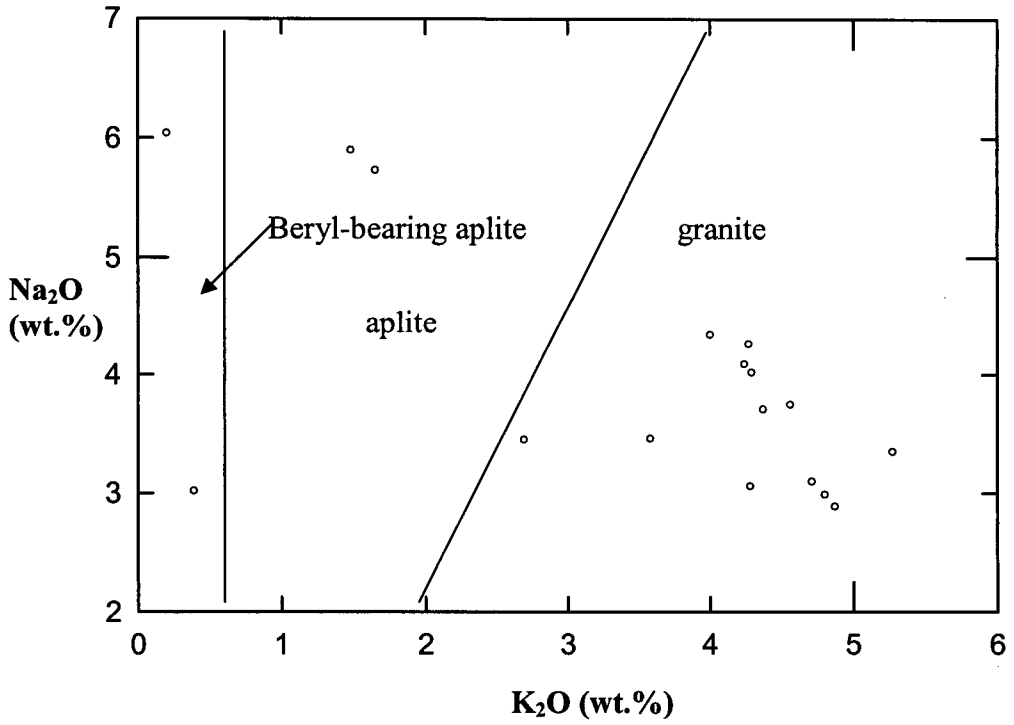

Figure 2.6. Sodium-versus potassium-oxide diagram for all Tsa da Glisza intrusive rocks. The potassium content of beryl- and emerald-bearing aplite dykes is lower than that of non-mineralized aplite dykes. The main intrusive body has the highest potassium content.

3. The timing of deformation relative to mineralization is now understood. In particular, mineralization was syn- to late-tectonic, coinciding with the waning stages of granite emplacement.

CHAPTER 3

[2]The Tsa da Glisza emerald deposit: New results and inferred genetic model.

3.1 INTRODUCTION

The Tsa da Glisza emerald occurrence is centered at 61°16.6' N latitude, 133°5.5' W longitude on National Topographical Survey map sheet 105G/7, in the Finlayson Lake district of southeastern Yukon, Canada (Fig. 3.1). The Tsa da Glisza occurrence contains the only known Cr-bearing emerald in the Canadian Cordillera. Emerald is an extremely valuable gemstone, and is rare because the required elements Be and Cr (with or without vanadium) are geochemically incompatible, and therefore are rarely found together in environments in which beryl is stable.

A previous study by Groat et al. (2002) reported on reconnaissance investigations of the geology of the mineralized region at Tsa da Glisza and the mineralogy of emerald and tourmaline, as well as initial fluid-inclusion work and limited geochronology and stable isotope results. Due to their limited data, the authors did not present a comprehensive genetic model for the formation of emerald at Tsa da Glisza. Additional fluid-inclusion studies which led to better constraints of the pressure, temperature and fluid conditions during emerald mineralization, presented in Marshall et al. (2003). The authors suggested that they could not distinguish between a tectonic-hydrothermal (shear zone-related) versus a magmatic or hybrid origin for the mineralizing fluid based on their data. Results of the 2002 and 2003 field seasons are summarized in Neufeld et al. (2003, 2004).

This paper compiles results from research on the Tsa da Glisza emerald deposit since 2002, outlines the various genetic models that might apply, and suggests the most likely genetic model for the deposit. Our objectives in this work were to investigate the role of a nearby granite pluton in the mineralizing process, determine the source of Cr and the sequence of events and evolution of fluid chemistry during the mineralization process, infer the structural dynamics during the mineralization event, and construct a genetic model to assist in further regional exploration for emerald in the northern Cordillera of North America.

---

[2] A version of this chapter is drafted for submission to Canadian Mineralogist. H.L.D. Neufeld, L.A. Groat, J.K. Mortensen, and S. Israel. The Tsa da Glisza emerald deposit: New results and inferred genetic model.

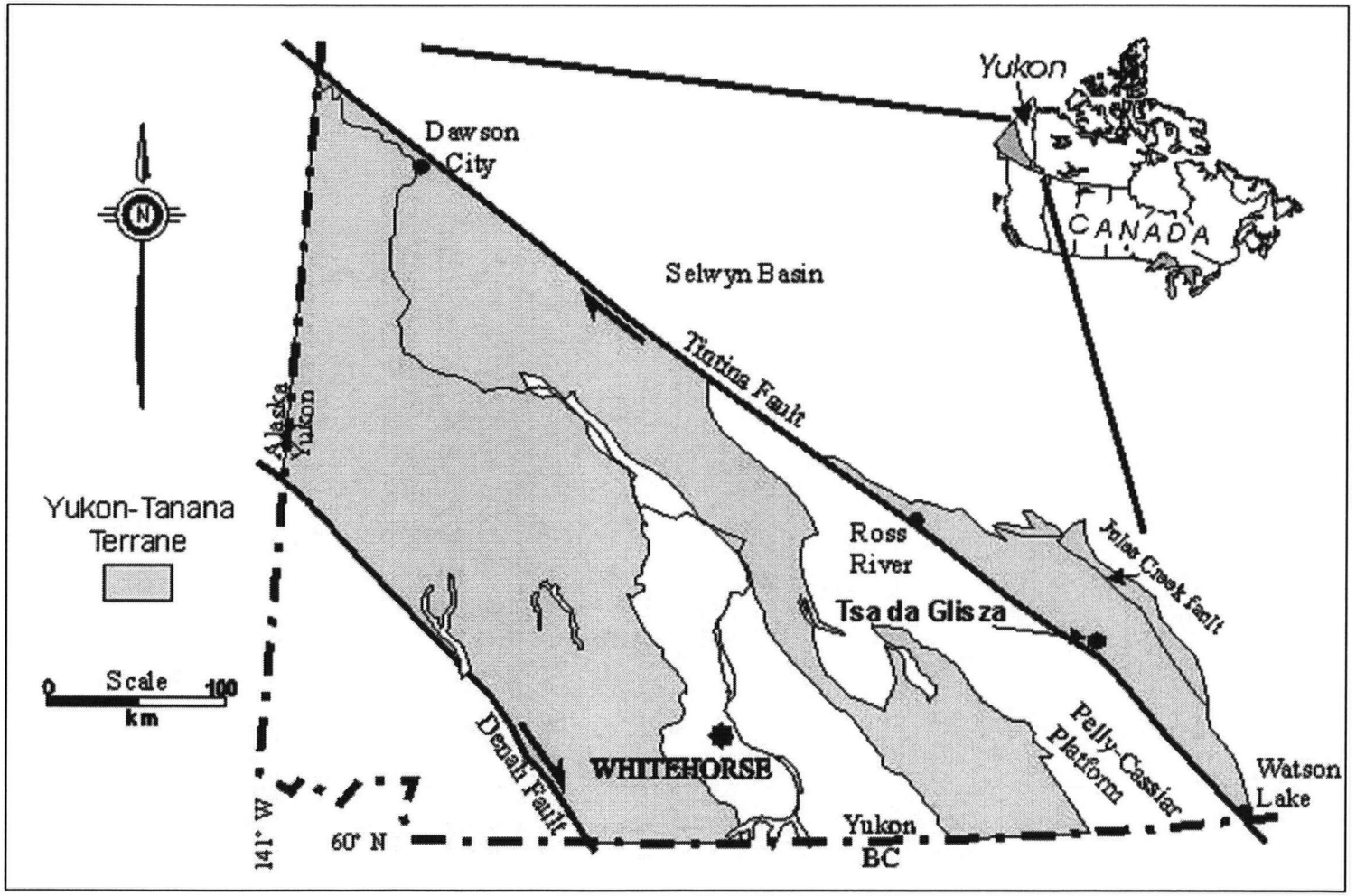

Figure 3.1. Location map of the Tsa da Glisza emerald occurrence, Yukon Territory, Canada.

The definition of "emerald" is still under considerable debate (e.g. Conklin, 2002; Schwartz and Schmetzer, 2002). In this paper, we define emerald as dark green, clear, gem-quality beryl, as distinct from opaque beryl crystals ranging in colour from white through dark green.

3.2 REGIONAL SETTING

The Finlayson Lake district is underlain by rocks of the Yukon-Tanana Terrane (Fig. 3.1), and is regionally bounded to the west by the Tintina Fault, and to the east by the Jules Creek Fault (Murphy, 2004). In this part of the Yukon Territory, the Yukon-Tanana terrane is composed of polydeformed pre-Late Devonian quartz-rich metaclastic rocks and carbonates and Late Devonian and Mississippian metavolcanic and metaplutonic rocks inferred to have formed within a continental magmatic arc (Mortensen & Jilson, 1985; Mortensen, 1992; Murphy and Piercey, 2000; Murphy, 2004) and back-arc settings (Piercey et al., 2000). The rocks were thrust onto the North American miogeocline between Late Triassic and Earliest Cretaceous time (Murphy, 2004). The structurally deepest rocks are contained within the Big Campbell thrust sheet, which is composed of the Upper Devonian Grass Lakes group, and the Lower Mississippian Wolverine Lake group. Both of these groups have associated metaplutonic rocks. The overlying Money Creek and Cleaver Lake thrust sheets occur further south in the Finlayson Lake district. The Tsa da Glisza occurrence is hosted within the Fire Lake Formation of the Grass Lakes group, which consists of mafic and felsic metavolcanic rocks and dark clastic rocks of the Fire Lake, Kudz Ze Kayah, and Wind Lake formations. The Fire Lake Formation is a mafic metavolcanic package composed mainly of chloritic phyllite, and is spatially associated with mafic and ultramafic plutonic rocks (Murphy, 2004; Piercey et al., 2004). The Kudz Ze Kayah Formation stratigraphically overlies the Fire Lake Formation and consists of carbonaceous phyllite and schist, felsic metavolcanic rocks, and rare quartzofeldspathic metaclastic rocks (Murphy, 2004). Rocks of the Wind Lake Formation do not occur proximal to Tsa da Glisza.

The rocks in the Finlayson Lake district are intruded by several *ca.* 112 to 110 Ma granitic bodies of the Cassiar-Anvil plutonic suite (Mortensen, unpublished data). The intrusions are syn- to post-kinematic with respect to the main Cretaceous deformation in the area. A recent structural interpretation of the Finlayson Lake region (Murphy, 2004) suggests that Cretaceous

deformation was more extensive than previously thought. The North River fault, a low-angle normal fault of mid-Cretaceous age, accommodated broadly north-south movement throughout the Finlayson Lake district. Rocks in the footwall have mid-Cretaceous Ar/Ar cooling ages, and were ductilely deformed prior to and during the emplacement of mid-Cretaceous granite plutons. The fault is interpreted to have accomodated the uplift and cooling of the footwall due to granitic pluton emplacement.

The Tintina Fault lies 14 km southwest of the Tsa da Glisza property (Fig. 3.1). Related volcanic rocks occur adjacent to the Tintina Fault, and faults and porphyritic dikes likely related to the event occur throughout the Finlayson Lake district (Jackson et al., 1986).

3.3 DEPOSIT GEOLOGY

3.3.1 Lithologic assemblages

3.3.1.1 Mid-Paleozoic age assemblage

3.3.1.1.1 Volcanic host-rocks

The main host rock for the emerald-bearing veins at Tsa da Glisza is a fine grained green-grey chlorite-plagioclase schist that locally contains biotite and actinolite porphyroblasts (Fig. 3.2 and Fig. 3.3a). This schist forms part of the mafic metavolcanic Upper Devonian Fire Lake Formation (unit DF of Murphy et al. 2002). Greenschist facies metamorphism altered most primary mafic minerals to chlorite and actinolite, while the groundmass consists mainly of quartz, chlorite, and actinolite with less abundant muscovite, biotite, and rare carbonate (Fig. 3.3a). The schist is strongly foliated and lineated and in some areas has a waxy phyllitic texture. Elongate sprays of tourmaline and porphyroblastic biotite occur locally within the foliation of the schist. Despite the pervasive deformation that the rock has experienced, some primary quartz amygdules are still locally recognizable. The main body of chlorite schist occurs on Tsa da Glisza and Howdee Ridge proper (Fig.3.2), but also crops out on the north and south slopes of the dominantly ultramafic ridge west of the mineralized areas. Chloritization likely occurred in the mid-Paleozoic.

A medium-grained, foliated actinolite-chlorite-plagioclase-quartz metavolcanic rock (unit DF of Murphy et al. 2002) is closely interfingered with the chlorite schist and could not be separated from the chlorite schist in some areas at the scale of our mapping (Fig. 3.2). The

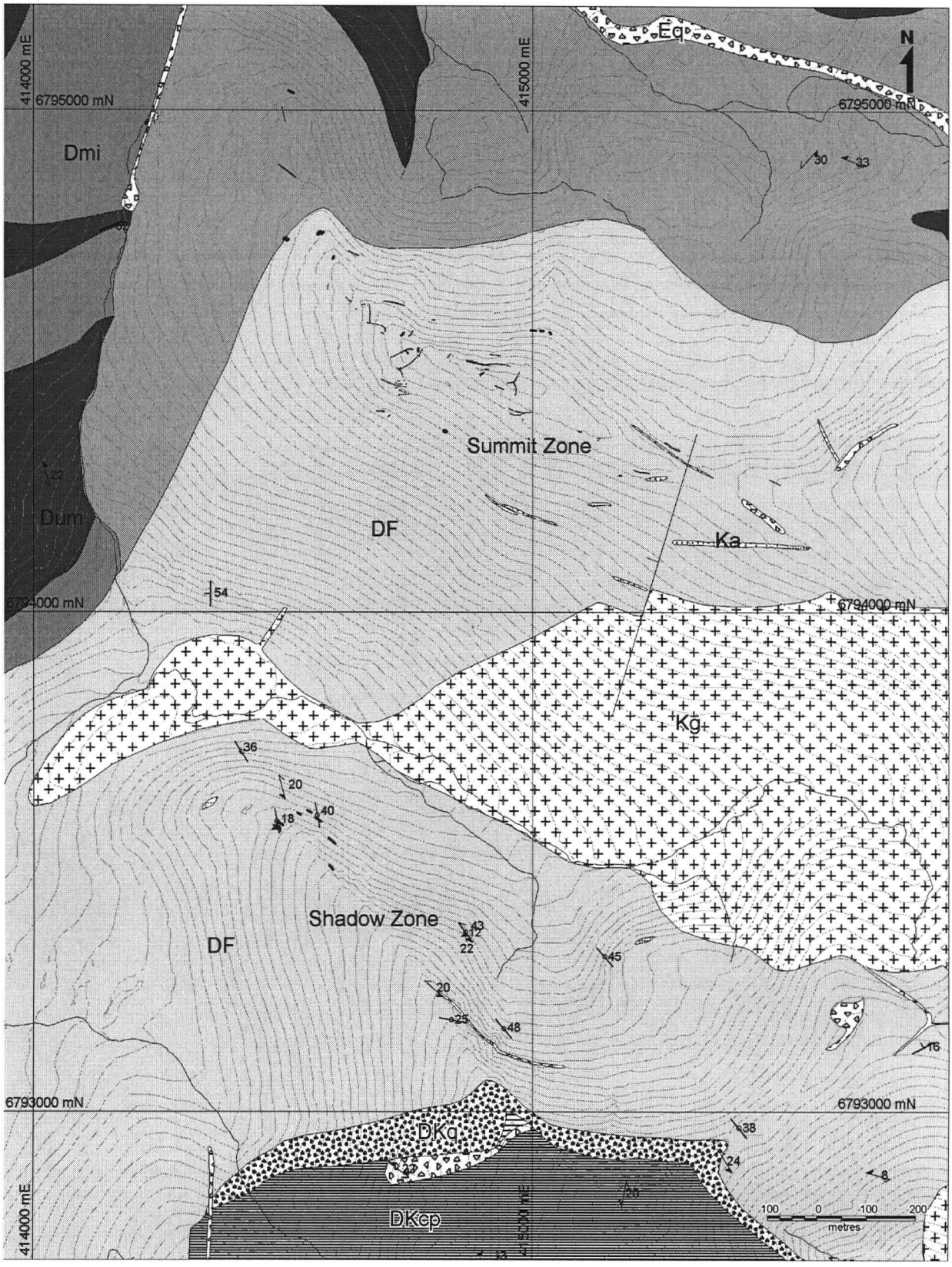

Figure 3.2. Geological map of the Tsa da Glisza property.

LEGEND

Rock Units

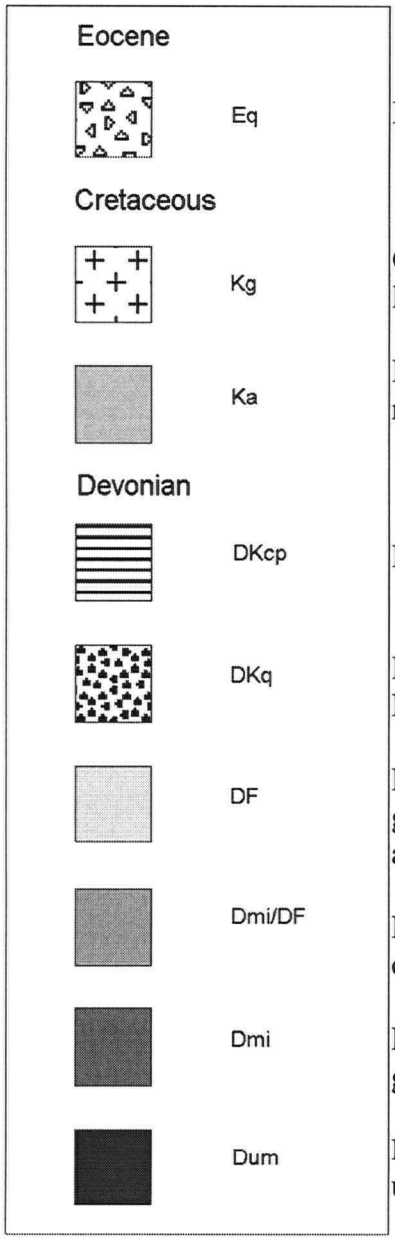

Eocene quartz-feldspar porphyry dikes and sills.

Cretaceous biotite-muscovite granite to muscovite leucogranite,with rare accessory garnet and tourmaline.

Leucogranitic and aplite-pegmatite sills and dikes with accessory muscovite, tourmaline, garnet, and rare beryl.

Devonian carbonaceous phyllite.

Devonian quartzite, locally rusty-weathering near contact with DF.

Devonian Fire Lake mafic metavolcanic unit, dark- to medium-green plagioclase-chlorite schist to phyllite, common biotite and actinolite porphyroblasts.

Interfingered actinolite-plagioclase-biotite leuco-gabbro and chlorite schist.

Devonian pyroxenite to actinolite-plagioclase-biotite leuco-gabbro.

Red-weathering, moderately serpentinized Devonian intrusive ultramafic rock.

Symbols

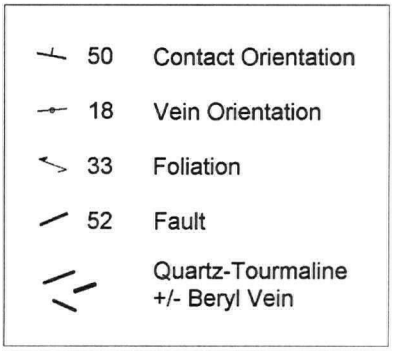

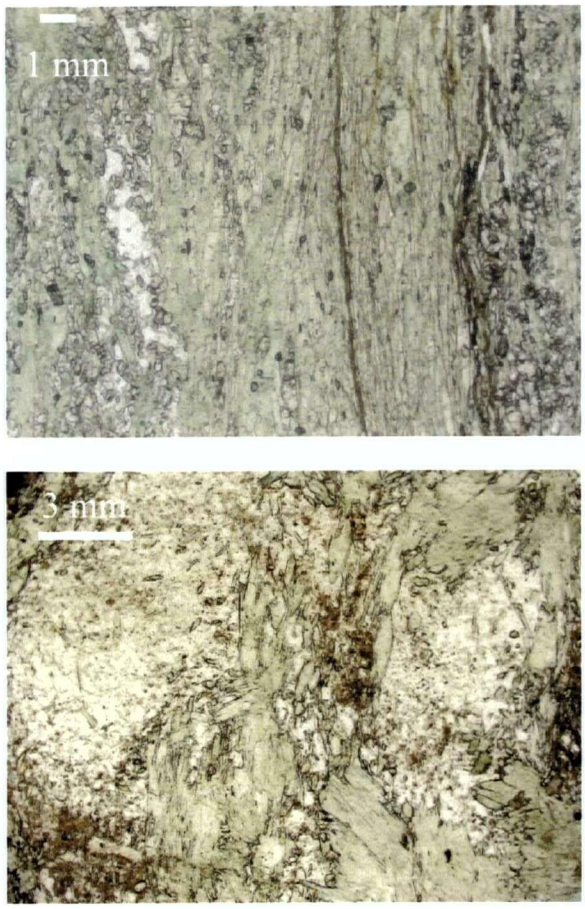

Figure 3.3. Photomicrographs of mid-Paleozoic rocks at the Tsa da Glisza property. **a)** fine grained green-grey chlorite-plagioclase schist. Greenschist facies metamorphism altered most primary mafic minerals to chlorite and actinolite, while the groundmass consists mainly of quartz, chlorite, and actinolite with less abundant muscovite, biotite, and rare carbonate. **b)** medium grained, foliated actinolite-chlorite-plagioclase-quartz metavolcanic rock

irregular contacts between the two rock types likely reflect primary interlayering of the volcanic rocks, which has been further complicated by subsequent transposition of the original contacts. The medium-grained foliated metavolcanic occurs toward the western nose of the ridge, near the fault contact with mafic and ultramafic intrusive rocks, and becomes less common eastward away from the fault. In hand sample, this rock is distinctly mottled green and white in color, with millimeter-scale actinolite, plagioclase, and clusters of fine-grained quartz causing the mottled texture (Fig. 3.3c). It is a more competent rock than the chlorite schist and is generally less altered by quartz veining, but geochemically it also falls in the range of high-Ca boninites (Neufeld et al., 2004).

Carbonaceous phyllite to quartzite (unit DKcp) occurs over much of the south-eastern region of the study area, at the top of the stratigraphic sequence. A 300-metre wide (maximum) band of quartz-plagioclase schist (unit DK) occurs on the south-facing slopes at the southern end of the study area. The schist contains numerous foliation-parallel quartz veins and stringers, which apparently do not contain tourmaline or beryl. A 50-metre wide band of biotite-rich unit DK, sandwiched between units DKcp and DF on the southern slopes, is also barren of quartz-tourmaline veining.

3.3.1.1.2 Mid-Paleozoic mafic and ultramafic intrusive rocks

Brown-weathering, dark green to black, variably serpentinized ultramafic rocks occur in the western and northern parts of the map area (Fig. 3.2). Murphy et al. (2002) suggested that the ultramafic bodies represent sills (unit Dum) that fed the overlying Fire Lake Formation volcanic rocks (unit DF) via gabbroic dikes (unit Dmi), however the ultramafic body at Tsa da Glisza has an equidimensional rather than tabular shape. The ultramafic body is highly serpentinized with localized alteration to talc. Metagabbro and metapyroxenite, altered to leuco-amphibolite and amphibolite, respectively, are likely the feeder dikes (Dmi), as suggested by Murphy et al., (2002). These rocks were grouped and mapped with the serpentinized ultramafic unit; near Tsa da Glisza all three rock types are cut by very few quartz veins and have not yet been found to host emerald-bearing quartz veins.

3.3.1.2 Cretaceous intrusive rocks

The pluton proximal to the Tsa da Glisza emerald occurrence is a part of the Anvil plutonic suite of 112-100 Ma felsic intrusions, which is regionally associated with W, Mo, Au, and Bi mineralization (Mortensen et al., 2000). Tsa da Glisza is situated above the shallowly-dipping western margin of a two-mica (biotite > muscovite) granite intrusion (Fig. 3.2). Property-scale mapping confirmed that the mafic host rocks for emerald mineralization at Tsa da Glisza are underlain by Cretaceous granite at a relatively shallow depth (minimum 250 metres at the eastern end of Tsa da Glisza) and the emerald occurrence is considerably closer to a granite contact than was previously inferred by Groat et al. (2002). The granite is weakly foliated to unfoliated, with shallowly dipping contacts. Muscovite content increases with proximity to contacts, as does the occurrence of rare quartz-tourmaline veins within the pluton. Garnet is present, but rare, and cordierite is absent. No miarolitic cavities were observed. A contact aureole extending approximately 500 metres from the granite contact is defined by the presence of biotite and tourmaline within the surrounding schist.

Numerous aplitic leucogranite dikes from 40 cm to five metres in width are present on the property, hosted within chlorite schist, actinolite schist, and pyroxenite (unit Ka, Fig. 3.2). The aplite dikes consist of two feldspars and quartz, as expected, but some of the dikes also contain small amounts of garnet. Optical methods indicate that the plagioclase in the aplite dikes at Tsa da Glisza ranges in composition from andesine to oligoclase (An_{28} to An_{40}), with some plagioclase in aplite being altered entirely to albite. The dikes are pervasively altered, with carbonate and muscovite partially replacing both feldspars, and are cut by veinlets of quartz-carbonate-sulfide (chalcopyrite, pyrrhotite, arsenopyrite, and molybdenite) (Fig. 3.4a). The extent of alteration surrounding the dikes is also highly variable, but where present, is similar to the tourmaline-jarosite-lepidocrocite-scheelite-sulfide assemblage which surrounds the quartz veins (described below). The dikes are variably strained, ranging from massive and essentially undeformed to locally strongly deformed. Most of the aplite dikes have pegmatitic and quartz-rich segregations either enclosed within the dikes or extending out into the host rock.

Quartz veins are abundant, and by far the majority of them appear to be related to the Cretaceous intrusive event. Pre-Cretaceous veins are typically less than 15 cm wide, parallel to the foliation, relatively sulfide-rich, and free of tourmaline. The Cretaceous veins are at least 10 cm wide, except where they have been boudinaged. All of the Cretaceous quartz veins, including those that contain beryl and emerald, are associated with at least some tourmaline, either within

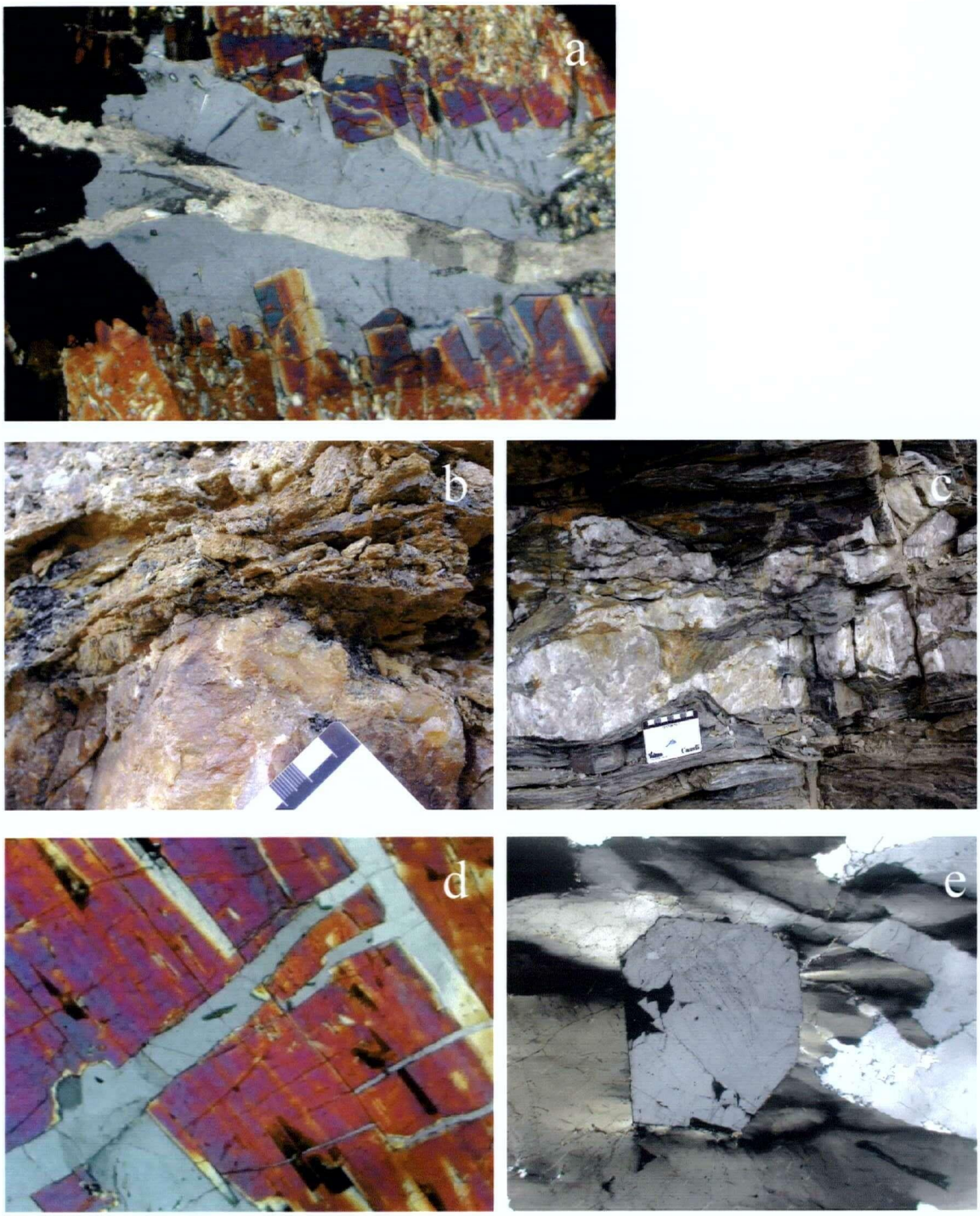

Figure 3.4. Photomicrographs of igneous rocks at the Tsa da Glisza emerald occurrence. **a)** Quartz veinlet within aplite, with late carbonate and sulphide filling a fracture in the veinlet. Tourmaline borders the veinlet. FOV ~7mm. **b)** Typical alteration assemblage adjacent to a quartz-tourmaline vein consists of tourmaline, jarosite, lepidocrocite, scheelite, and sulfide. **c)** Many of the quartz veins are strongly deformed. **d)** Brittle deformation of tourmaline. Fractures are ductilely infilled by quartz. FOV ~3mm. **e)** Undulatory extinction in quartz, and fractures in beryl, infilled by quartz. FOV ~7mm.

the veins or in the immediate vein selvage. The degree of visible alteration surrounding the veins varies from almost none to metre-wide envelopes.

3.3.1.3 Eocene porphyry rocks

Feldspar- and quartz-phyric, beige-, purple-grey-, and pink-weathering porphyry dikes and sills of probable Eocene age occur throughout the study area (Fig. 3.2), and commonly occur along the same zones of weakness exploited by the Cretaceous aplite and leucogranite dikes and sills, or along lithologic contacts. The porphyry intrusions are approximately 5 to 50 metres thick, and are commonly weathered to brown rounded pebbles. Some late faulting and alteration of host rocks and emerald could be attributed to this Eocene event, which was roughly synchronous with movement along the Tintina fault.

3.3.2 Mineralization and Associated Alteration Assemblages

At the Tsa da Glisza occurrence, emerald occurs: (1) in the alteration envelopes of quartz-tourmaline veins; (2) within both highly deformed, and undeformed quartz-tourmaline veins; and (3) in linear zones of highly altered schist, with no quartz-tourmaline veins immediately adjacent (Figs. 3.5 and 3.6). The emerald crystals show no preferred growth orientation relative to either the schist foliation, or to tourmaline-filled fractures within the quartz veins. Schist in direct contact with emerald-bearing quartz veins almost invariably shows alteration, but we note that mineralized veins may be hosted in unaltered chlorite schist (contrary to Groat et al. 2002), and altered schist zones do not always contain emerald (Fig. 3.5).

The Cretaceous event altered some of the chlorite schist to light brown jarosite- and phlogopite-rich schist. This schist is locally disaggregated, with scheelite and tourmaline also occurring close to quartz vein contacts. This prominent rust-coloured alteration, particularly near the top of Tsa da Glisza (also the most mineralized area), is likely due both to metasomatism on vein selvages and hydrothermal fluid circulation during the Cretaceous event (discussed in further detail below).

Modal abundances within the quartz veins are generally 80-95% quartz, with minor tourmaline, plagioclase, and muscovite, and rare beryl, scheelite and fluorite. Scheelite and fluorite crystals in vein and selvage are rarely larger than 1 mm in diameter. Alteration of the

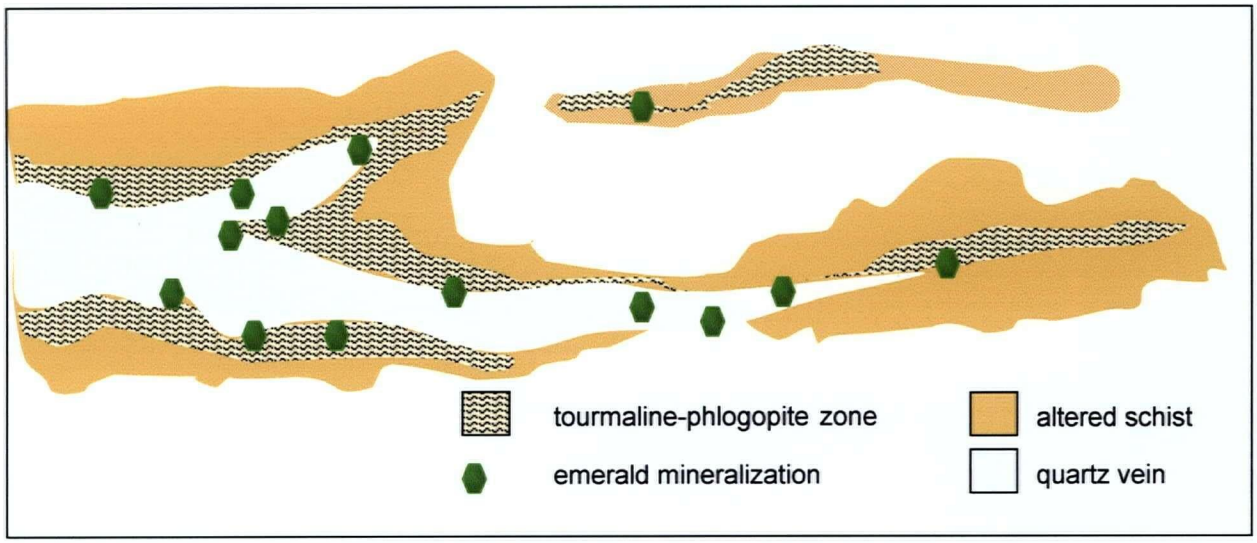

Figure 3.4. Cartoon of the various relationships between quartz vein, alteration, and emerald occurrences. No scale, as width of quartz veins and alteration is highly variable. Emerald occurs: (1) in the alteration envelopes of quartz-tourmaline veins; (2) within both highly deformed, and undeformed quartz-tourmaline veins; and (3) in linear zones of highly altered schist, with no quartz-tourmaline veins immediately adjacent. Schist in direct contact with emerald-bearing quartz veins almost invariably shows alteration, but mineralized veins may be hosted in unaltered chlorite schist, and altered schist zones do not always contain emerald.

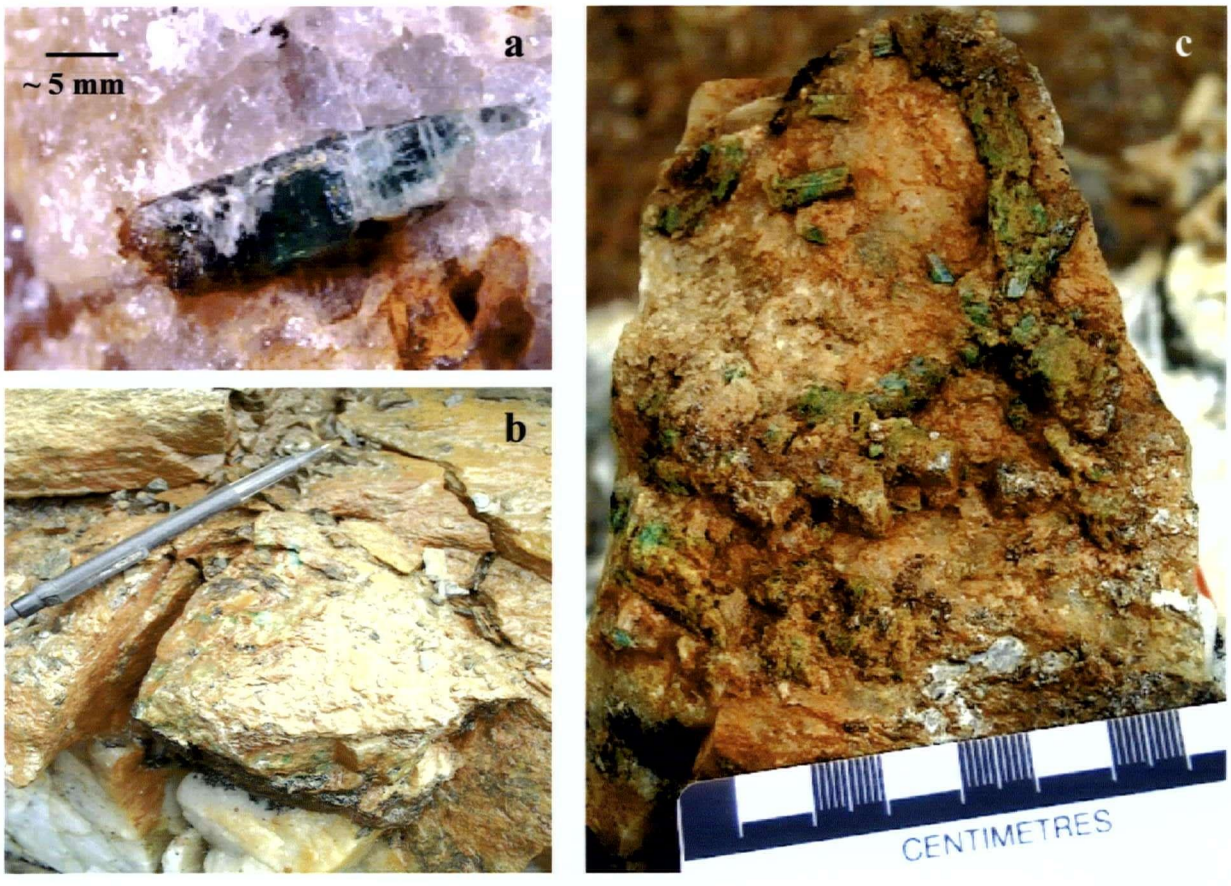

Figure 3.6. Emerald mineralization. Emerald occurs: **a)** within both highly deformed, and undeformed quartz-tourmaline veins; **b**) in the alteration envelopes of quartz-tourmaline veins; and **c**) in linear zones of highly altered schist, with no quartz-tourmaline veins immediately adjacent.

quartz-tourmaline vein selvages consists of jarosite, chlorite, tourmaline, muscovite, lepidocrosite and rare beryl (emerald), scheelite and fluorite in order of abundance. Distinct metasomatic zones cannot be delineated, but tourmaline and phlogopite are usually most abundant within the first 10 cm away from the vein-host contact, whereas more distal alteration mainly comprises jarosite within foliation planes of the chlorite schist. Where emerald occurs within the quartz-tourmaline vein material itself, phlogopite, fluorite, and scheelite are very rarely observed either within the vein, or on the selvage. Alteration envelopes are also less commonly associated with this type of mineralization. Emerald occurring within linear zones of strong alteration not directly adjacent to quartz vein has no associated quartz or plagioclase. Tourmaline, phlogopite, scheelite, fluorite, and rare carbonate are observed within the alteration zone.

A white beryl-bearing albite vein at Tsa da Glisza is somewhat similar to "desilicated pegmatites" described by Fersman (1960). These pegmatites are modified during crystallization by extensive reaction with mafic host rocks, and result in quartz-free plagioclase dikes with corundum, phlogopite selvages, and emerald within mica-rich assemblages. The beryl-bearing albite-quartz-muscovite vein at Tsa da Glisza is approximately 30 cm wide, and consists of an outer zone of plagioclase with blebs of quartz, and rare muscovite, and clear colourless and white opaque beryl to 2.5 cm in length occurring with quartz and tourmaline in a 2 cm-wide core of the dike. The albite vein locally pinches out, with emerald bearing quartz-tourmaline veins occurring within 1 m of the dike termination. Green beryl, and rare emerald, are found in quartz-rich segregations within two albitized aplite dikes at Tsa da Glisza. These segregations have some associated tourmaline, and rare white mica.

3.3.3 Structural Setting

3.3.3.1 Field Observations

The Tsa da Glisza area is characterized by complex structural relationships that are the result of several phases of deformation. This preliminary structural study of the area proximal to emerald mineralization has resulted in the following interpretation (Israel, 2003).

Early Mississippian (*ca.* 360 Ma) compressive deformation was responsible for transposition of the mafic metavolcanic unit and the formation of foliation-parallel, centimetre-scale, non-mineralized quartz veins. Transposition of the metavolcanic unit is indicated by

centimetre-scale isoclinal folds and the presence of preserved volcanic textures that indicate the existence of both upright and overturned bedding. The complex interfingering of rock types observed within the Fire Lake Formation is also likely related to this early event.

In the Early Cretaceous, rocks at Tsa da Glisza were subjected to non-coaxial simple shearing as a result of major contraction related to NW-verging, Cordillera-wide orogen-parallel deformation. Foliations related to this event and a re-orientation of the earlier transposed fabrics are generally west-northwest striking in the Tsa da Glisza area and dip shallowly to the north-northeast (Fig. 3.2). A crenulation fabric is developed in some of the rocks; this may have allowed for increased fluid flow, an hypothesis that is supported by the more pervasive alteration observed within these rocks. Several generations of quartz veins were formed and deformed during progressive movement of the shear system and resulted in considerable variability in the orientation and morphology of individual veins. Depending on their orientation and the point at which they were introduced to the system the veins may be isoclinally folded and boudinaged (Fig. 3.4c), planar or slightly folded. No distinct preferred orientation of emplacement for the veins is evident. There are at least two directions of lineations preserved on foliation planes and two directions of boudins exhibited by the most deformed veins at Tsa da Glisza. These features may be related to the emplacement of the pluton, which was likely syn-deformational and as well as providing fluids for vein formation (see discussion), may have been responsible for a re-orientation of the shear system with or without flattening across the system (transpression). Brittle-ductile shearing outlasted emplacement of the granite and aplite bodies, since strongly deformed shear zones are present within some of the aplite dikes. The aplite dikes are variably strained, ranging from massive and essentially undeformed to locally strongly deformed.

Late-stage, brittle deformation in the form of thrust and strike-slip faults and rusty-weathering alteration zones cross-cuts much of the earlier deformation observed on the property. This deformation could be associated with regional deformation related to movement along the Tintina Fault and emplacement of Eocene felsic porphyry dikes and sills. These dikes and brittle faults appear to follow the same zones of weakness that were exploited by the aplite bodies, and therefore late fluids from the Eocene dikes could easily have come into contact with emerald-bearing quartz veins and could be responsible for the formation of rinds on some of the emerald crystals.

A nearly vertical fault trends east-west at the top of the ridge (Fig. 3.2). Drill data suggests that the fault becomes shallow at depth. Alteration associated with the fault consists of pale green and white banded rocks near the fault itself, and bright red, powdery alteration surrounding

the fault. The fault appears to be younger than the emerald mineralization, although it could have contributed to fracturing of emerald crystals, which is most prevalent near the top of the ridge, and possibly to the intense alteration of the chlorite schist, particularly around quartz veins, whose altered selvages would have provided available as fluid pathways.

3.3.3.2 Petrographic Observations

Evidence of both ductile and brittle deformation is observed in petrographic sections of aplitic dikes and quartz veins. Deformed aplite dikes commonly contain quartz with strain shadows, and tourmaline that is fractured perpendicular to the c-axis and infilled with quartz (Fig. 3.4d). Within both aplite and quartz veins, beryl showing minor undulatory extinction, secondary fluid inclusions, and rare replacement by quartz (Fig. 3.4e) provides evidence of ductile conditions during and after mineralization. However, brittle crack-seal textures are present locally within some of the quartz veins and aplites, with tourmaline, calcite, quartz, and rare sulfides filling the fractures (Fig. 3.4a). Brittle deformation is evidenced in the aplite dikes by sharp contacts between the dikes and quartz veins within them, likely crack-seal textures, or fracture infilling. Brittle deformation has also affected some of the emerald, as evidenced by minor undulatory extinction, and the presence of both healed fractures (secondary fluid inclusion trails) and remaining fractures in emerald. Fracturing is most common in emerald from the Far West zone, an area near the emerald-bearing aplite. Mineralization in that area is associated with a quartz-tourmaline vein hosted within medium-grained foliated meta-volcanic rocks. Fracturing is rarely seen in emerald from the original discovery areas, near the top of the ridge (Fig. 3.7), where the emerald occurs in highly altered schist on the edge of quartz vein, or in emerald from the Mattscar zone, where emerald occurs in a highly altered linear zone of disaggregated rock. Emerald from the Southwest zone, where blasting was used to put in an adit, shows no more fracturing than emerald from other veins in that part of the ridge.

3.3.4 Geochronology

3.3.4.1 U-Pb

U-Pb (monzonite) analyses give ages of 112.4 +/- 1.1 Ma (Mortensen, unpublished data) for the granite pluton underlying Tsa da Glisza, 111 ± 1.6 Ma for an aplite dike approximately

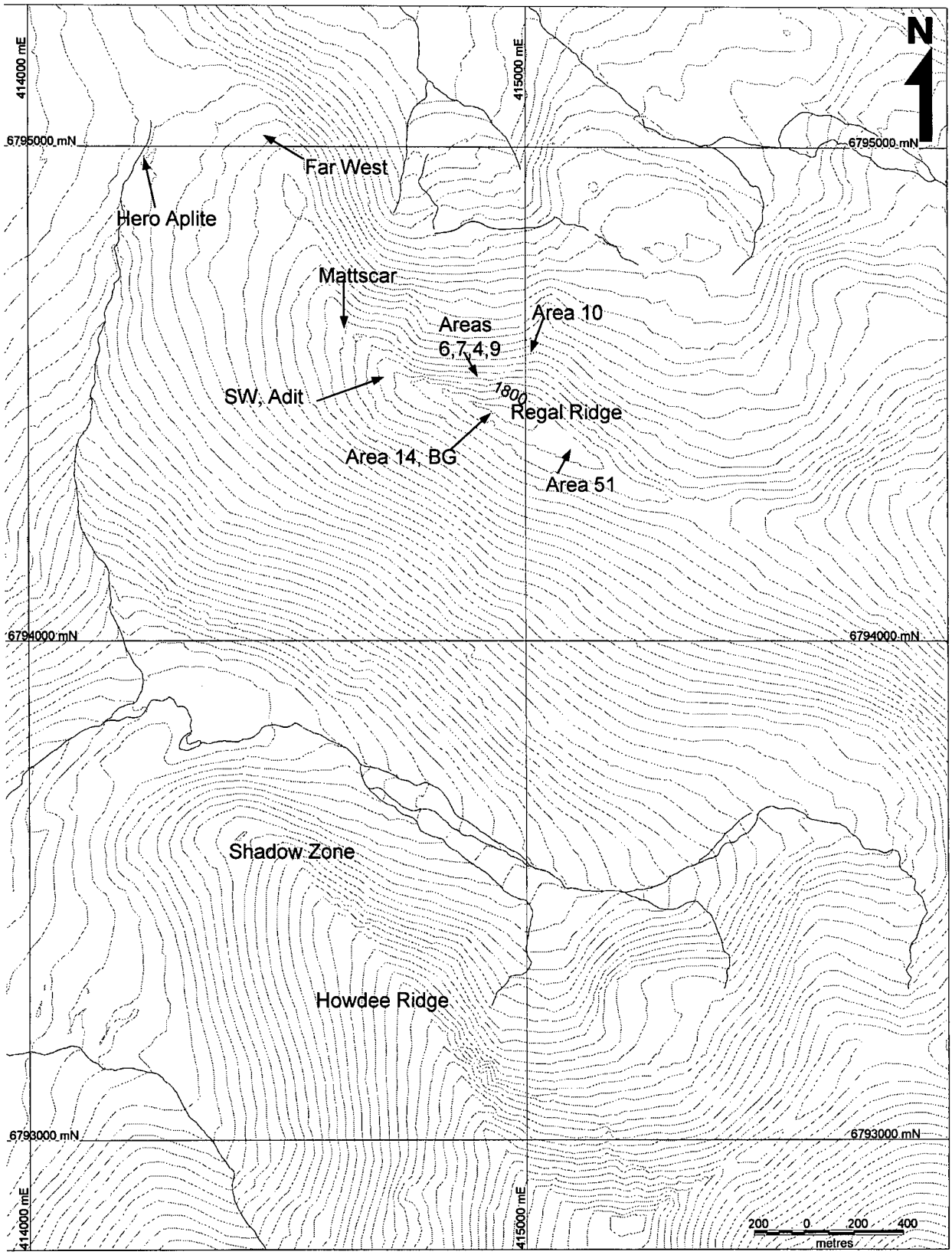

Figure 3.7. Location of named mineralized areas and ridges on the Tsa da Glisza property.

100 m above the granite and 200 metres from nearest emerald mineralization, and 112.2 +/- 0.5 Ma for an aplite-pegmatite dike within the ultramafic unit, approximately 500 metres from a granite outcrop (Fig. 3.8). The ages of other granitic intrusions in the region are also *ca.* 112 Ma (Mortensen, unpublished data).

3.3.4.2 $^{40}Ar/^{39}Ar$

Samples of mica for $^{40}Ar/^{39}Ar$ dating were taken from five drill-core samples and one hand sample to determine a thermal history of the area, including the approximate age of emplacement of aplites and quartz veins, and the timing of peak metamorphism. Analysed micas included foliation-parallel phlogopite within the chlorite schist, phlogopite from quartz vein selvage, muscovite from aplite, and muscovite from pegmatitic veins within aplite. The procedures are described in Appendix 1, and results of the study are presented in Table 3.1. Flat age spectra were obtained from each separate, resulting in plateau ages from *ca.* 110 to 112 Ma. Ages of *ca.* 113-109 Ma are reported for biotite in the footwall of the North River fault (Villeneuve and Murphy, unpublished data; in Murphy, 2004), and Groat et al. (2002) reported a single $^{40}Ar/^{39}Ar$ age of 108.7 ± 1.2 Ma for phlogopite within altered schist on the selvage of an emerald-bearing vein. The consistency of mica ages within the schist, aplite dikes, and quartz vein selvages indicates that the mineralizing event was closely tied to the intrusion of the granite body, and coincided with a regional metamorphic event. Unfortunately, because the ages are identical, a detailed thermal history of the occurrence cannot be determined.

Taken together, the U-Pb monazite ages and the Ar/Ar mica ages indicate that the region was at elevated temperatures (between 750 and 350° C) for 3 million years at most.

3.3.5 Geochemistry

3.3.5.1 Host Rock Geochemistry

Piercey et al. (1999, 2001, 2004), and Murphy and Piercey (2000) have shown that the Fire Lake formation regionally consists of rocks with geochemical signatures ranging from boninites (high-magnesium andesite to basalt) through island-arc tholeites, calc-alkaline and non-arc volcanic rocks. Compositions of the Tsa da Glisza chlorite schist all fall in the range of high-Ca

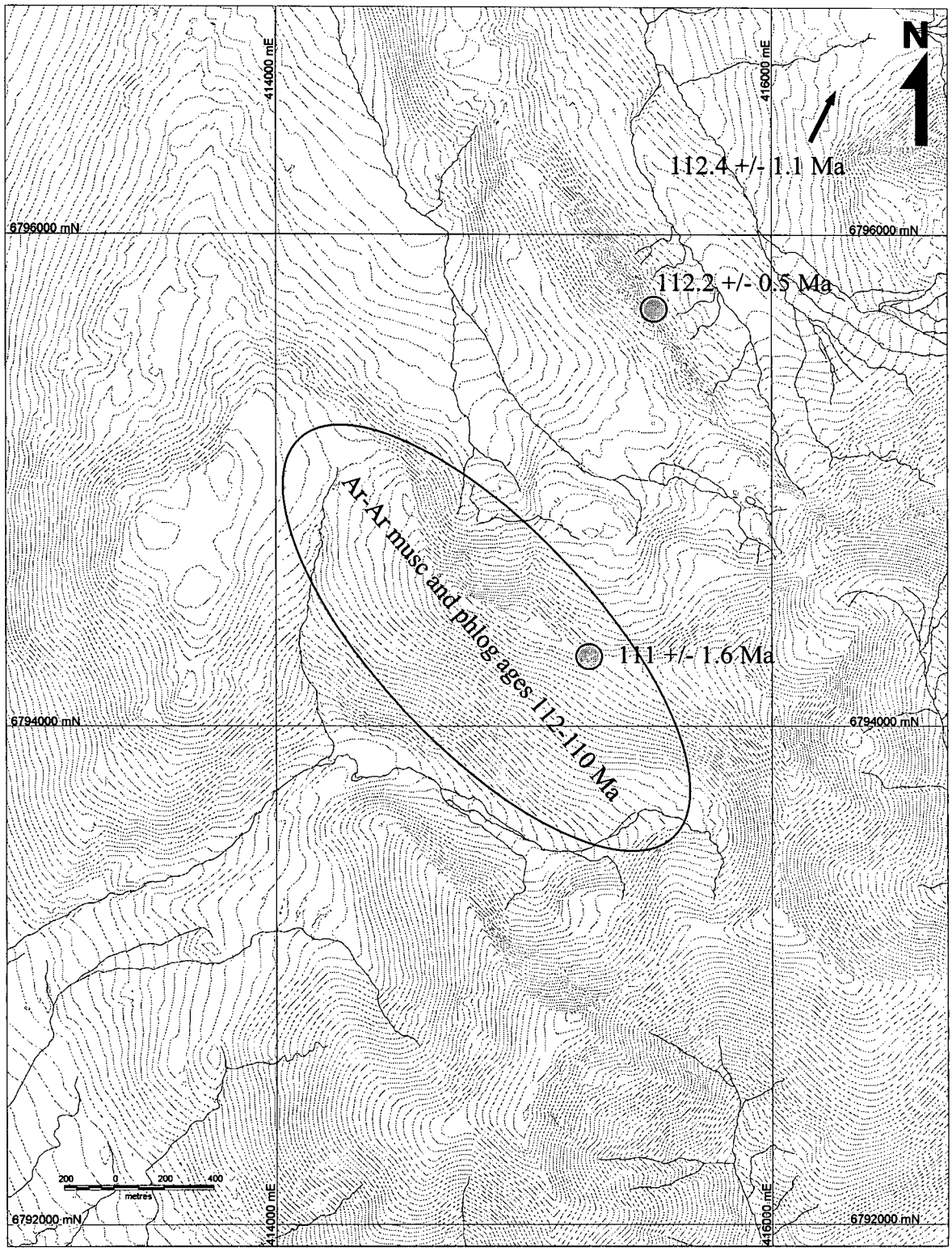

Figure 3.8. Location of geochronology samples (circles= U-Pb) taken from near Tsa da Glisza.

Table 3.1. $^{40}Ar/^{39}Ar$ Isotope Data, Tsa da Glisza emerald occurrence, Yukon Territory.

Sample	Description	Mica	Plateau Age
AD1-99	Selvage of quartz vein	phlogopite	110.5 ± 0.7 Ma (97% of ^{39}Ar)
RR-02-34	Pegmatitic phase within aplite	muscovite	111.2 ± 0.9 Ma (97% of ^{39}Ar)
AD1-21.9	Schist, 20cm from quartz vein	phlogopite	111.9 ± 0.6 Ma (92% of ^{39}Ar)
AD1-172	Aplite	muscovite	112.2 ± 1.3 Ma (62% of ^{39}Ar)
AD2-23.1	Altered schist, between quartz vein and fault	phlogopite	113.8 ± 1.2 Ma (93% of ^{39}Ar)

boninites (Neufeld et al., 2004; suite 5 of Piercey et al., 2004), a composition which is geochemically distinct from other mafic metavolcanic rocks within the Fire Lake Formation, and is characterized by high MgO, intermediate SiO_2, and anomalously high Cr, Ni, Co, and Sc values (Piercey et al., 2004). The chlorite schist at Tsa da Glisza has an average of 960 ppm Cr (Table 3.2). The foliated metavolcanic rock, also boninite in composition, has the lowest Cr content (average 220 ppm) of all mid-Paleozoic rocks at Tsa da Glisza, but is known to host mineralization, though less commonly than the chlorite schist. It has higher Ca and lower Fe content than the chlorite schist (Table 3.2). Of the rock units that are not associated with emerald mineralization, the ultramafic rocks have very high Cr contents (up to 3900 ppm Cr), and the leuco-amphibolite has much higher Ca, and lower Fe and Cr contents than the ultramafic rocks (Table 3.2).

The whole-rock geochemistry of twenty-seven host rock and vein selvage pairs were examined for element enrichments and depletions which might provide evidence for fluid interaction within the host rock due to vein formation (Appendix 2). Laurs et al. (1996) used this method at the Khaltaro emerald deposit, Pakistan to determine the extent of metasomatism around an emerald-bearing vein, and in particular, the movement of Cr from amphibolite towards pegmatite-quartz veins. The Khaltaro data set consisted of a single traverse across a mineralized vein. Although single traverses across Tsa da Glisza veins show distinct elemental variations, there was no statistically significant (greater than 1σ) enrichment or depletion of elements between the altered vein selvage samples and samples of unaltered host rock over our entire data set (Appendix 2). This is either an effect of the chemical variation inherent in the host rock, the more distal permeation of fluids into the host rock at Tsa da Glisza compared with Khaltaro (~20 cm, compared with metres at Tsa da Glisza), or perhaps due to over-printing of metasomatic alteration by continued fluid circulation. Typical patterns of element enrichment and depletion surrounding the emerald-bearing veins can be represented, however, and are discussed in detail in a following section.

3.3.5.2 Igneous Geochemistry

3.3.5.2.1 Granite

Geochemical results (Table 3.3) confirm that the pluton is an evolved peraluminous S-type granite; a Shand index plot shows that it is peraluminous (Fig. 3.9), and MORB-normalised rare-

Table 3.2. Whole rock geochemistry of mid-Paleozoic rocks at the Tsa da Glisza emerald occurrence.

	RR-02-8 414716 6796538	HN-2-1 413675.25 6794656.75	HN-2-2 413790.25 6794879.75	RR-02-10 416234 6794246	HN-2-17 415016.25 6794634.75	HN-2-28 414973 6794398	HN-2-30 414944.25 6794417.75	RR-02-21 414536 6794917	HN-2-66 414227 6794986	RR-02-14 415342 6794260	HN-2-45 414407.25 6795077.75
	serpentinized ultramafic	serpentinized ultramafic	gabbro	chlorite schist nearest granite	fissile chlorite schist	phlogopite-chlorite schist	fragmental basalt? chlorite schist	chlorite schist	actinolite-plagioclase schist	chlorite schist	actinolite-plagioclase schist
	Dum	Dum	Dmi	DF	DF	DF	DF	DF	DF	DF	DF
SiO2 (wt. %)	42.02	37.59	49.6	48.19	49.88	50.84	51.27	51.8	53.4	54.01	55.19
Al2O3	1.65	3.92	2.03	6.89	9.97	12.55	13.33	13.04	14.39	9.76	14.07
Fe2O3	9.75	13.31	7.51	10.81	13.24	9.78	9.19	9.3	9.03	8.52	5.51
CaO	0.04	0.81	9.51	9.5	5.07	8.41	7.36	9.51	8.41	9.34	8.8
MgO	35.99	32.86	25.03	19.39	15.2	11.94	11.26	11.17	9.59	13.33	9.2
Na2O	0.13	0.05	0.07	0.41	0.2	1.89	2.26	1.41	1.72	1.15	3.04
K2O	0.03	0.02	0.03	0.05	0.05	0.36	0.26	0.22	0.18	0.09	0.64
Cr2O3	0.43	0.52	0.37	0.38	0.18	0.08	0.06	0.08	0.03	0.08	0.02
TiO2	0.03	0.07	0.1	0.14	0.25	0.28	0.32	0.23	0.3	0.22	0.11
MnO	0.08	0.18	0.19	0.26	0.21	0.17	0.14	0.17	0.14	0.2	0.09
P2O5	0.01	0.01	<0.01	0.02	0.01	0.01	0.03	0.03	0.02	0.02	0.01
SrO	<0.01	0.01	0.01	0.01	0.01	0.02	0.01	0.01	0.03	0.03	0.02
BaO	<0.01	<0.01	<0.01	<0.01	0.01	0.02	0.02	0.01	0.01	0.01	0.04
LOI	9.53	10.25	4.15	3.07	4.78	2.19	3.22	1.89	2.27	1.72	1.33
Total	99.67	99.59	98.62	99.11	99.06	98.56	98.73	98.85	99.53	98.49	98.06
FeO (wt. %)	3.6	8.8	3.29	7.92	10.15	7.74	6.95	7.02	6.94	6.51	4.24
C	<0.05	<0.05	0.08	<0.05	0.05	<0.05	0.1	<0.05	0.08	<0.05	<0.05
CO2	<0.2	<0.2	0.3	<0.2	0.2	<0.2	0.4	<0.2	0.3	<0.2	<0.2
H2O-	0.38	0.24	0.07	0.07	0.23	0.18	0.21	0.08	0.16	0.06	0.04
H2O+	9.61	11.45	4.16	3.72	5.44	2.66	3.17	2.47	2.59	2.5	1.64
Cr2O3	0.43	0.52	0.35	0.39	0.18	0.1	0.09	0.09	0.05	0.1	0.04

continued on following page

hh

Table 3.2 continued.

	RR-02-8 Dum	HN-2-1 Dum	HN-2-2 Dmi	RR-02-10 DF	HN-2-17 DF	HN-2-28 DF	HN-2-30 DF	RR-02-21 DF	HN-2-66 DF	RR-02-14 DF	HN-2-45 DF
Ag (ppm)	<1	<1	<1	<1	<1	<1	<1	<1	<1	<1	<1
B	30	40	<20	<20	<20	<20	<20	<20	<20	<20	<20
Ba	2.4	4.2	15.4	7.9	3.5	191.5	110	38.7	80.7	106.5	310
Be	1.24	<0.05	0.25	0.12	0.27	0.24	0.15	0.19	0.8	0.23	0.2
Ce	0.6	1	0.7	2	1.1	2.1	1.7	2	1.8	1.9	0.8
Cl	<50	<50	<50	210	<50	<50	<50	160	<50	390	120
Co	120	124.5	54.2	70.5	65.2	41	40.2	45.6	44.9	42.2	32.5
Cr	3080	3900	2460	2730	1230	690	540	610	290	660	220
Cs	4.3	4.1	0.1	0.4	2	25.8	7.2	6	3.5	0.5	4.5
Cu	18	60	<5	24	6	57	190	<5	9	93	42
Dy	<0.1	0.3	0.4	0.7	0.9	1.2	1.2	1.1	1	0.9	0.3
Er	0.1	0.3	0.3	0.6	0.7	1	0.8	0.8	0.8	0.6	0.2
Eu	<0.1	<0.1	0.1	0.1	0.1	0.3	0.2	0.1	0.2	0.1	0.1
F	430	<20	<20	50	40	60	40	50	200	40	30
Ga	4	6	2	8	9	15	10	12	12	9	7
Gd	<0.1	0.2	0.2	0.5	0.5	0.7	0.7	0.6	0.6	0.5	0.2
Hf	<1	<1	<1	1	<1	1	<1	1	1	1	<1
Ho	<0.1	0.1	0.1	0.2	0.2	0.3	0.3	0.2	0.3	0.2	0.1
La	0.6	1	1	1.9	1.1	1.8	1.2	1.8	1.2	1.2	1.5
Li	7.1	1.9	1.4	57.7	54.8	68.8	83.7	76.3	57.1	13.8	25.1
Lu	<0.1	0.1	0.1	0.1	0.1	0.2	0.1	0.1	0.2	0.1	<0.1
Mo	3	3	3	3	2	2	3	3	3	3	3
Nd	<0.5	<0.5	<0.5	1.1	0.6	1.2	1.3	1.2	1	1.1	<0.5
Ni	1635	1415	303	801	345	169	134	246	111	179	142
Pb	<5	<5	<5	<5	<5	5	<5	5	6	5	<5
Pr	<0.1	0.1	0.1	0.2	0.1	0.3	0.2	0.2	0.2	0.2	0.1
Rb	1	0.9	0.3	0.6	1.1	31.9	18.3	8.4	10.2	1.6	17.6
Sc	5.7	11.8	24.2	26	46.5	51.5	46.8	46.9	54.4	38.5	34.9
Sm	<0.1	0.1	0.1	0.4	0.3	0.5	0.5	0.5	0.4	0.4	0.1
Sn	5	<1	<1	<1	<1	<1	1	1	1	1	<1
Sr	2.5	3.9	11.2	4.7	2.5	77.9	75.2	44.4	186	65.7	140
Ta	<0.5	<0.5	<0.5	<0.5	<0.5	<0.5	<0.5	<0.5	<0.5	<0.5	<0.5
Tb	<0.1	<0.1	<0.1	0.1	0.1	0.1	0.2	0.1	0.1	0.1	<0.1
Tl	<0.5	<0.5	<0.5	<0.5	<0.5	<0.5	<0.5	<0.5	<0.5	<0.5	<0.5
Tm	<0.1	0.1	<0.1	0.1	0.1	0.1	0.1	0.1	0.1	0.1	<0.1
U	<0.5	<0.5	<0.5	<0.5	<0.5	<0.5	<0.5	<0.5	<0.5	<0.5	<0.5
V	23	81	35	175	209	302	216	226	304	230	123
W	31	10	16	17	12	7	12	17	8	8	11
Y	<0.5	2.4	2.2	4.3	5.3	8.3	7.3	6.3	7	5.2	2
Yb	<0.1	0.5	0.3	0.7	0.8	1.2	0.9	0.9	1	0.8	0.3
Zn	57	57	33	72	72	62	69	77	34	71	36

Table 3.3. Whole rock geochemistry of Cretaceous intrusive rocks at the Tsa da Glisza emerald occurrence.

	HN-2-43	HN-2-37	HN-2-62A	RR-02-9B	RR-02-4	HN-2-40	RR-02-32	RR-02-26	RR-02-23	HN-2-8	RR-02-2	RR-02-28	RR-02-34
	414953	415953	415913	416371	415766	415589.25	415714	415286	415340	414227	415878	414744	415461
	6793979	6793962	6794754	6794799	6795348	6794102.75	6795539	6794325	6794566	6794986	6794254	6794473	6794704
	Kg, far south and west	Kg, base chem for	Outcrop Kg, near lake	aplite	aplite	aplite	aplite	aplite	aplite w/ tour	Hero aplite, beryl assoc.	aplite, beryl assoc.	aplite, beryl assoc.	pegmatitic dike
SiO2 (wt. %)	71.25	72.14	74.35	72.75	73.43	73.93	74.2	74.53	74.83	72.25	71.3	81.2	73.72
Al2O3	15.61	15.4	14.34	14.9	15.64	14.89	16.34	14.75	14.62	16.01	18.01	11.1	14.93
Fe2O3	1.69	1.41	1.08	0.63	0.88	0.66	0.54	0.62	0.63	0.2	0.46	0.25	0.44
CaO	0.94	1.17	0.71	1.47	1.5	0.53	0.8	0.59	0.69	2.75	0.66	3.01	0.55
MgO	0.58	0.4	0.49	0.23	0.29	0.22	0.13	0.02	0.08	0.06	0.07	0.07	0.01
Na2O	3.1	2.89	3.06	4.02	3.45	2.99	3.46	4.34	4.09	6.04	5.73	3.02	5.9
K2O	4.71	4.87	4.28	4.29	2.69	4.8	3.58	4	4.24	0.2	1.65	0.39	1.48
Cr2O3	0.01	0.01	0.01	0.01	0.01	0.01	0.01	0.01	0.01	<0.01	<0.01	0.02	0.01
TiO2	0.32	0.25	0.17	0.05	0.13	0.09	0.06	0.02	0.04	0.06	0.02	<0.01	0.01
MnO	0.02	0.02	0.01	0.01	0.01	<0.01	0.02	0.09	<0.01	0.03	0.08	<0.01	0.03
P2O5	0.14	0.1	0.08	0.06	0.06	0.07	0.03	0.02	0.04	0.01	0.03	0.01	0.01
SrO	0.02	0.01	0.01	<0.01	<0.01	0.01	0.01	<0.01	<0.01	0.05	0.01	0.01	0.01
BaO	0.05	0.04	0.03	0.01	0.01	<0.01	<0.01	<0.01	<0.01	0.02	0.02	<0.01	0.01
LOI	1.35	1.19	1.04	1.14	1.45	1.02	0.53	0.65	0.61	0.81	1.08	0.75	0.93
Total	99.78	99.9	99.66	99.58	99.55	99.23	99.7	99.64	99.89	98.5	99.13	99.81	98.02
FeO (wt. %)	1.18	0.9	0.72	0.39	0.64	0.39	0.32	0.39	0.45	0.21	0.26	0.32	0.39
C	<0.05	<0.05	<0.05			<0.05				0.05			
CO2	<0.2	<0.2	<0.2			<0.2				0.2			
H2O-	0.14	0.09	0.06	0.03	0.02	0.04	0.02	0.01	0.03	0.09	0.06	0.04	0.03
H2O+	0.86	0.66	0.63	0.5	1.01	0.64	0.36	0.4	0.42	0.26	0.86	0.22	0.69
Cr2O3	0.03	0.03	0.03			0.03				0.03			

continued on next page

Table 3.3 continued.

	HN-2-43	HN-2-37	HN-2-62A	RR-02-9B	RR-02-4	HN-2-40	RR-02-32	RR-02-26	RR-02-23	HN-2-8	RR-02-2	RR-02-28	RR-02-34
	Kg, far south and west	Kg, base chem for	Outcrop Kg, near lake	aplite	aplite	aplite	aplite	aplite	aplite w/ tour	Hero aplite, beryl assoc.	aplite, beryl assoc.	aplite, beryl assoc.	pegmatitic dike
Ag (ppm)	<1	<1	1	<1	<1	<1	<1	<1	<1	<1	<1	<1	<1
B	30	30	30			30				20			
Ba	415	419	161.5	62.3	76.3	41.4	8.5	18.5	13.9	117	132.5	16.8	56.8
Be	12.7	10.85	9.84	13.32	15.17	10.8	19.88	18.77	14.72	79.9	105.3	249.94	31.12
Ce	82.2	74.4	42.7	18.6	36.8	11.6	11.4	10.2	14.2	3.6	4.7	<0.5	8.7
Cl	<50	<50	<50	100	100	<50	<100	<100	<100	<50	<100	<100	<100
Co	4	3.7	3.2	0.6	1	1.4	0.6	0.6	0.7	2	0.7	0.6	0.6
Cr	130	150	120	110	100	130	130	140	130	140	110	170	120
Cs	26.3	25.2	15.2	14.4	9.5	14.5	14.2	13.3	12.7	3.2	11.4	22.4	6.8
Cu	<5	<5	<5	<5	<5	31	114	75	27	<5	8	<5	<5
Dy	2.2	2	2.2	1.8	1.7	1.7	3.4	3.5	3.1	2.2	1.5	0.2	2.4
Er	1.1	1	1.1	0.8	0.8	0.9	2.4	2.5	2	0.8	0.6	0.1	1.2
Eu	0.6	0.6	0.2	0.2	0.2	0.1	0.1	0.1	0.1	0.1	<0.1	0.1	<0.1
F	1320	1200	710	470	770	570	360	340	430	50	140	60	130
Ga	29	29	30	31	37	32	33	32	33	24	47	22	38
Gd	4.2	4.1	2.7	2	2.6	1.5	2.2	1.8	2.1	1.3	0.9	0.2	1.7
Hf	5	4	3	2	3	2	2	3	2	7	6	6	2
Ho	0.4	0.4	0.4	0.3	0.3	0.3	0.7	0.7	0.7	0.3	0.2	<0.1	0.4
La	38.6	36.6	19.8	8.3	17.5	5.3	4.7	4.3	6.4	2	2.2	<0.5	4.1
Li	213	161.5	97.5	36.23	95.61	80.1	87.28	47.43	60.39	29.2	4.71	10.23	6.87
Lu	0.1	0.1	0.1	0.1	0.1	0.1	0.4	0.4	0.3	0.1	0.1	<0.1	0.2
Mo	4	3	3	<2.00	<2.00	4	<2.00	<2.00	<2.00	4	<2.00	<2.00	<2.00
Nb	14	12	11	10	13	8	7	8	9	20	80	3	28
Nd	31.8	29.3	17.4	8.5	14.9	4.9	5.6	4.6	6.1	1.4	2.1	<0.5	4
Ni	8	9	10	7	9	7	6	6	6	7	6	7	8
Pb	51	50	40	30	17	44	25	32	28	13	8	6	12
Pr	9.2	8.5	4.9	2.2	4.1	1.3	1.4	1.2	1.7	0.4	0.5	<0.1	1.1
Rb	378	376	416	321	312	377	343	350	382	11.7	334	57	241
Sc	5	4.1	3.4	2.96	3.87	3	1.79	1.16	1.52	0.5	0.29	0.14	0.56
Sm	5.5	5.1	3.4	2.3	3	1.6	2	1.7	2	1.2	0.9	<0.1	1.7
Sn	22	16	21	13	49	25	22	17	23	4	65	<1.00	79
Sr	127	138	58.6	48.1	54.4	27.6	19.3	7.6	15.1	257	10.5	57.9	24.7
Ta	2	1.8	2.7	1.9	1.8	1	1.1	1.3	1.1	13.1	37	2.5	9.3
Tb	0.5	0.5	0.4	0.3	0.4	0.3	0.5	0.5	0.5	0.4	0.3	<0.1	0.4
Th	26	23	14	8	12	5	7	4	6	3	5	2	5
Tl	1.2	1.3	1.2	1	1	1	1	1	1	<0.5	1	<1	<1
Tm	0.1	0.1	0.2	<0.5	<0.5	0.1	<0.5	<0.5	<0.5	0.1	<0.5	<0.5	<0.5
U	7.8	4.5	13.1	17	13.7	4.6	8.4	7.2	20.4	12.2	3.6	8.5	14.8
V	18	14	9	<5.00	<5.00	<5	<5.00	<5.00	<5.00	<5	<5.00	<5.00	<5.00
W	28	29	24	3	4	13	3	4	9	22	22	2	3
Y	10.6	9.7	11.6	8.8	9.1	10	24.6	26.2	22.4	13.1	10.3	0.9	14.8
Yb	0.9	0.8	1	0.7	0.8	0.9	2.7	2.9	1.8	1.2	0.7	0.1	1.4
Zn	68	54	40	23	22	16	16	11	14	5	10	<5	5
Zr	125	116	53.4	27.8	116	21.8	19.5	31.5	33.8	36.6	38.6	30.5	46.2

Note: Most major elements were analyzed using XRF, and most trace elements by ICP-MS or ICP-ES. Li, Be, Cr, and Mo were determined by AAS, B and Cl by INAA, FeO by titration, CO_2 and H_2O by infrared spectroscopy, and F by specific ion potentiometry.

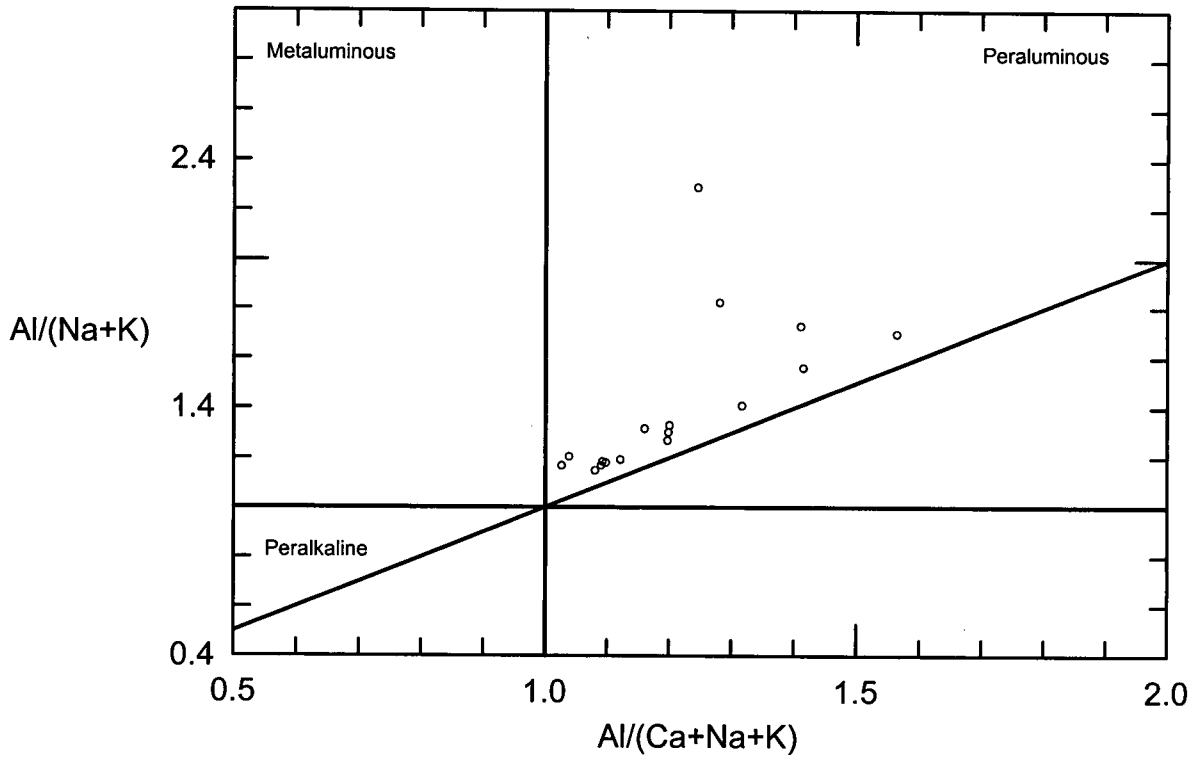

Figure 3.9. Shand index plot with igneous samples from the Tsa da Glisza property. All samples are peraluminous.

earth element data show trends typical of S-type granites (Fig. 3.10; compare Winter, 2001). No hornblende or magnetite occurs within the granite, but biotite and muscovite are common. The average Be content of the granite averages 11 ppm, which is relatively high compared to crustal Be values (3 ppm, Wedepohl 1995) and at the low end of the global average Be-content of granites (1-160 ppm, London and Evensen 2002) (Table 3.3). Li, P, and F contents are also high (Table 3.3).

3.3.5.2.2 Aplite

Most of the aplite dikes have pegmatitic and quartz-rich segregations either enclosed within the dikes or extending out into the host rock. These segregations have increased Be content relative to their hosts; at least two of the aplite dikes host pegmatitic or quartz segregations that locally contain beryl (Table 3.3). Aplite dikes with quartz-beryl segregations differ chemically from non-mineralized intrusions (both aplite dikes and the main granite body) by having higher Be and Na and lower Li, F, and Sn contents (Table 3.3). However, drill core samples of aplite, taken without removing altered selvages, show anomalously high F values (Appendix 2).

Alteration of feldspars in aplite to albite, muscovite, and carbonate assemblages may contribute to the high Ca:K and Na:K ratios of the aplites. The whole-rock geochemical data show that Na and Ca generally follow a simple linear replacement pattern, which suggests that the relationship between them is directly related to replacement in feldspars. Aplite dikes with beryl-bearing quartz segregations have distinctly high Ca:K ratios compared with the other intrusive rocks. The modified alkali-lime index (Frost et al., 2001) clearly distinguishes between beryl-bearing aplite dikes, and non-mineralized intrusive rocks (Fig. 3.11).

3.3.5.3 Vein Geochemistry

Whole-rock geochemistry of samples taken across numerous mineralized veins shows a consistent enrichment (relative to unaltered host rock) of Li, Sn, and F within the vein selvages, and rare enrichment of Be, Bi, and W usually within the vein itself, and rarely in the immediate vein contact (Fig. 3.12; Appendix 2). This is consistent with the abundant muscovite and rare fluorite in vein selvages. Boron is enriched in both the veins and selvages relative to unaltered chlorite schist, likely reflecting the abundant tourmaline in both veins and selvages. Beryllium

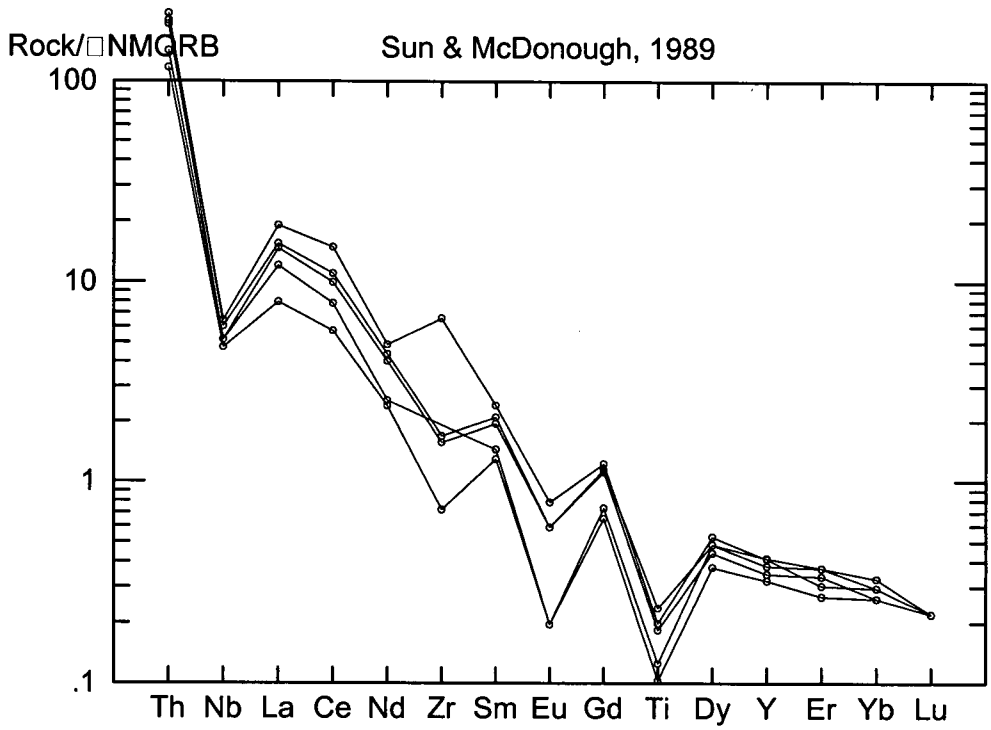

Figure 3.10. Rare-earth element patterns for granite samples from the pluton nearest the Tsa da Glisza property. Normalised to mid-ocean ridge basalt values of Sun and McDonough (1989). Pattern shown is typical of S-type granite (Winter, 2001).

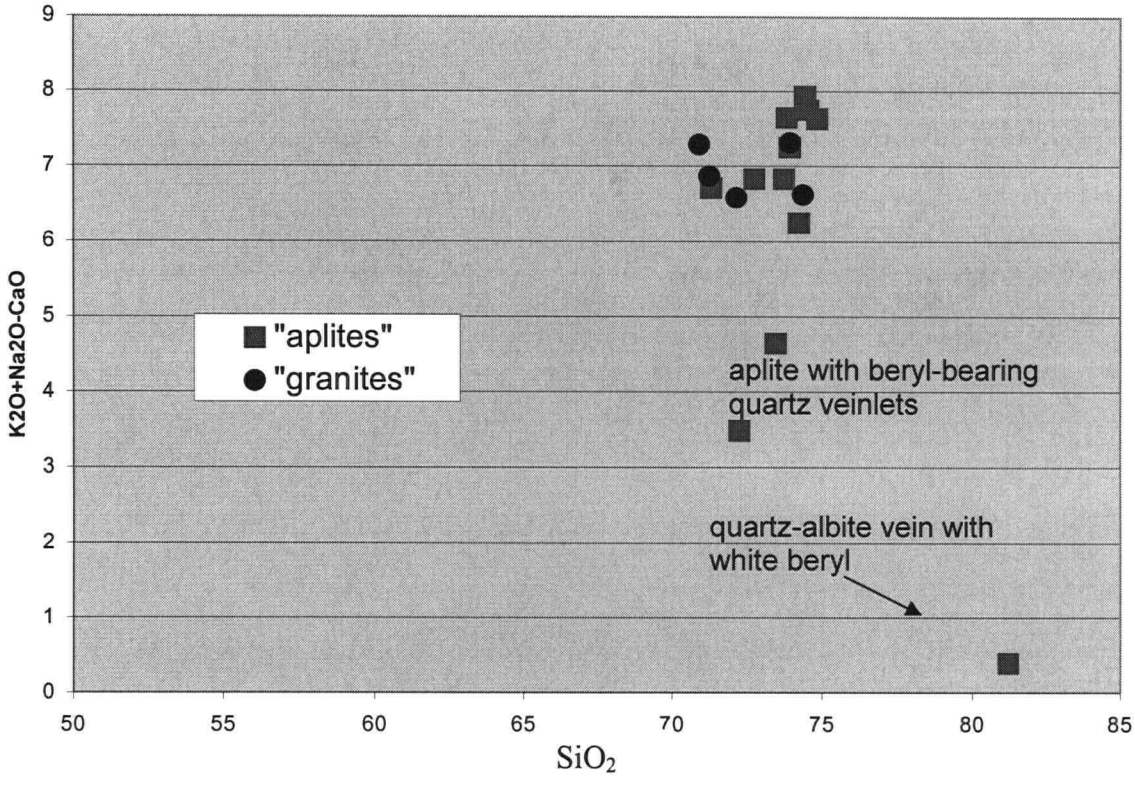

Figure 3.11. Modified alkali-lime index (MALI) for aplite and granite samples from the Tsa da Glisza property. Beryl-related aplite dikes have a higher Ca content than other intrusive samples.

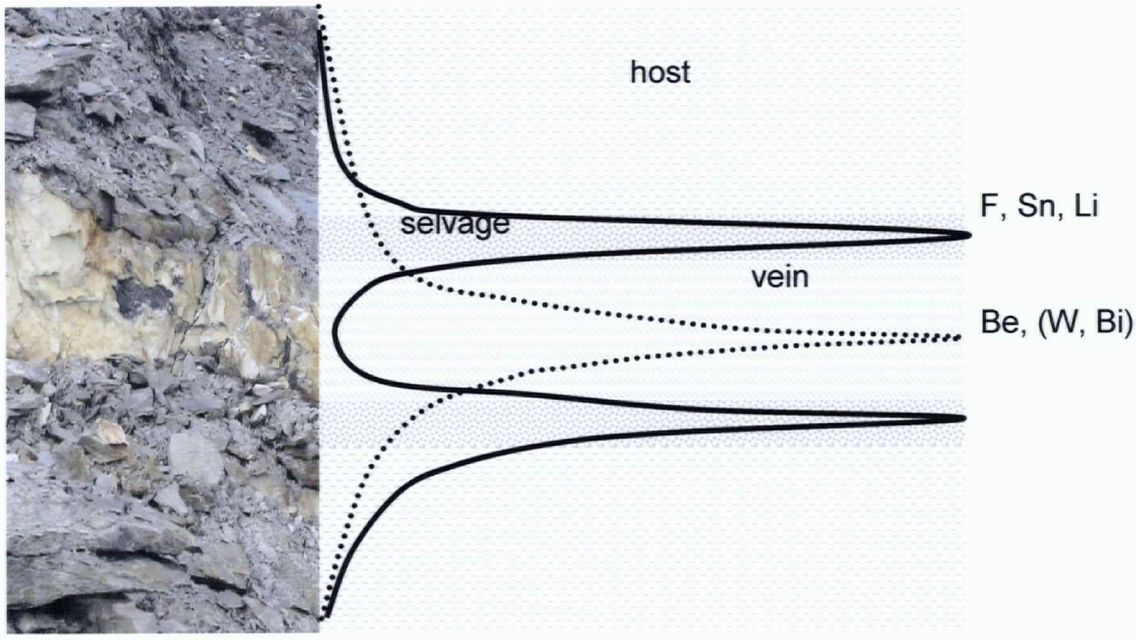

Figure 3.12. Typical pattern of geochemical enrichment relative to host schist, across a mineralized quartz-tourmaline vein. F, Sn, and Li values peak within the altered vein selvage (tourmaline-phlogopite zone), Be values peak sporadically within the vein itself, and Bi and W peak either within the vein, or in the immediate vein selvage.

values can differ by as much as 300 ppm over a distance of one metre along a vein. This likely in part reflects the "nugget effect".

Mineralization also occurs within zones of highly altered schist past quartz vein terminations. No characteristic geochemical fingerprint has yet been established for this type of mineralization; the Li, F, and Sn-rich envelopes are not apparent, and although there is some correlation of Be with W and Bi, it is sporadic and unreliable. The F contents of the emerald-bearing altered schist are generally high (>2700 ppm), and Li and Sn have moderate values (>150 and >25 ppm, respectively) (Appendix 2).

3.3.5.4 Soil Geochemistry

Soil geochemistry results from samples collected before 2003 show significant positive correlations (r values) between Be and Sn (0.82), Rb (0.80), Bi (0.74), Cs (0.67), and W (0.65) (Giroux, 2002,). However, different analytical methods used on samples give drastically varying results for Be. New soil geochemical data from the Tsa da Glisza property are expected to more clearly delineate element correlations, but this information is not yet available.

3.3.6 Mineral Chemistry and Textures

3.3.6.1 Emerald and Beryl

In an attempt to determine the chemical variability of the mineralizing fluid, 245 medium to dark green, clear beryl crystals from eleven mineralized zones at Tsa da Glisza (Fig. 3.7) were analyzed by electron microprobe. Details of the analytical procedure can be found in Appendix 1. Each emerald crystal was also examined with a scanning electron microscope for evidence of zoning, inclusions, and fracturing. None of the emerald crystals was chemically zoned to a degree that could be seen with back-scattered electron imaging; while white beryl rims surround some emerald crystals, the chemical variation is not enough to produce a back-scattered electron imaging contrast. Few internal cavities were observed in the emerald grains in this data set, although cavities have been observed in non-gem beryl from Tsa da Glisza.

The results show that the colour, number and type of inclusions, and fracturing vary considerably throughout the emerald sample set (Appendix 3). Colour varies considerably among

beryl crystals from each area, but no significant colour differences between areas could be discerned using this dataset. Two-thirds of the crystals studied were included. Quartz is the most common inclusion in emerald, followed by biotite, tourmaline, pyrite, and calcite, and rare chlorite, epidote, scheelite, and chromite (Fig. 3.13). The most inclusion-rich emeralds are those that occur in quartz veinlets within aplite. These emeralds host all the types of mineral inclusions found elsewhere on the property (listed above), except pyrite, calcite, and scheelite. The abundance of calcite inclusions in emerald generally appears to increase toward the top of Regal Ridge. Emerald grains with no inclusions were also less fractured in general.

There is no significant variation in major element chemistry for those beryls associated with quartz-tourmaline veins in chlorite schist (by far the majority). Emerald hosted in quartz veinlets within aplite (Figs. 3.14, 3.15; "aplite") has lower Al and Si, and higher Na, Mg, and Fe than most beryl associated with quartz-tourmaline veins within chlorite schist (Appendix 3). Totals vary in direct correlation with the amount of Si in the structure. Alkali enrichment in beryl is generally associated with albitic assemblages and late cavity-hosted crystals (Cerny, 2002). One crystal hosted within a quartz-rich segregation within aplite contains anomalously high alkali content.

A comparison of this data set with the smaller data set of emerald and beryl from the original discovery areas in Groat et al. (2002) shows an extension of the range of values, which is somewhat expected since this sample set includes emeralds from new areas of mineralization, up to 400 metres away from the original discovery areas. For a plot of Al *vs.* other *Y*-site ions, the only notable difference from the Groat et al. (2002) data is expansion of the range of values in both directions (Fig. 3.14). Emerald showing the most extensive replacement of Al is from a quartz veinlet within mineralized aplite. With the exception of this sample, a general trend of decreasing substitution in emerald from east to west, or with decreasing altitude, is apparent (this is potentially correlated to distance above the granite intrusion). A further comparison to data from Groat et al. (2002) can be made with a graph of (Mg + Fe) *vs.* (Na+ K + Cs) (Fig. 3.15). Again the data range is greater, with emerald from aplite showing the most extensive coupled substitution, and some emerald from the southwest vein (in the adit) with very little substitution. In general, emerald from the southwest vein shows less extensive substitution than emerald from other areas on the property.

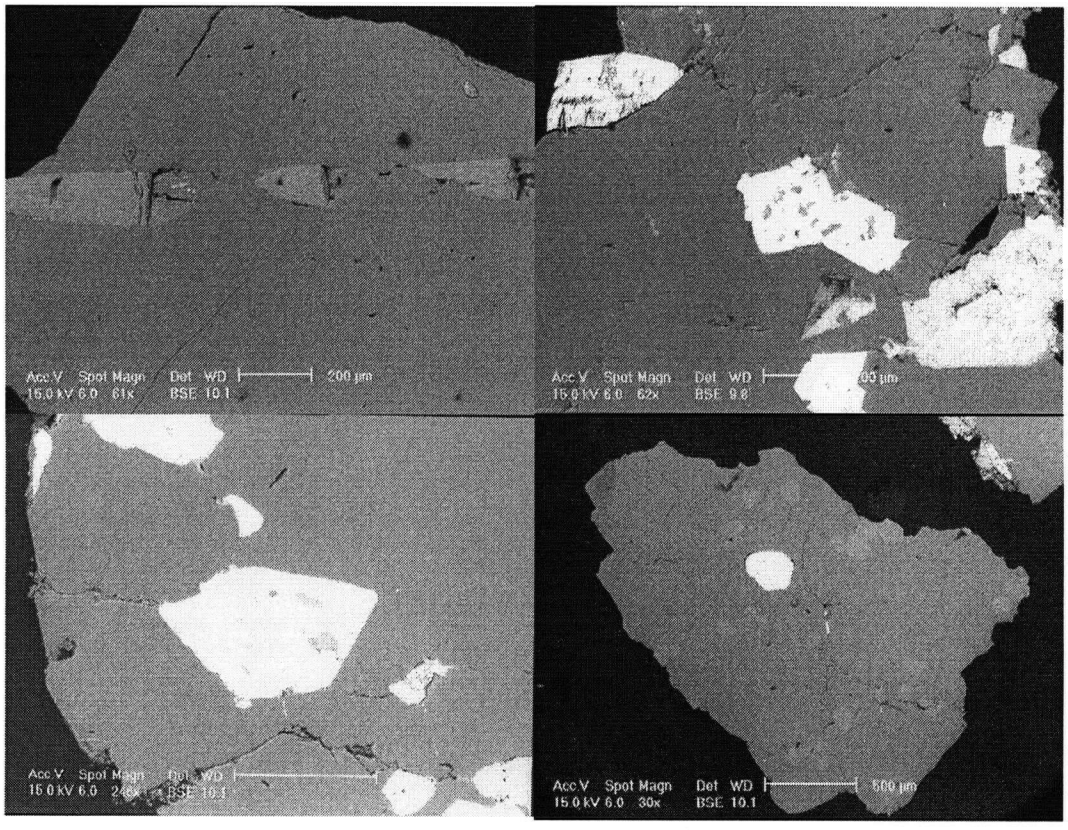

Figure 3.13. Scanning electron microscope back-scatter electron images of beryl (emerald) grains with various inclusions: a) tourmaline; b)scheelite (mid-grey, right edge), calcite, and mica; c) calcite (lighter) with small mica inclusions (darker); d) pyrite (white) and numerous rounded quartz grains.

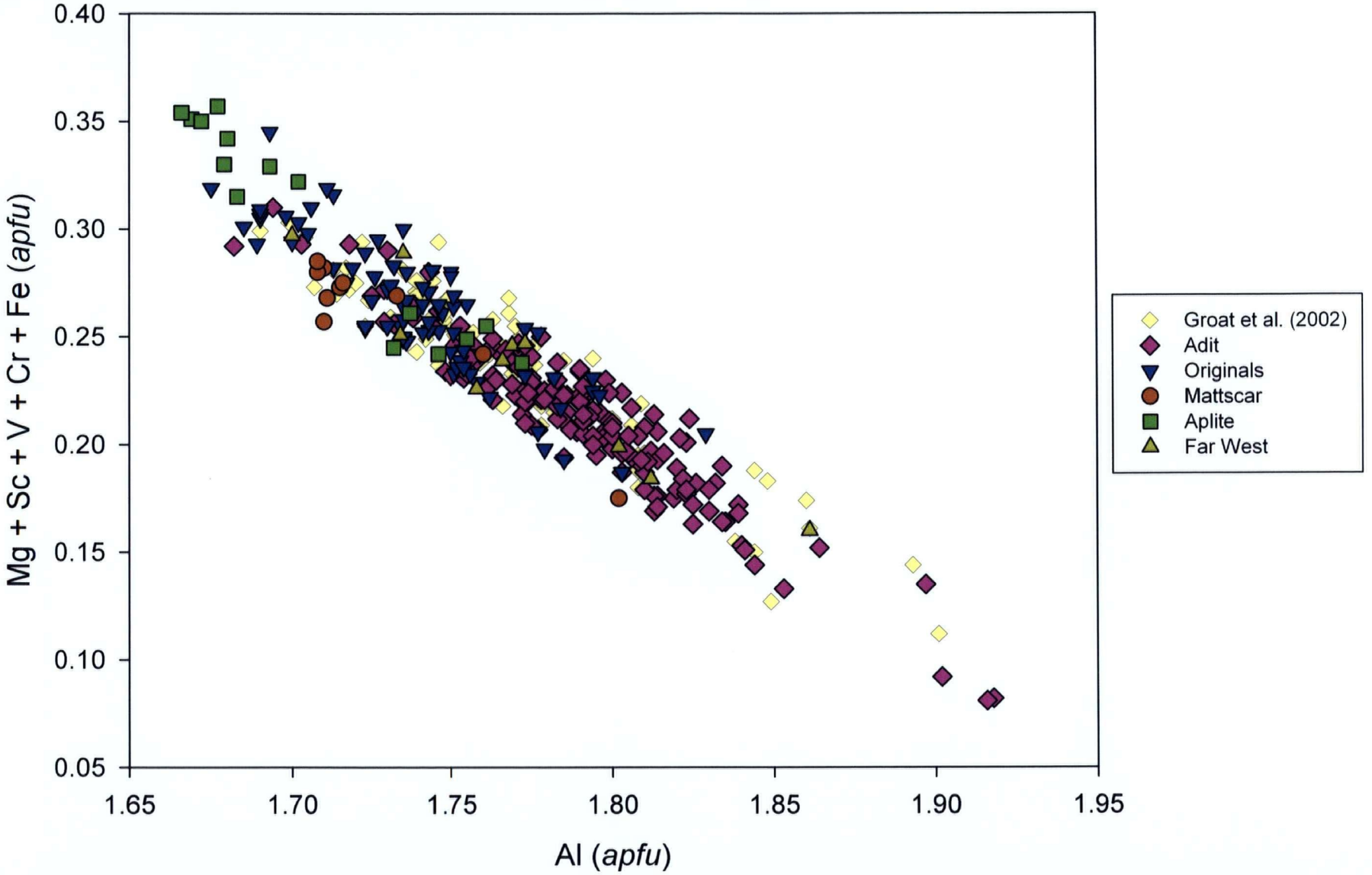

Figure 3.14. Al *versus* the sum of other *Y*-site cations, in atoms per formula unit, for analyses from this study and from Groat et al. (2002).

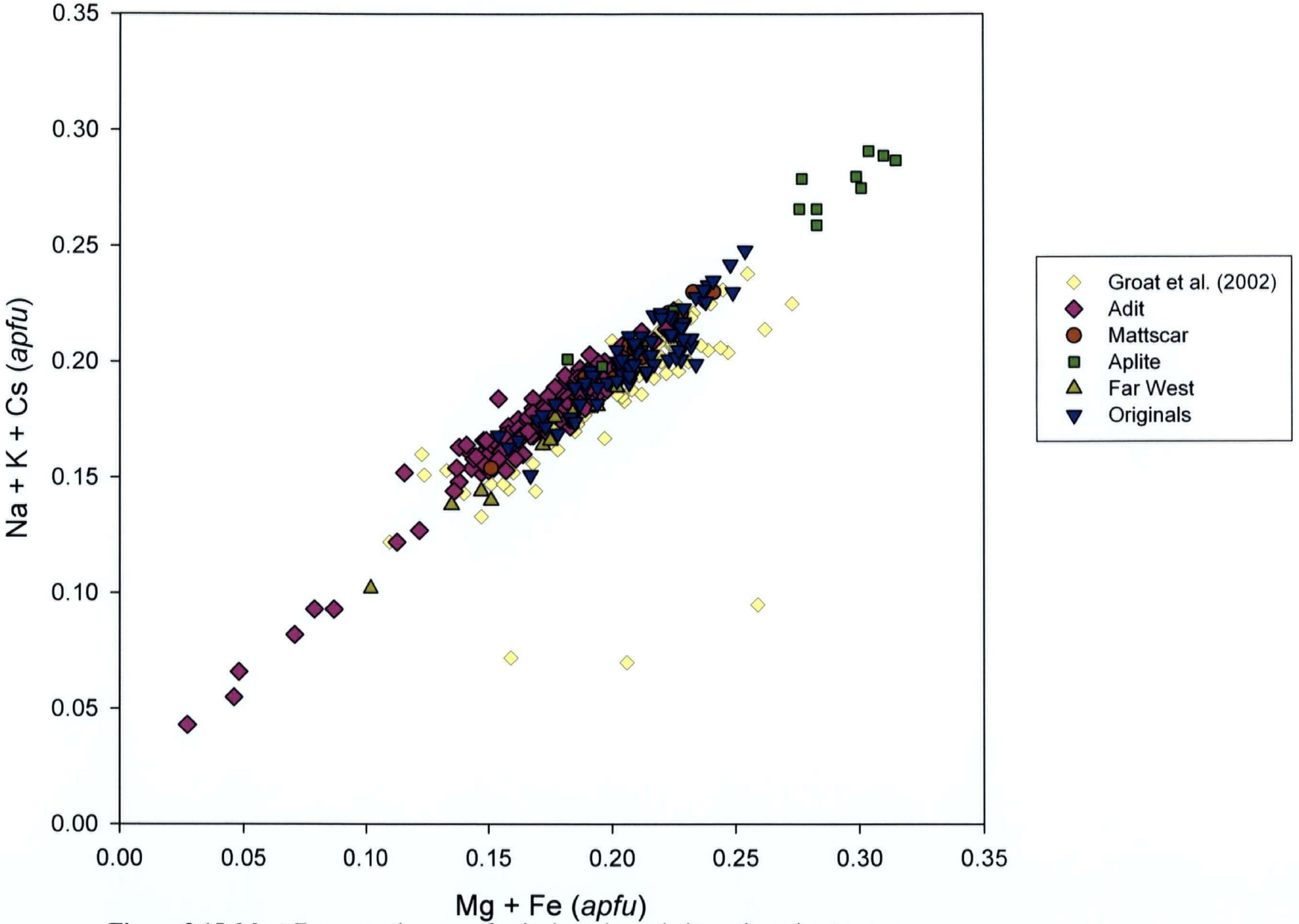

Figure 3.15. Mg + Fe *versus* the sum of univalent channel-site cations, in atoms per formula unit, for analyses from this study and from Groat *et al.* (2002).

3.3.6.2 Tourmaline

Tourmaline is ubiquitous at Tsa da Glisza. It occurs in quartz veins, aplites, and the granite, within alteration envelopes, and between cleavage planes of the host rocks. To help determine the chemistry of the mineralizing fluid, sixteen different rock samples containing tourmaline were studied with a scanning electron microscope, and the tourmaline crystals were analyzed with an electron microprobe. Details of the analytical procedure are presented in Appendix 1 and results can be found in Appendix 4. The tourmaline samples were separated into three groups based on host rock and compositional differences: (1) schist (with or without a quartz vein immediately adjacent); (2) aplite; (3) quartz vein. Average chemical compositions for each group are shown in Table 3.4. The Fe/(Fe + Mg) (*Y* site) and Ca/(Ca + Na) (*X* site) values (Fig. 3.16a) of tourmaline hosted within aplite lie in the middle of the range, and are dravite in composition, whereas tourmaline hosted within quartz segregations within aplite dikes falls toward the more Fe-, Na-dominated end of the range, from dravite to schorl in composition. The tourmaline with the highest Fe/(Fe + Mg) values is from a pegmatitic dike located approximately 100 m from the granite pluton. Schist-hosted tourmaline has a comparatively small range of Fe/(Fe + Mg) variability, and is Mg-rich (as is the schist), but covers a wide range of Ca/(Ca + Na) values, reaching up to uvite , although it is most commonly dravite. Schist-hosted tourmaline has fewer *X*-site vacancies and more Ca than tourmaline in aplite and quartz veins (Fig. 3.16b), likely related to the CaO (5 to 10 wt.%), and Na_2O (maximum 3 wt.%) contents of the chlorite schist (Table 3.2).

Three of the samples from quartz-rich segregations within aplite contain white beryl as well as tourmaline. These tourmalines are more Na- and Fe-rich, and have a higher proportion of *X*-site vacancies, than tourmaline that formed in the aplite hosting these quartz-rich segregations (Fig. 3.16b).

An analysis of the compositions of tourmaline cores and rims showed no compositional differences for schist-related tourmaline. Aplite- and quartz vein-related tourmaline generally shows an increase in Mg and Ca from core to rim (Appendix 4).

When these data are compared with the smaller data set in Groat et al. (2002), a discrepancy is apparent. The "tourmaline zone" and tourmalines within emerald that were analyzed by Groat et al. (2002) fall into the range defined by this study as schist-related, while

Table 3.4. Averaged electron microprobe compositions of tourmaline from the Tsa da Glisza property

	Schist-Related		Aplite-Related		Quartz-related	
	Avg. (97)	StdDev	Avg.(61)	StdDev	Avg.(122)	StdDev
SiO_2	36.36	6.62	35.23	1.098	34.90	2.816
TiO_2	0.43	0.20	0.43	0.306	0.48	0.357
B_2O_3 *	10.51	0.12	10.32	0.111	10.27	0.150
Al_2O_3	30.69	4.05	30.85	1.694	32.21	1.517
Cr_2O_3	0.12	0.10	0.06	0.058	0.01	0.016
MgO	8.93	1.43	7.69	1.753	5.07	2.205
CaO	1.72	1.02	1.14	0.657	0.74	0.532
MnO	0.04	0.04	0.16	0.086	0.24	0.129
FeO	5.26	1.12	6.63	1.595	9.12	2.708
Na_2O	1.81	0.26	2.13	0.263	2.08	0.452
K_2O	0.02	0.01	0.03	0.017	0.22	1.390
H_2O *	3.45	0.25	3.25	0.155	3.19	0.144
F	0.38	0.48	0.66	0.291	0.74	0.289
O=F	-0.16	0.20	-0.28	0.123	-0.31	0.121
Total	99.54	1.90	98.29	0.759	98.95	1.480
Si^{4+}	6.006	0.954	5.931	0.163	5.908	0.462
Ti^{4+}	0.053	0.025	0.055	0.039	0.061	0.046
B^{3+}	3.000	0.000	3.000	0.000	3.000	0.000
Al^{3+}	5.989	0.789	6.123	0.352	6.427	0.300
Cr^{3+}	0.015	0.013	0.008	0.008	0.001	0.002
Mg^{2+}	2.203	0.350	1.926	0.426	1.274	0.544
Ca^{2+}	0.306	0.179	0.204	0.117	0.133	0.095
Mn^{2+}	0.005	0.006	0.023	0.012	0.034	0.019
Fe^{2+}	0.729	0.158	0.935	0.234	1.295	0.400
Na^{+}	0.581	0.084	0.695	0.087	0.683	0.146
K^{+}	0.004	0.003	0.006	0.004	0.048	0.305
H^{+}	3.803	0.254	3.648	0.156	3.606	0.153
F^{-}	0.197	0.254	0.352	0.156	0.394	0.153
O^{2-}	30.962	0.631	30.754	0.169	30.787	0.497
CATSUM	18.891	0.159	18.905	0.085	18.863	0.271
AN SUM	31.160	0.566	31.106	0.089	31.181	0.488

Note: Compositions were recalculated on the basis of 15 (Mg^{2+}, Mn^{2+}, Fe^{2+}, Al^{3+}, Cr^{3+}, Si^{4+}, Ti^{4+}) *apfu*.

*Determined by stoichiometry, assuming 3 B *apfu* and 4 (OH, F,) *apfu*.

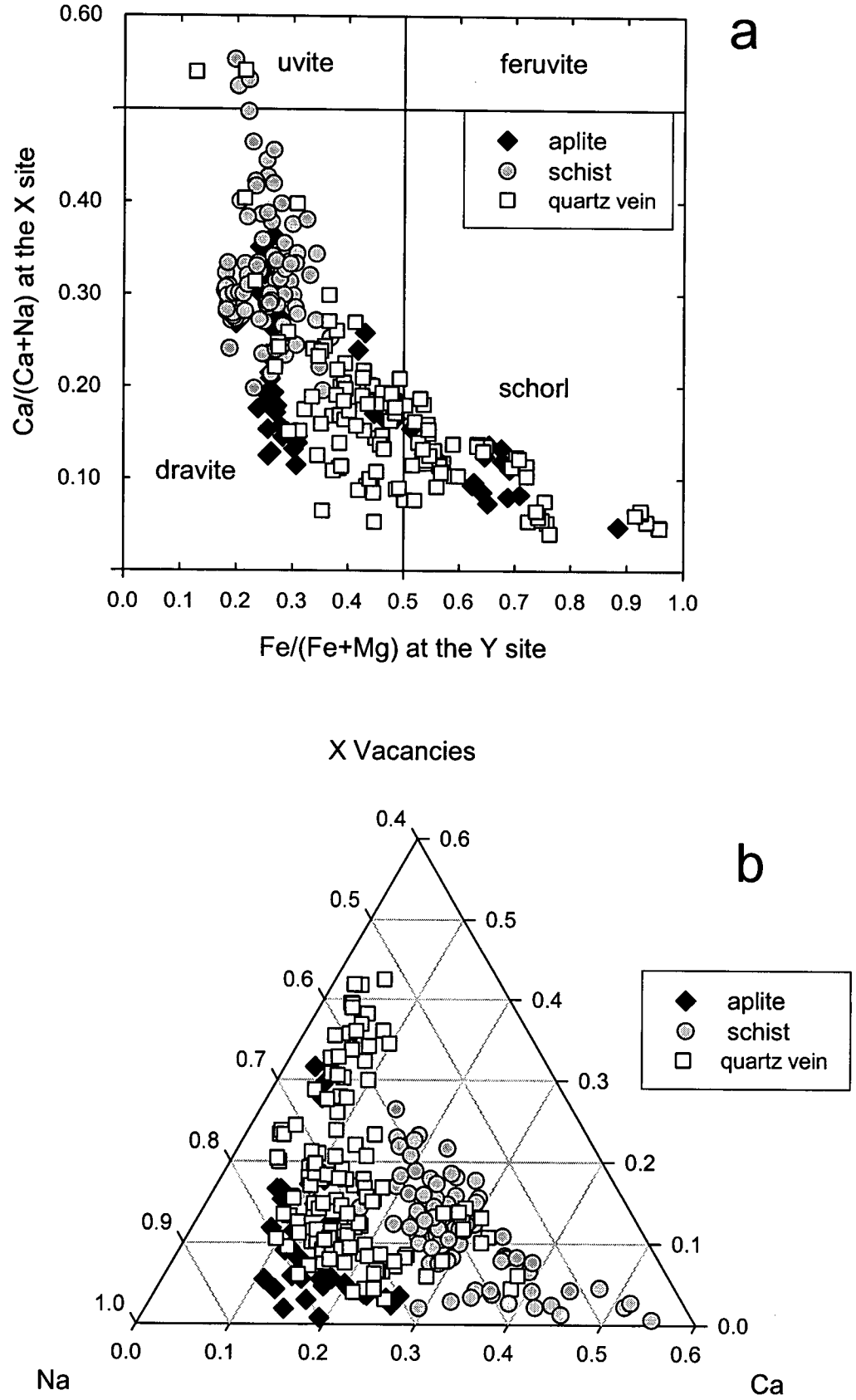

Figure 3.16. **(a)** Diagram of Fe/(Fe + Mg) at the *Y* site *versus* Ca/(Ca + Na) at the *X* site for tourmaline samples from this study. **(b)** Triangular diagram of *X*-site vacancies-Na-Ca for tourmaline samples from this study.

their "host" tourmaline lies well below the cut-off range implied by this study for schist-hosted tourmaline. The difference, however, is largely in semantics. "Tourmaline zone" tourmaline is that which occurs on the edge of a quartz vein, just within the schist. Approximately half of the "schist-hosted" samples from this study were exactly such. The other half were hosted solely within schist, though generally within a metre of a quartz vein or aplite dike. No compositional differences can be distinguished between the two, thus easily reconciling the Groat et al. (2002) tourmaline zone data. Their "host" tourmaline sample, however, does contain more Fe than any of the schist-related samples from this study, and these samples were likely either hosted in a rock type not encountered in this study, or were collected very near an aplite dike. The data collected by Groat et al. (2002) for tourmaline inclusions in emerald directly overlap the schist-related tourmaline compositions from this study.

3.3.7 Stable Isotopes

Oxygen isotope data were obtained from quartz and muscovite mineral separates, and four whole-rock samples of nine different rock samples, to characterize the fluid-rock interaction during mineralization. If the fluids have an oxygen isotopic composition different from that of the host schist, then the extent of fluid infiltration around a vein can be traced, and the amount of chemical mixing inferred. The results are reported in Table 3.5, and details of the analytical method are in Appendix 1.

Four whole-rock samples of the host schist were analyzed for oxygen isotopes. The entire schist package was chloritized, so we define altered schist as the brown-weathering, jarosite-tourmaline-lepidocrosite-scheelite-fluorite rock that locally occurs adjacent to mineralized quartz veins. Two samples were considered unaltered. Although there is no significant difference in the isotopic signature of the altered and unaltered schist samples, it is of note that the altered schist sample with the highest $\delta^{18}O$ value was obtained directly adjacent to an emerald-bearing vein. The unaltered schist sample with the lowest $\delta^{18}O$ was taken from an area with no noticeable veining. O'Neil & Chappell (1977) suggested that where chloritic alteration takes place in the presence of a fluid that is in near oxygen isotopic equilibrium with a cooling pluton, the lower temperature chloritization process results in an increased $\delta^{18}O$ value for the altered rock.

Quartz separates from five intrusive samples returned two groups of results. Three samples have $\delta^{18}O$ values near 13.7‰, whereas two samples returned values of approximately 11.6‰

Table 3.5. Stable isotope data, Tsa da Glisza property, Yukon Territory.

Sample	Mineral	$d^{18}O$ ($^0/_{00}$, SMOW)	dD ($^0/_{00}$, SMOW)	H_2O channel (wt. %)
aplite near mineralized veins	musc	10.4	-99	5
granite, likely roof	musc	10.8	-90	5
unaltered schist	whole rock	8.0		
altered schist, near white-beryl-bearing aplite	whole rock	8.9		
unaltered schist	whole rock	9.3		
altered schist, near emerald-bearing quartz vein	whole rock	9.8		
emerald-bearing quartz vein	quartz	11.7		
aplite near mineralized veins	quartz	11.6		
granite, likely roof	quartz	13.6		
quartz-tourmaline vein	quartz	13.7		
white-beryl-bearing aplite	quartz	13.8		

(Table 3.5). The two samples with low values are from an emerald-bearing quartz vein, and a large aplitic body quite near a mineralized zone of veining. The higher $\delta^{18}O$ samples include a sample of the granite, a quartz vein, and an aplite that contains white beryl.

The results indicate that the extent of fluid interaction with the schist can be assessed by oxygen isotopic composition of the vein selvage and surrounding rock. Further studies could test the usefulness of stable isotopes as a tool for emerald exploration, as evidence for fluid interaction increases the likelihood that a vein contains emerald, rather than colourless beryl.

Muscovite separates from two intrusive samples were analyzed for both hydrogen and oxygen isotopes. Both samples are highly depleted in D and have slightly enriched $\delta^{18}O$ values compared to SMOW. Based on the $\delta^{18}O_{qtz\text{-}musc}$ value of 2.8 for the granite, the quartz-muscovite geothermometer of Matthews & Schliestedt (1984) yields temperature of formation of approximately 470 °C. On the basis of fluid-inclusion isochoric data (Marshall et al., 2003), our temperature obtained for the granite corresponds to pressures of approximately 1.5 to 2.3 kbar, and inferred depths of 5.7 to 8.7 km. These new results correspond well with previous quartz-tourmaline geothermometer (Kotzer et al., 1993) results for a Regald Ridge quartz vein sample, which yielded temperatures ranging from 365 to 498 °C, and inferred depths of 3 to 7.7 km (Marshall et al., 2003).

3.4 DISCUSSION

3.4.1 Overview of Genetic Models for Emerald Deposits

Emerald deposits may be related to pegmatitic, magmatic-hydrothermal, or non-magmatic processes. A recent review of Be mineralogy, petrology, and geochemistry (Grew, 2002) compiled and delineated the various genetic models proposed for emerald deposits worldwide (e.g., Cerny, 2002; Franz and Morteani, 2002; Barton and Young, 2002) . Due to discrepancies in nomenclature in the literature, this discussion uses the terms outlined by Barton and Young (2002) in their review.

Emerald occurring in pegmatite is usually associated with mid-level pegmatites of the rare-element class (Cerny, 2002). There is a continuum from Be-enriched magmas to pegmatites to hydrothermal vein deposits (London and Evensen, 2002). Most magmas which produce Be-rich residual fluids have low CaO and high F contents.

Metasomatism driven by granitic magmatism, where pegmatites or quartz-muscovite-feldspar veins intrude ultramafic or mafic Cr-bearing host rocks, is invoked to explain most emerald deposits (Kazmi and Snee, 1989; Sinkankas, 1989). Quartz-poor and biotite-rich contact-parallel metasomatic zones usually accompany the emerald-bearing dikes and veins (Barton and Young, 2002). Related intrusive rocks are usually peraluminous biotite and biotite-muscovite granites with mineralogically simple veins, although some deposits are associated with mineralogically complex pegmatites. Emerald occurs within both vein alteration envelopes and within the veins (dominantly quartz, muscovite, and plagioclase) themselves, which commonly show evidence of reaction with the host mafic or ultramafic rocks. Although metasomatic desilicification of pegmatites is commonly associated with emerald mineralization, it is often difficult to determine the timing of metasomatism relative to emplacement, and also to determine whether the altering fluids were dominantly hydrothermal or magmatic (Barton and Young, 2002).

Many of the world-renowned emerald deposits are hosted within ultramafic rocks, and show defined multiple metasomatic zones, known as "blackwall" assemblages (e.g., Franqueira, Spain; Reft River, Russia; Menzies, Australia; Habachtal, Austria; Carnaiba, Brazil). Emerald usually occurs in the innermost biotite-rich zone, and is commonly associated with fluorite and F-bearing phlogopite, a coincidence which suggests that the Mg-Ca-rich host rocks triggered F precipitation, in turn precipitating Ba and Al as emerald (e.g., Soboleva et al., 1972).

Mafic-hosted emerald-bearing veins do not show multiple metasomatic zones on their selvages, but are commonly enveloped by a single biotite-rich layer, likely due to the higher Si and Ca, and lower Mg contents of mafic relative to ultramafic rocks (e.g., Khaltaro, Pakistan; Laurs et al., 1996) (Barton and Young, 2002). At Khaltaro, the formation of fluorite and biotite released the Cr and Fe necessary to form emerald at the contact of albite-quartz-muscovite veins with amphibolite (Laurs et al., 1996).

Non-magmatic origins are established for some emerald deposits. These are currently split into two groups: brine-related and metamorphic (schist-type, or shear zone) occurrences. Emerald deposits in Columbia are basinal brine-related, occurring in tension gash carbonate-quartz-albite-pyrite veins within Be-rich basinal sedimentary rocks. Franz and Morteani (2002) classify all emerald deposits formed in the context of metamorphism, as "schist-type" deposits. They argue that emerald in these deposits, being generally less than 2 cm in length, the typical size of metamorphic porphyroblasts, has grown at the contact between metamorphosed Cr-rich mafic to ultramafic rocks and Be-rich K-N-Al quartzofeldspathic rocks (including meta-

pegmatites and aplites), during post-intrusive deformation and metamorphism that locally redistributed and reprecipitated Be. Franz and Morteani (2002) suggest that the intrusion of small igneous bodies cannot provide the necessary large amounts of fluid for the extensive alteration envelopes commonly associated with mineralized bodies, whereas metasomatic reactions can easily explain the envelopes. This hydrothermal-metasomatic model is referred to by Barton and Young (2002) as "shear-zone-related".

The formation of shear zone-related emerald is still under considerable debate. The importance of "blackwall" zoning and regional metamorphism in emerald formation at the Habachtal, Austria and Gravelotte, South Africa deposits was identified by Grundmann and Morteani (1989), Nwe and Grundmann (1990) and Nwe and Morteani (1993). Their model invokes a regional tectonic event to redistribute Be present in K-Na-Al silicate rocks at their intrusive or tectonic contact with ultramafic Cr- and Mg-rich rocks. Beryl, phenakite, and chrysoberyl precipitate at this contact, within multiple metasomatic "blackwall" zones. Although their occurrence within biotite-rich zones in metamorphosed mafic and ultramafic rocks appears similar to many igneous-related deposits, shear-zone emeralds, grown during regional metamorphism, usually have textures demonstrating their synkinematic overgrowths of other minerals (Grundmann and Morteani, 1989). These emeralds also have higher Fe and Mg than emerald from other deposit types (Barton and Young, 2002). CO_2-bearing inclusions and non-magmatic oxygen isotope ratios are common for these moderate-salinity systems with no associated igneous rocks, that form deposits in Austria, Afghanistan, Pakistan, and Brazil (Kazmi and Snee, 1989; Giuliani et al., 1990).

The distinction between magmatic-hydrothermal, and non-magmatic (hydrothermal-metasomatic, shear zone) origins is difficult in deposits where both igneous bodies and evidence for regional metamorphism occur (e.g. Franqueira, Spain; Martin-Izard et al., 1995, Franz et al., 1996 and Gravelotte, South Africa; Nwe and Morteani, 1993). The Franqueira deposit contains emerald after phenakite, and emerald after chrysoberyl, within phlogopite-tourmaline alteration zones on the edge of quartz-albite-muscovite-K-feldspar veins within dunite. The emerald overgrowths, and multiple zones of alteration within an ultramafic rocks, allow for a shear-zone metamorphic interpretation for emerald formation, but the evidence does not necessarily preclude coeval magma emplacement. Similar overgrowth of emerald on phenakite and chrysoberyl during deformation could occur with synkinematic intrusion accompanied by progressive growth of metasomatic zones (Barton and Young, 2002). Similarly, the Gravelotte deposit in South Africa contains beryl after phenakite within biotite-rich alteration zones

(Grundmann and Morteani, 1989; Nwe and Morteani, 1993; Robb and Robb, 1986). Non-gem beryl occurs within both foliated and unfoliated albite-quartz-muscovite veins intruded into mafic host rocks. Franz and Morteani (2002) suggest that with detailed investigation of structural relationships between deformation features in the metamorphic rocks, beryl growth and intrusion, many deposits currently classified as magmatic-hydrothermal will fit the shear zone-related model.

3.4.2 Evidence Bearing on the Genesis of Emerald at Tsa da Glisza

Emerald at Tsa da Glisza is associated with relatively small aplite dikes and quartz-tourmaline veins that could result from either (1) local bimetasomatic exchange by intergranular diffusion during Cretaceous regional metamorphism (shear zone-related, e.g., Habachtal, Austria) or (2) infiltration possibly paired with diffusion metasomatism driven by a shorter-lived Cretaceous magmatic-hydrothermal event (magmatic-hydrothermal, e.g., Khaltaro, Pakistan) (Barton and Young, 2002).

Results from research on the Tsa da Glisza emerald occurrenceprovide the basis for a model for the genesis of emerald mineralization in the area. Critical factors in this model include the extent of metamorphic processes on the emerald formation, the relative timing of events and mineral precipitation, and the fluid chemistry. The results are summarised below.

The Cretaceous tectonic setting of the Tsa da Glisza emerald deposit fits either a regional metamorphism-driven genetic model, or a magmatic-hydrothermal model. The Finlayson Lake district was subjected to a period of deformation associated with north-south movement along the North River fault to accommodate uplift due to intrusion of several granitic bodies. The timing of movement along the North River Fault is not well constrained, but is broadly Early Cretaceous. If this event occurred during or after the emplacement of the Tsa da Glisza granitic pluton, it could have either assisted in Be-bearing fluid mobilisation, or completely remobilised Be (by metasomatism) from Be-bearing, or rock-forming minerals within aplite or pegmatite dikes. The intrusion of the granitic pluton nearest Tsa da Glisza, however, provides the heat and fluids implicit in a magmatic-hydrothermal model. Emerald deposits are most commonly associated with peraluminous biotite-muscovite granites, as they provide the elevated Al_2O_3 activities required to form beryl (Barton and Young, 2002). Although it is conceivable that Be-minerals other than beryl were formed in aplite and pegmatite dikes, and were the source for Be

later remobilised metasomatically, no other Be minerals (e.g., phenakite, chrysoberyl) have been identified at Tsa da Glisza.

The host unit for emerald mineralization, a permeable, but Cr-rich chlorite schist of boninite composition (Fire Lake Formation suite 5 of Piercey et al., 2004), is fairly rare in the Finlayson Lake district. Chloritization (likely a mid-Paleozoic event) and development of crenulation fabric (likely Cretaceous) led to increased permeability to fluids. Most shear zone-related emerald deposits occur in ultramafic rocks, where Cr is very abundant. While the host rock at Tsa da Glisza is mafic in composition, the same metasomatic reactions advocated in the shear zone model could apply. However, if shear zone metasomatism was the dominant process responsible for forming emerald, one would expect to see metasomatic zones and emerald associated with the aplite-pegmatite dikes that intrude the ultramafic rocks. No such alteration is observed.

Where beryl and emerald are found within quartz-rich segregations within aplite, beryl may form from late-crystallizing fluids trapped within the aplite. These residual fluids would be expected to be rich in Be. Alternatively, these occurrences may indicate that some Be was sourced from plagioclase, which, when altered by sodium-rich fluids to a more albitic composition, releases the minor amount of Be that was originally incorporated into the plagioclase structure (cf. Charoy, 1999), or from other Be minerals crystallized within the aplite. The albite-quartz vein containing colourless beryl could represent an intermediate phase of the process by which Be-rich fluids continued out from the aplite and pegmatite dikes to form mineralized quartz veins.

Emerald at Tsa da Glisza is found not only on the altered vein selvages, which could be interpreted as solely metasomatic, but also within quartz veins adjacent to weakly altered or unaltered host rock. The shear zone model cannot account for such mineralization. However, emerald is also found within linear zones of highly-altered schist, which are most easily explained by shear zone reactions since they contain no quartz. These zones do have high concentrations of typically magmatic elements such as W and Bi, which require that their formation involved some magmatic fluid input.

Structural evidence at Tsa da Glisza points to a complex structural regime, with multiple phases of deformation, and re-orientations of the shear systems. Many of the quartz veins appear to have been emplaced within a deformational environment, and strongly-deformed zones are locally apparent in the aplite dikes. The schist is metamorphosed to upper greenschist facies, and

shows a crenulation cleavage. The veins and aplites were intruded into a brittle-ductile deformational regime.

Ar-Ar dating of biotite/phlogopite and muscovite gave ages within the error of U-Pb ages of zircon and monazite from the granite pluton and aplite dikes. This implies that the local metamorphic event was directly related to the intrusion of the granite, and high temperature conditions did not persist long past the granite emplacement event. Any later regional metamorphic event with temperatures high enough to remobilise Be would have reset the mica Ar-Ar ratios. This is clear evidence that a magmatic-hydrothermal model is most applicable for emerald mineralization at Tsa da Glisza. Furthermore, younger regional metamorphism would likely have produced a foliation or other evidence for deformation within the granitic rocks; however, the granite is at most weakly foliated, and some aplite dikes and quartz veins show no evidence of deformation.

The broad alteration envelopes surrounding the quartz-tourmaline veins are not likely to have formed solely from magmatic fluids, and indicate a significant involvement of hydrothermal fluids, or a sustained period of contact metasomatic reaction (e.g., Franz and Morteani, 2002). The geochemistry of the mineralized veins, their alteration envelopes, and soils in the area, however, is evidence for a magmatic-dominated fluid system. Beryllium is strongly correlated with a number of typically magmatic elements: W, Bi, Li, Sn, F, B. Any remobilisation of Be from crystallized aplite and pegmatite would therefore have involved remobilisation of all of these elements. It seems more likely that a dominantly magmatic fluid intruded the mafic host rocks in a single event, crystallizing aplite, rare pegmatite, and abundant quartz veins as it mixed with hydrothermal schist-equilibrated fluids.

The emeralds are not overgrowths on other Be minerals such as phenakite or chrysoberyl, and they do not contain anomalously high amounts of Fe or Mg, both of which are typical for shear zone deposits. Inclusions of tourmaline, phlogopite, and scheelite within emerald confirm that beryl formed synchronous with, or later than, these minerals. The phlogopite inclusions do not form a preferential orientation within emerald. The emeralds do contain fluid inclusion trails along healed fractures, which attest to the fact that they formed during deformation. This deformation is easily explained by the structural regime acting on rocks at the margin of a cooling pluton. The emeralds are not necessarily foliation-parallel where they occur in the vein selvages, but more often grow in "pockets" along the vein wall.

The geochemistry of tourmaline at the Tsa da Glisza occurrence suggests that there was significant interaction of the magmatic fluids with the host schist. Mg and Ca content (both high

in the schist geochemistry) increases towards the rims of tourmaline hosted within quartz veins and aplites. This implies that fluid interaction with the schist draws tourmaline toward a more Mg- and Ca-rich composition, and that emerald at Tsa da Glisza is more likely to be associated with dravite and uvite, than with schorl. Inclusions of tourmaline within emerald also have a high Mg and Ca content. This implies that emerald crystallized after tourmaline which crystallized from fluids that had interacted with the host schist. This involvement of fluids that had some chemical interaction with the host schist is very important for the introduction of Cr into the fluids, allowing for green beryl to crystallize, and may also suggest that these fluids provided some sort of impetus for either beryl or tourmaline crystallization.

Stable isotope ratios indicate that the extent of fluid interaction with the schist can be assessed by oxygen isotopic composition of the vein selvage and surrounding rock. Mineralized veins had a lower ratio than non-mineralized veins, attesting to their mixing with schist-reacted fluids. An analysis of white-beryl-bearing aplite, which shows no isotopic evidence for buffering by the host schist, supports our hypothesis that the Cr necessary for producing green beryl is provided by the schist, and enters the fluids through interaction with the schist.

On the weight of all of the lines of evidence listed above we suggest that the most reasonable interpretation is that emerald formation at Tsa da Glisza was associated with the interaction of magmatic and hydrothermal fluids within the actively-deforming roof pendant of a peraluminous granite. The mineralizing event was mainly syn- to late- tectonic, coinciding with the waning stages of granite emplacement, and peak metamorphic upper greenschist conditions. The Tsa da Glisza deposit therefore fits best the magmatic-hydrothermal, strongly peraluminous W-Mo (biotite-muscovite) granite occurrence type defined by Barton and Young (2002).

3.4.3 Genetic Model for Tsa da Glisza Emerald Mineralization

The genetic model we propose for emerald mineralization at Tsa da Glisza based on observations summarized above, is shown in schematic form in Figure 3.17. Beryllium, with other magmatic elements, including B, W, Li, Bi, and F, moved out from the granite within highly evolved magmatic fluids. Beryllium is increasingly mobile in fluids containing B and P, and may complex with F, Cl, and hydroxyl ions. The high F contents within mineralized vein selvages (likely within phlogopite as well as small fluorite crystals) suggests that Be most likely travelled as a fluoride or possibly hydroxide complex. Aplite and pegmatite dikes formed with

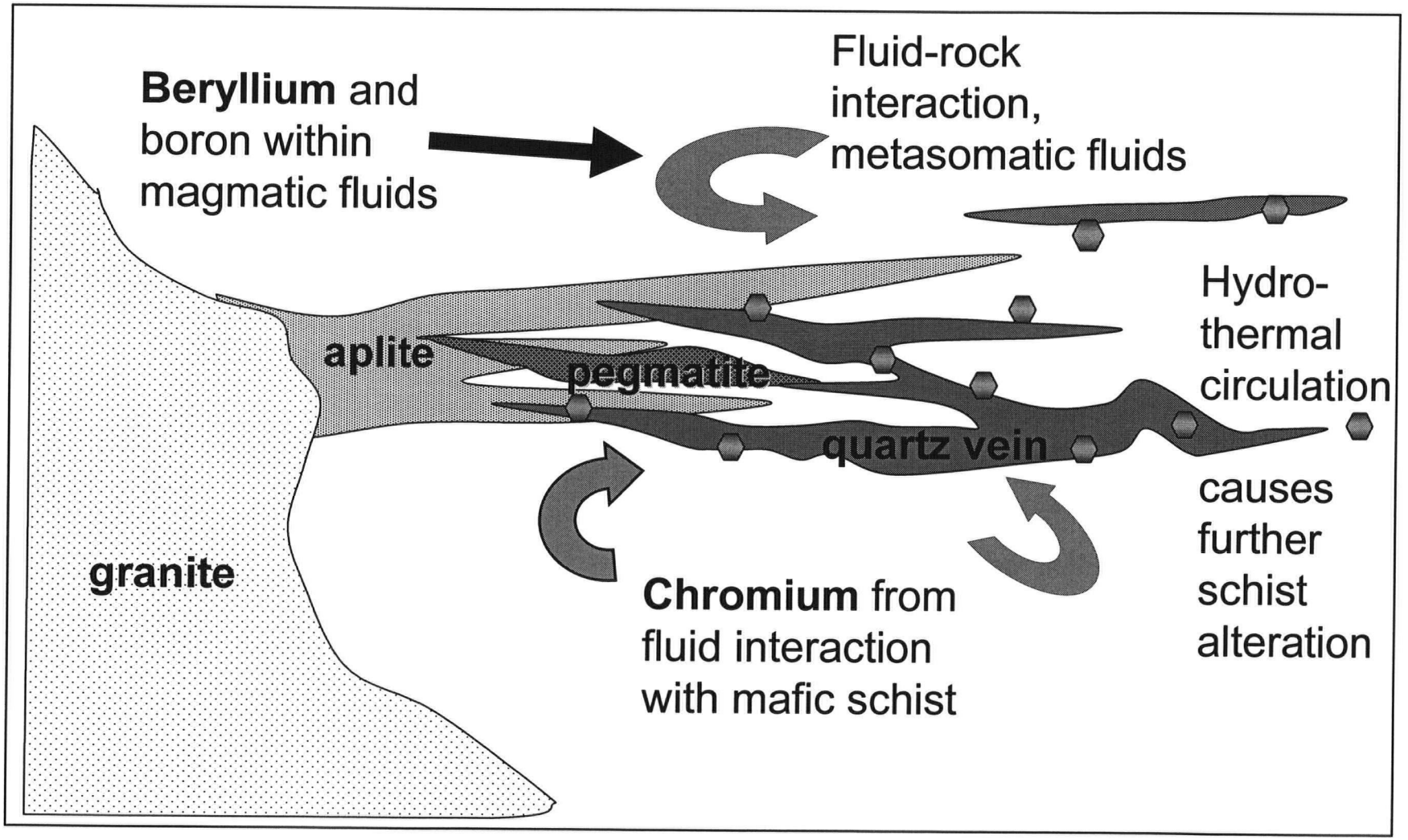

Figure 3.17. Schematic of proposed genetic model for emerald mineralization at Tsa da Glisza. The mineralizing fluids are a mixture of both magmatic-hydrothermal and metasomatic fluids. Mineralized veins occur within, adjacent to, and distal from aplite and pegmatite dikes.

the onset of cooling. Although the dikes locally contain Be concentrations of up to 100 ppm, Be was mostly not incorporated into the aplite-forming minerals, and continued to move through the host rocks, within dominantly magmatic fluids.

A hydrothermal fluid cell was initiated in the host rocks after emplacement of the granite. These fluids percolated through the chlorite schist, and leached Cr from the mafic groundmass. Geochemical transects from unaltered chlorite schist through altered schist, to quartz-tourmaline veins give no indication of how far Cr may have travelled within these fluids (Neufeld et al., 2004). Cr may have been directly sourced from host rock within centimetres of quartz-tourmaline veins through contact metasomatism, or may have travelled some distance along hydrothermal fluid pathways.

Beryl crystallization may have been triggered by several factors: (1) mixing with cooler hydrothermal fluids; (2) crystallization of tourmaline, which would have removed B and possibly some Li and F from the fluids and/or lowered the aluminium activity of the fluids, all of which would have resulted in a reduced solubility of Be in the fluid (cf. London and Evensen, 2002); (3) an increase in the Ca content of the fluids due to interaction with the host schist; (4) an increase in host-rock permeability or porosity due to either rock type differences or fracture propagation related to deformation accommodating cooling of the granite pluton below; (5) precipitation of fluorite within the vein selvage, removing F (ligand) from the fluids; (6) or simply due to decreases in pressure and/or temperature. Likely all of these factors played some role in initiating beryl precipitation, particularly where mineralization is contained within highly altered vein selvages. Where emerald occurs solely within the quartz veins, factors (3) and (5) above are probably not involved, and where emerald occurs within linear zones of alteration away from quartz-tourmaline veins, low silica activity may also be a factor in prompting precipitation of beryl (London and Evensen, 2002).

3.5 CONCLUSIONS

The new descriptive model for the emerald mineralization at Tsa da Glisza, and the genetic model that derives from it, are currently being used to develop a series of criteria to constrain exploration throughout the northern Canadian Cordillera and perhaps elsewhere in the world. The Tsa da Glisza deposit is unique in that it involves processes from both magmatic-hydrothermal, and shear zone established models. While the mineralizing fluids were dominantly

magmatic, the deformational environment acting on the mafic schist host rocks allowed for increased fluid permeation of the host and consequent increased reaction to source Cr, causing an extensive mineralized vein and alteration assemblage system.

CHAPTER 4.

[3]The Tsa da Glisza (Regal Ridge) emerald occurrence, Finlayson Lake district (105G/7), Yukon: New results, and implications for continued regional exploration.

4.1 INTRODUCTION

The Tsa da Glisza (previously known as Regal Ridge) emerald occurrence is centered at 61°16.6' N latitude, 133°5.5' W longitude on NTS map sheet 105G/7, in the Finlayson Lake district within the Pelly Mountains of south-eastern Yukon (Fig. 4.1). Emerald is an extremely valuable gemstone, and is rare because the required elements Be and Cr (with or without V) are geochemically incompatible, and therefore are rarely found together in environments in which beryl is stable. The Tsa da Glisza occurrence hosts the only known Cr-bearing emerald in the Canadian Cordillera. The definition of "emerald" is still under considerable debate (e.g., Schwartz and Schmetzer, 2002). In this paper, we define emerald as bright green, clear, gem-quality beryl, as distinct from both opaque beryl ranging in colour from white through dark green, and clear beryl that is less than bright green.

This paper compiles results from both field and laboratory research on the Tsa da Glisza emerald occurrence since 2003, interprets the results to develop a genetic model, and outlines an updated exploration model to develop targets for emerald mineralization similar to that found at Tsa da Glisza.

4.2 REGIONAL GEOLOGY

The Tsa da Glisza study area is located in the Finlayson Lake district of the Yukon (Fig. 4.1). The area was mapped most recently by Murphy (1997), Murphy and Piercey (1999),

---

[3] A version of this chapter has been submitted for publication. Neufeld, H.L.D., Mortensen, J.K., and Groat, L.A., 2004. The Tsa da Glisza (Regal Ridge) emerald occurrence, Finlayson Lake district (105G/7), Yukon: New results, and implications for continued regional exploration. Submitted to: Yukon Exploration and Geology 2004, D.S. Emond and L.L. Lewis (eds.), Yukon Geological Survey.

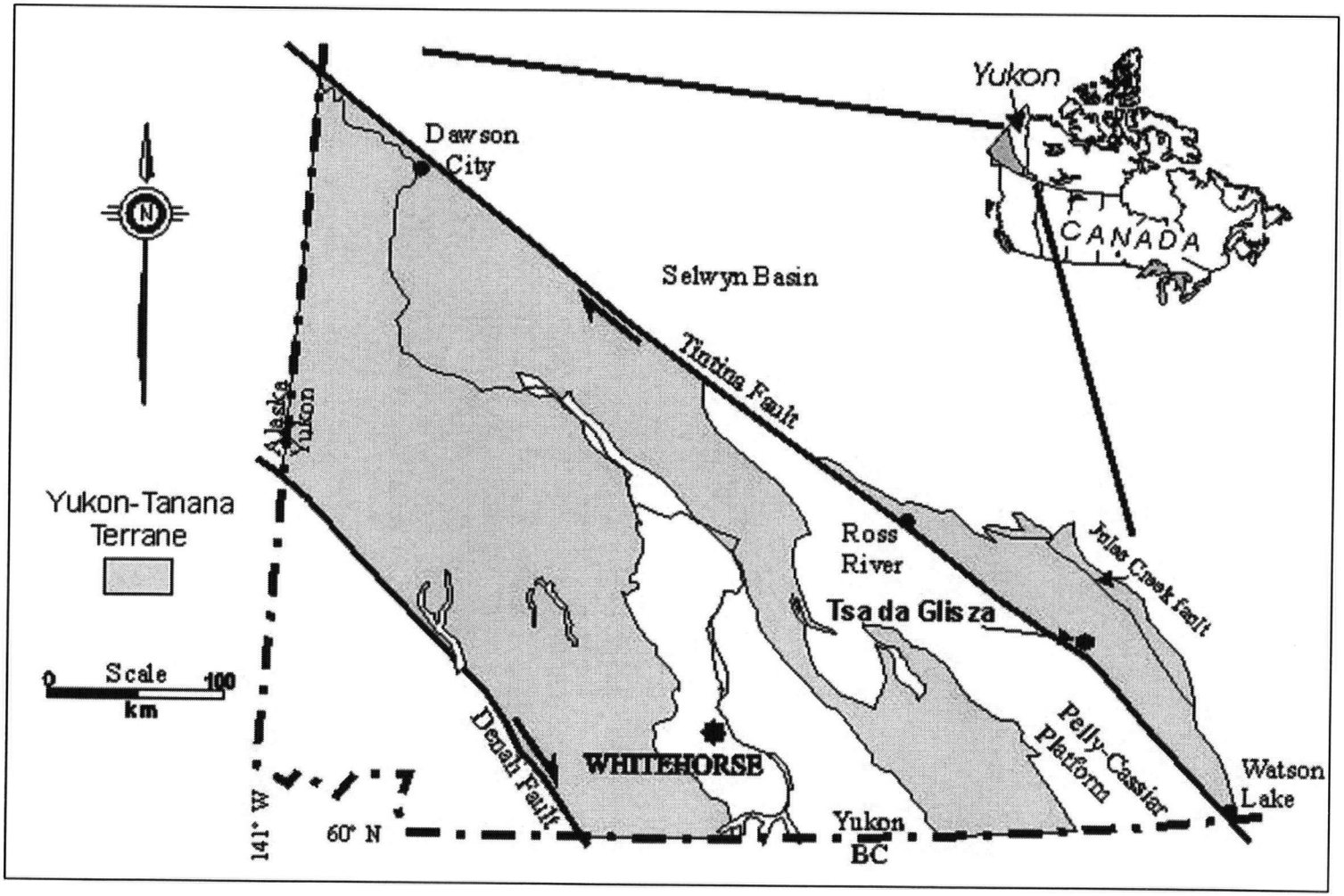

Figure 4.1. Location map of the Tsa da Glisza emerald occurrence, Yukon Territory, Canada.

Murphy et al. (2001), and Murphy et al. (2004). The geologic setting of the region was described in detail by Murphy (2004), and Murphy et al. 2002. Neufeld et al. (2004) discussed the geological setting of the Tsa da Glisza emerald occurrence in some detail, and in this paper we provide a brief review of the lithologies that are present within the immediate vicinity of the Tsa da Glisza property and highlight recent changes in that interpretation.

The Finlayson Lake district consists of rocks of the Yukon-Tanana Terrane, which is regionally bounded to the west by the Tintina Fault, and to the east by the Jules Creek Fault (Fig. 4.1; Murphy, 2004). The structurally deepest rocks are contained within the Big Campbell thrust sheet, which is composed of the Upper Devonian Grass Lakes group, and the Lower Mississippian Wolverine Lake group. Both of these groups have associated metaplutonic rocks. The overlying Money Creek and Cleaver Lake thrust sheets occur further south in the Finlayson Lake district. The Tsa da Glisza occurrence is hosted within the Grass Lakes group, which consists of mafic and felsic metavolcanic rocks and dark clastic rocks of the Fire Lake, Kudz Ze Kayah, and Wind Lake formations. The Fire Lake Formation is a mafic metavolcanic package composed mainly of chloritic phyllite, and is spatially associated with mafic and ultramafic plutonic rocks (Murphy 2004, Piercey et al., 2004). The Kudz Ze Kayah Formation stratigraphically overlies the Fire Lake Formation and consists of carbonaceous phyllite and schist, felsic metavolcanic rocks, and rare quartzofeldspathic metaclastic rocks (Murphy, 2004). The rocks in the Finlayson Lake district are intruded by several *ca.* 112 to 110 Ma granitic bodies of the Cassiar-Anvil plutonic suite (Mortensen, unpublished data). The intrusions are syn- to post-kinematic with respect to the main Cretaceous deformation in the area.

A recent structural interpretation of the Finlayson Lake region (Murphy, 2004) suggests that the Finlayson Lake district experienced a period of strong deformation during the Cretaceous. As the numerous felsic plutons in the region were emplaced, movement along the east-west trending North River normal fault was initiated to accommodate uplift and cooling of rocks in the footwall of the fault. Movement of the hanging wall of the fault was broadly north to south. Rock units in the footwall have mid-Cretaceous Ar-Ar cooling ages, and were ductily deformed prior to and during the emplacement of mid-Cretaceous granite plutons. Tsa da Glisza occurs within the footwall of this fault, within 10 km of the present-day fault trace. The Tintina Fault lies 14 km southwest of the Tsa da Glisza property (Fig. 4.1). Early Tertiary volcanic rocks occur adjacent to the Tintina Fault, and faults and porphyritic dikes likely related to Tertiary movement along the Tintina occur throughout the Finlayson Lake district (Jackson et al., 1986).

4.3 PROPERTY GEOLOGY

Neufeld et al. (2004) described the geology associated with mineralization at the Summit Zone (Regal Ridge proper). This area is underlain by rocks of the Fire Lake Formation, as well as Cretaceous and Eocene intrusive rocks. A two-week mapping program conducted in July 2004 covered the entire claim block, and resulted in a 1:10,000 scale geologic map (Fig. 4.2). A brief description of the rock units is given below, along with some new observations. Rock unit nomenclature is from YGS mapping (Murphy et al., 2001).

The Tsa da Glisza property is mainly underlain by rocks of the Fire Lake Formation, a suite of Devonian mafic metavolcanic rocks and associated mafic and ultramafic plutonic rocks. The emerald occurrence is mainly hosted within the Fire Lake mafic metavolcanic unit (unit DF). This rock unit was studied extensively by Piercey (1999, 2000, 2004; Murphy and Piercey 2000). It occurs as dark- to medium-green plagioclase-chlorite schist to phyllite, with common biotite and actinolite porphyroblasts. Greenschist facies metamorphism altered most primary mafic minerals to chlorite and actinolite. The groundmass consists mainly of quartz, chlorite, and actinolite with less abundant muscovite, biotite, and rare carbonate. At Tsa Da Glisza, the composition of the chlorite schist is equivalent to that of high-calcium-bearing boninite, a composition which is geochemically distinct from other mafic metavolcanics within the Fire Lake Formation by high MgO, intermediate SiO_2, and anomalous Cr, Ni, Co, and Sc (Piercey et al., 2004). Chloritization likely occurred prior to the Cretaceous deformation event, during which some of the chlorite schist was altered to jarosite- and mica-rich schist, with scheelite and tourmaline also occurring close to quartz vein contacts. This altered schist occurs mainly at the top of Regal Ridge. Red-weathering, moderately serpentinized ultramafic rock (unit Dum), and actinolite-plagioclase-biotite leuco-gabbro to more common pyroxenite (unit Dmi) occur mainly to the west of the mineralized areas (Fig. 4.2). Quartz-tourmaline veins within these units are very rare, likely due to both the extremely competent nature of the rock type, and distance from the granite. Geological mapping of the property (Fig. 4.2) suggests that the ultramafic unit is not present at depth between the granite and unit DF.

Carbonaceous phyllite (unit DKcp) occurs over much of the southeastern part of the property, and makes up the upper part of the rock sequence in this area. A thin band of rusty quartzite marks the contact between the chlorite schist and carbonaceous phyllite units. The rusty quartzite was included within unit DKcp by Murphy et al. (2001), but was mapped separately in

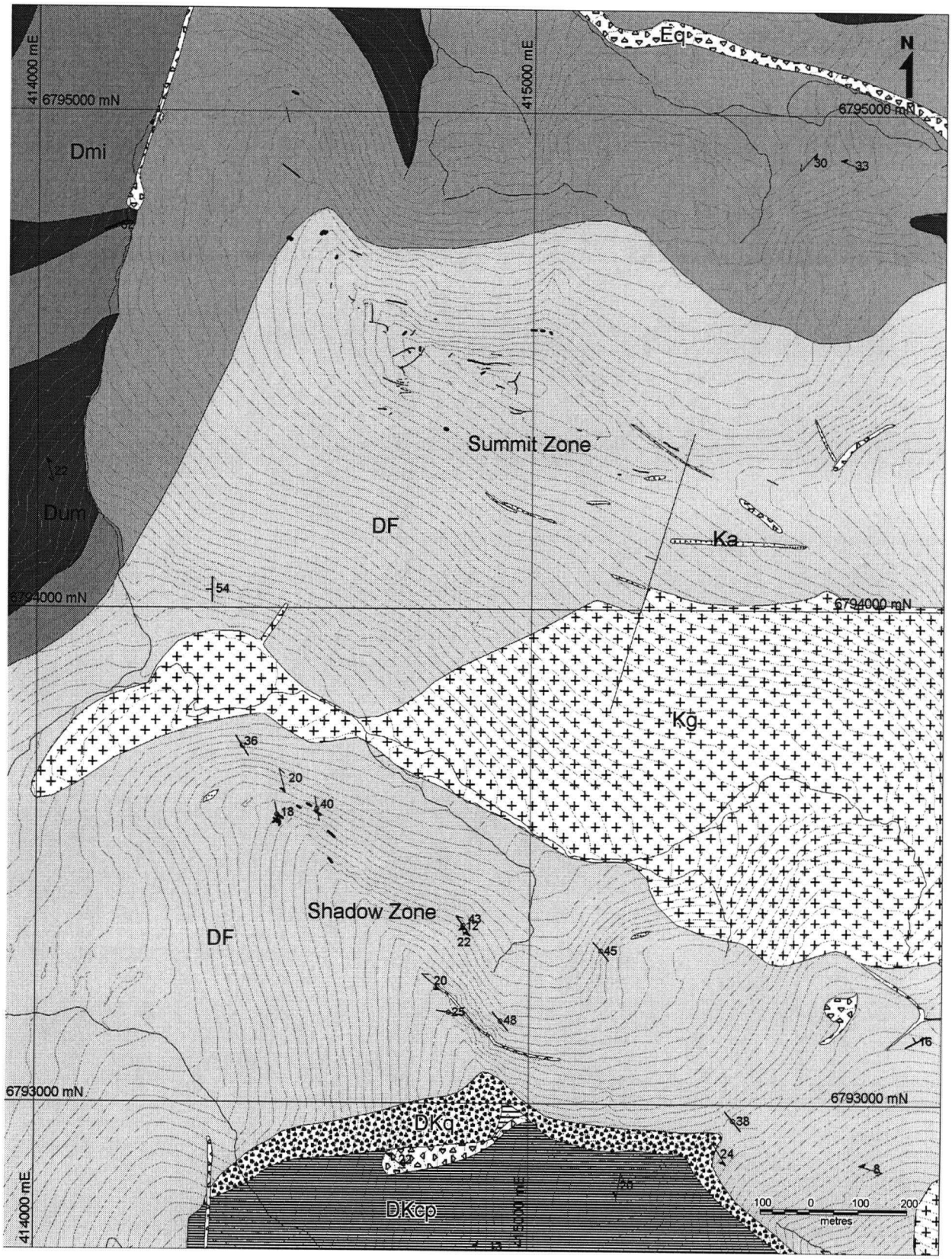

Figure 4.1. Geological map of the Tsa da Glisza property.

LEGEND

Rock Units

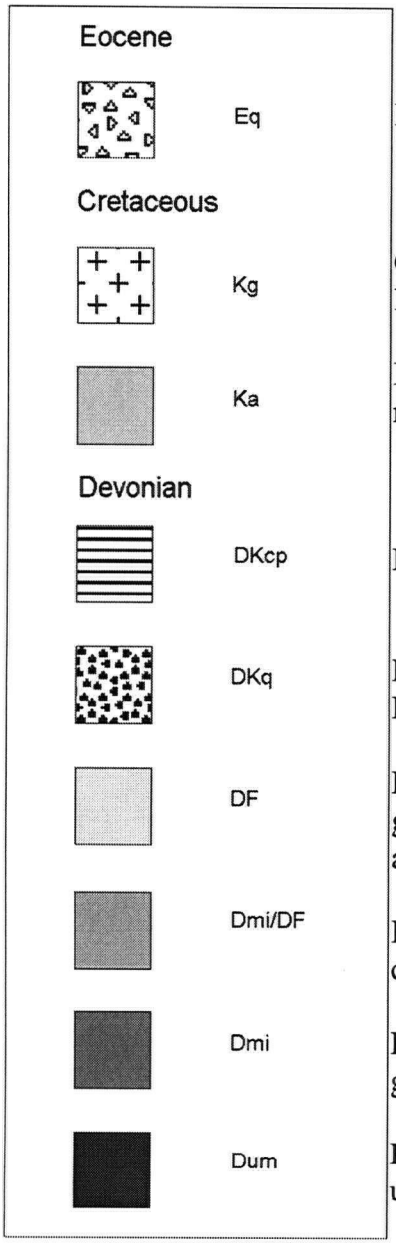

Eocene quartz-feldspar porphyry dikes and sills.

Cretaceous biotite-muscovite granite to muscovite leucogranite,with rare accessory garnet and tourmaline.

Leucogranitic and aplite-pegmatite sills and dikes with accessory muscovite, tourmaline, garnet, and rare beryl.

Devonian carbonaceous phyllite.

Devonian quartzite, locally rusty-weathering near contact with DF.

Devonian Fire Lake mafic metavolcanic unit, dark- to medium-green plagioclase-chlorite schist to phyllite, common biotite and actinolite porphyroblasts.

Interfingered actinolite-plagioclase-biotite leuco-gabbro and chlorite schist.

Devonian pyroxenite to actinolite-plagioclase-biotite leuco-gabbro.

Red-weathering, moderately serpentinized Devonian intrusive ultramafic rock.

Symbols

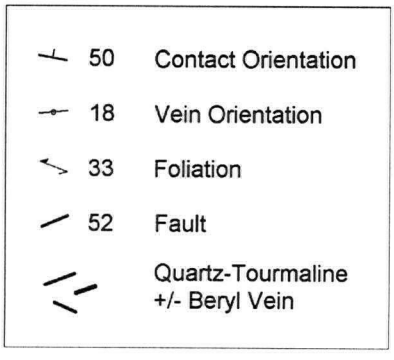

this study as unit DKq. Neither the carbonaceous phyllite or quartzite within the Kudz Ze Kayah Formation have been found to host quartz-tourmaline or emerald-bearing veins.

A biotite-muscovite granite to muscovite leucogranite crops out in the valley between the two mineralized ridges (unit Kg; Fig. 4.2). The 112.2 +/- 0.5 Ma pluton (Mortensen, unpublished data) contains rare garnet, and does not contain miarolitic cavities. A contact aureole extending approximately 500 m from granite contacts is defined by the presence of biotite and tourmaline within the surrounding schist.

Numerous leucogranite and aplite-pegmatite dikes and sills (unit Ka, not mapped separately by Murphy et al., 2001) from 30 cm to ten m in width are present on the property. The aplite dikes consist of plagioclase, quartz, muscovite, and minor potassium feldspar, tourmaline, and garnet. Pegmatite is rare, and has the same mineralogy as the aplites, but with increased amounts of muscovite. Both white and green beryl occur in quartz-rich segregations within at least two of the aplite dikes. Some of the aplite and pegmatite show alteration, containing feldspars mainly albite in composition, intergrowths of albite and muscovite, and rare interstitial calcite and sulphides.

Beige-, purple-grey-, and pink-weathering feldspar- and quartz-phyric porphyry dikes and sills (unit Eq) of inferred Eocene age occur throughout the property, and appear to intrude along the same zones of weakness exploited by the Cretaceous aplite and leucogranite dikes and sills, or along geologic contacts. The porphyry intrusions are approximately 5 to 50 m thick, and are commonly intensely altered to brown rounded pebbles. Some late faulting and alteration of host rocks and emerald at Tsa da Glisza could be attributed to this Eocene event.

4.4 MINERALIZATION AND ALTERATION

At the Tsa da Glisza occurrence, emerald occurs: (1) in the altered selvages of quartz-tourmaline veins; (2) within quartz-tourmaline veins; and (3) in linear zones of highly-altered schist, with no quartz-tourmaline veins immediately adjacent. As discussed in Neufeld et al. (2004), the quartz veins are interpreted to be syn- to late-tectonic, coinciding with the waning stages of granite emplacement. No distinct preferred orientation of emplacement for the veins is evident, and the degree of deformation is variable; some veins appear relatively linear and tabular, whereas others are extensively boudinaged. Mineralization is associated with both extremes of vein type. The emerald crystals show no preferred growth orientation relative to

either the schist foliation, or to tourmaline-filled fractures within the quartz veins. Alteration of the quartz-tourmaline vein selvages consists of jarosite, tourmaline, lepidolite (F and Li- rich mica), and scheelite and fluorite crystals (less than 1mm in size), in order of abundance. Tourmaline and mica are most abundant within the first 10 cm away from the vein-host contact, whereas more distal alteration mainly comprises jarosite within foliation planes of the chlorite schist. Whole-rock geochemistry of samples taken across numerous mineralized veins shows a consistent enrichment of Li, Sn, and F within the vein selvages, and rare enrichment of Be, Bi, and W within the vein itself (Fig. 4.3; Appendix 3). This is consistent with the abundant lepidolite in vein selvages. Boron is enriched in both the veins and selvages relative to unaltered chlorite schist, likely reflecting the abundant tourmaline in both veins and selvages.

Beryl, and rare emerald, are found in quartz-rich segregations within two albitized aplite dikes at Tsa da Glisza. Beryl within the aplite dikes may form from late-crystallizing fluids trapped within the aplite. These residual fluids would be expected to be rich in Be. Alternately, these occurrences may indicate that some Be was sourced from plagioclase, which, when altered by sodium-rich fluids to a more albitic composition, releases the minor amount of Be that was originally incorporated into the plagioclase structure (cf. Charoy, 1999). It is highly unlikely that all of the Be within the mineralizing fluids was sourced from the aplites after they had crystallized, since most mineralized quartz vein selvages are geochemically anomalous in several typically magmatic elements (B, W, Bi, F, Sn, Li) and it seems unlikely that all of these would have been remobilized from aplite during a later metasomatic event.

4.5 GENETIC MODEL

Emerald formation at Tsa da Glisza is considered to have been associated with the interaction of magmatic and hydrothermal fluids within the actively-deforming zone in relatively close proximity to a peraluminous granite. The mineralizing event was mainly syn- to late-tectonic, coinciding with the waning stages of granite emplacement and peak metamorphic (upper greenschist) conditions. The Tsa da Glisza deposit best fits the magmatic-hydrothermal, strongly peraluminous W-Mo (biotite-muscovite) granite occurrence type as defined by Barton and Young (2002), but seems to have also been related to a relatively short period of deformation of the host schists, directly related to emplacement and cooling of the granitic pluton. Any genetic model for emerald mineralization must account for the incompatibility of two necessary

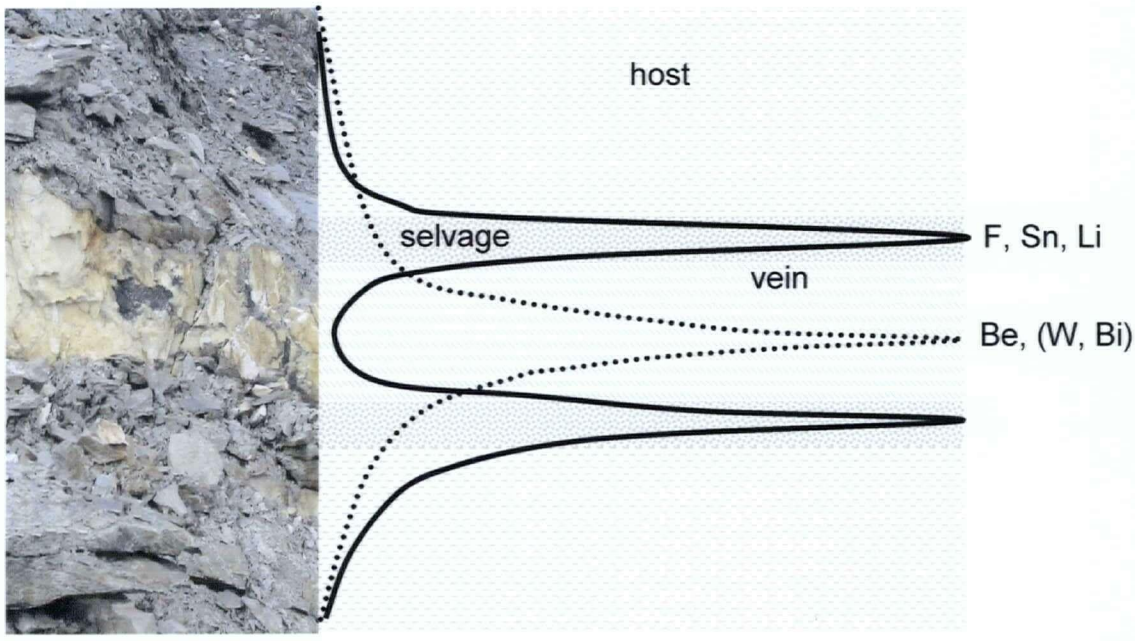

Figure 4.3. Typical pattern of geochemical enrichment relative to host schist, across a mineralized quartz-tourmaline vein. F, Sn, and Li values peak within the altered vein selvage (tourmaline-phlogopite zone), Be values peak sporadically within the vein itself, and Bi and W peak either within the vein, or in the immediate vein selvage.

elements for emerald formation, Be and Cr, which are rarely found together in environments in which beryl is stable.

The genetic model we propose for emerald mineralization at Tsa da Glisza is shown in schematic form in Figure 4.4. Beryllium, with other magmatic elements, including B, W, Li, Bi, and F, moves out from the granite within highly evolved magmatic fluids. Beryllium is increasingly mobile in fluids containing B and phosphate, and may complex with F, chlorine, and hydroxyl ions (London and Evensen, 2002). The high F contents within mineralized vein selvages suggests that Be most likely travelled as a fluoride or possibly hydroxide complex. Aplite and pegmatite dikes formed with the onset of cooling. Although the dikes locally contain Be concentrations of up to 100 ppm, Be was mostly not incorporated into the aplite-forming minerals, and continued to move through the host rocks, within dominantly magmatic fluids.

A hydrothermal fluid cell was initiated in the host rocks with emplacement of the granite. These fluids percolated through the chlorite schist, and leached Cr from the mafic groundmass. Geochemical transects from unaltered chlorite schist through altered schist, to quartz-tourmaline veins give no indication of how far Cr may have travelled within these fluids. Cr may have been directly sourced from host rock within centimetres of quartz-tourmaline veins through contact metasomatism, or may have travelled some distance along hydrothermal fluid pathways.

Beryl crystallization may have been triggered by several factors: (1) mixing with cooler hydrothermal fluids; (2) crystallization of tourmaline, which would have removed B and possibly some Li and F from the fluids and/or lowered the aluminium activity of the fluids, all of which would have resulted in a reduced solubility of Be in the fluid (cf. London and Evensen, 2002); (3) an increase in the Ca content of the fluids due to interaction with the host schist; (4) an increase in host-rock permeability or porosity due to either rock type differences or fracture propagation related to deformation accommodating cooling of the granite pluton below; (5) precipitation of lepidolite within the vein selvage, removing F (ligand) and Li (buffer) from the fluids; (6) or simply due to decreases in pressure and/or temperature. Likely all of these factors played some role in initiating beryl precipitation, particularly where mineralization is contained within highly altered vein selvages. Where emerald occurs solely within the quartz veins, factors (3) and (5) above are probably not involved, and where emerald occurs within linear zones of alteration away from quartz-tourmaline veins, low silica activity may also be a factor in prompting precipitation of beryl (London and Evensen, 2002).

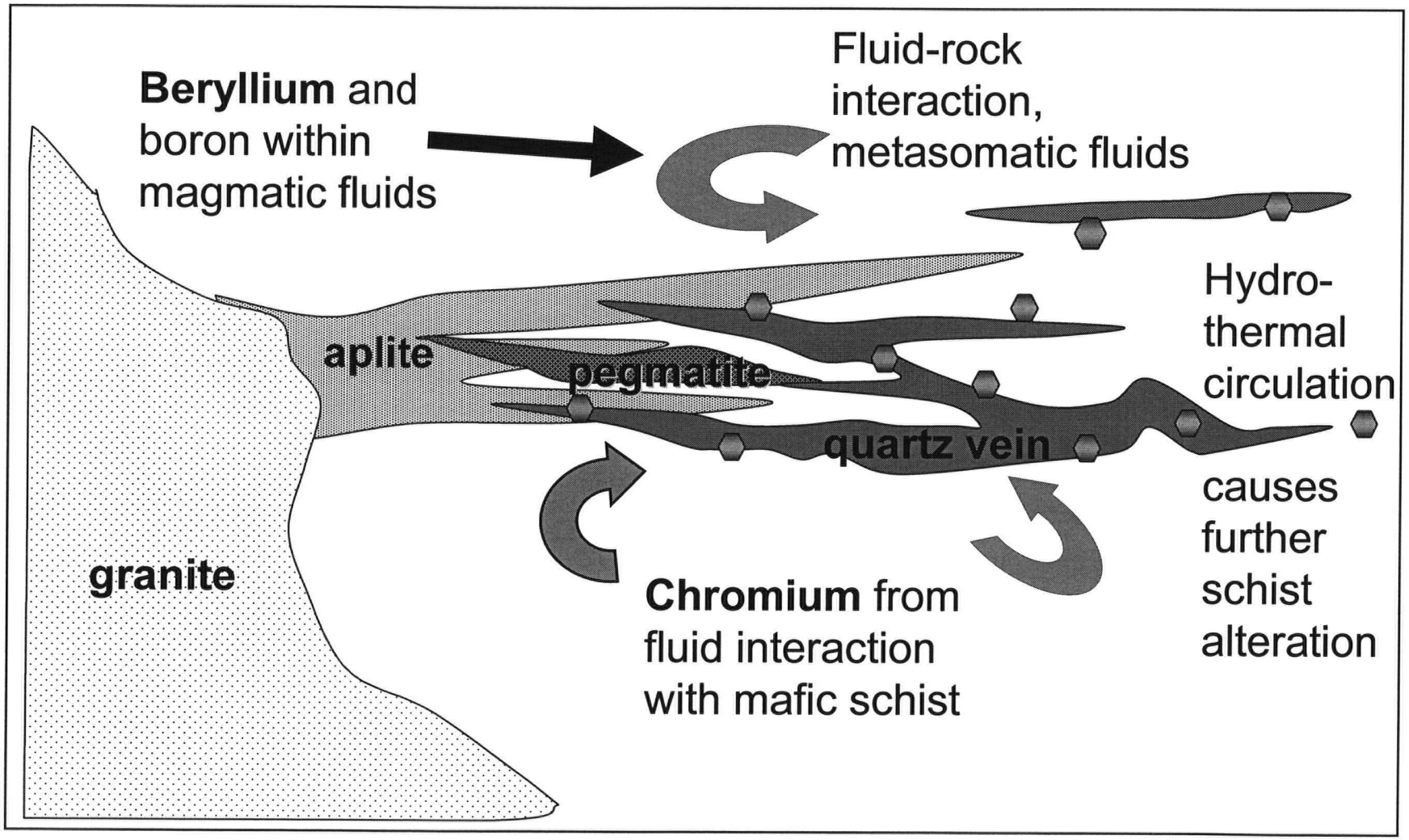

Figure 4.4. Schematic of proposed genetic model for emerald mineralization at Tsa da Glisza. The mineralizing fluids are a mixture of both magmatic-hydrothermal and metasomatic fluids. Mineralized veins occur within, adjacent to, and distal from aplite and pegmatite dikes.

4.6 EXPLORATION MODEL

Emerald exploration in the Yukon has been ongoing since at least 1999, and has resulted in the 2003 discovery of aquamarine at the True Blue occurrence (Deklerk, 2003, Guano claims, 105F 081). Emerald mineralization was also discovered one kilometre away from known mineralization at the Tsa da Glisza property in 2004 (Shadow Zone, Fig. 4.2). Walton (1996) first discussed the possibility of gem mineralization in the Yukon, and the various models for emerald formation world-wide as applicable to Yukon exploration are discussed by Walton (2004). In this paper, we discuss the specifics of an exploration model based solely on the style of emerald mineralization at the Tsa da Glisza occurrence. Such a model may be applicable to much of the Canadian Cordillera, but is specifically aimed at the Finlayson Lake district of the Yukon-Tanana Terrane. Key aspects of the model are discussed below.

4.6.1 Host Rock

4.6.1.1 Geochemistry

The amount of emerald mineralization within quartz-tourmaline veins is limited by the availability and transport of Cr from the host rock (Laurs et al. 1996). The main host rock for emerald mineralization at Tsa da Glisza is a fine-grained chlorite schist (unit DF) of boninitic composition, with an average Cr content of 800 ppm, which is higher than any other mafic metavolcanic rocks in the Finlayson Lake district, including other rock compositions within unit DF (Table 4.1) (Neufeld et al, 2004; Piercey et al., 2004). This suggests that emerald exploration within the Finlayson Lake district should focus on host rocks of boninitic composition, found regionally within unit DF. Although the Cr content of the ultramafic unit is much higher than that of the chlorite schist (Table 4.1), two factors argue against it being the source of Cr in the mineralizing fluids. First, geological mapping of the property indicates that the ultramafic unit is not present at depth beneath the deposit (i.e. between the granite and the mineralized region) (Fig. 4.2). Secondly, aplite and quartz veins within the ultramafic unit generally display little or no surrounding alteration, suggesting a more limited interaction between the host and the hydrothermal fluids. The more likely source of the Cr in the Tsa da Glisza occurrence is the chlorite schist, which, due to its schistosity and high mica content, is both highly permeable and reactive. Therefore, exploration should target high-Cr content, permeable mafic schist hosts

Table 4.1. Whole rock geochemistry of mid-Paleozoic rocks at the Tsa da Glisza emerald occurrence.

	RR-02-8 414716 6796538	HN-2-1 413675.25 6794656.75	HN-2-2 413790.25 6794879.75	RR-02-10 416234 6794246	HN-2-17 415016.25 6794634.75	HN-2-28 414973 6794398	HN-2-30 414944.25 6794417.75	RR-02-21 414536 6794917	HN-2-66 414227 6794986	RR-02-14 415342 6794260	HN-2-45 414407.25 6795077.75
	serpentinized ultramafic	serpentinized ultramafic	gabbro	chlorite schist nearest granite	fissile chlorite schist	phlogopite-chlorite schist	fragmental basalt? chlorite schist	chlorite schist	actinolite-plagioclase schist	chlorite schist	actinolite-plagioclase schist
	Dum	Dum	Dmi	DF	DF	DF	DF	DF	DF	DF	DF
SiO2 (wt. %)	42.02	37.59	49.6	48.19	49.88	50.84	51.27	51.8	53.4	54.01	55.19
Al2O3	1.65	3.92	2.03	6.89	9.97	12.55	13.33	13.04	14.39	9.76	14.07
Fe2O3	9.75	13.31	7.51	10.81	13.24	9.78	9.19	9.3	9.03	8.52	5.51
CaO	0.04	0.81	9.51	9.5	5.07	8.41	7.36	9.51	8.41	9.34	8.8
MgO	35.99	32.86	25.03	19.39	15.2	11.94	11.26	11.17	9.59	13.33	9.2
Na2O	0.13	0.05	0.07	0.41	0.2	1.89	2.26	1.41	1.72	1.15	3.04
K2O	0.03	0.02	0.03	0.05	0.05	0.36	0.26	0.22	0.18	0.09	0.64
Cr2O3	0.43	0.52	0.37	0.38	0.18	0.08	0.06	0.08	0.03	0.08	0.02
TiO2	0.03	0.07	0.1	0.14	0.25	0.28	0.32	0.23	0.3	0.22	0.11
MnO	0.08	0.18	0.19	0.26	0.21	0.17	0.14	0.17	0.14	0.2	0.09
P2O5	0.01	0.01	<0.01	0.02	0.01	0.01	0.03	0.03	0.02	0.02	0.01
SrO	<0.01	0.01	0.01	0.01	0.01	0.02	0.01	0.01	0.03	0.03	0.02
BaO	<0.01	<0.01	<0.01	<0.01	0.01	0.02	0.02	0.01	0.01	0.01	0.04
LOI	9.53	10.25	4.15	3.07	4.78	2.19	3.22	1.89	2.27	1.72	1.33
Total	99.67	99.59	98.62	99.11	99.06	98.56	98.73	98.85	99.53	98.49	98.06
FeO (wt. %)	3.6	8.8	3.29	7.92	10.15	7.74	6.95	7.02	6.94	6.51	4.24
C	<0.05	<0.05	0.08	<0.05	0.05	<0.05	0.1	<0.05	0.08	<0.05	<0.05
CO2	<0.2	<0.2	0.3	<0.2	0.2	<0.2	0.4	<0.2	0.3	<0.2	<0.2
H2O-	0.38	0.24	0.07	0.07	0.23	0.18	0.21	0.08	0.16	0.06	0.04
H2O+	9.61	11.45	4.16	3.72	5.44	2.66	3.17	2.47	2.59	2.5	1.64
Cr2O3	0.43	0.52	0.35	0.39	0.18	0.1	0.09	0.09	0.05	0.1	0.04

continued on following page

Table 4.1 continued.

	RR-02-8 Dum	HN-2-1 Dum	HN-2-2 Dmi	RR-02-10 DF	HN-2-17 DF	HN-2-28 DF	HN-2-30 DF	RR-02-21 DF	HN-2-66 DF	RR-02-14 DF	HN-2-45 DF
Ag (ppm)	<1	<1	<1	<1	<1	<1	<1	<1	<1	<1	<1
B	30	40	<20	<20	<20	<20	<20	<20	<20	<20	<20
Ba	2.4	4.2	15.4	7.9	3.5	191.5	110	38.7	80.7	106.5	310
Be	1.24	<0.05	0.25	0.12	0.27	0.24	0.15	0.19	0.8	0.23	0.2
Ce	0.6	1	0.7	2	1.1	2.1	1.7	2	1.8	1.9	0.8
Cl	<50	<50	<50	210	<50	<50	<50	160	<50	390	120
Co	120	124.5	54.2	70.5	65.2	41	40.2	45.6	44.9	42.2	32.5
Cr	3080	3900	2460	2730	1230	690	540	610	290	660	220
Cs	4.3	4.1	0.1	0.4	2	25.8	7.2	6	3.5	0.5	4.5
Cu	18	60	<5	24	6	57	190	<5	9	93	42
Dy	<0.1	0.3	0.4	0.7	0.9	1.2	1.2	1.1	1	0.9	0.3
Er	0.1	0.3	0.3	0.6	0.7	1	0.8	0.8	0.8	0.6	0.2
Eu	<0.1	<0.1	0.1	0.1	0.1	0.3	0.2	0.1	0.2	0.1	0.1
F	430	<20	<20	50	40	60	40	50	200	40	30
Ga	4	6	2	8	9	15	10	12	12	9	7
Gd	<0.1	0.2	0.2	0.5	0.5	0.7	0.7	0.6	0.6	0.5	0.2
Hf	<1	<1	<1	1	<1	1	<1	1	1	1	<1
Ho	<0.1	0.1	0.1	0.2	0.2	0.3	0.3	0.2	0.3	0.2	0.1
La	0.6	1	1	1.9	1.1	1.8	1.2	1.8	1.2	1.2	1.5
Li	7.1	1.9	1.4	57.7	54.8	68.8	83.7	76.3	57.1	13.8	25.1
Lu	<0.1	0.1	0.1	0.1	0.1	0.2	0.1	0.1	0.2	0.1	<0.1
Mo	3	3	3	3	2	2	3	3	3	3	3
Nd	<0.5	<0.5	<0.5	1.1	0.6	1.2	1.3	1.2	1	1.1	<0.5
Ni	1635	1415	303	801	345	169	134	246	111	179	142
Pb	<5	<5	<5	<5	<5	5	<5	5	6	5	<5
Pr	<0.1	0.1	0.1	0.2	0.1	0.3	0.2	0.2	0.2	0.2	0.1
Rb	1	0.9	0.3	0.6	1.1	31.9	18.3	8.4	10.2	1.6	17.6
Sc	5.7	11.8	24.2	26	46.5	51.5	46.8	46.9	54.4	38.5	34.9
Sm	<0.1	0.1	0.1	0.4	0.3	0.5	0.5	0.5	0.4	0.4	0.1
Sn	5	<1	<1	<1	<1	<1	1	1	1	1	<1
Sr	2.5	3.9	11.2	4.7	2.5	77.9	75.2	44.4	186	65.7	140
Ta	<0.5	<0.5	<0.5	<0.5	<0.5	<0.5	<0.5	<0.5	<0.5	<0.5	<0.5
Tb	<0.1	<0.1	<0.1	0.1	0.1	0.1	0.2	0.1	0.1	0.1	<0.1
Tl	<0.5	<0.5	<0.5	<0.5	<0.5	<0.5	<0.5	<0.5	<0.5	<0.5	<0.5
Tm	<0.1	0.1	<0.1	0.1	0.1	0.1	0.1	0.1	0.1	0.1	<0.1
U	<0.5	<0.5	<0.5	<0.5	<0.5	<0.5	<0.5	<0.5	<0.5	<0.5	<0.5
V	23	81	35	175	209	302	216	226	304	230	123
W	31	10	16	17	12	7	12	17	8	8	11
Y	<0.5	2.4	2.2	4.3	5.3	8.3	7.3	6.3	7	5.2	2
Yb	<0.1	0.5	0.3	0.7	0.8	1.2	0.9	0.9	1	0.8	0.3
Zn	57	57	33	72	72	62	69	77	34	71	36

rather than ultramafic rock. Lewis et al. (2003) produced a map outlining locations of intermediate to mafic volcanic and metamorphic rocks in the Yukon Territory that may help in targeting appropriate host lithologies.

4.6.1.2 Alteration

Emerald mineralization at Tsa da Glisza is commonly associated with narrow, highly altered vein envelopes and selvages, and zones of less altered host rock that extend up to several metres away from the quartz veins. This style of alteration is an indication that the system was permeable to fluids, and if present, increases the potential for emerald mineralization within a prospective area.

4.6.2 Related Intrusive Rocks

Nearby intrusion of an evolved felsic magma is obviously implicit in the model for magmatic-hydrothermal emerald deposits. Tsa da Glisza is one of numerous emerald deposits worldwide that are closely associated with a peraluminous granite (Guiliani, 1990; Barton and Young, 2002). In addition, the presence of aplite and pegmatite dikes outside of the pluton indicates that not only did the magma produce evolved fluids, but also that at least some of those fluids were able to move out into the surrounding rocks, rather than cooling and crystallizing within the pluton itself. While beryl is a common component of pegmatites within granitic plutons, emerald will not form unless some amount of mixing of the magmatic fluids with a Cr or vanadium source has occurred.

4.6.2.1 Age

At Tsa da Glisza, the 112.2 +/- 0.6 Ma biotite-muscovite granite underlying the property is part of the Anvil plutonic suite (Mortensen et al., 2000). The Cretaceous age of the related intrusive is not a restrictive factor of the model; however, it is a good "rule of thumb" for emerald exploration within the Yukon, as the Cretaceous Cassiar and Tungsten magmatic suites also contain evolved, felsic granites (Lewis et al., 2003).

4.6.2.2 Mineralogy

The mineralogy of a granitic pluton can be used by a prospector to determine whether Be was likely a component of the evolved magmatic fluids, or was accommodated into the structure of common minerals within the pluton itself. Cordierite, muscovite, and plagioclase can all accommodate some Be into their structure during crystallization. Cordierite has by far the highest Be partition coefficient of these three minerals, but plagioclase of composition An_{30} (oligoclase-andesine) can also remove substantial amounts of Be from the magmatic fluids. A pluton that contains cordierite or abundant oligoclase-andesine is unlikely to have produced Be-rich residual fluids during crystallization.

The mineralogy of associated aplite dikes provides important information for the exploration model. For example, if aplite dikes are found that contain white beryl, this could either be interpreted as a positive factor in that Be moved out of the pluton, or it could be interpreted as negative, since white beryl is evidence of little to no mixing of fluids with host rocks. In general, aplite bodies with more albite than potassium feldspar (Laurs et al., 1996), and those that contain tourmaline, are increasingly likely to be associated with emerald mineralization.

4.6.2.3 Geochemistry

The Be content of the granite at Tsa da Glisza averages 11 ppm (Table 4.2), which is relatively high compared to crustal Be values (3 ppm, Wedepohl 1995) and at the low end of the global average Be-content of granites (1-160 ppm, London and Evensen 2002). Yukon granites with associated beryl tend to have between 12-20 ppm Be (Lewis et al. 2003). Lithium, F, phosphorous, and B contents are also high (Table 4.2). As discussed previously, high amounts of these potential ligands and buffers within a fluid increases the mobility of Be within that fluid.

The geochemistry of aplite dikes is unlikely to assist in assessing a target for emerald potential, although high Na/K ratio, and Be contents greater than 30 ppm may indicate the presence of Be-F within a sodic fluid during crystallization of the aplite (Neufeld, 2004).

Table 4.2. Whole rock geochemistry of Cretaceous intrusive rocks at the Tsa da Glisza emerald occurrence.

	HN-2-43	HN-2-37	HN-2-62A	RR-02-9B	RR-02-4	HN-2-40	RR-02-32	RR-02-26	RR-02-23	HN-2-8	RR-02-2	RR-02-28	RR-02-34
	414953	415953	415913	416371	415766	415589.25	415714	415286	415340	414227	415878	414744	415461
	6793979	6793962	6794754	6794799	6795348	6794102.75	6795539	6794325	6794566	6794986	6794254	6794473	6794704
	Kg, far south and west	Kg, base chem for	Outcrop Kg, near lake	aplite	aplite	aplite	aplite	aplite	aplite w/ tour	Hero aplite, beryl assoc.	aplite, beryl assoc.	aplite, beryl assoc.	pegmatitic dike
SiO2 (wt. %)	71.25	72.14	74.35	72.75	73.43	73.93	74.2	74.53	74.83	72.25	71.3	81.2	73.72
Al2O3	15.61	15.4	14.34	14.9	15.64	14.89	16.34	14.75	14.62	16.01	18.01	11.1	14.93
Fe2O3	1.69	1.41	1.08	0.63	0.88	0.66	0.54	0.62	0.63	0.2	0.46	0.25	0.44
CaO	0.94	1.17	0.71	1.47	1.5	0.53	0.8	0.59	0.69	2.75	0.66	3.01	0.55
MgO	0.58	0.4	0.49	0.23	0.29	0.22	0.13	0.02	0.08	0.06	0.07	0.07	0.01
Na2O	3.1	2.89	3.06	4.02	3.45	2.99	3.46	4.34	4.09	6.04	5.73	3.02	5.9
K2O	4.71	4.87	4.28	4.29	2.69	4.8	3.58	4	4.24	0.2	1.65	0.39	1.48
Cr2O3	0.01	0.01	0.01	0.01	0.01	0.01	0.01	0.01	0.01	<0.01	<0.01	0.02	0.01
TiO2	0.32	0.25	0.17	0.05	0.13	0.09	0.06	0.02	0.04	0.06	0.02	<0.01	0.01
MnO	0.02	0.02	0.01	0.01	0.01	<0.01	0.02	0.09	<0.01	0.03	0.08	<0.01	0.03
P2O5	0.14	0.1	0.08	0.06	0.06	0.07	0.03	0.02	0.04	0.01	0.03	0.01	0.01
SrO	0.02	0.01	0.01	<0.01	<0.01	0.01	0.01	<0.01	<0.01	0.05	0.01	0.01	0.01
BaO	0.05	0.04	0.03	0.01	0.01	<0.01	<0.01	<0.01	<0.01	0.02	0.02	<0.01	0.01
LOI	1.35	1.19	1.04	1.14	1.45	1.02	0.53	0.65	0.61	0.81	1.08	0.75	0.93
Total	99.78	99.9	99.66	99.58	99.55	99.23	99.7	99.64	99.89	98.5	99.13	99.81	98.02
FeO (wt. %)	1.18	0.9	0.72	0.39	0.64	0.39	0.32	0.39	0.45	0.21	0.26	0.32	0.39
C	<0.05	<0.05	<0.05			<0.05				0.05			
CO2	<0.2	<0.2	<0.2			<0.2				0.2			
H2O-	0.14	0.09	0.06	0.03	0.02	0.04	0.02	0.01	0.03	0.09	0.06	0.04	0.03
H2O+	0.86	0.66	0.63	0.5	1.01	0.64	0.36	0.4	0.42	0.26	0.86	0.22	0.69
Cr2O3	0.03	0.03	0.03			0.03				0.03			

continued on next page

Table 4.2 continued.

	HN-2-43	HN-2-37	HN-2-62A	RR-02-9B	RR-02-4	HN-2-40	RR-02-32	RR-02-26	RR-02-23	HN-2-8	RR-02-2	RR-02-28	RR-02-34
	Kg, far south and west	Kg, base chem for	Outcrop Kg, near lake	aplite	aplite	aplite	aplite	aplite	aplite w/ tour	Hero aplite, beryl assoc.	aplite, beryl assoc.	aplite, beryl assoc.	pegmatitic dike
Ag (ppm)	<1	<1	1	<1	<1	<1	<1	<1	<1	<1	<1	<1	<1
B	30	30	30			30				20			
Ba	415	419	161.5	62.3	76.3	41.4	8.5	18.5	13.9	117	132.5	16.8	56.8
Be	12.7	10.85	9.84	13.32	15.17	10.8	19.88	18.77	14.72	79.9	105.3	249.94	31.12
Ce	82.2	74.4	42.7	18.6	36.8	11.6	11.4	10.2	14.2	3.6	4.7	<0.5	8.7
Cl	<50	<50	<50	100	100	<50	<100	<100	<100	<50	<100	<100	<100
Co	4	3.7	3.2	0.6	1	1.4	0.6	0.6	0.7	2	0.7	0.6	0.6
Cr	130	150	120	110	100	130	130	140	130	140	110	170	120
Cs	26.3	25.2	15.2	14.4	9.5	14.5	14.2	13.3	12.7	3.2	11.4	22.4	6.8
Cu	<5	<5	<5	<5	<5	31	114	75	27	<5	8	<5	<5
Dy	2.2	2	2.2	1.8	1.7	1.7	3.4	3.5	3.1	2.2	1.5	0.2	2.4
Er	1.1	1	1.1	0.8	0.8	0.9	2.4	2.5	2	0.8	0.6	0.1	1.2
Eu	0.6	0.6	0.2	0.2	0.2	0.1	0.1	0.1	0.1	0.1	<0.1	0.1	<0.1
F	1320	1200	710	470	770	570	360	340	430	50	140	60	130
Ga	29	29	30	31	37	32	33	32	33	24	47	22	38
Gd	4.2	4.1	2.7	2	2.6	1.5	2.2	1.8	2.1	1.3	0.9	0.2	1.7
Hf	5	4	3	2	3	2	2	3	2	7	6	6	2
Ho	0.4	0.4	0.4	0.3	0.3	0.3	0.7	0.7	0.7	0.3	0.2	<0.1	0.4
La	38.6	36.6	19.8	8.3	17.5	5.3	4.7	4.3	6.4	2	2.2	<0.5	4.1
Li	213	161.5	97.5	36.23	95.61	80.1	87.28	47.43	60.39	29.2	4.71	10.23	6.87
Lu	0.1	0.1	0.1	0.1	0.1	0.1	0.4	0.4	0.3	0.1	0.1	<0.1	0.2
Mo	4	3	3	<2.00	<2.00	4	<2.00	<2.00	<2.00	4	<2.00	<2.00	<2.00
Nb	14	12	11	10	13	8	7	8	9	20	80	3	28
Nd	31.8	29.3	17.4	8.5	14.9	4.9	5.6	4.6	6.1	1.4	2.1	<0.5	4
Ni	8	9	10	7	9	7	6	6	6	7	6	7	8
Pb	51	50	40	30	17	44	25	32	28	13	8	6	12
Pr	9.2	8.5	4.9	2.2	4.1	1.3	1.4	1.2	1.7	0.4	0.5	<0.1	1.1
Rb	378	376	416	321	312	377	343	350	382	11.7	334	57	241
Sc	5	4.1	3.4	2.96	3.87	3	1.79	1.16	1.52	0.5	0.29	0.14	0.56
Sm	5.5	5.1	3.4	2.3	3	1.6	2	1.7	2	1.2	0.9	<0.1	1.7
Sn	22	16	21	13	49	25	22	17	23	4	65	<1.00	79
Sr	127	138	58.6	48.1	54.4	27.6	19.3	7.6	15.1	257	10.5	57.9	24.7
Ta	2	1.8	2.7	1.9	1.8	1	1.1	1.3	1.1	13.1	37	2.5	9.3
Tb	0.5	0.5	0.4	0.3	0.4	0.3	0.5	0.5	0.5	0.4	0.3	<0.1	0.4
Th	26	23	14	8	12	5	7	4	6	3	5	2	5
Tl	1.2	1.3	1.2	1	1	1	1	1	1	<0.5	1	<1	<1
Tm	0.1	0.1	0.2	<0.5	<0.5	0.1	<0.5	<0.5	<0.5	0.1	<0.5	<0.5	<0.5
U	7.8	4.5	13.1	17	13.7	4.6	8.4	7.2	20.4	12.2	3.6	8.5	14.8
V	18	14	9	<5.00	<5.00	<5	<5.00	<5.00	<5.00	<5	<5.00	<5.00	<5.00
W	28	29	24	3	4	13	3	4	9	22	22	2	3
Y	10.6	9.7	11.6	8.8	9.1	10	24.6	26.2	22.4	13.1	10.3	0.9	14.8
Yb	0.9	0.8	1	0.7	0.8	0.9	2.7	2.9	1.8	1.2	0.7	0.1	1.4
Zn	68	54	40	23	22	16	16	11	14	5	10	<5	5
Zr	125	116	53.4	27.8	116	21.8	19.5	31.5	33.8	36.6	38.6	30.5	46.2

Note: Most major elements were analyzed using XRF, and most trace elements by ICP-MS or ICP-ES. Li, Be, Cr, and Mo were determined by AAS, B and Cl by INAA, FeO by titration, CO_2 and H_2O by infrared spectroscopy, and F by specific ion potentiometry.

4.6.3 Structural Environment

As discussed above, the Tsa da Glisza occurrence lies in the footwall of the Cretaceous North River Fault, within 10 km of the present-day fault trace. This indicates that unloading of the rock units at Tsa da Glisza was relatively late in the local tectonic regime. The structural geology at Tsa da Glisza is complex and deserves further study; however the Cretaceous structural setting as discussed by Neufeld et al. (2004) clearly shows a re-orientation of the shear system late in the Cretaceous event. Emerald mineralization was syn-to post-tectonic, and possibly coincided with this environment of rapid unloading, which would have decreased lithostatic pressure and increased the permeability of the host rocks to fluids.

Cretaceous granites within the Finlayson Lake district show a moderate emplacement depth (Mortensen et al., 2000). The quartz-tourmaline veins at Tsa da Glisza were emplaced into greenschist facies rocks near the brittle-ductile transition (Marshall et al., 2003; Neufeld et al., 2004). Beryllium saturation, although dependent on alumina activity, commonly occurs at temperatures of 450 to 550 °C (e.g. Barton, 1986). Mineralization has thus far been found within 800 m of outcropping granite, and between 200 and 500 m above granite at depth.

4.6.4 Geochemical Indicators

Preliminary element correlation studies on soil geochemical data from the Tsa da Glisza property highlight a correlation of Be, W, Sn and Bi anomalies near emerald mineralization (Giroux, 2002). However, different analytical methods used on samples give drastically varying results for Be (Lewis and Hart, 2004). New soil geochemical data from the Tsa da Glisza property are expected to more clearly delineate element correlations, but this information is not yet available. In general, Be values greater than 10 ppm in soil are considered anomalous. However, high Be values do not necessarily indicate the presence of beryl. During regional exploration for emerald at various locations throughout the Yukon in 2004, several Be soil geochemistry anomalies were attributed to Be-rich mica occurring on pegmatite selvages, or to clay minerals, rather than to beryl. Conversely, some mineralized areas at Tsa da Glisza are not geochemically anomalous. This is most likely when emerald occurs within relatively impermeable quartz veins, rather than on altered selvages where it is more susceptible to weathering and mobilization. While they do not conform to this model, areas with Be-rich clays

might be considered for Columbian-style emerald mineralization, where emerald forms within thrust faults and shear zones. Areas with abundant Be-rich micas are relatively unlikely to contain beryl mineralization, since beryl will typically form prior to mica, and remove Be from the residual fluid. Many of the elements that are strongly correlated with mineralized quartz veins and selvages (e.g., B, F, Li) in geochemical transects across the veins, are relatively mobile elements and do not correlate well with Be in soil geochemistry.

Regional soil geochemistry can be used to distinguish rock types with high Cr contents. However, as mentioned above, ultramafic rocks, which give the highest regional Cr values, do not appear to be a viable host for emerald mineralization such as that seen at Tsa da Glisza. By correlating regional geophysical data with Cr soil geochemisty (e.g. using Bond et al., 2002), high-Cr rocks that are not magnetic (therefore not likely to be ultramafic) can be identified (Fig. 4.5). Since regional geochemical coverage may be scarce, this method likely will require some scavenging through old assessment reports for property-scale soil geochemistry programs.

4.6.5 Geophysical Indicators

The quartz-tourmaline veins associated with emerald at Tsa da Glisza are not magnetically distinct on any scale. They occur within a mafic metavolcanic host rock that is neither a magnetic high nor low on regional geophysical maps (Fig. 4.6; Bond et al., 2002). The associated pluton produces a distinct magnetic low, attesting to its S-type, peraluminous nature (lack of magnetite or hornblende). The nearby ultramafic unit is regionally a strong magnetic high. As mentioned above, a correlation between magnetic highs and high Cr soil geochemistry may help to narrow the target zones, since ultramafic rocks are not a requirement of the exploration model. Areas with a medium magnetic response and medium to high Cr soil geochemistry are viable targets as mafic metavolcanic host rocks for emerald mineralization, particularly where they occur near a felsic pluton.

4.7 CONCLUSIONS

Although the coincidence at Tsa da Glisza of the many necessary factors for emerald formation is fortuitous, it is not necessarily unique. Many of the factors are often found together,

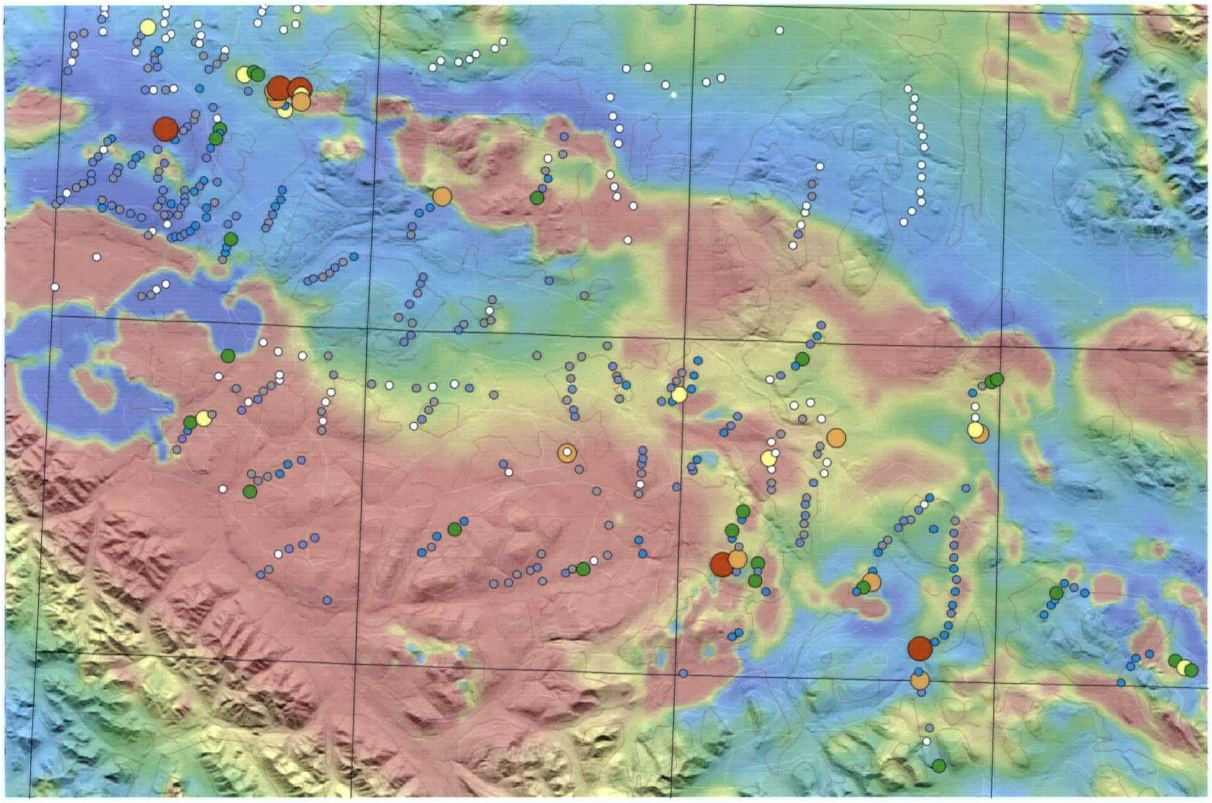

Figure 4.5. Geophysical magnetic anomaly map of the northern part of the Finlayson Lake district, with Cr soil geochemistry overlay. Areas showing a medium magnetic response, and high Cr values are viable target host rocks for emerald mineralization. Cr soil geochemical values cut off as follows: red=, orange=, yellow=, green=, blue=, purple=, grey=. Geophysical map and soil geochemical values from Bond et al. (2002). This figure does not show the Tsa da Glisza property. Regional geochemical soil sampling coverage in that is very scarce; this area has better coverage and was chosen merely to illustrate the point.

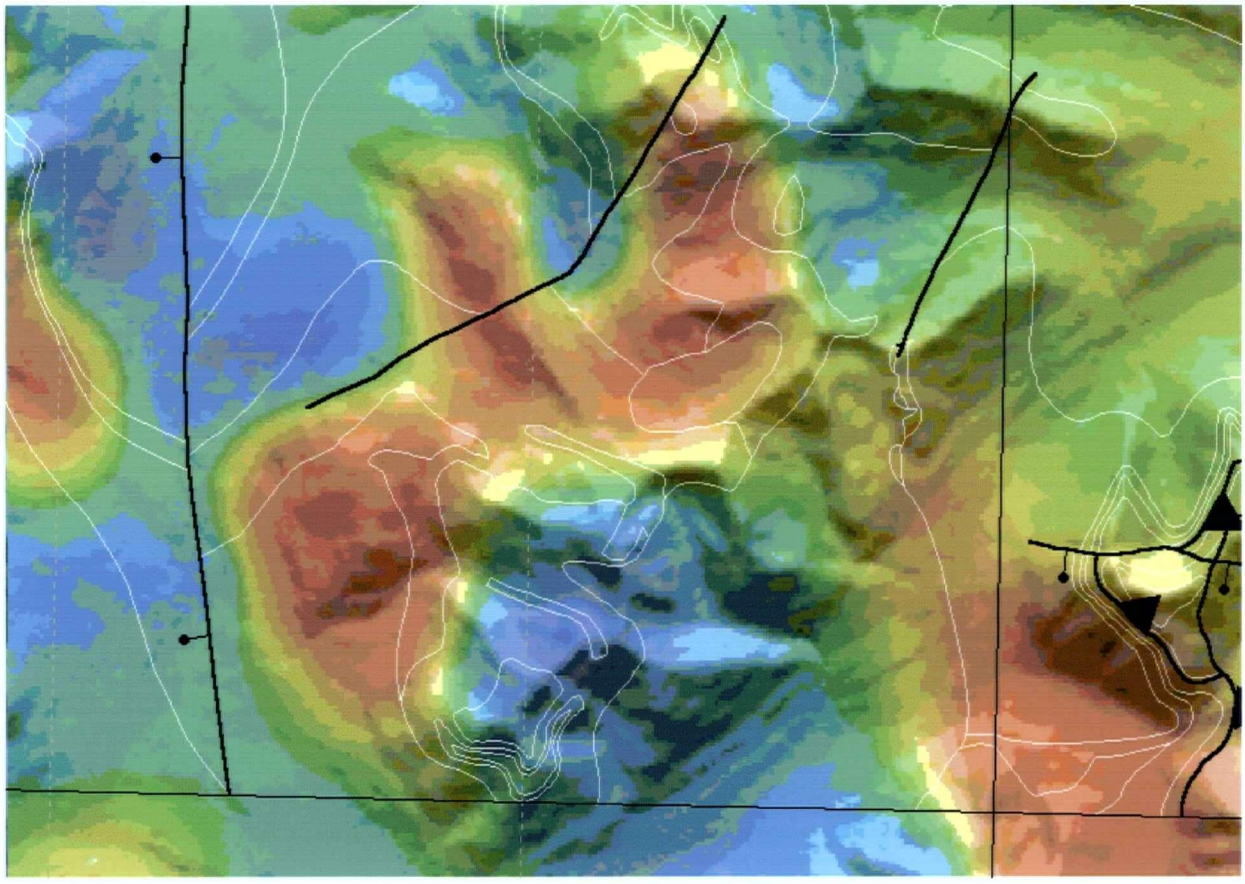

Figure 4.6. Geophysical magnetic response map for rocks in the region of the Tsa da Glisza property (from Bond et al., 2002, with overlain outlines of regional geologic contacts). The mafic metavolcanic host rock for emerald mineralization is neither a magnetic high nor low (green to yellow)). The associated pluton produces a distinct magnetic low (blue), attesting to its S-type, peraluminous nature (lack of magnetite or hornblende). The ultramafic unit is regionally a strong magnetic high (red).

such as granitic plutons, and the deformational environment above and adjacent to them, or mafic host rocks with schistose, and therefore permeable, textures. Emerald occurrences are small areas, and difficult to find using typical exploration methods such as soil geochemistry and geophysical surveys. Highly prospective targets can be identified using the exploration model outlined above and its constraints on host rock, associated intrusive rocks, structural environments, and geochemical and geophysical indicators. Detailed prospecting of those specific targets is the most effective method of exploration for emerald.

CHAPTER 5

CONCLUSIONS

5.1 CONCLUSIONS

This work has resulted in a number of important findings, as listed below:

1) Descriptive model.

   Property- and trench-scale mapping led to an increased understanding of the mineralogy of the mineralized veins and the alteration assemblages enveloping them, and the variability in the character of the host rock. Several new areas with prospective geology were mapped, and two new areas of emerald mineralization (Hero aplite, Shadow zone) were discovered as a direct result of the mapping project. Mapping suggests that the granite underlies the deposit at an estimated depth of 300 metres, with depth increasing to the west-northwest, much closer to mineralization than was previously suggested. The mineralogy of the various Cretaceous intrusive rocks has confirmed the role of both the granite pluton, and aplite dikes in the mineralizing event.

2) Genetic model.

   The Tsa da Glisza deposit is unique in that it involves processes from both magmatic-hydrothermal, and shear zone established models. While the mineralizing fluids were dominantly magmatic, the deformational environment acting on the mafic schist host rocks allowed for increased fluid permeation of the host and consequent increased reaction surface from which to source Cr, causing an extensive mineralized vein and alteration assemblage system. Emerald formation at Tsa da Glisza is considered to have been associated with the interaction of magmatic and hydrothermal fluids within the actively-deforming zone in relatively close proximity to a peraluminous granite. The mineralizing event was mainly syn- to late-tectonic, coinciding with the waning stages of granite emplacement and peak metamorphic (upper greenschist) conditions. The Tsa da Glisza deposit best fits the magmatic-hydrothermal, strongly peraluminous W-Mo (biotite-muscovite) granite occurrence type as defined by Barton and Young (2002). However, deformation related to the intrusion of the granite is critical to the genetic

model, as it assisted fluid circulation through the host schist, which led to the formation of emerald.

3) Exploration model.

   Although the coincidence at Tsa da Glisza of the many necessary factors for emerald formation is fortuitous, it is not necessarily unique. Many of the factors are often found together, such as granitic plutons, and the deformational environment above and adjacent to them, or mafic host rocks with schistose, and therefore permeable, textures. Highly prospective targets can be identified using the exploration model outlined and its constraints on host rock, associated intrusive rocks, structural environments, and geochemical and geophysical indicators. Detailed prospecting of those specific targets is the most effective method of exploration for emerald.

5.2 FUTURE RESEARCH

Possibilities for further research on emerald mineralization at the Tsa da Glisza emerald occurrence became evident during the course of this study:

1) Boron isotope study of the tourmaline. Chemical analyses suggest distinctions between tourmaline within the host rocks (regional, metamorphic tourmaline), tourmaline within the granite, and tourmaline intimately associated with emerald mineralization. Identification of the boron isotopic composition of these tourmaline types could help to fingerprint the composition of the mineralizing fluids, in particular, the proportion of hydrothermal to magmatic fluids at the time of emerald deposition.

2) Additional whole-rock geochemistry and O-H isotope linked studies. Preliminary work suggests that emerald mineralization is associated with areas of high isotopic homogenization. Data linking the whole-rock geochemistry of samples across a mineralized vein, with the oxygen and hydrogen isotopic compositions of those rocks, may help to determine the fluid chemistry at the time of mineralization, or pinpoint the chemical triggers for emerald deposition.

3) A detailed structural study of the deposit, to determine how critical the deformational environment was to the emerald-forming event, and to better constrain the dynamics of the system, is necessary to further develop the genetic model.

4) A regional geochemical study of rock unit DF to determine the regional extent of the boninitic high-Cr and high-Mg rocks, which host emerald mineralization at Regal Ridge (i.e. a follow-up of the work done on the boninitic rocks of the region by Steve Piercey and Don Murphy). The presence of these anomalously high Cr-bearing, permeable rocks seems to be crucial for the formation of dark green beryl. The location of this specific rock type throughout the Finlayson region might be the key to the location of more emerald mineralization.

REFERENCES

Barton, M.D., 1986. Phase equilibria and thermodynamic properties of minerals in the BeO-Al2O3-SiO2-H2O (BASH) system, with petrologic applications. American Mineralogist, vol. 71, p. 277-300.

Barton, M.D., and Young, S., 2002. Non-pegmatitic Deposits of Beryllium: Mineralogy, Geology, Phase Equilibria and Origin. In: Beryllium: Mineralogy, Petrology and Geochemistry, E.S. Grew, (ed.). Reviews in Mineralogy and Geochemistry, vol. 50, p.591-691.

Bond, J.D., Murphy, D.C., Colpron, M., Gordey, S.P., Plouffe, A., Roots, C.F., Lipovsky, P.S., Stronghill, G., and Abbott, J.G., 2002. Digital compilation of bedrock geology and till geochemistry of northern Finlayson Lake area, southeastern Yukon (105G). Exploration and Geological Services Division, Yukon, Indian and Northern Affairs Canada, Open File 2002-7 (D) and Geological Survey of Canada Open File 4243.

Breitsprecher, K. , Mortensen, J.K. and Villeneuve, M.E. (comp.) 2003. YukonAge 2002, A database of isotopic age determinations for rock units from Yukon Territory in Yukon digital geology, Version 2.0, S.P. Gordey and A.J. Makepeace (comp.); Geological Survey of Canada Open File 1749 and Yukon Geological Survey Open File 2003-9(D)

Cerny, P., 2002. Mineralogy of beryllium in granitic pegmatites. In: Beryllium: Mineralogy, Petrology and Geochemistry, E.S. Grew, (ed.). Reviews in Mineralogy and Geochemistry, vol. 50, p. 405-444.

Charoy, B., 1999. Beryllium speciation in evolved granitic magmas: phosphates versus silicates. European Journal of Mineralogy, vo. 11, p. 135-148.

Conklin, 2002. What is emerald?: Fact and opinion. In: Emeralds of the world, extraLapis English No. 2: the legendary green beryl. Lapis International, East Hampton, 100p.

Deklerk, R., 2002 (compiler). Yukon MINFILE 2002. Exploration and Geological Services Division, Yukon, Indian and Northern Affairs Canada.

Fersman, A.E., 1960. Selected works VI. Pegmatites. Reprint of 3rd ed, 1940. Akad Nauk, SSSR Moscow, 747p.

Franz, G., Gilg, H.A., Grundmann, G., and Morteani, G., 1996. Metasomatism at a granitic pegmatite-dunite contact in Galicia: the Franqueira occurrence of chrysoberyl (alexandrite), emerald, and phenakite: Discussion. Canadian Mineralogist, vol. 34, p. 1329-1331.

Franz, G. and Morteani, G., 2002. Be-minerals: Synthesis, stability, and occurrence in metamorphic rocks. In: Beryllium: Mineralogy, Petrology and Geochemistry (E.S. Grew, ed.). Reviews in Mineralogy and Geochemistry, vol. 50, p. 551-590.

Frost B.R., Barnes C.G., Collins W.J., Arculus R.J., Ellis D.J., Frost C.D., 2001. A geochemical classification for granitic rocks. Journal of Petrology, vol. 42, p. 2033–2048.

Giroux, G.H., 2002. True North Geochemical Study. True North Gems Inc., company report.

Giuliani, G.G., D'El Rey, S.L.J., and Couto, P.A., 1990. Origin of emerald deposits of Brazil. Mineralium Deposita, vol. 25, p. 57-64.

Gordey, S.P. and Makepeace, A.J. (comp.), 2003: Yukon digital geology, Version 2.0; Geological Survey of Canada Open File 1749 and Yukon Geological Survey Open File 2003-9(D).

Grew, E.S., (ed.) 2002. Beryllium: Mineralogy, Petrology and Geochemistry, Reviews in Mineralogy and Geochemistry, vol. 50, p. 445-486.

Groat, L.A., Marshall, D.D., Giuliani, G., Murphy, D.C., Piercey, S.J., Jambor, J.L., Mortensen, J.K., Ercit, T.S., Gault, R.A., Mattey, D.P., Schwartz, D.P., Maluski, H., Wise, M.A., Wengzynowski, W. and Eaton, W.D., 2002. Mineralogical and geochemical study of the Regal Ridge showing emeralds, southeastern Yukon. Canadian Mineralogist, vol. 40, no. 5, p. 1313-1338.

Grundmann, G., and Morteani, G., 1989. Emerald mineralization during regional metamorphism: The Habachtal (Austria) and Leydsdorp (Transvaal, South Africa) deposits. Economic Geology, vol. 84, p. 1835-1849.

Israel, S., 2003. Preliminary investigation of the structural characteristics of the Regal Ridge property, Finlayson Lake area, Yukon. True North Gems, Inc. company report.

Jackson, L.E., Gordey, S.P., Armstrong, R.L. and Harakal, J.E., 1986. Bimodal Paleogene volcanics near Tintina Fault, east-central Yukon, and their possible relationship to placer gold. Yukon Geology, Exploration and Geological Services Division, Yukon, Indian and Northern Affairs Canada, vol. 1, p.139-147.

Kazmi, A.H. and Snee, L.W., 1989. Emeralds of Pakistan: geology, gemology and genesis. Van Nostrand Reinhold Co., N.Y., USA.

Kotzer, T.G., Kyser, T.K., King, R.W. & Kerrich, R., 1993. An empirical oxygen- and hydrogen-isotope geothermometer for quartz-tourmaline and tourmaline-water. Geochimica et Comochimica Acta, vol. 57, p. 3421-3426.

Laurs, B.M., Dilles, J.H., and Snee, L.W., 1996. Emerald mineralization and metasomatism of amphibolite, Khaltaro granitic pegmatite-hydrothermal vein system, Haramosh mountains, northern Pakistan. Canadian Mineralogist, vol. 34, p. 1253-1286.

Lewis, L., and Hart, C., 2004. Maximizing beryllium anomalies for successful emerald exploration. Poster, Yukon Geoscience Forum.

Lewis, L., Hart, C., and Murphy, D.C., 2003. Roll out the beryl. http://www.geology.gov.yk.ca/publications/miscellaneous/placemats/beryl_placemat.pdf Yukon Geological Survey website, publications download.

London, D. and Evensen, J.M., 2002. Beryllium in silicic magmas: origin of beryl-bearing pegmatites. In: Beryllium: Mineralogy, Petrology and Geochemistry, E.S. Grew, (ed.). Reviews in Mineralogy and Geochemistry, vol. 50, p. 445-486.

Lowe, C., Miles, W., and Kung, R. and Makepeace, A.J., 2003. Aeromagnetic data over the Yukon Territory. In: Yukon digital geology, Version 2.0, S.P. Gordey and A.J. Makepeace (comp.); Geological Survey of Canada Open File 1749 and Yukon Geological Survey Open File 2003-9(D)

Marshall, D. D., Groat, L.A., Giuliani, G., Murphy, D.C., Mattey, D., Ercit, T.S., Wise, M.A., Wengzynowski, W. & Eaton, W.D., 2003. Pressure, temperature and fluid conditions during emerald precipitation, Southeastern Yukon: Fluid inclusion and stable isotope evidence. Chemical Geology, vol. 194, p. 187-199.

Martin-Izard, A., Paniagua, A., Moreiras, D., Acevedo, R.D., and Marcos-Pascual, C., 1995. Metasomatism at a granitic pegmatite-dunite contact in Galicia: the Franqueira occurrence of chrysoberyl (alexandrite), emerald, and phenakite. Canadian Mineralogist, vol. 33, p. 775-792.

Matthews, A. & Schliestedt, M., 1984. Evolution of the blueschist and greenschist facies rocks of Sifnos, Cyclades, Greece: A stable isotope study of subduction-related metamorphism. Contributions to Mineralogy and Petrology, vol. 88, p. 150-163.

Mortensen, J.K., 1992. Pre-Mid-Mesozoic tectonic evolution of the Yukon-Tanana Terrane, Yukon and Alaska. Tectonics, vol. 11, p.836-853.

Mortensen, J.K. & Jilson, G.A., 1985. Evolution of the Yukon-Tanana Terrane: Evidence from southeastern Yukon Territory. Geology, vol. 13, p.806-810.

Mortensen, J.K., Hart, C.J.R., Murphy, D.C. & Heffernan, S., 2000. Temporal evolution of early and mid-Cretaceous magmatism in the Tintina Gold Belt. In: The Tintina Gold Belt: Concepts, Exploration and Discoveries, J.L. Jambor, ed.. British Columbia and Yukon Chamber of Mines, Special Volume 2, p.49-57.

Murphy, D.C., 1997. Preliminary geological map of Grass Lakes area, Pelly Mountains, southeastern Yukon (105G/7). Exploration and geological services division, Yukon Region, Indian and Northern Affairs Canada, Open File 1999-4, 1:100 000 scale.

Murphy, D.C., 1998a. Mafic and ultramafic meta-plutonic rocks south of Finlayson Lake, Yukon: setting and implications for the early geological and metallogenic evolution of Yukon-Tanana Terrane. *In:* Cordillera Revisited: Recent Developments in Cordilleran Geology, Tectonics and Mineral Deposits, P. Mustard & S. Gareau, eds.. Geological Association of Canada Cordilleran Section Short Course, Extended Abstracts, p.102-109.

Murphy, D.C., 2004. Devonian-Mississippian metavolcanic stratigraphy, massive sulphide potential and structural re-interpretation of Yukon-Tanana Terrane south of the Finlayson Lake massive sulphide district, southeastern Yukon (105G/1, 105H/3,4,5). In: Yukon Exploration and Geology 2003, D.S. Emond and L.L. Lewis (eds.), Yukon Geological Survey, p. 157-175.

Murphy, D.C. and Piercey, S.J., 1999. Geological map of parts of Finlayson Lake (105G/7,8 and parts of 1, 2, and 9) and Frances Lake (parts of 105H/5 and 12) areas, southeastern Yukon. Exploration and geological services division, Yukon Region, Indian and Northern Affairs Canada, Open File 1997-3, 1:50 000 scale.

Murphy, D.C. and Piercey, S.J., 2000. Syn-mineralization faults and their re-activation, Finlayson Lake massive sulphide district, Yukon-Tanana Terrane, southeastern Yukon. In: Yukon Exploration and Geology 1999, D.S. Emond and L.H. Weston, (eds.), Exploration and Geological Services Division, Yukon Region, Indian and Northern Affairs Canada (55-66).

Murphy, D.C., Colpron, M., Gordey, S.P., Roots, C.F., Abbott, J.G., and Lipovsky, P.S., 2001. Preliminary geological map of northern Finlayson Lake area (NTS 105 G), Yukon Territory (1:100 000 scale). Exploration and Geological Services Division, Yukon Region, Indian and Northern Affairs Canada, Open File 2001-33.

Murphy, D.C., Colpron, M., Roots, C.F., Gordey, S.P., and Abbott, J.G., 2002. Finlayson Lake targeted geoscience initiative (southeastern Yukon), Part 1: Bedrock geology. In: Yukon Exploration and Geology 2001, D.S. Emond, L.H. Weston and L.L. Lewis, (eds.), Exploration and Geological Services Division, Yukon Region, Indian and Northern Affairs Canada, p. 189-207.

Murphy, D.C., Kennedy, R., and Tizzard, A., 2004. Geological map of part of Waters Creek and Fire Lake map areas (NTS 105G/1, part of 105G/2), southeastern Yukon (1:50 000 scale). Yukon Geological Survey, Open File 2004-11.

Neufeld, H.L.D., Groat, L.A., and Mortensen, J.K., 2003. Preliminary investigations of emerald mineralization in the Regal Ridge area, Finlayson Lake district, southeastern Yukon. In: Yukon Exploration and Geology 2002, D.S. Emond and L L Lewis (eds.), Exploration and Geological Services Division, Yukon Region, Indian and Northern Affairs Canada, p. 281-284.

Neufeld, H.L.D., Israel, S., Groat, L.A. and Mortensen, J.K., 2004. Geology and structural setting of the Regal Ridge emerald property, Finlayson Lake district, southeastern Yukon. In: Yukon Exploration and Geology 2003, D.S. Emond and L.L. Lewis (eds.), Yukon Geological Survey, p. 281-288. (CHAPTER 2, this work)

Neufeld, H.L.D., Groat, L.A., Mortensen, J.K., and Israel, S., in press 2005. The Regal Ridge emerald deposit: New mineralogical, geochemical, isotopic, and petrologic results, and inferred genetic model. Canadian Mineralogist. (CHAPTER 3, this work)

Nwe, Y.Y., and Grundmann, G., 1990. Evolution of metamorphic fluids in shear zones: The record from emeralds of Habachtal, Tauern Window, Austria. Lithos, vol. 25, p. 281-304.

Nwe, Y.Y., and Morteani, G., 1993. Fluid evolution in the H_2O-CH_4-CO_2-NaCl system during emerald mineralization at Gravelotte, Murchison Greenstone Belt, Northeast Transvaal, South Africa. Geochimica et Cosmochimica Acta, vol. 57, p. 89-103.

O'Neil, J.R. & Chappell, B.W., 1977. Oxygen and hydrogen isotope relations in the Berridale batholith. Journal of the Geological Society of London, vol. 133, p. 559-571.

Piercey, S.J., Hunt, J.A. & Murphy, D.C., 1999. Lithogeochemistry of meta-volcanic rocks from Yukon-Tanana Terrane, Finlayson Lake region: preliminary results. In: Yukon Exploration and Geology 1998, C.F. Roots & D.S. Emond, (eds.), Exploration and Geological Services Division, Yukon, Indian and Northern Affairs Canada p.55-66.

Piercey, S.J., Murphy, D.C., Mortensen, J.K. and Paradis, S.A., 2000a. Arc-rifting and ensialic back-arc basin magmatism in the northern Canadian Cordillera: evidence from the Yukon-Tanana Terrane, Finlayson Lake region, Yukon. Lithoprobe Report, vol.72, p.129-138.

Piercey, S.J., Murphy, D.C., and Mortensen, J.K., 2000b. Magmatic diversity in a pericratonic realm: tales from the Yukon-Tanana Terrane in the Finlayson Lake region, southeastern Yukon, Canada. Geol. Soc. Am. Program with Abstracts vol. 32, A-62.

Piercey, S.J., Murphy, D.C., Mortensen, J.K. and Paradis, S.A., 2001. Boninitic magmatism in an continental margin, Yukon-Tanana terrane, southeastern Yukon, Canada. Geology, vol. 29, p.731-734.

Piercey , S.J., Murphy, D.C., Mortensen, J.K., and Creaser, R.A., 2004. Mid-Paleozoic initiation of the northern Cordilleran marginal backarc basin: Geologic, geochemical, and neodymium isotope evidence from the oldest mafic magmatic rocks in the Yukon-Tanana terrane, Finlayson Lake district, southeast Yukon, Canada. Geological Society of America Bulletin: vol. 116, No. 9, p. 1087–1106.

Pouchou, J.-L. & Pichoir, F., 1991. Quantitative analysis of homogeneous or stratified microvolumes applying the model "PAP". In: Electron Probe Quantitation, K.F.J. Heinrich & D.E. Newbury (eds.), Plenum Press, New York, N.Y., p.31-75.

Renne, P.R., Swisher, C.C., Deino, A.L., Karner, D.B., Owens, T. & Depaolo, D.J., 1998. Intercalibration of standards, absolute ages and uncertainties in 39Ar/40Ar dating. Chemical Geology, vol. 145, p.117-152.

Schwartz, D., and Schmetzer, K., 2002. The definition of emerald: the green variety of beryl colored by chromium and/or vanadium. In: Emeralds of the world, extraLapis English No. 2: the legendary green beryl. Lapis International, East Hampton, 100p.

Shervais, J.W., 1982. Ti-V plots and the petrogenesis of modern and ophiolotic lavas. Earth and Planetary Scientific Letters, vol. 59, p. 101-118.

Sinkankas, J., 1989. Emerald and other beryls. Geoscience Press, Az., USA.

Soboleva, G.I., Tugarinov, I.A., and Khitarov, D.N., 1972. Role of calcium and magnesium in country rocks during chrysoberyl mineralization. Geokhimiya, p. 1392-1395.

Sun, S.S., and McDonough, W.F., 1989. Chemical and isotopic systematics of oceanic basalts: Implications for mantle composition and process. In: Magmatism in the ocean basins, Saunders, A.D., and Norry, M.J. (eds.). Geological society of London special publication 42, p. 313-345.

Walton, L., 1996. Exploration criteria for gemstone deposits and their application to Yukon geology. Exploration and Geological Services Division, Yukon Region, Indian and Northern Affairs Canada, Open File 1996-2.

Walton, L., 2004. Exploration criteria for gemstone deposits in the Yukon. Yukon Geological Survey Open File 2004-10.

Wedepohl, K.H., 1995. The composition of the continental crust. Geochimica et Cosmochimica Acta, Vol. 59, p.1217-1232.

Winter, J.D., 2001. An Introduction to Igneous and Metamorphic Petrology. Prentice-Hall, N.J., 697p.

APPENDIX 1.
ANALYTICAL PROCEDURES

A Philips XL30 scanning electron microscope equipped with a Princeton Gamma-Tech energy-dispersion X-ray spectrometer was used to examine polished thin sections and microprobe mounts using back-scattered-electron imaging and to obtain qualitative chemical data for mineral identification.

Electron-probe micro-analyses of beryl were obtained with a fully automated CAMECA SX-50 instrument, operating in the wavelength-dispersion mode with the following operating conditions: excitation voltage, 15 kV; beam current, 20 nA; peak count time, 50 s for Mg, Sc, K, Ca, Ti, V, Cr, Mn, Fe, Cs, 20 s for Al, Na, Si; background count-time, one-half of the peak count time; spot diameter, 30 μm. The following standards were used: albite (Na, Al, Si), diopside (Mg, Ca), orthoclase (K), rutile (Ti), scandium (Sc), vanadium (V), magnesiochromite (Cr), synthetic fayalite (Fe^{3+}), synthetic rhodonite (Mn), and pollucite (Cs). $K\alpha$ lines were used for all elements except for Cs ($L\alpha$). Data reduction was done using the 'PAP' $\phi(\rho Z)$ method (Pouchou & Pichoir 1991).

Electron-probe micro-analyses of tourmaline were obtained with the same instrument and operating conditions except peak and background count times, which were 20 and 10 s, respectively. B was fixed at the nominal value. For the elements considered, the following standards, X-ray lines and crystals were used: topaz, F$K\alpha$, TAP; albite, Na$K\alpha$, TAP; diopside, Mg$K\alpha$, Si$K\alpha$, TAP; kyanite, Al$K\alpha$, TAP; orthoclase, K$K\alpha$, PET; diopside, Ca$K\alpha$, PET; rutile, Ti$K\alpha$, PET; synthetic magnesiochromite, Cr$K\alpha$, LIF; synthetic rhodonite, Mn$K\alpha$, LIF; synthetic fayalite, Fe$K\alpha$, LIF; synthetic Ni_2SiO_4, Ni$K\alpha$, LIF.

Powder-diffraction data were collected at UBC with a Siemens D5000 diffractometer equipped with a diffracted-beam graphite monochromator and a Cu X-ray tube operated at 40 kV and 40 mA. Data were collected from 3 to 60° 2θ with a scanning step of 0.02° 2θ.

Hydrogen and oxygen isotope data data for primary igneous quartz, biotite, and muscovite from the granite and for coexisting quartz and tourmaline from the quartz veins associated with the emerald mineralization were obtained at Queen's University. Water was removed from the sample using a 5 kW radio-frequency generator. A bromine pentafluoride extraction line was used for the oxygen, and deplected uranium was used for hydrogen. The isotopes were measured with a Finnigan Mat 252 Mass spectrometer.

Whole-rock analyses of the granite and vein quartz were done by ALS Chemex Limited of North Vancouver. Lithium, Be, Cr, and Mo concentrations were determined by atomic absorption spectroscopy, B and Cl by neutron activation analysis, and F by specific ion potentiometry. All other elements were measured by induction-coupled plasma mass spectrometry (ICP-MS) or X-ray fluorescence (XRF). Whole-rock data for the schists and boninites were supplied by the Geological Survey of Canada in Ottawa. Most major elements were analyzed by XRF, FeO by wet-chemical methods, and CO_2 and H_2O by infrared spectroscopy. Trace elements data were obtained by ICP-ES (emission spectrometry) and -MS.

For $^{40}Ar/^{39}Ar$ dating each sample was first crushed and sieved to obtain fragments ranging in size from 0.5 to 2 mm. A hand magnet was passed over the samples to remove magnetic minerals and metallic crusher fragments/spall. The samples were washed in deionized water, rinsed and then air-dried at room temperature. Mineral separates were hand-picked, wrapped in aluminum foil and stacked in an irradiation capsule with similar-aged samples and neutron flux monitors (Fish Canyon Tuff sanidine, 28.02 Ma, Renne *et al.* 1998, and MAC-83 biotite, 24.36 Ma, Villeneuve *et al.* 2000). The samples were irradiated on October 14-16, 2003 at the McMaster Nuclear Reactor in Hamilton, Ontario, for 72 MWH, with a neutron flux of approximately 3×10^{16} neutrons/cm^2. Analyses ($n = 33$) of 11 neutron flux monitors irradiated with the samples produced errors of <0.25% in the J value. The samples were analyzed on March 9-10, 2004, at the Noble Gas Laboratory, Pacific Centre for Isotopic and Geochemical Research, University of British Columbia, Vancouver. The separates were step-heated at incrementally higher powers in the defocused beam of a 10W CO_2 laser (New Wave Research MIR10) until fused. The gas evolved from each step was analyzed with a VG5400 mass spectrometer equipped with an ion-counting electron multiplier. All measurements were corrected for total system blank, mass spectrometer sensitivity, mass discrimination, radioactive decay during and subsequent to irradiation, as well as interfering Ar from atmospheric contamination and the irradiation of Cl, K, and Ca. Details of the analyses are presented in Tables X and X. Errors are quoted at the 2σ (95% confidence) level and are propagated from all sources except mass spectrometer sensitivity and age of the flux monitor.

Appendix 2. Geochemistry of vein transects, True North Gems, Inc. data.

		TS2003-001 selvage	TS2003-002 qtz vn	TS2003-003 selvage	TS2003-004 host	TS2003-005 qtz vn
Be norm	ppm	57.29	10.12	100.00	16.55	1.61
Bi norm	ppm	100.00	5.56	74.07	0.76	1.44
Li norm	ppm	46.31	5.82	100.00	337.00	15.40
Sn norm	ppm	56.73	6.12	100.00	55.60	5.90
W norm	ppm	37.11	100.00	52.20	8.40	195.00
F norm	ppm	52.06	31.47	100.00	5850.00	5730.00
Be	ppm	14.15	2.5	24.7	16.55	1.61
Bi	ppm	1.62	0.09	1.2	0.76	1.44
Li	ppm	85.9	10.8	185.5	337	15.4
Sn	ppm	55.6	6	98	55.6	5.9
W	ppm	5.9	15.9	8.3	8.4	195
F	ppm	1770	1070	3400	5850	5730
Ag	ppm	0.13	<0.02	0.11	0.09	0.02
Al	%	5.83	1.22	6.49	4.09	1.2
As	ppm	<0.2	1.5	<0.2	<0.2	0.9
Ba	ppm	60	<10.0	130	550	10
Ca	%	5.89	0.68	5.79	5.12	1.5
Cd	ppm	0.23	<0.02	0.06	0.09	0.02
Ce	ppm	1.72	0.21	1.44	1.04	0.27
Co	ppm	48.9	6	47.9	36.3	4.1
Cr	ppm	445	91	412	390	138
Cs	ppm	133	4.12	254	374	1.36
Cu	ppm	201	16.4	121	146	23.8
Fe	%	7.43	0.85	7.36	5.65	0.65
Ga	ppm	9.84	2.96	12.85	9.85	4.51
Ge	ppm	0.18	0.05	0.16	0.13	0.05
Hf	ppm	0.2	<0.1	0.2	0.1	<0.1
In	ppm	0.047	0.006	0.031	0.023	<0.005
K	%	0.83	0.02	1.8	2.63	0.05
La	ppm	0.7	<0.5	0.6	<0.5	<0.5
Mg	%	8.54	0.68	8.27	7.21	0.58
Mn	ppm	1820	168	1760	1345	155
Mo	ppm	0.36	0.63	0.39	0.19	2.15
Na	%	0.47	0.1	0.65	0.25	0.1
Nb	ppm	0.8	0.1	0.9	1.6	<0.1
Ni	ppm	245	27	232	204	14.6
P	ppm	40	<10	30	70	10
Pb	ppm	1.8	0.6	2.3	1.6	1.1
Rb	ppm	177.5	4	384	600	8.6
Re	ppm	0.004	0.003	0.006	0.003	0.003
S	%	0.04	0.04	0.08	0.33	0.03
Sb	ppm	0.13	<0.05	0.09	<0.05	0.06
Se	ppm	1	1	<1	<1	<1
Sr	ppm	14.5	13.8	20.9	19.2	8.5
Ta	ppm	<0.05	<0.05	<0.05	0.05	<0.05
Te	ppm	<0.05	<0.05	<0.05	<0.05	<0.05
Th	ppm	<0.2	<0.2	<0.2	<0.2	<0.2
Ti	%	0.15	0.02	0.17	0.11	0.01
Tl	ppm	1.5	0.02	2.65	3.45	0.1
U	ppm	<0.1	<0.1	<0.1	<0.1	<0.1
V	ppm	251	27	275	176	19
Y	ppm	8.2	0.6	7.8	4.7	3.2
Zn	ppm	115	17	124	149	26
Zr	ppm	2.7	0.6	3.1	1.2	<0.5

SAMPLE	TS2003-010 selvage	TS2003-011 qtz vn	TS2003-012 selvage	TS2003-013 selvage/gouge	TS2003-014 qtz vn	TS2003-015 selvage/gouge
Be norm	14.60	72.43	100.00	30.00	85.71	100.00
Bi norm	34.00	100.00	88.00	100.00	5.88	70.59
Li norm	100.00	24.50	87.40	100.00	26.17	98.20
Sn norm	12.09	27.25	100.00	17.65	100.00	58.82
W norm	1.61	1.14	100.00	18.26	100.00	16.17
F norm	14.34	86.82	100.00	100.00	92.31	84.62
Be	2.49	12.35	17.05	0.21	0.6	0.7
Bi	0.34	1	0.88	0.17	0.01	0.12
Li	262	64.2	229	167	43.7	164
Sn	5.1	11.5	42.2	0.3	1.7	1
W	2.4	1.7	149.5	6.1	33.4	5.4
F	370	2240	2580	130	120	110
Ag	0.02	<0.02	0.06	0.03	0.02	0.05
Al	5.27	2.75	5.6	7.81	4.79	7.07
As	0.3	0.4	<0.2	<0.2	0.9	0.4
Ba	30	10	60	20	10	20
Ca	4.13	1.18	4.87	4.78	2.37	3.58
Cd	0.07	<0.02	0.21	0.05	0.03	0.06
Ce	0.98	0.44	0.94	1.2	0.48	1.33
Co	46.8	5.1	41.1	37.2	9.8	31.4
Cr	525	188	432	138	82	72
Cs	186	5.87	141	171	67.9	131.5
Cu	3.7	17.3	84.2	59.6	29.3	97.7
Fe	5.93	1.2	5.6	5.71	1.32	5.16
Ga	10.35	12.95	10.35	13.4	4.93	10.1
Ge	0.13	0.08	0.15	0.14	0.07	0.12
Hf	0.1	<0.1	0.1	0.2	<0.1	0.1
In	0.03	<0.005	0.045	0.046	0.009	0.033
K	0.66	0.08	0.98	0.17	0.15	0.13
La	<0.5	<0.5	<0.5	0.5	<0.5	0.6
Mg	7.63	0.94	6.78	5.69	1.33	5.06
Mn	1090	333	1260	957	397	859
Mo	0.07	1.63	0.18	0.21	0.31	0.25
Na	0.77	0.26	1.02	1.65	0.92	1.85
Nb	0.3	0.5	0.3	0.4	0.1	0.4
Ni	269	20.2	192.5	103	18	57.1
P	30	90	60	60	10	60
Pb	2.4	1.4	2.3	1.4	1.3	1.2
Rb	105	15.4	193	16.1	16.7	12.4
Re	<0.002	<0.002	0.002	<0.002	<0.002	<0.002
S	<0.01	<0.01	0.01	<0.01	<0.01	0.01
Sb	<0.05	<0.05	<0.05	0.06	0.05	0.08
Se	<1	<1	<1	<1	<1	<1
Sr	24.4	9.4	34.2	77.6	40	51.1
Ta	<0.05	<0.05	<0.05	<0.05	<0.05	<0.05
Te	<0.05	<0.05	<0.05	<0.05	<0.05	<0.05
Th	<0.2	<0.2	<0.2	<0.2	<0.2	<0.2
Ti	0.13	0.02	0.12	0.15	0.03	0.15
Tl	0.78	0.1	1.62	0.16	0.15	0.11
U	0.1	<0.1	0.2	0.2	<0.1	0.1
V	260	28	211	256	49	222
Y	6.6	0.8	5.9	7.8	2.4	7.2
Zn	103	75	122	77	19	75
Zr	1.6	<0.5	2.2	2.8	0.6	2.4

SAMPLE	TS2003-007 qtz vn	TS2003-008 qtz vn	TS2003-009 host	TS2003-016 aplite	TS2003-018 qtz vn	TS2003-019 qtz vn
Be norm	0.91	7.76	2.05	45.40	10.75	1.90
Bi norm	0.07	0.73	0.11	0.27	0.19	0.09
Li norm	20.80	30.10	75.60	101.00	44.40	5.50
Sn norm	3.90	35.10	15.10	11.30	27.00	6.80
W norm	11.00	82.70	22.60	4.50	360.00	4.80
F norm	600.00	1230.00	1020.00	1330.00	2910.00	760.00
Be	0.91	7.76	2.05	45.4	10.75	1.9
Bi	0.07	0.73	0.11	0.27	0.19	0.09
Li	20.8	30.1	75.6	101	44.4	5.5
Sn	3.9	35.1	15.1	11.3	27	6.8
W	11	82.7	22.6	4.5	360	4.8
F	600	1230	1020	1330	2910	760
Ag	<0.02	0.19	0.03	0.03	0.1	0.03
Al	4.07	4.22	4.5	6.61	4.36	1.79
As	0.7	<0.2	17.4	0.4	0.7	0.9
Ba	10	<10.0	20	30	50	<10.0
Ca	1.46	2.03	8.85	1.82	0.82	0.54
Cd	<0.02	0.14	0.05	0.03	<0.02	0.02
Ce	0.23	0.72	0.68	2.46	0.66	0.39
Co	9.1	30.3	14.3	7.2	28.8	43
Cr	130	224	132	56	227	201
Cs	1.84	5.09	15.15	48.7	18.7	0.63
Cu	5.9	547	52.6	44.5	217	51.5
Fe	1.32	3.94	4.18	1.36	3.26	3.21
Ga	5.33	8.43	7.46	23.2	16.4	4.17
Ge	0.07	0.12	0.1	0.07	0.1	0.09
Hf	<0.1	0.1	0.1	1.5	<0.1	<0.1
In	0.005	0.014	0.016	0.01	0.015	0.006
K	0.01	0.02	0.25	0.64	0.2	0.01
La	<0.5	<0.5	<0.5	1.1	<0.5	<0.5
Mg	1.29	3.52	3.99	1.14	3.48	1.42
Mn	191	506	1115	408	269	241
Mo	1.03	1.21	0.37	5.61	1.18	1.33
Na	0.35	0.33	0.02	3.02	0.26	0.09
Nb	0.1	0.2	0.3	3.2	0.1	0.4
Ni	32	61.1	38.3	16.8	105	36.2
P	30	150	30	30	110	50
Pb	1.2	2.1	0.9	12.4	2.1	0.9
Rb	0.7	1	48.3	107.5	28.4	0.9
Re	<0.002	0.006	<0.002	0.002	0.002	0.009
S	0.01	0.49	0.02	0.02	0.02	0.44
Sb	<0.05	0.07	0.11	<0.05	0.1	<0.05
Se	<1	1	<1	<1	<1	<1
Sr	35.1	30.2	28	39.4	32.3	33.2
Ta	<0.05	<0.05	<0.05	0.23	<0.05	<0.05
Te	<0.05	<0.05	<0.05	<0.05	<0.05	<0.05
Th	<0.2	<0.2	<0.2	3.1	<0.2	<0.2
Ti	0.06	0.09	0.08	0.03	0.06	0.04
Tl	0.02	0.13	0.28	0.72	0.3	<0.02
U	<0.1	0.1	0.1	12.4	1.1	0.4
V	67	127	150	61	106	60
Y	0.4	4.6	4.4	10.2	4.9	1.4
Zn	21	44	46	28	53	15
Zr	<0.5	2.1	1.3	20	0.5	0.7

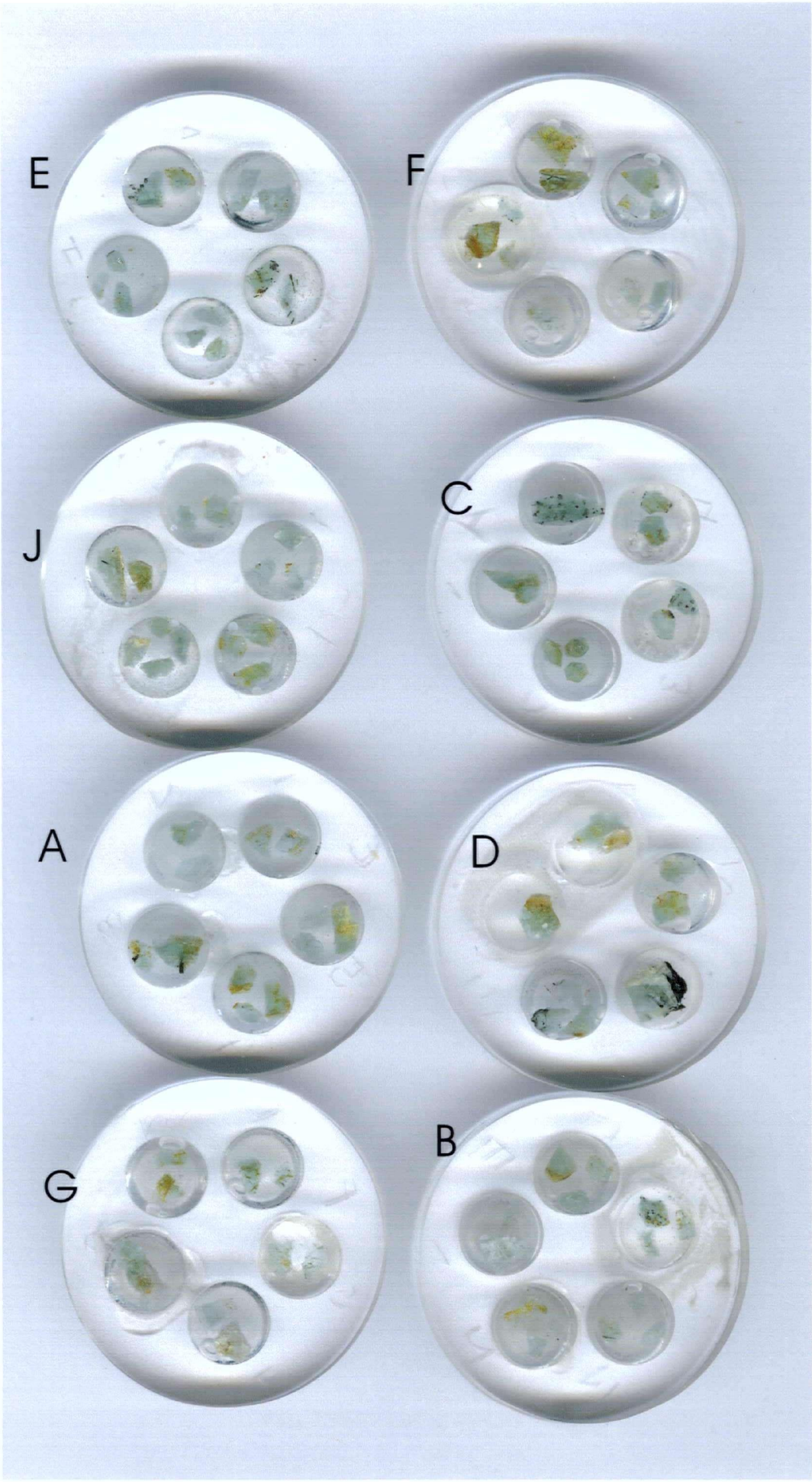
E
F
J
C
A
D
G
B

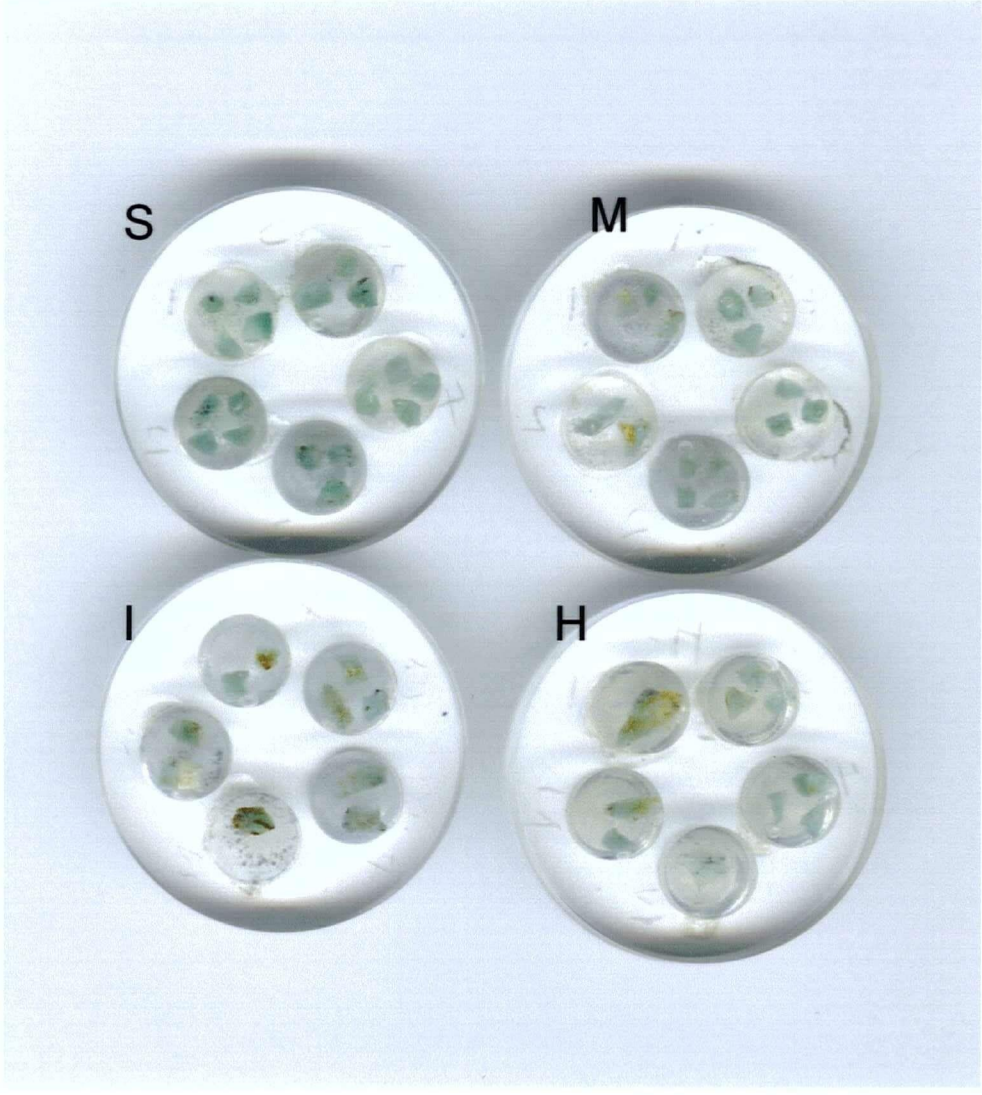
S
M
I
H

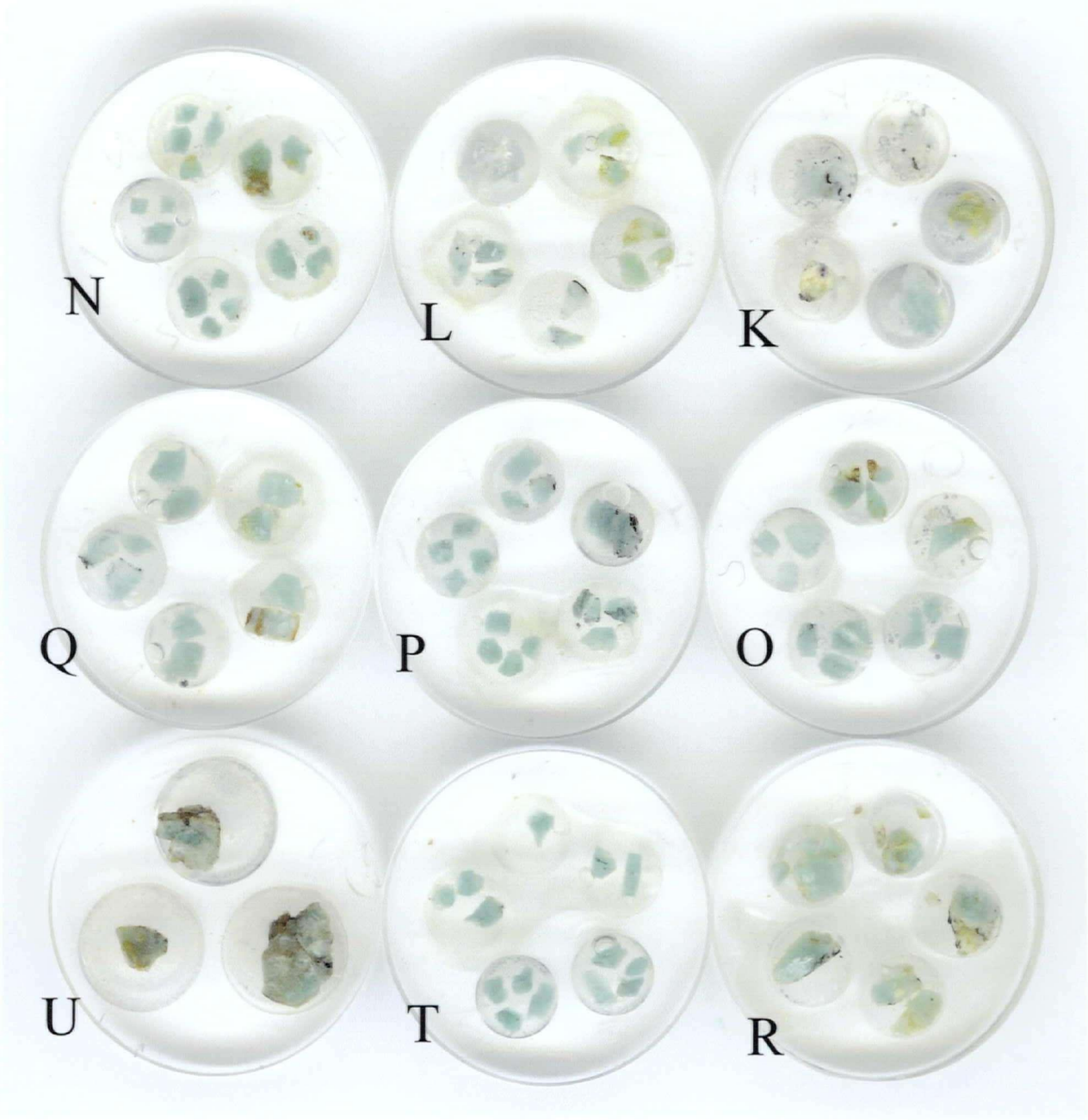
N
L
K
Q
P
O
U
T
R

Point	SAMPLE		Area												
			(R is for round in adit)	Colour 1-good, 3-crap	Fractured	Inclusions									
						Calcite	Quartz	Biotite	Pyrite	Chlorite	Scheelite	Epidote	Tour	Fluorite	Chromite
R-1	A1		R 9/10	2	sw	y		y	y						
R-2	A2	a	R 9/10	2	n					y					
R-3	A2	b	R 9/10	2	n	y	y				y				
R-4	A2	c	R 9/10	2	n	y		y	y						
R-5	A3	a	R 9/10	2	sw			y	y			y			
R-6	A3	b	R 9/10	2	y		y		y						
R-7	A4	a	R 9/10	1	sw	y									
R-8	A4	b	R 9/10	1	sw				y						
R-9	A5		R 9/10	1	?		y		y						
R-10	B1	a	R 9/10	2	y								y		
R-11	B1	b	R 9/10	2	?				y						
R-12	B2	a	R 9/10	1	y										
R-13	B2	b	R 9/10	1	?	y									
R-14	B3	a	R 9/10	1	sw	y		y	y						
R-15	B3	b	R 9/10	1	?		y		y						
R-16	B4	a	R 11	2	?										
R-17	B4	b	R 11	2	?		y								
R-18	B4	c	R 11	2	?	y	y								
R-19	B5	a	R 11	2	sw		y	y							
R-20	B5	b	R 11	2	y							y			
R-21	B5	c	R 11	2	sw										
R-22	C1	a	R 11	3	n		y								
R-23	C1	b	R 11	3	sw			y			y				
R-24	C2	a	R 11	2	n										
R-25	C2	b	R 11	2	sw	y									
R-26	C3	a	R 11	1	y	y				y	y				
R-27	C3	b	R 11	1	?		y	y	y						
R-28	C4	a	R 12	2	sw										
R-29	C4	b	R 12	2	n		y								
R-30	C4	c	R 12	2	sw		y								
R-31	C5	a	R 12	3	few	y	y								
R-32	C5	b	R 12	3	sw	y	y								
R-33	C5	c	R 12	3	?	y?									
R-34	D1	a	R 12	3	sw										
R-35	D1	b	R 12	3	sw	y									
R-36	D1	c	R 12	3	few										
R-37	D2	a	R 12	3	few		y		y						
R-38	D2	b	R 12	3	few		y								
R-39	D2	c	R 12	3	sw							y			
R-40	D3	a	R 8	3	few	y	y								
R-41	D3	b	R 8	3	n		y								
R-42	D4	a	R 8	3	sw		y								
R-43	D4	b	R 8	3	n	y	y								
R-44	D5	a	R 8	3	sw		y								
R-45	D5	b	R 8	3	y		y								
R-46	D5	c	R 8	3	?	y									
R-47	D5	d	R 8	3	?	y						y			
R-48	E1	a	R 8	3	y		y								
R-49	E1	b	R 8	3	sw										
R-50	E2	a	R 8	3	y	y									
R-51	E2	b	R 8	3	few		y						y		
R-52	E2	c	R 8	3	?							y			
R-53	E3	a	R 8	3	few										
R-54	E3	b	R 8	3	y										
R-55	E3	c	R 8	3	few										
R-56	E4	a	R 13	3	few										
R-57	E4	b	R 13	3	y	y		y	y						
R-58	E4	c	R 13	3	few				y						
R-59	E5	a	R 13	2	y	y									
R-60	E5	b	R 13	2	sw										
R-61	E5	c	R 13	2	n										
R-62	F1	a	R 13	2	few										
R-63	F1	b	R 13	2	sw										
R-64	F2	a	R 13	3	sw		y				y				
R-65	F2	b	R 13	3	few										
R-66	F5		R 14	2	sw	y	y								
R-67	F5	a	R 14	3	n										
R-68	F4	b	R 14	3	y	y	y			y			y		

Point	SAMPLE		Area												
			(R is for round in adit)	Colour 1-good, 3-crap	Fractured	Inclusions									
						Calcite	Quartz	Biotite	Pyrite	Chlorite	Scheelite	Epidote	Tour	Fluorite	Chromite
R-69	F4	a	R 14	3	y	y		y							
R-70	F3	b	R 14	3	few	y		y	y				y		
R-71	G1		R 14	3	few										
R-72	G2	a	R 14	3	n	y	y								
R-73	G2	b	R 14	3	y	y									
R-74	G3	a	R 7	3	n										
R-75	G3	b	R 7	3	few	y									
R-76	G3	c	R 7	3	n										
R-77	G4	a	R 7	2	few		y								
R-78	G4	b	R 7	2	few	y	y		y						
R-79	G5	a	R 7	2	n	y			y						
R-80	G5	b	R 7	2	few		y		y						
R-81	G5	c	R 7	2	few										
R-90	H1		R 7	3	few				y			y			
R-91	H2	a	R 7	3	few			y?				y	y?		
R-92	H2	b	R 7	3	n										
R-93	H3		R 7	3	n										
R-94	H4	a	R 15	2	y										
R-95	H4	b	R 15	2	y	y						y			
R-96	H4	c	R 15	2	few										
R-97	H5	a	R 15	3	few		y								
R-98	H5	b	R 15	3	sw										
R-99	H5	c	R 15	3	n			y	y						
R-100	I1	a	R 15	2	sw	y						y			
R-101	I1	b	R 15	2	y		y	y							
R-102	I2	a	R 15	2	n	y	y								
R-103	I2	b	R 15	2	sw	y	y							y	
R-104	I3		R 15	2	sw	y	y								
R-105	I4	a	R 16	3	few	y	y	y	y						
R-106	I4	b	R 16	3	few		y								
R-107	I5	a	R 16	3	few	y		y	y						
R-108	I5	b	R 16	3	n	y									
R-109	I5	c	R 16	3	few	y									
R-82	J1		R 16	3	y	y							y		
R-83	J2	a	R 16	2	y										
R-84	J2	b	R 16	2	few	y	y					y			
R-85	J3		R 16	2	y		y		y						
R-86	J4		R 16	1	few	y		y			y				
R-87	J5	a	R 17	3	few										
R-88	J5	b	R 17	3	sw		y	y	y		y				
R-89	J5	c	R 17	3					y			y			
R-156	K1		R 17	3	y				y			y			
R-157	K2		R 17	3	y				y			y			
R-158	K3		R 17	2	n							y			
R-159	K4		R 17	3	sw						y	y			
R-160	K5	a	R 3	3	few				y			y			
R-161	K5	b	R 3	3	n										
R-162	K5	c	R 3	3	n				y			y			
R-143	L1		R 3	2	y	y	y								
R-144	L2	a	R 3	2	n		y		y						
R-145	L2	b	R 3	2	sw							y			
R-146	L2	c	R 3	2	few		y					y			
R-147	L3	a	R 3	3	few	y	y		y						
R-148	L3	b	R 3	3	few	y			y						
R-149	L3	b	R 3	3	few	y			y						
R-150	L4	a	R 4	3	few	y			y						
R-151	L4	b	R 4	3	sw	y									
R-152	L4	c	R 4	3	few	y									
R-153	L5	a	R 4	3	n										
R-154	L5	b	R 4	3	n			y	y						
R-155	L5	c	R 4	3	n	y									
R-128	M1	a	R 4	3	few										
R-129	M1	b	R 4	3	few										
R-130	M1	c	R 4	3	n										
R-131	M2	a	R 4	2	few	y									
R-132	M2	b	R 4	2		y			y						

Point	SAMPLE		Area												
			(R is for round in adit)	Colour 1-good, 3-crap	Fractured	Inclusions									
						Calcite	Quartz	Biotite	Pyrite	Chlorite	Scheelite	Epidote	Tour	Fluorite	Chromite
R-133	M3	a	MattScar	2	few		y	y							
R-134	M3	b	MattScar	2	few										
R-135	M3	c	MattScar	2	y			y							
R-136	M3	d	MattScar	2	few			y							
R-137	M4	a	MattScar	2	few										
R-138	M4	b	MattScar	2	few										
R-139	M4	c	MattScar	2	few		y								
R-140	M5	a	MattScar	2	n										
R-141	M5	b	MattScar	2			y								
R-142	M5	c	MattScar	2	n										
R-163	N1	a	Far West	1	y		y								
R-164	N1	b	Far West	1	sw										
R-165	N1	c	Far West	1	few		y	y							
R-166	N2	a	Far West	1	y			y	y						
R-167	N2	b	Far West	1	sw										
R-168	N2	c	Far West	1			y		y						
R-169	N2	d	Far West	1	y		y	y							
R-170	N3	a	Far West	1	y								y		
R-171	N3	b	Far West	1	sw						y				
R-172	N3	c	Far West	1	few		y								
R-173	N4	a	Area 51	1	y		y		y						
R-174	N4	b	Area 51	1	sw			y							
R-175	N5	a	Area 51	1	few		y	y							
R-176	N5	b	Area 51	1	y										
R-177	N5	c	Area 51	1	few		y	y							
R-178	N5	d	Area 51	1	few		y								
R-179	O1	a	Area 51	1	n		y		y				y		
R-180	O1	b	Area 51	1	few										
R-181	O1	c	Area 51	1	few								y		
R-182	O2	a	Area 10	2	n										
R-183	O2	b	Area 10	2	n										
R-184	O2	c	Area 10	2	n										
R-185	O3	a	Area 10	1	y		y								
R-186	O3	b	Area 10	1	n										
R-187	O3	c	Area 10	1	few								y		
R-188	O4	a	Area 10	1	n				y						
R-189	O4	b	Area 10	1	sw										
R-190	O4	c	Area 10	1	sw										
R-191	O5		Area 10	1	n			y							
R-192	O5		Area 10	1	n			y							
R-193	P1	a	Area 4	1	few										
R-194	P1	b	Area 4	1	y										
R-195	P1	c	Area 4	1	y										
R-196	P1	d	Area 4	1	n										
R-197	P2	a	Area 4	1	few		y								
R-198	P2	b	Area 4	1	sw		y								
R-199	P2	c	Area 4	1	n										
R-200	P2	d	Area 4	1	n										
R-201	P3	a	Area 4	1	few				y						
R-202	P3	b	Area 4	1	y										
R-203	P3	c	Area 4	1	n										
R-204	P4		SW Vein	1	sw	y			y						
R-205	P4		SW Vein	1	sw	y			y						
R-206	P5	c	SW Vein	1	y	y			y						
R-207	P5	a	SW Vein	1	n										
R-208	P5	b	SW Vein	1	few										
R-209	Q1	a	SW Vein	1	few										
R-210	Q1	b	SW Vein	1	y						y				
R-211	Q2	a	SW Vein	2	few										
R-212	Q2	b	SW Vein	2	n								y		
R-213	Q2	c	SW Vein	2	n	y			y						
R-214	Q3	a	SW Vein	1	y										
R-215	Q3	b	SW Vein	1	y										

Point	SAMPLE		Area (R is for round in adit)	Colour 1-good, 3-crap	Fractured	Inclusions									
						Calcite	Quartz	Biotite	Pyrite	Chlorite	Scheelite	Epidote	Tour	Fluorite	Chromite
R-216	Q4	a	Area 14	2	n										
R-217	Q4	b	Area 14	2	y	y		y	y		y				
R-218	Q5	a	Area 14	2	y				y						
R-219	Q5	b	Area 14	2	few										
R-234	R1	a	Area 14	1	few										
R-235	R1	c	Area 14	1	sw						y				
R-236	R2		Area 14	1	few								y		
R-237	R3	a	Area 14	2	sw						y				
R-238	R3	b	Area 14	2	sw										
R-239	R3	c	Area 14	2	y										
R-240	R4		Area 14	1	few								y		
R-241	R5	a	Area 14	2	y										
R-242	R5	b	Area 14	2	y										
R-110	S1	a	Area 9	1	n			y	y						
R-111	S1	b	Area 9	1	n		y		y			y			
R-112	S1	c	Area 9	1	few				y						y
R-113	S1	d	Area 9	1	n										
R-114	S2	a	Area 9	1	few				y				y		
R-115	S2	b	Area 9	1	n										
R-116	S2	c	Area 9	1	n										
R-117	S2	d	Area 9	1	few			y							
R-118	S3	a	Area 9	1	n	y	y								y
R-119	S3	b	Area 9	1	n										
R-120	S3	c	Area 9	1	n										
R-121	S4	a	Area 6	2	n										
R-122	S4	b	Area 6	2	n										
R-123	S4	c	Area 6	2	y										
R-124	S4	d	Area 6	2	sw										
R-125	S5	a	Area 6	1	y										
R-126	S5	b	Area 6	1	n										
R-127	S5	c	Area 6	1	few		y			y					
R-220	T1	a	Area 6	1	y								y		
R-221	T1	b	Area 6	1	y	y							y		
R-222	T1	c	Area 6	1	n								y		
R-223	T2	a	Area 6-7	1	n			y							
R-224	T2	b	Area 6-7	1	few										
R-225	T2	c	Area 6-7	1	few		y	y	y						
R-226	T2	d	Area 6-7	1	n										
R-227	T3	a	Area 6-8	1	sw			y							
R-228	T3	b	Area 6-8	1	few		y								
R-229	T3	c	Area 6-8	1	n										
R-230	T3	d	Area 6-8	1	few		y								
R-231	T4	a	Area 6-9	1	n										
R-232	T4	b	Area 6-9	1	few								y		
R-233	T5		Area 6-10	1	few		y	y							
R-243	U3	1	HeroAplite	2	few		y	y		y			y		
R-244	U3	2	HeroAplite	2	few		y	y		y			y		
R-245	U3	3	HeroAplite	2	few		y	y		y			y		
R-246	U3	4	HeroAplite	2	few		y	y		y			y		
R-247	U3	5	HeroAplite	2	few		y	y		y			y		
R-248	U1	1	HeroAplite	1	sw		y					y			
R-249	U1	2	HeroAplite	1	sw		y					y			
R-250	U1	3	HeroAplite	1	sw		y					y			
R-251	U1	4	HeroAplite	1	sw		y					y			
R-252	U1	5	HeroAplite	1	sw		y					y			
R-253	U2	1	HeroAplite	1	few		y	y		y			y		y
R-254	U2	2	HeroAplite	1	few		y	y		y			y		y
R-255	U2	3	HeroAplite	1	few		y	y		y			y		y
R-256	U2	4	HeroAplite	1	few		y	y		y			y		y
R-257	U2	5	HeroAplite	1	few		y	y		y			y		y

Data for emerald from Mattscar Zone

Point	133	134	135	136	137	138	139	140	141	142	Mattscar AVG	STDEV
NA2O	1.10	1.18	1.24	1.08	0.81	1.09	1.03	1.22	1.17	1.03	1.10	0.12
MGO	1.24	1.38	1.52	1.25	0.86	1.22	1.20	1.41	1.34	1.13	1.26	0.17
AL2O3	15.68	15.67	15.69	15.67	16.53	15.56	15.64	15.60	15.56	16.00	15.76	0.28
SIO2	64.97	64.70	64.93	63.95	65.04	64.51	64.94	64.35	64.46	64.21	64.61	0.35
K2O	0.02	0.04	0.03	0.02	0.04	0.03	0.03	0.04	0.04	0.02	0.03	0.01
CAO	0.03	0.03	0.06	0.02	0.02	0.03	0.03	0.03	0.04	0.03	0.03	0.01
SC2O3	0.06	0.04	0.01	0.06	0.03	0.07	0.06	0.03	0.05	0.03	0.04	0.02
TIO2	0.00	0.00	0.00	0.00	0.00	0.01	0.02	0.02	0.00	0.01	0.01	0.01
V2O3	0.03	0.02	0.02	0.01	0.02	0.05	0.04	0.03	0.05	0.03	0.03	0.01
CR2O3	0.74	0.56	0.54	0.69	0.29	0.85	0.66	0.52	0.74	0.67	0.63	0.15
MNO	0.00	0.00	0.02	0.01	0.00	0.00	0.00	0.00	0.00	0.03	0.01	0.01
FEO	0.47	0.48	0.40	0.47	0.42	0.49	0.45	0.47	0.47	0.41	0.45	0.03
CS2O	0.13	0.10	0.10	0.10	0.10	0.14	0.11	0.10	0.13	0.12	0.11	0.01
BEO *	13.49	13.45	13.50	13.31	13.50	13.41	13.46	13.38	13.41	13.38	13.43	0.06
H2O	2.19	2.26	2.31	2.18	1.95	2.19	2.13	2.30	2.25	2.13	2.19	0.10
TOTAL	100.15	99.91	100.37	98.82	99.61	99.65	99.80	99.50	99.71	99.23	99.68	0.42
NA+	0.197	0.212	0.222	0.196	0.145	0.197	0.185	0.221	0.211	0.186	0.197	0.021
MG2+	0.171	0.191	0.210	0.175	0.119	0.169	0.166	0.196	0.186	0.157	0.174	0.024
AL3+	1.711	1.715	1.710	1.733	1.802	1.708	1.710	1.716	1.708	1.760	1.727	0.029
SI4+	6.015	6.008	6.005	6.000	6.015	6.008	6.024	6.004	6.004	5.993	6.008	0.008
K+	0.002	0.005	0.004	0.002	0.005	0.004	0.004	0.005	0.005	0.002	0.004	0.001
CA2+	0.003	0.003	0.006	0.002	0.002	0.003	0.003	0.003	0.004	0.003	0.003	0.001
SC3+	0.005	0.003	0.001	0.005	0.002	0.006	0.005	0.002	0.004	0.002	0.004	0.002
TI4+	0.000	0.000	0.000	0.000	0.000	0.001	0.001	0.001	0.000	0.001	0.000	0.000
V3+	0.002	0.001	0.001	0.001	0.001	0.004	0.003	0.002	0.004	0.002	0.002	0.001
CR3+	0.054	0.041	0.039	0.051	0.021	0.063	0.048	0.038	0.054	0.049	0.046	0.011
MN2+	0.000	0.000	0.002	0.001	0.000	0.000	0.000	0.000	0.000	0.002	0.001	0.001
FE2+	0.036	0.037	0.031	0.037	0.032	0.038	0.035	0.037	0.037	0.032	0.035	0.002
CS+	0.005	0.004	0.004	0.004	0.004	0.006	0.004	0.004	0.005	0.005	0.005	0.001
BE2+	3.000	3.000	3.000	3.000	3.000	3.000	3.000	3.000	3.000	3.000	3.000	0.000
CATSUM	11.202	11.222	11.234	11.207	11.149	11.205	11.188	11.230	11.222	11.196	11.206	0.024

Data for emerald from Aplite

Point	243	244	245	246	247	248	249	250	251	252
NA2O	1.53	1.47	1.46	1.55	1.43	1.52	1.48	1.39	1.42	1.18
MGO	1.81	1.65	1.79	1.78	1.63	1.84	1.77	1.70	1.68	1.36
AL2O3	15.00	15.32	15.08	15.14	15.22	15.09	15.07	15.29	15.11	16.06
SIO2	63.56	63.42	63.67	63.54	63.96	63.39	63.72	63.72	63.56	64.00
K2O	0.03	0.04	0.04	0.02	0.01	0.03	0.03	0.02	0.02	0.02
CAO	0.04	0.02	0.03	0.03	0.02	0.04	0.02	0.03	0.04	0.01
SC2O3	0.01	0.02	0.01	0.01	0.01	0.02	0.03	0.00	0.02	0.02
TIO2	0.00	0.00	0.01	0.01	0.00	0.02	0.01	0.00	0.00	0.02
V2O3	0.04	0.03	0.00	0.04	0.02	0.01	0.03	0.02	0.01	0.02
CR2O3	0.54	0.55	0.65	0.46	0.49	0.52	0.65	0.59	0.59	0.12
MNO	0.01	0.02	0.00	0.01	0.00	0.02	0.01	0.00	0.03	0.02
FEO	0.71	0.57	0.63	0.68	0.61	0.71	0.65	0.57	0.60	0.45
CS2O	0.15	0.13	0.10	0.16	0.13	0.13	0.15	0.10	0.09	0.14
BEO *	13.26	13.25	13.28	13.26	13.31	13.24	13.29	13.29	13.24	13.34
H2O	2.56	2.51	2.50	2.58	2.47	2.55	2.52	2.44	2.47	2.26
TOTAL	99.25	99.00	99.25	99.27	99.31	99.13	99.43	99.16	98.88	99.02
NA+	0.279	0.269	0.266	0.283	0.260	0.278	0.270	0.253	0.260	0.214
MG2+	0.254	0.232	0.251	0.250	0.228	0.259	0.248	0.238	0.236	0.190
AL3+	1.666	1.702	1.672	1.680	1.683	1.677	1.669	1.693	1.679	1.772
SI4+	5.988	5.980	5.988	5.984	6.003	5.978	5.987	5.988	5.994	5.991
K+	0.004	0.005	0.005	0.002	0.001	0.004	0.004	0.002	0.002	0.002
CA2+	0.004	0.002	0.003	0.003	0.002	0.004	0.002	0.003	0.004	0.001
SC3+	0.001	0.002	0.001	0.001	0.001	0.002	0.002	0.000	0.002	0.002
TI4+	0.000	0.000	0.001	0.001	0.000	0.001	0.001	0.000	0.000	0.001
V3+	0.003	0.002	0.000	0.003	0.002	0.001	0.002	0.002	0.001	0.002
CR3+	0.040	0.041	0.048	0.034	0.036	0.039	0.048	0.044	0.044	0.009
MN2+	0.001	0.002	0.000	0.001	0.000	0.002	0.001	0.000	0.002	0.002
FE2+	0.056	0.045	0.050	0.054	0.048	0.056	0.051	0.045	0.047	0.035
CS+	0.006	0.005	0.004	0.006	0.005	0.005	0.006	0.004	0.004	0.006
BE2+	3.000	3.000	3.000	3.000	3.000	3.000	3.000	3.000	3.000	3.000
CATSUM	11.302	11.286	11.288	11.302	11.269	11.305	11.291	11.272	11.276	11.226

Data for emerald from Aplite

Point	253	254	255	256	257	Aplite AVG	STD DEV
NA2O	1.05	1.04	1.05	1.10	1.02	1.31	0.20
MGO	1.20	1.13	1.06	1.27	1.11	1.52	0.28
AL2O3	15.90	15.87	15.88	15.67	15.64	15.42	0.36
SIO2	63.71	63.90	64.33	63.78	64.00	63.75	0.24
K2O	0.03	0.04	0.03	0.03	0.03	0.03	0.01
CAO	0.02	0.04	0.02	0.02	0.02	0.03	0.01
SC2O3	0.06	0.05	0.04	0.04	0.05	0.03	0.02
TIO2	0.01	0.00	0.00	0.00	0.00	0.01	0.01
V2O3	0.04	0.03	0.05	0.03	0.03	0.03	0.01
CR2O3	0.60	0.63	0.72	0.57	0.65	0.56	0.13
MNO	0.01	0.01	0.01	0.01	0.00	0.01	0.01
FEO	0.43	0.49	0.45	0.46	0.45	0.56	0.10
CS2O	0.09	0.09	0.18	0.11	0.15	0.13	0.03
BEO *	13.29	13.31	13.38	13.27	13.29	13.29	0.04
H2O	2.15	2.14	2.15	2.19	2.13	2.37	0.17
TOTAL	98.59	98.77	99.35	98.55	98.57	99.04	0.29
NA+	0.191	0.189	0.190	0.201	0.186	0.239	0.037
MG2+	0.168	0.158	0.147	0.178	0.156	0.213	0.040
AL3+	1.761	1.755	1.746	1.737	1.732	1.708	0.037
SI4+	5.987	5.994	6.002	6.000	6.015	5.992	0.009
K+	0.004	0.005	0.004	0.004	0.004	0.003	0.001
CA2+	0.002	0.004	0.002	0.002	0.002	0.003	0.001
SC3+	0.005	0.004	0.003	0.003	0.004	0.002	0.001
TI4+	0.001	0.000	0.000	0.000	0.000	0.000	0.000
V3+	0.003	0.002	0.004	0.002	0.002	0.002	0.001
CR3+	0.045	0.047	0.053	0.042	0.048	0.041	0.010
MN2+	0.001	0.001	0.001	0.001	0.000	0.001	0.001
FE2+	0.034	0.038	0.035	0.036	0.035	0.044	0.008
CS+	0.004	0.004	0.007	0.004	0.006	0.005	0.001
BE2+	3.000	3.000	3.000	3.000	3.000	3.000	0.000
CATSUM	11.205	11.201	11.195	11.211	11.190	11.255	0.043

Data for emerald from Far West zone.

Point	163	164	165	166	167	168	169	170	171	172	FarWest AVG	STD DEV
NA2O	0.95	0.89	0.54	0.74	0.73	0.94	0.76	0.88	0.95	1.00	0.84	0.14
MGO	1.13	1.07	0.59	0.87	0.77	1.08	0.84	1.05	1.16	1.22	0.98	0.19
AL2O3	16.06	16.17	17.06	16.56	16.48	16.24	16.11	15.85	15.66	15.53	16.17	0.43
SIO2	64.07	65.16	64.66	65.01	64.31	64.95	64.09	64.74	63.67	64.63	64.53	0.45
K2O	0.02	0.02	0.02	0.03	0.01	0.04	0.01	0.02	0.03	0.03	0.02	0.01
CAO	0.05	0.04	0.01	0.03	0.02	0.04	0.01	0.03	0.03	0.04	0.03	0.01
SC2O3	0.05	0.02	0.02	0.04	0.04	0.00	0.02	0.04	0.03	0.06	0.03	0.02
TIO2	0.00	0.01	0.00	0.00	0.00	0.01	0.00	0.00	0.00	0.00	0.00	0.00
V2O3	0.05	0.03	0.04	0.02	0.03	0.01	0.02	0.00	0.02	0.05	0.03	0.02
CR2O3	0.73	0.69	0.72	0.60	0.59	0.83	1.32	0.99	1.22	1.17	0.89	0.26
MNO	0.02	0.01	0.00	0.00	0.01	0.01	0.00	0.01	0.01	0.01	0.01	0.01
FEO	0.35	0.33	0.27	0.40	0.36	0.36	0.39	0.38	0.40	0.43	0.37	0.04
CS2O	0.09	0.07	0.07	0.10	0.13	0.07	0.13	0.16	0.11	0.12	0.11	0.03
BEO *	13.36	13.54	13.49	13.53	13.38	13.53	13.37	13.45	13.29	13.44	13.44	0.08
H2O	2.07	2.02	1.72	1.89	1.88	2.06	1.91	2.01	2.07	2.11	1.97	0.11
TOTAL	99.00	100.07	99.21	99.82	98.74	100.17	98.98	99.61	98.65	99.84	99.41	0.53
NA+	0.172	0.159	0.097	0.132	0.132	0.168	0.138	0.158	0.173	0.180	0.15	0.024
MG2+	0.157	0.147	0.081	0.120	0.107	0.149	0.117	0.145	0.163	0.169	0.14	0.027
AL3+	1.769	1.758	1.861	1.802	1.812	1.766	1.773	1.734	1.735	1.700	1.77	0.043
SI4+	5.987	6.011	5.984	6.001	6.000	5.994	5.985	6.011	5.984	6.003	6.00	0.010
K+	0.002	0.002	0.002	0.004	0.001	0.005	0.001	0.002	0.004	0.004	0.00	0.001
CA2+	0.005	0.004	0.001	0.003	0.002	0.004	0.001	0.003	0.003	0.004	0.00	0.001
SC3+	0.004	0.002	0.002	0.003	0.003	0.000	0.002	0.003	0.002	0.005	0.00	0.001
TI4+	0.000	0.001	0.000	0.000	0.000	0.001	0.000	0.000	0.000	0.000	0.00	0.000
V3+	0.004	0.002	0.003	0.001	0.002	0.001	0.001	0.000	0.002	0.004	0.00	0.001
CR3+	0.054	0.050	0.053	0.044	0.044	0.061	0.097	0.073	0.091	0.086	0.07	0.019
MN2+	0.002	0.001	0.000	0.000	0.001	0.001	0.000	0.001	0.001	0.001	0.00	0.001
FE2+	0.027	0.025	0.021	0.031	0.028	0.028	0.030	0.030	0.031	0.033	0.03	0.003
CS+	0.004	0.003	0.003	0.004	0.005	0.003	0.005	0.006	0.004	0.005	0.00	0.001
BE2+	3.000	3.000	3.000	3.000	3.000	3.000	3.000	3.000	3.000	3.000	3.00	0.000
CATSUM	11.187	11.165	11.108	11.144	11.138	11.179	11.151	11.167	11.192	11.194	11.16	0.026

Data for emerald from Original discovery zones

Point	110	111	112	113	114	115	116	117	118	119	120	121
NA2O	1.05	1.01	0.90	1.03	0.87	0.86	0.92	1.01	1.07	0.91	1.03	0.78
MGO	1.26	1.15	1.06	1.30	0.96	0.91	0.99	1.23	1.34	1.04	1.32	0.94
AL2O3	15.25	15.93	15.90	15.19	16.19	16.54	16.25	15.37	15.36	15.87	15.53	16.20
SIO2	63.49	63.32	64.23	63.19	64.11	63.64	63.80	63.83	63.56	63.81	63.09	63.77
K2O	0.03	0.02	0.02	0.04	0.04	0.02	0.02	0.02	0.03	0.02	0.03	0.03
CAO	0.03	0.02	0.01	0.03	0.04	0.03	0.01	0.04	0.04	0.02	0.02	0.00
SC2O3	0.04	0.02	0.02	0.02	0.00	0.02	0.03	0.06	0.02	0.02	0.04	0.02
TIO2	0.01	0.00	0.00	0.01	0.02	0.00	0.00	0.00	0.00	0.00	0.00	0.00
V2O3	0.03	0.01	0.03	0.00	0.04	0.02	0.02	0.05	0.01	0.02	0.01	0.04
CR2O3	1.15	0.71	0.77	1.46	0.89	0.58	0.66	1.17	1.05	1.05	0.91	0.71
MNO	0.00	0.01	0.00	0.01	0.00	0.02	0.00	0.00	0.00	0.01	0.00	0.00
FEO	0.48	0.45	0.38	0.65	0.36	0.39	0.41	0.45	0.52	0.48	0.53	0.44
CS2O	0.15	0.11	0.10	0.13	0.08	0.12	0.15	0.12	0.17	0.18	0.21	0.12
BEO *	13.22	13.22	13.35	13.20	13.37	13.31	13.32	13.29	13.25	13.31	13.18	13.29
H2O	2.15	2.12	2.02	2.13	2.00	1.99	2.04	2.12	2.17	2.03	2.13	1.92
TOTAL	98.34	98.10	98.79	98.39	98.97	98.45	98.62	98.76	98.59	98.77	98.03	98.26
NA+	0.192	0.185	0.163	0.189	0.158	0.156	0.167	0.184	0.196	0.166	0.189	0.142
MG2+	0.177	0.162	0.148	0.183	0.134	0.127	0.138	0.172	0.188	0.145	0.186	0.132
AL3+	1.698	1.773	1.753	1.693	1.782	1.829	1.796	1.702	1.706	1.755	1.735	1.794
SI4+	5.998	5.980	6.008	5.977	5.987	5.971	5.984	5.998	5.991	5.986	5.979	5.991
K+	0.004	0.002	0.002	0.005	0.005	0.002	0.002	0.002	0.004	0.002	0.004	0.004
CA2+	0.003	0.002	0.001	0.003	0.004	0.003	0.001	0.004	0.004	0.002	0.002	0.000
SC3+	0.003	0.002	0.002	0.002	0.000	0.002	0.002	0.005	0.002	0.002	0.003	0.002
TI4+	0.001	0.000	0.000	0.001	0.001	0.000	0.000	0.000	0.000	0.000	0.000	0.000
V3+	0.002	0.001	0.002	0.000	0.003	0.002	0.002	0.004	0.001	0.002	0.001	0.003
CR3+	0.086	0.053	0.057	0.109	0.066	0.043	0.049	0.087	0.078	0.078	0.068	0.053
MN2+	0.000	0.001	0.000	0.001	0.000	0.002	0.000	0.000	0.000	0.001	0.000	0.000
FE2+	0.038	0.036	0.030	0.051	0.028	0.031	0.032	0.035	0.041	0.038	0.042	0.035
CS+	0.006	0.004	0.004	0.005	0.003	0.005	0.006	0.005	0.007	0.007	0.008	0.005
BE2+	3.000	3.000	3.000	3.000	3.000	3.000	3.000	3.000	3.000	3.000	3.000	3.000
CATSUM	11.208	11.201	11.170	11.220	11.170	11.173	11.180	11.199	11.218	11.183	11.218	11.159

Data for emerald from Original discovery zones

Point	122	123	124	125	126	127	173	174	175	176	177	178
NA2O	1.08	1.11	1.15	1.20	1.03	1.18	1.03	1.04	1.15	1.10	1.12	1.08
MGO	1.24	1.27	1.33	1.45	1.24	1.38	1.21	1.23	1.35	1.40	1.34	1.27
AL2O3	15.94	15.73	15.22	15.72	15.62	15.34	15.86	15.83	15.50	15.24	15.61	15.97
SIO2	63.17	63.82	63.71	63.28	63.69	63.20	64.22	64.45	63.77	64.43	63.77	64.93
K2O	0.03	0.03	0.04	0.04	0.02	0.03	0.03	0.03	0.03	0.04	0.03	0.03
CAO	0.04	0.02	0.04	0.05	0.02	0.03	0.02	0.03	0.02	0.06	0.03	0.05
SC2O3	0.05	0.05	0.07	0.02	0.04	0.04	0.06	0.07	0.07	0.01	0.06	0.05
TIO2	0.00	0.01	0.00	0.00	0.01	0.00	0.00	0.00	0.01	0.00	0.01	0.00
V2O3	0.04	0.04	0.05	0.04	0.05	0.01	0.03	0.02	0.02	0.03	0.02	0.03
CR2O3	0.58	0.62	0.98	0.55	0.92	1.03	0.82	0.76	1.06	1.14	0.85	0.72
MNO	0.01	0.01	0.01	0.02	0.00	0.00	0.00	0.00	0.00	0.01	0.00	0.00
FEO	0.34	0.43	0.47	0.38	0.43	0.54	0.46	0.43	0.51	0.47	0.48	0.36
CS2O	0.07	0.13	0.11	0.07	0.09	0.14	0.11	0.08	0.07	0.08	0.09	0.07
BEO *	13.20	13.30	13.26	13.22	13.28	13.20	13.39	13.42	13.32	13.39	13.31	13.52
H2O	2.18	2.20	2.24	2.28	2.13	2.26	2.13	2.14	2.24	2.19	2.21	2.18
TOTAL	97.97	98.77	98.68	98.32	98.57	98.38	99.37	99.53	99.12	99.59	98.93	100.26
NA+	0.198	0.202	0.210	0.220	0.188	0.216	0.186	0.188	0.209	0.199	0.204	0.193
MG2+	0.175	0.178	0.187	0.204	0.174	0.195	0.168	0.171	0.189	0.195	0.187	0.175
AL3+	1.777	1.741	1.690	1.750	1.732	1.711	1.743	1.736	1.713	1.675	1.727	1.739
SI4+	5.975	5.994	6.002	5.976	5.991	5.980	5.990	5.998	5.981	6.008	5.985	5.998
K+	0.004	0.004	0.005	0.005	0.002	0.004	0.004	0.004	0.004	0.005	0.004	0.004
CA2+	0.004	0.002	0.004	0.005	0.002	0.003	0.002	0.003	0.002	0.006	0.003	0.005
SC3+	0.004	0.004	0.006	0.002	0.003	0.003	0.005	0.006	0.006	0.001	0.005	0.004
TI4+	0.000	0.001	0.000	0.000	0.001	0.000	0.000	0.000	0.001	0.000	0.001	0.000
V3+	0.003	0.003	0.004	0.003	0.004	0.001	0.002	0.001	0.002	0.002	0.002	0.002
CR3+	0.043	0.046	0.073	0.041	0.068	0.077	0.060	0.056	0.079	0.084	0.063	0.053
MN2+	0.001	0.001	0.001	0.002	0.000	0.000	0.000	0.000	0.000	0.001	0.000	0.000
FE2+	0.027	0.034	0.037	0.030	0.034	0.043	0.036	0.033	0.040	0.037	0.038	0.028
CS+	0.003	0.005	0.004	0.003	0.004	0.006	0.004	0.003	0.003	0.003	0.004	0.003
BE2+	3.000	3.000	3.000	3.000	3.000	3.000	3.000	3.000	3.000	3.000	3.000	3.000
CATSUM	11.214	11.214	11.222	11.240	11.202	11.237	11.201	11.199	11.227	11.215	11.221	11.203

Data for emerald from Original discovery zones

Point	179	180	181	182	183	184	185	186	187	188	189	190
NA2O	1.16	1.07	1.23	1.08	0.94	1.08	1.12	1.08	1.11	1.25	1.17	1.12
MGO	1.34	1.21	1.53	1.36	1.09	1.36	1.35	1.38	1.39	1.50	1.39	1.36
AL2O3	15.72	15.78	15.33	16.19	16.22	15.83	15.79	15.81	15.89	15.58	15.81	15.68
SIO2	64.33	64.75	64.47	64.53	64.30	64.60	64.02	64.16	64.05	64.07	63.91	64.05
K2O	0.04	0.03	0.03	0.03	0.02	0.02	0.03	0.02	0.04	0.03	0.02	0.03
CAO	0.04	0.01	0.03	0.03	0.03	0.02	0.03	0.03	0.03	0.04	0.03	0.03
SC2O3	0.04	0.08	0.04	0.03	0.05	0.02	0.04	0.02	0.03	0.02	0.05	0.05
TIO2	0.01	0.00	0.00	0.00	0.00	0.01	0.01	0.00	0.00	0.00	0.00	0.00
V2O3	0.03	0.05	0.03	0.01	0.03	0.03	0.04	0.03	0.03	0.00	0.02	0.02
CR2O3	0.68	0.75	0.64	0.18	0.36	0.42	0.60	0.37	0.44	0.55	0.62	0.59
MNO	0.01	0.02	0.02	0.00	0.00	0.00	0.00	0.00	0.00	0.00	0.00	0.01
FEO	0.47	0.45	0.46	0.36	0.41	0.44	0.45	0.44	0.49	0.38	0.45	0.44
CS2O	0.13	0.11	0.10	0.10	0.08	0.09	0.13	0.10	0.10	0.06	0.07	0.13
BEO *	13.40	13.47	13.39	13.44	13.38	13.43	13.35	13.35	13.36	13.34	13.34	13.34
H2O	2.25	2.17	2.30	2.18	2.06	2.18	2.21	2.18	2.20	2.32	2.25	2.21
TOTAL	99.65	99.95	99.60	99.52	98.97	99.53	99.17	98.97	99.16	99.14	99.13	99.06
NA+	0.210	0.192	0.222	0.195	0.170	0.195	0.203	0.196	0.201	0.227	0.212	0.203
MG2+	0.186	0.167	0.213	0.188	0.152	0.189	0.188	0.192	0.194	0.209	0.194	0.190
AL3+	1.726	1.725	1.685	1.773	1.784	1.735	1.741	1.743	1.751	1.719	1.744	1.731
SI4+	5.994	6.005	6.013	5.997	6.000	6.009	5.989	6.003	5.989	5.999	5.983	5.998
K+	0.005	0.004	0.004	0.004	0.002	0.002	0.004	0.002	0.005	0.004	0.002	0.004
CA2+	0.004	0.001	0.003	0.003	0.003	0.002	0.003	0.003	0.003	0.004	0.003	0.003
SC3+	0.003	0.006	0.003	0.002	0.004	0.002	0.003	0.002	0.002	0.002	0.004	0.004
TI4+	0.001	0.000	0.000	0.000	0.000	0.001	0.001	0.000	0.000	0.000	0.000	0.000
V3+	0.002	0.004	0.002	0.001	0.002	0.002	0.003	0.002	0.002	0.000	0.002	0.002
CR3+	0.050	0.055	0.047	0.013	0.027	0.031	0.044	0.027	0.033	0.041	0.046	0.044
MN2+	0.001	0.002	0.002	0.000	0.000	0.000	0.000	0.000	0.000	0.000	0.000	0.001
FE2+	0.037	0.035	0.036	0.028	0.032	0.034	0.035	0.034	0.038	0.030	0.035	0.034
CS+	0.005	0.004	0.004	0.004	0.003	0.004	0.005	0.004	0.004	0.002	0.003	0.005
BE2+	3.000	3.000	3.000	3.000	3.000	3.000	3.000	3.000	3.000	3.000	3.000	3.000
CATSUM	11.224	11.200	11.233	11.209	11.179	11.205	11.220	11.210	11.222	11.237	11.228	11.218

Data for emerald from Original discovery zones

Point	191	192	193	194	195	196	197	198	199	200	201	202
NA2O	1.06	1.05	1.07	1.07	1.16	1.07	1.20	1.04	1.03	0.99	1.17	1.19
MGO	1.24	1.29	1.23	1.24	1.31	1.34	1.42	1.14	1.12	1.09	1.39	1.37
AL2O3	16.26	15.98	16.02	16.01	15.82	15.62	15.72	15.88	15.90	15.83	15.60	15.84
SIO2	63.88	64.52	64.58	64.71	63.84	64.05	63.32	64.43	64.26	64.51	64.33	64.38
K2O	0.02	0.02	0.02	0.03	0.04	0.04	0.05	0.02	0.03	0.03	0.04	0.02
CAO	0.04	0.05	0.03	0.02	0.03	0.04	0.03	0.03	0.02	0.01	0.03	0.03
SC2O3	0.05	0.04	0.03	0.04	0.06	0.05	0.05	0.05	0.05	0.06	0.05	0.00
TIO2	0.00	0.01	0.01	0.00	0.00	0.00	0.00	0.00	0.00	0.00	0.00	0.00
V2O3	0.04	0.01	0.03	0.02	0.01	0.02	0.04	0.03	0.02	0.03	0.02	0.00
CR2O3	0.23	0.25	0.50	0.48	0.39	0.76	0.45	0.74	0.88	0.92	0.55	0.44
MNO	0.00	0.00	0.00	0.01	0.02	0.00	0.00	0.00	0.00	0.03	0.01	0.01
FEO	0.43	0.45	0.43	0.43	0.43	0.51	0.47	0.45	0.45	0.49	0.46	0.38
CS2O	0.09	0.08	0.13	0.12	0.09	0.15	0.12	0.10	0.14	0.14	0.14	0.09
BEO *	13.34	13.41	13.44	13.46	13.30	13.34	13.22	13.41	13.39	13.43	13.38	13.39
H2O	2.16	2.15	2.17	2.17	2.25	2.17	2.28	2.14	2.13	2.10	2.25	2.27
TOTAL	98.84	99.31	99.69	99.81	98.75	99.16	98.37	99.46	99.42	99.66	99.42	99.41
NA+	0.192	0.190	0.193	0.192	0.211	0.194	0.220	0.188	0.186	0.179	0.212	0.215
MG2+	0.173	0.179	0.170	0.171	0.183	0.187	0.200	0.158	0.156	0.151	0.193	0.190
AL3+	1.794	1.754	1.754	1.750	1.751	1.723	1.750	1.743	1.747	1.735	1.717	1.741
SI4+	5.981	6.009	5.999	6.003	5.995	5.995	5.980	6.000	5.992	6.000	6.006	6.003
K+	0.002	0.002	0.002	0.004	0.005	0.005	0.006	0.002	0.004	0.004	0.005	0.002
CA2+	0.004	0.005	0.003	0.002	0.003	0.004	0.003	0.003	0.002	0.001	0.003	0.003
SC3+	0.004	0.003	0.002	0.003	0.005	0.004	0.004	0.004	0.004	0.005	0.004	0.000
TI4+	0.000	0.001	0.001	0.000	0.000	0.000	0.000	0.000	0.000	0.000	0.000	0.000
V3+	0.003	0.001	0.002	0.001	0.001	0.002	0.003	0.002	0.001	0.002	0.001	0.000
CR3+	0.017	0.018	0.037	0.035	0.029	0.056	0.034	0.054	0.065	0.068	0.041	0.032
MN2+	0.000	0.000	0.000	0.001	0.002	0.000	0.000	0.000	0.000	0.002	0.001	0.001
FE2+	0.034	0.035	0.033	0.033	0.034	0.040	0.037	0.035	0.035	0.038	0.036	0.030
CS+	0.004	0.003	0.005	0.005	0.004	0.006	0.005	0.004	0.006	0.006	0.006	0.004
BE2+	3.000	3.000	3.000	3.000	3.000	3.000	3.000	3.000	3.000	3.000	3.000	3.000
CATSUM	11.209	11.200	11.202	11.202	11.222	11.215	11.241	11.195	11.197	11.189	11.224	11.221

Data for emerald from Original discovery zones

Point	203	216	217	218	219	220	221	222	223	224	225	226
NA2O	1.12	1.03	0.90	0.93	1.13	1.11	1.06	0.88	0.95	1.05	1.07	1.10
MGO	1.34	1.26	1.03	1.02	1.38	1.19	1.28	0.91	1.13	1.24	1.26	1.25
AL2O3	15.68	16.06	16.34	16.51	15.89	15.72	15.33	16.10	15.90	15.86	15.60	15.33
SIO2	63.75	64.70	64.89	64.82	64.29	64.21	64.22	64.67	64.12	64.71	64.44	64.29
K2O	0.04	0.03	0.03	0.03	0.02	0.03	0.02	0.03	0.03	0.03	0.04	0.03
CAO	0.02	0.03	0.01	0.02	0.04	0.01	0.03	0.04	0.02	0.05	0.03	0.03
SC2O3	0.05	0.00	0.01	0.02	0.04	0.05	0.07	0.00	0.04	0.04	0.04	0.03
TIO2	0.00	0.00	0.00	0.00	0.01	0.00	0.00	0.01	0.01	0.00	0.00	0.00
V2O3	0.04	0.02	0.04	0.02	0.02	0.07	0.05	0.02	0.02	0.03	0.04	0.03
CR2O3	0.60	0.28	0.22	0.16	0.43	0.76	1.05	0.91	0.89	0.46	0.89	0.99
MNO	0.02	0.02	0.00	0.00	0.00	0.03	0.00	0.00	0.00	0.00	0.00	0.02
FEO	0.51	0.43	0.40	0.40	0.48	0.52	0.50	0.36	0.48	0.48	0.45	0.54
CS2O	0.14	0.11	0.14	0.15	0.10	0.15	0.13	0.14	0.14	0.15	0.16	0.16
BEO *	13.29	13.44	13.47	13.48	13.40	13.37	13.35	13.45	13.37	13.44	13.40	13.36
H2O	2.21	2.13	2.02	2.05	2.22	2.20	2.16	2.01	2.07	2.15	2.17	2.19
TOTAL	98.81	99.54	99.50	99.61	99.45	99.42	99.25	99.53	99.17	99.69	99.59	99.35
NA+	0.204	0.186	0.162	0.167	0.204	0.201	0.192	0.158	0.172	0.189	0.193	0.199
MG2+	0.188	0.174	0.142	0.141	0.192	0.166	0.178	0.126	0.157	0.172	0.175	0.174
AL3+	1.736	1.758	1.785	1.803	1.746	1.730	1.690	1.762	1.751	1.736	1.713	1.689
SI4+	5.990	6.010	6.016	6.006	5.993	5.996	6.007	6.006	5.990	6.012	6.004	6.012
K+	0.005	0.004	0.004	0.004	0.002	0.004	0.002	0.004	0.004	0.004	0.005	0.004
CA2+	0.002	0.003	0.001	0.002	0.004	0.001	0.003	0.004	0.002	0.005	0.003	0.003
SC3+	0.004	0.000	0.001	0.002	0.003	0.004	0.006	0.000	0.003	0.003	0.003	0.002
TI4+	0.000	0.000	0.000	0.000	0.001	0.000	0.000	0.001	0.001	0.000	0.000	0.000
V3+	0.003	0.001	0.003	0.001	0.001	0.005	0.004	0.001	0.001	0.002	0.003	0.002
CR3+	0.045	0.021	0.016	0.012	0.032	0.056	0.078	0.067	0.066	0.034	0.066	0.073
MN2+	0.002	0.002	0.000	0.000	0.000	0.002	0.000	0.000	0.000	0.000	0.000	0.002
FE2+	0.040	0.033	0.031	0.031	0.037	0.041	0.039	0.028	0.037	0.037	0.035	0.042
CS+	0.006	0.004	0.006	0.006	0.004	0.006	0.005	0.006	0.006	0.006	0.006	0.006
BE2+	3.000	3.000	3.000	3.000	3.000	3.000	3.000	3.000	3.000	3.000	3.000	3.000
CATSUM	11.224	11.196	11.167	11.174	11.220	11.212	11.204	11.162	11.190	11.200	11.206	11.209

Data for emerald from Original discovery zones

Point	227	228	229	230	231	232	233	234	235	236	237	238
NA2O	1.03	0.97	0.93	0.92	1.00	0.95	1.33	1.16	1.04	1.02	1.09	1.03
MGO	1.15	1.09	1.07	1.09	1.16	1.02	1.58	1.34	1.28	1.23	1.26	1.18
AL2O3	15.78	16.08	15.97	15.82	15.76	15.98	15.39	15.78	15.79	16.02	15.96	16.25
SIO2	64.94	64.62	64.64	64.60	64.85	64.69	64.38	64.39	64.70	64.77	64.33	64.80
K2O	0.03	0.02	0.02	0.02	0.03	0.03	0.03	0.04	0.04	0.03	0.04	0.02
CAO	0.01	0.02	0.01	0.02	0.02	0.02	0.05	0.04	0.02	0.02	0.02	0.02
SC2O3	0.02	0.03	0.03	0.02	0.04	0.04	0.00	0.03	0.04	0.01	0.05	0.00
TIO2	0.00	0.00	0.00	0.00	0.00	0.00	0.02	0.00	0.00	0.00	0.00	0.00
V2O3	0.02	0.04	0.03	0.03	0.04	0.04	0.02	0.02	0.04	0.01	0.03	0.00
CR2O3	0.81	0.68	0.62	0.81	0.75	0.95	0.73	0.36	0.47	0.44	0.24	0.23
MNO	0.00	0.01	0.02	0.02	0.02	0.02	0.00	0.00	0.00	0.00	0.00	0.02
FEO	0.42	0.47	0.45	0.44	0.44	0.47	0.45	0.44	0.47	0.41	0.44	0.33
CS2O	0.12	0.12	0.14	0.14	0.12	0.17	0.10	0.10	0.11	0.11	0.12	0.10
BEO *	13.48	13.45	13.43	13.42	13.46	13.47	13.40	13.38	13.43	13.46	13.37	13.46
H2O	2.13	2.08	2.05	2.04	2.11	2.07	2.39	2.25	2.14	2.13	2.19	2.13
TOTAL	99.94	99.68	99.41	99.39	99.80	99.92	99.87	99.33	99.57	99.66	99.14	99.57
NA+	0.185	0.175	0.168	0.166	0.180	0.171	0.240	0.210	0.187	0.184	0.197	0.185
MG2+	0.159	0.151	0.148	0.151	0.160	0.141	0.219	0.186	0.177	0.170	0.175	0.163
AL3+	1.723	1.759	1.751	1.735	1.723	1.746	1.690	1.735	1.730	1.752	1.756	1.777
SI4+	6.016	5.999	6.012	6.013	6.016	5.998	5.998	6.009	6.015	6.011	6.007	6.011
K+	0.004	0.002	0.002	0.002	0.004	0.004	0.004	0.005	0.005	0.004	0.005	0.002
CA2+	0.001	0.002	0.001	0.002	0.002	0.002	0.005	0.004	0.002	0.002	0.002	0.002
SC3+	0.002	0.002	0.002	0.002	0.003	0.003	0.000	0.002	0.003	0.001	0.004	0.000
TI4+	0.000	0.000	0.000	0.000	0.000	0.000	0.001	0.000	0.000	0.000	0.000	0.000
V3+	0.001	0.003	0.002	0.002	0.003	0.003	0.001	0.001	0.003	0.001	0.002	0.000
CR3+	0.059	0.050	0.046	0.060	0.055	0.070	0.054	0.027	0.035	0.032	0.018	0.017
MN2+	0.000	0.001	0.002	0.002	0.002	0.002	0.000	0.000	0.000	0.000	0.000	0.002
FE2+	0.033	0.036	0.035	0.034	0.034	0.036	0.035	0.034	0.037	0.032	0.034	0.026
CS+	0.005	0.005	0.006	0.006	0.005	0.007	0.004	0.004	0.004	0.004	0.005	0.004
BE2+	3.000	3.000	3.000	3.000	3.000	3.000	3.000	3.000	3.000	3.000	3.000	3.000
CATSUM	11.188	11.185	11.175	11.175	11.186	11.182	11.252	11.218	11.198	11.192	11.206	11.188

Data for emerald from Original discovery zones

Point	239	240	241	242	Original AVG	STD DEV
NA2O	1.11	1.29	1.24	1.02	1.06	0.10
MGO	1.29	1.56	1.47	1.16	1.25	0.15
AL2O3	15.85	15.47	15.53	16.37	15.81	0.30
SIO2	64.69	64.40	64.39	65.18	64.21	0.49
K2O	0.03	0.04	0.04	0.03	0.03	0.01
CAO	0.03	0.03	0.03	0.05	0.03	0.01
SC2O3	0.04	0.02	0.03	0.00	0.04	0.02
TIO2	0.00	0.00	0.00	0.01	0.00	0.00
V2O3	0.03	0.03	0.03	0.02	0.03	0.01
CR2O3	0.56	0.57	0.72	0.16	0.67	0.27
MNO	0.01	0.04	0.00	0.02	0.01	0.01
FEO	0.39	0.40	0.47	0.33	0.45	0.05
CS2O	0.10	0.10	0.14	0.08	0.12	0.03
BEO *	13.45	13.40	13.41	13.54	13.37	0.08
H2O	2.20	2.36	2.31	2.13	2.16	0.09
TOTAL	99.78	99.71	99.81	100.10	99.22	0.53
NA+	0.200	0.233	0.224	0.182	0.192	0.019
MG2+	0.179	0.217	0.204	0.160	0.174	0.021
AL3+	1.734	1.700	1.705	1.779	1.740	0.030
SI4+	6.006	6.003	5.998	6.012	5.998	0.011
K+	0.004	0.005	0.005	0.004	0.004	0.001
CA2+	0.003	0.003	0.003	0.005	0.003	0.001
SC3+	0.003	0.002	0.002	0.000	0.003	0.002
TI4+	0.000	0.000	0.000	0.001	0.000	0.000
V3+	0.002	0.002	0.002	0.001	0.002	0.001
CR3+	0.041	0.042	0.053	0.012	0.049	0.020
MN2+	0.001	0.003	0.000	0.002	0.001	0.001
FE2+	0.030	0.031	0.037	0.025	0.035	0.004
CS+	0.004	0.004	0.006	0.003	0.005	0.001
BE2+	3.000	3.000	3.000	3.000	3.000	0.000
CATSUM	11.207	11.245	11.238	11.186	11.205	0.021

Data for emerald from Adit

Point	1	2	3	4	5	6	7	8	9	10	11	12
NA2O	0.93	0.94	0.98	0.99	1.04	0.93	1.02	1.06	0.95	0.93	1.09	1.01
MGO	0.99	1.05	1.08	1.18	1.16	0.99	1.16	1.19	1.00	0.99	1.24	1.09
AL2O3	16.34	16.17	16.49	16.38	16.01	16.22	15.89	16.30	16.04	16.33	15.82	16.03
SIO2	64.25	64.61	64.35	64.83	64.40	64.71	64.26	63.85	64.16	65.07	64.35	63.84
K2O	0.03	0.03	0.05	0.04	0.03	0.03	0.05	0.04	0.03	0.03	0.04	0.03
CAO	0.02	0.02	0.02	0.04	0.03	0.03	0.02	0.03	0.03	0.01	0.03	0.03
SC2O3	0.05	0.05	0.04	0.02	0.06	0.04	0.06	0.05	0.03	0.03	0.04	0.05
TIO2	0	0.01	0.01	0.01	0.00	0.00	0.01	0.00	0.00	0.01	0.00	0.00
V2O3	0.04	0.04	0.04	0.00	0.04	0.04	0.02	0.03	0.03	0.04	0.03	0.05
CR2O3	0.63	0.51	0.41	0.30	0.52	0.59	0.79	0.37	0.90	0.48	0.69	0.69
MNO	0.03	0.01	0.01	0.00	0.00	0.03	0.02	0.02	0.03	0.02	0.00	0.00
FEO	0.45	0.44	0.40	0.36	0.46	0.42	0.48	0.40	0.45	0.40	0.48	0.44
CS2O	0.14	0.15	0.08	0.11	0.10	0.09	0.13	0.08	0.13	0.14	0.11	0.09
BEO *	13.41	13.44	13.44	13.50	13.41	13.46	13.39	13.34	13.38	13.53	13.40	13.32
H2O	2.049868	2.058364	2.09	2.10	2.14	2.05	2.13	2.16	2.07	2.05	2.19	2.12
TOTAL	99.35987	99.52836	99.49	99.86	99.40	99.63	99.43	98.92	99.23	100.06	99.51	98.79
NA+	0.168	0.169	0.177	0.178	0.188	0.167	0.184	0.192	0.172	0.166	0.197	0.184
MG2+	0.137	0.145	0.150	0.163	0.161	0.137	0.161	0.166	0.139	0.136	0.172	0.152
AL3+	1.793	1.77	1.806	1.786	1.758	1.773	1.746	1.798	1.764	1.777	1.738	1.771
SI4+	5.982	6.002	5.979	5.998	5.998	6.002	5.991	5.975	5.988	6.008	5.997	5.985
K+	0.004	0.004	0.006	0.005	0.004	0.004	0.006	0.005	0.004	0.004	0.005	0.004
CA2+	0.002	0.002	0.002	0.004	0.003	0.003	0.002	0.003	0.003	0.001	0.003	0.003
SC3+	0.004	0.004	0.003	0.002	0.005	0.003	0.005	0.004	0.002	0.002	0.003	0.004
TI4+	0	0.001	0.001	0.001	0.000	0.000	0.001	0.000	0.000	0.001	0.000	0.000
V3+	0.003	0.003	0.003	0.000	0.003	0.003	0.001	0.002	0.002	0.003	0.002	0.004
CR3+	0.046	0.037	0.030	0.022	0.038	0.043	0.058	0.027	0.066	0.035	0.051	0.051
MN2+	0.002	0.001	0.001	0.000	0.000	0.002	0.002	0.002	0.002	0.002	0.000	0.000
FE2+	0.035	0.034	0.031	0.028	0.036	0.033	0.037	0.031	0.035	0.031	0.037	0.034
CS+	0.006	0.006	0.003	0.004	0.004	0.004	0.005	0.003	0.005	0.006	0.004	0.004
BE2+	3	3	3.000	3.000	3.000	3.000	3.000	3.000	3.000	3.000	3.000	3.000
CATSUM	11.183	11.179	11.192	11.190	11.197	11.174	11.200	11.209	11.184	11.171	11.209	11.196

Data for emerald from Adit

Point	13	14	15	16	17	18	19	20	21	22	23	24
NA2O	0.84	1.09	0.85	0.90	0.99	1.00	0.82	0.90	0.89	0.94	0.79	1.00
MGO	0.81	1.33	0.89	0.91	0.94	1.11	0.86	0.97	0.99	1.01	0.81	1.04
AL2O3	16.68	16.12	15.93	16.49	16.70	15.97	16.56	16.29	16.50	16.35	16.50	16.52
SIO2	64.47	63.89	64.32	63.72	64.24	63.92	64.73	64.32	63.68	63.90	64.49	64.21
K2O	0.03	0.04	0.04	0.02	0.03	0.03	0.02	0.03	0.01	0.02	0.03	0.03
CAO	0.00	0.03	0.01	0.03	0.03	0.03	0.02	0.02	0.02	0.02	0.01	0.03
SC2O3	0.02	0.05	0.03	0.04	0.01	0.05	0.05	0.04	0.05	0.04	0.03	0.02
TIO2	0.00	0.00	0.00	0.01	0.00	0.01	0.00	0.00	0.01	0.00	0.00	0.00
V2O3	0.02	0.03	0.02	0.02	0.02	0.04	0.03	0.04	0.03	0.02	0.02	0.04
CR2O3	0.50	0.37	0.99	0.48	0.36	0.71	0.39	0.50	0.45	0.61	0.57	0.28
MNO	0.00	0.03	0.00	0.02	0.01	0.02	0.00	0.00	0.00	0.00	0.00	0.01
FEO	0.38	0.40	0.40	0.42	0.31	0.44	0.42	0.40	0.45	0.42	0.45	0.46
CS2O	0.16	0.14	0.12	0.12	0.03	0.10	0.12	0.10	0.13	0.10	0.15	0.12
BEO *	13.44	13.35	13.37	13.31	13.42	13.33	13.47	13.39	13.32	13.35	13.43	13.41
H2O	1.97	2.19	1.98	2.02	2.10	2.11	1.96	2.02	2.02	2.06	1.93	2.11
TOTAL	99.32	99.06	98.95	98.51	99.19	98.87	99.45	99.02	98.55	98.84	99.21	99.28
NA+	0.151	0.198	0.154	0.164	0.179	0.182	0.147	0.163	0.162	0.171	0.142	0.181
MG2+	0.112	0.186	0.124	0.127	0.130	0.155	0.119	0.135	0.138	0.141	0.112	0.144
AL3+	1.826	1.778	1.754	1.823	1.832	1.763	1.810	1.790	1.824	1.803	1.808	1.814
SI4+	5.989	5.978	6.008	5.977	5.979	5.988	6.001	5.998	5.972	5.978	5.997	5.982
K+	0.004	0.005	0.005	0.002	0.004	0.004	0.002	0.004	0.001	0.002	0.004	0.004
CA2+	0.000	0.003	0.001	0.003	0.003	0.003	0.002	0.002	0.002	0.002	0.001	0.003
SC3+	0.002	0.004	0.002	0.003	0.001	0.004	0.004	0.003	0.004	0.003	0.002	0.002
TI4+	0.000	0.000	0.000	0.001	0.000	0.001	0.000	0.000	0.001	0.000	0.000	0.000
V3+	0.001	0.002	0.001	0.002	0.001	0.003	0.002	0.003	0.002	0.002	0.001	0.003
CR3+	0.037	0.027	0.073	0.036	0.026	0.053	0.029	0.037	0.033	0.045	0.042	0.021
MN2+	0.000	0.002	0.000	0.002	0.001	0.002	0.000	0.000	0.000	0.000	0.000	0.001
FE2+	0.030	0.031	0.031	0.033	0.024	0.034	0.033	0.031	0.035	0.033	0.035	0.036
CS+	0.006	0.006	0.005	0.005	0.001	0.004	0.005	0.004	0.005	0.004	0.006	0.005
BE2+	3.000	3.000	3.000	3.000	3.000	3.000	3.000	3.000	3.000	3.000	3.000	3.000
CATSUM	11.158	11.220	11.158	11.176	11.182	11.195	11.154	11.170	11.180	11.184	11.152	11.193

Data for emerald from Adit

Point	25	26	27	28	29	30	31	32	33	34	35	36
NA2O	0.90	0.79	1.01	0.87	1.02	0.85	0.94	0.90	0.79	1.01	0.97	0.89
MGO	0.90	0.84	1.09	0.92	1.12	0.87	1.06	0.92	0.68	1.15	1.08	1.06
AL2O3	16.39	16.48	16.00	16.56	16.02	16.48	16.08	16.37	17.24	16.01	16.38	16.28
SIO2	63.66	64.21	64.19	64.22	63.96	64.14	63.99	64.31	63.92	64.00	64.21	64.13
K2O	0.03	0.03	0.04	0.03	0.04	0.03	0.03	0.03	0.04	0.03	0.02	0.04
CAO	0.02	0.01	0.03	0.02	0.02	0.02	0.01	0.02	0.01	0.00	0.03	0.03
SC2O3	0.04	0.03	0.06	0.03	0.02	0.05	0.04	0.06	0.00	0.07	0.06	0.08
TIO2	0.00	0.00	0.00	0.00	0.01	0.01	0.00	0.01	0.00	0.01	0.01	0.00
V2O3	0.02	0.04	0.02	0.05	0.03	0.01	0.02	0.04	0.01	0.04	0.04	0.04
CR2O3	0.65	0.57	0.66	0.30	0.60	0.47	0.60	0.66	0.24	0.56	0.39	0.56
MNO	0.00	0.02	0.00	0.01	0.00	0.01	0.00	0.00	0.00	0.00	0.01	0.01
FEO	0.45	0.42	0.46	0.42	0.43	0.41	0.43	0.38	0.27	0.42	0.47	0.46
CS2O	0.10	0.14	0.12	0.13	0.13	0.14	0.15	0.15	0.10	0.12	0.10	0.15
BEO *	13.30	13.38	13.37	13.39	13.33	13.37	13.33	13.41	13.38	13.34	13.40	13.39
H2O	2.02	1.93	2.12	2.00	2.13	1.98	2.06	2.02	1.93	2.12	2.08	2.02
TOTAL	98.48	98.89	99.17	98.95	98.86	98.84	98.74	99.28	98.61	98.88	99.25	99.14
NA+	0.164	0.143	0.183	0.157	0.185	0.154	0.171	0.162	0.143	0.183	0.175	0.161
MG2+	0.126	0.117	0.152	0.128	0.156	0.121	0.148	0.128	0.095	0.161	0.150	0.147
AL3+	1.813	1.812	1.761	1.820	1.769	1.814	1.775	1.796	1.897	1.767	1.799	1.790
SI4+	5.976	5.991	5.994	5.990	5.992	5.990	5.995	5.987	5.967	5.992	5.982	5.983
K+	0.004	0.004	0.005	0.004	0.005	0.004	0.004	0.004	0.005	0.004	0.002	0.005
CA2+	0.002	0.001	0.003	0.002	0.002	0.002	0.001	0.002	0.001	0.000	0.003	0.003
SC3+	0.003	0.002	0.005	0.002	0.002	0.004	0.003	0.005	0.000	0.006	0.005	0.007
TI4+	0.000	0.000	0.000	0.000	0.001	0.001	0.000	0.001	0.000	0.001	0.001	0.000
V3+	0.002	0.003	0.001	0.004	0.002	0.001	0.002	0.003	0.001	0.003	0.003	0.003
CR3+	0.048	0.042	0.049	0.022	0.044	0.035	0.044	0.049	0.018	0.041	0.029	0.041
MN2+	0.000	0.002	0.000	0.001	0.000	0.001	0.000	0.000	0.000	0.000	0.001	0.001
FE2+	0.035	0.033	0.036	0.033	0.034	0.032	0.034	0.030	0.021	0.033	0.037	0.036
CS+	0.004	0.006	0.005	0.005	0.005	0.006	0.006	0.006	0.004	0.005	0.004	0.006
BE2+	3.000	3.000	3.000	3.000	3.000	3.000	3.000	3.000	3.000	3.000	3.000	3.000
CATSUM	11.177	11.155	11.194	11.168	11.197	11.164	11.183	11.172	11.151	11.195	11.190	11.183

Data for emerald from Adit

Point	37	38	39	40	41	42	43	44	45	46	47	48
NA2O	0.94	0.99	0.94	0.91	1.18	0.86	0.94	1.01	0.89	0.76	0.45	0.67
MGO	1.00	1.07	0.98	0.93	1.32	0.81	1.03	1.06	0.91	0.76	0.38	0.70
AL2O3	16.49	15.72	16.36	16.44	15.66	16.73	16.38	16.19	16.65	16.58	17.10	16.76
SIO2	64.81	64.22	64.37	64.04	63.83	64.39	64.53	63.70	64.74	64.66	65.64	65.48
K2O	0.03	0.04	0.02	0.04	0.02	0.03	0.02	0.04	0.03	0.03	0.01	0.02
CAO	0.01	0.03	0.02	0.02	0.03	0.00	0.03	0.03	0.01	0.01	0.01	0.02
SC2O3	0.02	0.04	0.06	0.03	0.06	0.04	0.06	0.06	0.04	0.03	0.01	0.03
TIO2	0.00	0.03	0.00	0.00	0.00	0.00	0.00	0.01	0.00	0.00	0.00	0.00
V2O3	0.01	0.03	0.01	0.02	0.06	0.04	0.04	0.04	0.02	0.01	0.01	0.00
CR2O3	0.45	1.10	0.56	0.51	0.74	0.27	0.41	0.61	0.18	0.48	0.98	0.75
MNO	0.00	0.03	0.02	0.00	0.00	0.04	0.01	0.00	0.01	0.00	0.01	0.01
FEO	0.43	0.48	0.43	0.47	0.51	0.34	0.41	0.43	0.41	0.43	0.25	0.22
CS2O	0.12	0.13	0.12	0.17	0.13	0.10	0.15	0.11	0.13	0.18	0.03	0.03
BEO *	13.50	13.38	13.42	13.37	13.32	13.42	13.45	13.31	13.47	13.45	13.65	13.61
H2O	2.06	2.10	2.06	2.03	2.26	1.99	2.06	2.12	2.02	1.91	1.64	1.83
TOTAL	99.87	99.39	99.37	98.98	99.12	99.06	99.52	98.72	99.51	99.29	100.17	100.13
NA+	0.169	0.179	0.170	0.165	0.215	0.155	0.169	0.184	0.160	0.137	0.080	0.119
MG2+	0.138	0.149	0.136	0.130	0.185	0.112	0.143	0.148	0.126	0.105	0.052	0.096
AL3+	1.798	1.729	1.794	1.810	1.730	1.835	1.793	1.790	1.819	1.814	1.844	1.813
SI4+	5.995	5.993	5.989	5.983	5.985	5.992	5.993	5.976	6.001	6.004	6.006	6.009
K+	0.004	0.005	0.002	0.005	0.002	0.004	0.002	0.005	0.004	0.004	0.001	0.002
CA2+	0.001	0.003	0.002	0.002	0.003	0.000	0.003	0.003	0.001	0.001	0.001	0.002
SC3+	0.002	0.003	0.005	0.002	0.005	0.003	0.005	0.005	0.003	0.002	0.001	0.002
TI4+	0.000	0.002	0.000	0.000	0.000	0.000	0.000	0.001	0.000	0.000	0.000	0.000
V3+	0.001	0.002	0.001	0.001	0.005	0.003	0.003	0.003	0.001	0.001	0.001	0.000
CR3+	0.033	0.081	0.041	0.038	0.055	0.020	0.030	0.045	0.013	0.035	0.071	0.054
MN2+	0.000	0.002	0.002	0.000	0.000	0.003	0.001	0.000	0.001	0.000	0.001	0.001
FE2+	0.033	0.037	0.033	0.037	0.040	0.026	0.032	0.034	0.032	0.033	0.019	0.017
CS+	0.005	0.005	0.005	0.007	0.005	0.004	0.006	0.004	0.005	0.007	0.001	0.001
BE2+	3.000	3.000	3.000	3.000	3.000	3.000	3.000	3.000	3.000	3.000	3.000	3.000
CATSUM	11.177	11.192	11.179	11.179	11.229	11.158	11.180	11.198	11.165	11.144	11.077	11.117

Data for emerald from Adit

Point	49	50	51	52	53	54	55	56	57	58	59	60
NA2O	0.86	1.05	0.81	0.87	0.85	0.50	0.85	0.90	1.04	0.97	1.03	1.09
MGO	0.85	1.15	0.79	0.87	0.85	0.39	0.90	0.98	1.08	1.02	1.19	1.22
AL2O3	16.61	16.00	16.50	16.58	16.64	16.87	16.63	16.09	16.03	16.44	15.80	16.19
SIO2	64.83	64.83	64.73	64.83	64.92	64.84	64.59	64.64	64.47	64.53	64.31	64.04
K2O	0.03	0.04	0.02	0.03	0.03	0.01	0.04	0.03	0.04	0.02	0.04	0.04
CAO	0.00	0.02	0.02	0.01	0.01	0.01	0.02	0.03	0.03	0.03	0.03	0.03
SC2O3	0.03	0.05	0.02	0.02	0.04	0.02	0.02	0.07	0.04	0.01	0.06	0.04
TIO2	0.01	0.00	0.00	0.00	0.00	0.00	0.01	0.01	0.00	0.00	0.00	0.00
V2O3	0.03	0.03	0.02	0.03	0.03	0.00	0.03	0.03	0.01	0.02	0.03	0.04
CR2O3	0.30	0.47	0.56	0.33	0.23	0.99	0.23	0.60	0.65	0.32	0.70	0.37
MNO	0.01	0.01	0.00	0.00	0.02	0.00	0.02	0.00	0.02	0.04	0.01	0.00
FEO	0.43	0.45	0.44	0.40	0.41	0.32	0.43	0.43	0.47	0.40	0.44	0.45
CS2O	0.13	0.14	0.14	0.12	0.14	0.05	0.12	0.14	0.11	0.11	0.15	0.09
BEO *	13.49	13.47	13.47	13.48	13.50	13.49	13.45	13.43	13.42	13.44	13.38	13.37
H2O	1.99	2.15	1.95	2.00	1.98	1.68	1.98	2.02	2.14	2.08	2.13	2.19
TOTAL	99.60	99.86	99.47	99.57	99.65	99.17	99.32	99.40	99.55	99.43	99.30	99.16
NA+	0.154	0.189	0.146	0.156	0.152	0.090	0.153	0.162	0.188	0.175	0.186	0.197
MG2+	0.117	0.159	0.109	0.120	0.117	0.054	0.125	0.136	0.150	0.141	0.166	0.170
AL3+	1.813	1.748	1.803	1.810	1.814	1.840	1.820	1.763	1.758	1.800	1.738	1.783
SI4+	6.003	6.010	6.003	6.004	6.006	6.001	5.997	6.009	5.998	5.996	6.001	5.982
K+	0.004	0.005	0.002	0.004	0.004	0.001	0.005	0.004	0.005	0.002	0.005	0.005
CA2+	0.000	0.002	0.002	0.001	0.001	0.001	0.002	0.003	0.003	0.003	0.003	0.003
SC3+	0.002	0.004	0.002	0.002	0.003	0.002	0.002	0.006	0.003	0.001	0.005	0.003
TI4+	0.001	0.000	0.000	0.000	0.000	0.000	0.001	0.001	0.000	0.000	0.000	0.000
V3+	0.002	0.002	0.001	0.002	0.002	0.000	0.002	0.002	0.001	0.001	0.002	0.003
CR3+	0.022	0.034	0.041	0.024	0.017	0.072	0.017	0.044	0.048	0.024	0.052	0.027
MN2+	0.001	0.001	0.000	0.000	0.002	0.000	0.002	0.000	0.002	0.003	0.001	0.000
FE2+	0.033	0.035	0.034	0.031	0.032	0.025	0.033	0.033	0.037	0.031	0.034	0.035
CS+	0.005	0.006	0.006	0.005	0.006	0.002	0.005	0.006	0.004	0.004	0.006	0.004
BE2+	3.000	3.000	3.000	3.000	3.000	3.000	3.000	3.000	3.000	3.000	3.000	3.000
CATSUM	11.158	11.195	11.150	11.159	11.156	11.088	11.163	11.168	11.195	11.182	11.199	11.212

Data for emerald from Adit

Point	61	62	63	64	65	66	67	68	69	70	71	72
NA2O	0.83	0.92	1.13	0.97	0.94	0.96	0.84	0.95	0.23	1.00	0.96	1.00
MGO	0.93	0.95	1.28	1.04	1.09	1.04	0.84	0.97	0.14	1.05	0.99	1.04
AL2O3	16.25	16.20	15.75	16.07	16.49	16.28	16.78	16.74	17.81	16.29	16.50	16.28
SIO2	64.14	64.58	64.57	64.60	64.91	64.33	65.08	64.86	65.62	64.69	64.77	64.70
K2O	0.04	0.04	0.04	0.03	0.03	0.04	0.02	0.03	0.00	0.03	0.04	0.03
CAO	0.01	0.01	0.04	0.01	0.01	0.02	0.00	0.02	0.00	0.02	0.02	0.02
SC2O3	0.04	0.06	0.05	0.07	0.03	0.03	0.04	0.07	0.00	0.04	0.06	0.05
TIO2	0.00	0.00	0.00	0.00	0.00	0.02	0.00	0.00	0.00	0.00	0.00	0.01
V2O3	0.03	0.03	0.03	0.02	0.04	0.03	0.03	0.04	0.01	0.03	0.04	0.04
CR2O3	0.71	0.72	0.70	0.58	0.20	0.57	0.14	0.09	0.75	0.54	0.31	0.50
MNO	0.04	0.00	0.00	0.01	0.01	0.00	0.00	0.02	0.00	0.00	0.00	0.00
FEO	0.45	0.44	0.45	0.41	0.43	0.43	0.41	0.44	0.10	0.42	0.47	0.43
CS2O	0.13	0.12	0.09	0.09	0.07	0.12	0.15	0.14	0.04	0.10	0.16	0.12
BEO *	13.37	13.45	13.44	13.43	13.51	13.42	13.53	13.52	13.67	13.48	13.49	13.47
H2O	1.96	2.04	2.22	2.08	2.06	2.08	1.97	2.07	1.46	2.11	2.08	2.11
TOTAL	98.93	99.56	99.79	99.41	99.82	99.37	99.83	99.96	99.83	99.80	99.89	99.80
NA+	0.150	0.166	0.204	0.175	0.168	0.173	0.150	0.170	0.041	0.180	0.172	0.180
MG2+	0.129	0.132	0.177	0.144	0.150	0.144	0.116	0.134	0.019	0.145	0.137	0.144
AL3+	1.789	1.773	1.725	1.761	1.797	1.786	1.825	1.822	1.918	1.779	1.800	1.778
SI4+	5.991	5.998	6.002	6.007	6.001	5.988	6.006	5.991	5.996	5.995	5.994	5.996
K+	0.005	0.005	0.005	0.004	0.004	0.005	0.002	0.004	0.000	0.004	0.005	0.004
CA2+	0.001	0.001	0.004	0.001	0.001	0.002	0.000	0.002	0.000	0.002	0.002	0.002
SC3+	0.003	0.005	0.004	0.006	0.002	0.002	0.003	0.006	0.000	0.003	0.005	0.004
TI4+	0.000	0.000	0.000	0.000	0.000	0.001	0.000	0.000	0.000	0.000	0.000	0.001
V3+	0.002	0.002	0.002	0.001	0.003	0.002	0.002	0.003	0.001	0.002	0.003	0.003
CR3+	0.052	0.053	0.051	0.043	0.015	0.042	0.010	0.007	0.054	0.040	0.023	0.037
MN2+	0.003	0.000	0.000	0.001	0.001	0.000	0.000	0.002	0.000	0.000	0.000	0.000
FE2+	0.035	0.034	0.035	0.032	0.033	0.033	0.032	0.034	0.008	0.033	0.036	0.033
CS+	0.005	0.005	0.004	0.004	0.003	0.005	0.006	0.006	0.002	0.004	0.006	0.005
BE2+	3.000	3.000	3.000	3.000	3.000	3.000	3.000	3.000	3.000	3.000	3.000	3.000
CATSUM	11.166	11.173	11.213	11.178	11.178	11.185	11.153	11.179	11.038	11.186	11.182	11.186

Data for emerald from Adit

Point	73	74	75	76	77	78	79	80	81	82	83	84
NA2O	0.80	0.90	0.85	0.90	0.95	0.92	0.96	0.92	0.85	0.94	1.02	1.06
MGO	0.79	0.98	0.86	0.94	0.99	0.92	1.04	0.95	0.78	0.94	1.08	1.22
AL2O3	16.86	16.85	16.56	16.41	16.28	16.48	16.43	16.29	16.78	16.72	16.29	16.20
SIO2	64.77	65.33	64.79	65.00	64.57	65.13	65.22	65.10	64.98	64.50	64.21	64.52
K2O	0.03	0.02	0.02	0.03	0.03	0.04	0.03	0.03	0.04	0.02	0.04	0.05
CAO	0.01	0.02	0.01	0.01	0.01	0.02	0.01	0.00	0.00	0.02	0.02	0.03
SC2O3	0.02	0.01	0.03	0.02	0.01	0.04	0.01	0.03	0.03	0.03	0.02	0.06
TIO2	0.00	0.00	0.01	0.00	0.00	0.00	0.02	0.00	0.00	0.00	0.00	0.00
V2O3	0.04	0.01	0.00	0.02	0.01	0.02	0.02	0.05	0.04	0.02	0.04	0.04
CR2O3	0.12	0.25	0.51	0.59	0.51	0.55	0.24	0.59	0.36	0.13	0.46	0.47
MNO	0.00	0.01	0.03	0.00	0.01	0.01	0.01	0.01	0.00	0.01	0.01	0.01
FEO	0.36	0.30	0.47	0.47	0.46	0.47	0.42	0.44	0.44	0.46	0.43	0.46
CS2O	0.15	0.08	0.16	0.13	0.12	0.15	0.13	0.13	0.19	0.12	0.11	0.10
BEO *	13.48	13.60	13.50	13.53	13.44	13.56	13.55	13.53	13.53	13.45	13.39	13.46
H2O	1.94	2.02	1.98	2.02	2.07	2.04	2.08	2.04	1.98	2.06	2.13	2.16
TOTAL	99.37	100.38	99.78	100.07	99.46	100.35	100.17	100.11	100.00	99.42	99.25	99.84
NA+	0.144	0.160	0.153	0.161	0.171	0.164	0.172	0.165	0.152	0.169	0.184	0.191
MG2+	0.109	0.134	0.119	0.129	0.137	0.126	0.143	0.131	0.107	0.130	0.150	0.169
AL3+	1.841	1.823	1.806	1.785	1.783	1.789	1.785	1.772	1.825	1.830	1.790	1.771
SI4+	6.002	5.997	5.995	6.001	6.001	5.998	6.012	6.008	5.996	5.989	5.987	5.986
K+	0.004	0.002	0.002	0.004	0.004	0.005	0.004	0.004	0.005	0.002	0.005	0.006
CA2+	0.001	0.002	0.001	0.001	0.001	0.002	0.001	0.000	0.000	0.002	0.002	0.003
SC3+	0.002	0.001	0.002	0.002	0.001	0.003	0.001	0.002	0.002	0.002	0.002	0.005
TI4+	0.000	0.000	0.001	0.000	0.000	0.000	0.001	0.000	0.000	0.000	0.000	0.000
V3+	0.003	0.001	0.000	0.001	0.001	0.001	0.001	0.004	0.003	0.001	0.003	0.003
CR3+	0.009	0.018	0.037	0.043	0.037	0.040	0.017	0.043	0.026	0.010	0.034	0.034
MN2+	0.000	0.001	0.002	0.000	0.001	0.001	0.001	0.001	0.000	0.001	0.001	0.001
FE2+	0.028	0.023	0.036	0.036	0.036	0.036	0.032	0.034	0.034	0.036	0.034	0.036
CS+	0.006	0.003	0.006	0.005	0.005	0.006	0.005	0.005	0.007	0.005	0.004	0.004
BE2+	3.000	3.000	3.000	3.000	3.000	3.000	3.000	3.000	3.000	3.000	3.000	3.000
CATSUM	11.148	11.165	11.162	11.169	11.178	11.172	11.175	11.168	11.158	11.177	11.196	11.208

Data for emerald from Adit

Point	85	86	87	88	89	90	91	92	93	94	95	96
NA2O	0.98	0.93	0.83	0.91	0.87	0.89	0.84	1.14	0.82	0.86	0.94	0.85
MGO	1.05	1.00	0.84	0.94	0.86	0.91	0.87	1.33	0.86	0.91	0.97	0.95
AL2O3	16.22	15.97	16.53	16.56	16.60	16.36	16.44	15.84	16.57	16.32	16.24	16.08
SIO2	64.46	64.21	64.45	64.36	64.20	64.77	64.45	64.24	64.21	64.36	63.95	65.13
K2O	0.03	0.03	0.02	0.02	0.02	0.03	0.02	0.04	0.03	0.03	0.03	0.02
CAO	0.04	0.02	0.02	0.02	0.03	0.01	0.03	0.02	0.03	0.00	0.02	0.03
SC2O3	0.05	0.05	0.01	0.05	0.02	0.04	0.02	0.04	0.04	0.03	0.06	0.05
TIO2	0.00	0.00	0.00	0.00	0.00	0.01	0.00	0.00	0.01	0.00	0.00	0.00
V2O3	0.04	0.02	0.03	0.05	0.03	0.03	0.03	0.04	0.02	0.02	0.03	0.00
CR2O3	0.65	0.86	0.55	0.35	0.64	0.53	0.52	0.35	0.28	0.80	0.66	0.92
MNO	0.01	0.02	0.02	0.01	0.00	0.00	0.02	0.02	0.01	0.00	0.00	0.01
FEO	0.53	0.50	0.43	0.41	0.43	0.48	0.43	0.48	0.43	0.41	0.46	0.39
CS2O	0.12	0.14	0.17	0.13	0.18	0.10	0.11	0.08	0.14	0.16	0.14	0.11
BEO *	13.45	13.38	13.43	13.42	13.42	13.48	13.42	13.37	13.38	13.42	13.35	13.53
H2O	2.09	2.05	1.96	2.03	2.00	2.02	1.97	2.23	1.96	1.99	2.06	1.98
TOTAL	99.72	99.18	99.29	99.26	99.30	99.66	99.17	99.22	98.79	99.31	98.91	100.05
NA+	0.176	0.168	0.150	0.164	0.157	0.160	0.152	0.206	0.148	0.155	0.171	0.152
MG2+	0.145	0.139	0.116	0.130	0.119	0.126	0.121	0.185	0.120	0.126	0.135	0.131
AL3+	1.775	1.757	1.811	1.816	1.821	1.787	1.803	1.744	1.823	1.790	1.791	1.750
SI4+	5.986	5.995	5.992	5.988	5.976	6.002	5.997	6.001	5.995	5.990	5.983	6.012
K+	0.004	0.004	0.002	0.002	0.002	0.004	0.002	0.005	0.004	0.004	0.004	0.002
CA2+	0.004	0.002	0.002	0.002	0.003	0.001	0.003	0.002	0.003	0.000	0.002	0.003
SC3+	0.004	0.004	0.001	0.004	0.002	0.003	0.002	0.003	0.003	0.002	0.005	0.004
TI4+	0.000	0.000	0.000	0.000	0.000	0.001	0.000	0.000	0.001	0.000	0.000	0.000
V3+	0.003	0.001	0.002	0.004	0.002	0.002	0.002	0.003	0.001	0.001	0.002	0.000
CR3+	0.048	0.063	0.040	0.026	0.047	0.039	0.038	0.026	0.021	0.059	0.049	0.067
MN2+	0.001	0.002	0.002	0.001	0.000	0.000	0.002	0.002	0.001	0.000	0.000	0.001
FE2+	0.041	0.039	0.033	0.032	0.033	0.037	0.033	0.038	0.034	0.032	0.036	0.030
CS+	0.005	0.006	0.007	0.005	0.007	0.004	0.004	0.003	0.006	0.006	0.006	0.004
BE2+	3.000	3.000	3.000	3.000	3.000	3.000	3.000	3.000	3.000	3.000	3.000	3.000
CATSUM	11.192	11.181	11.159	11.174	11.171	11.165	11.159	11.218	11.159	11.166	11.183	11.157

Data for emerald from Adit

Point	97	98	99	100	101	102	103	104	105	106	107	108
NA2O	0.93	0.90	0.99	1.09	0.99	0.84	0.30	0.99	0.97	0.82	0.93	0.82
MGO	1.00	0.98	1.11	1.19	1.16	0.84	0.23	1.09	1.11	0.91	1.07	0.86
AL2O3	16.12	16.41	15.97	15.82	16.04	16.56	17.60	15.42	16.13	16.26	16.41	16.57
SIO2	64.01	64.79	64.33	63.95	64.82	64.66	65.45	64.31	64.34	64.90	64.76	64.86
K2O	0.02	0.03	0.03	0.03	0.01	0.02	0.00	0.03	0.03	0.01	0.04	0.03
CAO	0.03	0.01	0.03	0.03	0.03	0.03	0.02	0.03	0.02	0.02	0.04	0.02
SC2O3	0.04	0.04	0.04	0.03	0.05	0.03	0.01	0.07	0.05	0.04	0.05	0.05
TIO2	0.00	0.00	0.01	0.01	0.00	0.01	0.00	0.02	0.00	0.01	0.00	0.00
V2O3	0.05	0.05	0.01	0.03	0.01	0.03	0.02	0.03	0.03	0.02	0.03	0.02
CR2O3	0.64	0.45	0.67	0.98	0.66	0.61	0.61	1.46	0.58	0.66	0.31	0.59
MNO	0.03	0.00	0.00	0.01	0.02	0.00	0.00	0.01	0.03	0.00	0.02	0.02
FEO	0.39	0.39	0.42	0.48	0.42	0.36	0.20	0.55	0.42	0.40	0.44	0.39
CS2O	0.10	0.07	0.07	0.12	0.08	0.12	0.04	0.08	0.08	0.13	0.11	0.13
BEO *	13.34	13.48	13.39	13.36	13.48	13.47	13.62	13.39	13.41	13.48	13.48	13.51
H2O	2.05	2.02	2.10	2.19	2.10	1.97	1.51	2.10	2.08	1.96	2.05	1.96
TOTAL	98.75	99.62	99.17	99.32	99.87	99.55	99.61	99.58	99.28	99.62	99.74	99.83
NA+	0.169	0.162	0.179	0.198	0.178	0.151	0.053	0.179	0.175	0.147	0.167	0.147
MG2+	0.140	0.135	0.154	0.166	0.160	0.116	0.031	0.151	0.154	0.126	0.148	0.118
AL3+	1.779	1.791	1.756	1.743	1.751	1.809	1.902	1.694	1.771	1.775	1.791	1.805
SI4+	5.993	6.001	6.001	5.979	6.003	5.993	6.001	5.996	5.994	6.011	5.997	5.995
K+	0.002	0.004	0.004	0.004	0.001	0.002	0.000	0.004	0.004	0.001	0.005	0.004
CA2+	0.003	0.001	0.003	0.003	0.003	0.003	0.002	0.003	0.002	0.002	0.004	0.002
SC3+	0.003	0.003	0.003	0.002	0.004	0.002	0.001	0.006	0.004	0.003	0.004	0.004
TI4+	0.000	0.000	0.001	0.001	0.000	0.001	0.000	0.001	0.000	0.001	0.000	0.000
V3+	0.004	0.004	0.001	0.002	0.001	0.002	0.001	0.002	0.002	0.001	0.002	0.001
CR3+	0.047	0.033	0.049	0.072	0.048	0.045	0.044	0.108	0.043	0.048	0.023	0.043
MN2+	0.002	0.000	0.000	0.001	0.002	0.000	0.000	0.001	0.002	0.000	0.002	0.002
FE2+	0.031	0.030	0.033	0.038	0.033	0.028	0.015	0.043	0.033	0.031	0.034	0.030
CS+	0.004	0.003	0.003	0.005	0.003	0.005	0.002	0.003	0.003	0.005	0.004	0.005
BE2+	3.000	3.000	3.000	3.000	3.000	3.000	3.000	3.000	3.000	3.000	3.000	3.000
CATSUM	11.177	11.167	11.186	11.213	11.186	11.157	11.053	11.191	11.187	11.151	11.181	11.156

Data for emerald from Adit

Point	109	128	129	130	131	132	143	144	145	146	147	148
NA2O	1.03	1.08	1.08	0.99	0.51	0.96	0.36	0.87	0.98	0.90	0.97	0.91
MGO	1.06	1.27	1.24	1.16	0.51	1.14	0.24	0.89	1.01	0.94	0.98	0.97
AL2O3	16.36	15.89	15.29	16.16	17.12	16.01	17.63	16.45	15.97	16.43	16.38	16.10
SIO2	64.80	64.03	64.50	64.01	65.41	64.29	65.05	64.43	64.40	64.49	64.52	64.08
K2O	0.03	0.04	0.04	0.03	0.01	0.03	0.02	0.03	0.03	0.02	0.03	0.02
CAO	0.02	0.04	0.04	0.02	0.02	0.02	0.01	0.01	0.03	0.02	0.03	0.02
SC2O3	0.04	0.06	0.06	0.04	0.01	0.07	0.00	0.04	0.06	0.04	0.05	0.05
TIO2	0.00	0.00	0.00	0.00	0.00	0.00	0.00	0.00	0.00	0.00	0.01	0.00
V2O3	0.05	0.05	0.02	0.02	0.01	0.04	0.00	0.03	0.02	0.01	0.03	0.01
CR2O3	0.52	0.51	1.01	0.37	0.61	0.42	0.45	0.49	0.72	0.58	0.29	0.70
MNO	0.03	0.01	0.00	0.00	0.00	0.00	0.00	0.02	0.02	0.01	0.02	0.02
FEO	0.45	0.40	0.49	0.46	0.22	0.42	0.20	0.43	0.43	0.44	0.41	0.47
CS2O	0.13	0.12	0.14	0.11	0.03	0.11	0.00	0.18	0.11	0.11	0.13	0.14
BEO *	13.51	13.34	13.38	13.34	13.60	13.37	13.55	13.42	13.40	13.44	13.43	13.35
H2O	2.13	2.18	2.18	2.10	1.69	2.08	1.57	2.00	2.09	2.02	2.08	2.03
TOTAL	100.16	99.02	99.47	98.81	99.75	98.96	99.08	99.29	99.27	99.45	99.36	98.87
NA+	0.185	0.196	0.195	0.180	0.091	0.174	0.064	0.157	0.177	0.162	0.175	0.165
MG2+	0.146	0.177	0.173	0.162	0.070	0.159	0.033	0.123	0.140	0.130	0.136	0.135
AL3+	1.782	1.753	1.682	1.783	1.853	1.763	1.916	1.804	1.755	1.799	1.795	1.775
SI4+	5.989	5.993	6.019	5.992	6.008	6.006	5.997	5.994	6.004	5.990	6.000	5.995
K+	0.004	0.005	0.005	0.004	0.001	0.004	0.002	0.004	0.004	0.002	0.004	0.002
CA2+	0.002	0.004	0.004	0.002	0.002	0.002	0.001	0.001	0.003	0.002	0.003	0.002
SC3+	0.003	0.005	0.005	0.003	0.001	0.006	0.000	0.003	0.005	0.003	0.004	0.004
TI4+	0.000	0.000	0.000	0.000	0.000	0.000	0.000	0.000	0.000	0.000	0.001	0.000
V3+	0.004	0.004	0.001	0.002	0.001	0.003	0.000	0.002	0.001	0.001	0.002	0.001
CR3+	0.038	0.038	0.075	0.027	0.044	0.031	0.033	0.036	0.053	0.043	0.021	0.052
MN2+	0.002	0.001	0.000	0.000	0.000	0.000	0.000	0.002	0.002	0.001	0.002	0.002
FE2+	0.035	0.031	0.038	0.036	0.017	0.033	0.015	0.033	0.034	0.034	0.032	0.037
CS+	0.005	0.005	0.006	0.004	0.001	0.004	0.000	0.007	0.004	0.004	0.005	0.006
BE2+	3.000	3.000	3.000	3.000	3.000	3.000	3.000	3.000	3.000	3.000	3.000	3.000
CATSUM	11.194	11.211	11.202	11.194	11.089	11.184	11.062	11.167	11.182	11.171	11.180	11.176

Data for emerald from Adit

Point	149	150	151	152	153	154	155	156	157	158	159	160
NA2O	0.96	1.04	0.75	0.67	1.02	0.94	1.06	0.98	1.03	0.84	1.13	0.89
MGO	0.97	1.13	0.72	0.67	1.10	1.05	1.12	1.13	1.10	0.80	1.33	0.96
AL2O3	16.20	16.15	16.67	16.99	16.16	16.32	16.13	16.51	16.32	16.84	15.60	16.39
SIO2	64.35	64.55	64.37	64.29	64.56	64.36	64.67	64.46	64.67	64.59	64.12	64.13
K2O	0.02	0.04	0.01	0.02	0.03	0.03	0.05	0.04	0.03	0.02	0.03	0.02
CAO	0.03	0.03	0.02	0.02	0.02	0.02	0.01	0.03	0.03	0.03	0.03	0.03
SC2O3	0.03	0.05	0.01	0.04	0.03	0.06	0.05	0.04	0.05	0.02	0.07	0.03
TIO2	0.01	0.00	0.00	0.00	0.02	0.00	0.00	0.00	0.00	0.00	0.00	0.00
V2O3	0.02	0.05	0.03	0.03	0.02	0.03	0.06	0.02	0.06	0.06	0.05	0.01
CR2O3	0.62	0.41	0.41	0.34	0.28	0.38	0.42	0.12	0.30	0.29	0.83	0.44
MNO	0.00	0.01	0.00	0.00	0.00	0.03	0.02	0.01	0.01	0.00	0.03	0.02
FEO	0.48	0.42	0.46	0.37	0.43	0.43	0.47	0.44	0.47	0.44	0.47	0.43
CS2O	0.13	0.10	0.21	0.09	0.12	0.11	0.14	0.17	0.10	0.16	0.13	0.13
BEO *	13.40	13.44	13.40	13.41	13.42	13.41	13.46	13.44	13.47	13.47	13.36	13.37
H2O	2.08	2.14	1.90	1.83	2.13	2.06	2.16	2.09	2.13	1.97	2.22	2.02
TOTAL	99.30	99.56	98.96	98.77	99.34	99.23	99.82	99.48	99.77	99.53	99.40	98.87
NA+	0.173	0.187	0.135	0.121	0.184	0.170	0.191	0.177	0.185	0.151	0.205	0.161
MG2+	0.135	0.157	0.100	0.093	0.153	0.146	0.155	0.157	0.152	0.111	0.185	0.134
AL3+	1.779	1.769	1.830	1.864	1.773	1.791	1.764	1.808	1.783	1.839	1.718	1.805
SI4+	5.995	5.999	5.997	5.985	6.009	5.994	6.000	5.990	5.995	5.986	5.991	5.992
K+	0.002	0.005	0.001	0.002	0.004	0.004	0.006	0.005	0.004	0.002	0.004	0.002
CA2+	0.003	0.003	0.002	0.002	0.002	0.002	0.001	0.003	0.003	0.003	0.003	0.003
SC3+	0.002	0.004	0.001	0.003	0.002	0.005	0.004	0.003	0.004	0.002	0.006	0.002
TI4+	0.001	0.000	0.000	0.000	0.001	0.000	0.000	0.000	0.000	0.000	0.000	0.000
V3+	0.001	0.004	0.002	0.002	0.001	0.002	0.004	0.001	0.004	0.004	0.004	0.001
CR3+	0.046	0.030	0.030	0.025	0.021	0.028	0.031	0.009	0.022	0.021	0.061	0.033
MN2+	0.000	0.001	0.000	0.000	0.000	0.002	0.002	0.001	0.001	0.000	0.002	0.002
FE2+	0.037	0.033	0.036	0.029	0.033	0.033	0.036	0.034	0.036	0.034	0.037	0.034
CS+	0.005	0.004	0.008	0.004	0.005	0.004	0.006	0.007	0.004	0.006	0.005	0.005
BE2+	3.000	3.000	3.000	3.000	3.000	3.000	3.000	3.000	3.000	3.000	3.000	3.000
CATSUM	11.180	11.195	11.144	11.131	11.188	11.182	11.199	11.194	11.194	11.160	11.221	11.173

Data for emerald from Adit

Point	161	162	204	205	206	207	208	209	210	211	212	213
NA2O	0.87	0.91	0.92	0.95	0.85	0.91	0.93	0.97	0.99	1.21	0.85	0.94
MGO	0.96	0.97	0.97	1.01	0.84	1.04	1.01	1.13	1.13	1.41	0.84	0.97
AL2O3	16.38	16.14	16.29	16.43	16.79	16.63	16.20	16.41	16.00	15.46	16.70	16.36
SIO2	64.27	64.40	64.40	64.45	64.71	63.91	64.59	64.73	63.68	64.21	64.09	64.50
K2O	0.04	0.02	0.03	0.03	0.04	0.03	0.03	0.02	0.05	0.04	0.03	0.03
CAO	0.01	0.03	0.01	0.02	0.02	0.02	0.02	0.02	0.02	0.04	0.01	0.01
SC2O3	0.04	0.04	0.03	0.03	0.00	0.03	0.04	0.04	0.02	0.07	0.01	0.02
TIO2	0.00	0.02	0.02	0.01	0.00	0.00	0.00	0.00	0.00	0.01	0.00	0.00
V2O3	0.01	0.03	0.02	0.01	0.04	0.06	0.02	0.04	0.02	0.04	0.02	0.02
CR2O3	0.53	0.66	0.68	0.44	0.18	0.06	0.58	0.12	0.63	0.64	0.23	0.39
MNO	0.02	0.00	0.02	0.01	0.00	0.01	0.00	0.00	0.00	0.01	0.00	0.01
FEO	0.44	0.40	0.46	0.43	0.41	0.43	0.48	0.42	0.47	0.52	0.41	0.43
CS2O	0.14	0.10	0.15	0.09	0.20	0.15	0.13	0.10	0.16	0.08	0.19	0.11
BEO *	13.40	13.40	13.43	13.44	13.48	13.34	13.44	13.47	13.28	13.36	13.36	13.42
H2O	2.00	2.03	2.04	2.07	1.98	2.03	2.05	2.08	2.10	2.29	1.98	2.06
TOTAL	99.11	99.15	99.47	99.42	99.54	98.65	99.52	99.55	98.55	99.39	98.72	99.27
NA+	0.157	0.164	0.166	0.171	0.153	0.165	0.168	0.174	0.180	0.219	0.154	0.170
MG2+	0.133	0.135	0.134	0.140	0.116	0.145	0.140	0.156	0.158	0.196	0.117	0.135
AL3+	1.800	1.773	1.785	1.800	1.834	1.834	1.774	1.794	1.773	1.703	1.839	1.794
SI4+	5.991	6.001	5.989	5.990	5.996	5.981	6.001	6.003	5.986	6.002	5.990	6.001
K+	0.005	0.002	0.004	0.004	0.005	0.004	0.004	0.002	0.006	0.005	0.004	0.004
CA2+	0.001	0.003	0.001	0.002	0.002	0.002	0.002	0.002	0.002	0.004	0.001	0.001
SC3+	0.003	0.003	0.002	0.002	0.000	0.002	0.003	0.003	0.002	0.006	0.001	0.002
TI4+	0.000	0.001	0.001	0.001	0.000	0.000	0.000	0.000	0.000	0.001	0.000	0.000
V3+	0.001	0.002	0.001	0.001	0.003	0.005	0.001	0.003	0.002	0.003	0.001	0.001
CR3+	0.039	0.049	0.050	0.032	0.013	0.004	0.043	0.009	0.047	0.047	0.017	0.029
MN2+	0.002	0.000	0.002	0.001	0.000	0.001	0.000	0.000	0.000	0.001	0.000	0.001
FE2+	0.034	0.031	0.036	0.033	0.032	0.034	0.037	0.033	0.037	0.041	0.032	0.033
CS+	0.006	0.004	0.006	0.004	0.008	0.006	0.005	0.004	0.006	0.003	0.008	0.004
BE2+	3.000	3.000	3.000	3.000	3.000	3.000	3.000	3.000	3.000	3.000	3.000	3.000
CATSUM	11.171	11.169	11.178	11.181	11.161	11.183	11.177	11.183	11.199	11.231	11.164	11.174

Data for emerald from Adit

Point	214	215	Adit AVG	STD DEV
NA2O	1.02	1.08	0.92	0.14
MGO	1.16	1.22	0.98	0.20
AL2O3	15.78	15.77	16.35	0.38
SIO2	64.51	64.58	64.47	0.40
K2O	0.03	0.02	0.03	0.01
CAO	0.02	0.03	0.02	0.01
SC2O3	0.04	0.04	0.04	0.02
TIO2	0.00	0.00	0.00	0.01
V2O3	0.04	0.04	0.03	0.01
CR2O3	0.75	0.61	0.52	0.22
MNO	0.00	0.00	0.01	0.01
FEO	0.44	0.47	0.42	0.06
CS2O	0.14	0.16	0.12	0.03
BEO *	13.41	13.42	13.43	0.07
H2O	2.13	2.18	2.04	0.12
TOTAL	99.47	99.62	99.37	0.40
NA+	0.184	0.195	0.165	0.026
MG2+	0.161	0.169	0.136	0.028
AL3+	1.732	1.729	1.791	0.037
SI4+	6.008	6.009	5.995	0.009
K+	0.004	0.002	0.004	0.001
CA2+	0.002	0.003	0.002	0.001
SC3+	0.003	0.003	0.003	0.001
TI4+	0.000	0.000	0.000	0.000
V3+	0.003	0.003	0.002	0.001
CR3+	0.055	0.045	0.038	0.016
MN2+	0.000	0.000	0.001	0.001
FE2+	0.034	0.037	0.033	0.005
CS+	0.006	0.006	0.005	0.001
BE2+	3.000	3.000	3.000	0.000
CATSUM	11.192	11.202	11.174	0.029

Data for tourmaline from schist

HN-2-14	T14-1	T14-2	T14-3	T14-4	T14-5	T14-6	T14-7	T14-8	T14-9	14-Oct	14-Nov	14-Dec	14-13
F	0	0.02	0.04	0.07	0.01	0.04	0.05	0	0	0	0	0	0
NA2O	1.99	2.02	1.95	1.93	1.93	1.83	1.86	1.89	1.92	0.75	1.94	1.97	1.77
MGO	9.25	9.58	9.23	9.56	9.14	9.62	9.45	9.11	9.06	15.9	9.77	9.44	9.4
AL2O3	32.23	32.1	32.53	31.78	32.08	32.04	32.03	32.83	32.06	12.92	31.4	31.83	31.6
SIO2	35.61	35.44	34.54	35.89	36.07	35.09	35.99	35.65	35.33	47.42	35.4	35.69	35.86
K2O	0	0.03	0.02	0.01	0	0.01	0.02	0.01	0	0.01	0.02	0.01	0
CAO	1.34	1.43	1.34	1.52	1.41	1.58	1.48	1.08	1.3	8.37	1.57	1.39	1.43
TIO2	0.51	0.53	0.6	0.53	0.5	0.66	0.68	0.39	0.56	0.28	0.59	0.57	0.66
CR2O3	0.1	0.11	0.09	0.16	0.15	0.11	0.23	0.2	0.1	0.05	0.08	0.08	0.25
MNO	0	0	0.04	0	0.04	0.04	0.04	0.02	0.01	0.17	0	0	0
FEO	3.88	3.96	4.32	3.71	4.13	3.78	3.79	3.74	3.98	5.93	3.96	3.74	3.8
B2O3 *	10.55	10.58	10.52	10.57	10.6	10.54	10.63	10.6	10.48	10.63	10.52	10.53	10.54
H2O *	3.64	3.64	3.61	3.61	3.65	3.62	3.64	3.66	3.62	3.67	3.63	3.63	3.64
O=F	0	-0.01	-0.02	-0.03	0	-0.02	-0.02	0	0	0	0	0	0
TOTAL	99.11	99.44	98.82	99.31	99.71	98.94	99.87	99.18	98.42	106.09	98.88	98.89	98.95
F-	0	0.01	0.021	0.036	0.005	0.021	0.026	0	0	0	0	0	0
NA+	0.635	0.643	0.625	0.615	0.614	0.585	0.59	0.601	0.617	0.238	0.621	0.63	0.566
MG2+	2.271	2.345	2.273	2.343	2.234	2.365	2.304	2.226	2.24	3.877	2.406	2.322	2.31
AL3+	6.255	6.212	6.333	6.159	6.199	6.226	6.173	6.342	6.266	2.491	6.114	6.191	6.14
SI4+	5.864	5.819	5.705	5.901	5.914	5.786	5.886	5.843	5.858	7.756	5.849	5.89	5.912
K+	0	0.006	0.004	0.002	0	0.002	0.004	0.002	0	0.002	0.004	0.002	0
CA2+	0.236	0.252	0.237	0.268	0.248	0.279	0.259	0.19	0.231	1.467	0.278	0.246	0.253
TI4+	0.063	0.065	0.075	0.066	0.062	0.082	0.084	0.048	0.07	0.034	0.073	0.071	0.082
CR3+	0.013	0.014	0.012	0.021	0.019	0.014	0.03	0.026	0.013	0.006	0.01	0.01	0.033
MN2+	0	0	0.006	0	0.006	0.006	0.006	0.003	0.001	0.024	0	0	0
FE2+	0.534	0.544	0.597	0.51	0.566	0.521	0.518	0.513	0.552	0.811	0.547	0.516	0.524
B3+	3	3	3	3	3	3	3	3	3	3	3	3	3
H+	4	3.99	3.979	3.964	3.995	3.979	3.974	4	4	4	4	4	4
O2-	31.115	31.064	30.983	31.097	31.134	31.04	31.101	31.066	31.107	32.126	31.075	31.123	31.115
CATSUM	18.872	18.901	18.866	18.885	18.861	18.866	18.853	18.792	18.848	19.707	18.904	18.878	18.818
AN SUM	31.115	31.074	31.004	31.133	31.139	31.061	31.127	31.066	31.107	32.126	31.075	31.123	31.115

Data for tourmaline from schist

HN-2-10	T10-1	T10-2	T10-3	T10-4	T10-5	T10-6	T10-7	T10-8	T10-9	10-10	10-11	10-12	10-13
F	0	0.02	0.03	0.06	0	0	0	0.06	0	0	0.03	0.05	0
NA2O	1.83	1.89	1.89	1.91	1.91	2	1.85	0.01	1.81	1.74	1.78	1.96	1.93
MGO	8.75	8.94	8.64	8.94	9.01	8.49	8.36	0	8.34	8.36	9.07	9.06	9.08
AL2O3	31.81	31.51	31.05	31.65	31.24	31.58	32.83	0.01	32.2	32.51	32.12	32.01	31.52
SIO2	34.8	35.18	35.11	35.42	35.2	35.04	35.21	99.04	34.7	35.32	35.67	36.19	35.35
K2O	0.02	0.02	0.02	0.01	0.02	0.02	0	0	0.02	0.03	0.01	0.03	0.02
CAO	1.32	1.39	1.58	1.29	1.42	1.31	1.05	0.01	1.59	1.27	1.39	1.39	1.5
TIO2	0.48	0.5	0.48	0.57	0.47	0.53	0.25	0	0.29	0.39	0.56	0.34	0.45
CR2O3	0.26	0.2	0.34	0.26	0.14	0.07	0.15	0.04	0.05	0.24	0.17	0.19	0.14
MNO	0	0.01	0	0	0.04	0	0.01	0	0.02	0	0	0	0.04
FEO	5.35	5.39	5.9	5.04	5.5	5.96	5.51	0.13	5.97	5.58	4.14	4.41	5.18
B2O3 *	10.47	10.51	10.45	10.53	10.49	10.47	10.58	11.49	10.47	10.57	10.55	10.6	10.53
H2O *	3.61	3.62	3.59	3.61	3.62	3.61	3.65	3.94	3.61	3.65	3.63	3.63	3.63
O=F	0	-0.01	-0.01	-0.03	0	0	0	-0.03	0	0	-0.01	-0.02	0
TOTAL	98.7	99.17	99.06	99.26	99.06	99.08	99.45	114.7	99.07	99.66	99.11	99.85	99.37
F-	0	0.01	0.016	0.031	0	0	0	0.029	0	0	0.016	0.026	0
NA+	0.589	0.606	0.61	0.611	0.613	0.644	0.589	0.003	0.583	0.555	0.568	0.623	0.618
MG2+	2.165	2.204	2.143	2.199	2.225	2.101	2.048	0	2.064	2.049	2.227	2.214	2.235
AL3+	6.222	6.142	6.089	6.156	6.099	6.179	6.358	0.002	6.3	6.299	6.236	6.183	6.134
SI4+	5.776	5.818	5.842	5.845	5.831	5.817	5.786	14.977	5.761	5.806	5.875	5.932	5.837
K+	0.004	0.004	0.004	0.002	0.004	0.004	0	0	0.004	0.006	0.002	0.006	0.004
CA2+	0.235	0.246	0.282	0.228	0.252	0.233	0.185	0.002	0.283	0.224	0.245	0.244	0.265
TI4+	0.06	0.062	0.06	0.071	0.059	0.066	0.031	0	0.036	0.048	0.069	0.042	0.056
CR3+	0.034	0.026	0.045	0.034	0.018	0.009	0.019	0.005	0.007	0.031	0.022	0.025	0.018
MN2+	0	0.001	0	0	0.006	0	0.001	0	0.003	0	0	0	0.006
FE2+	0.743	0.746	0.821	0.696	0.762	0.827	0.757	0.016	0.829	0.767	0.57	0.604	0.715
B3+	3	3	3	3	3	3	3	3	3	3	3	3	3
H+	4	3.99	3.984	3.969	4	4	4	3.971	4	4	3.984	3.974	4
O2-	30.995	31.006	31.042	31.014	31.009	31.034	30.985	36.455	31.027	31.023	31.089	31.11	31.045
CATSUM	18.828	18.857	18.896	18.841	18.87	18.881	18.774	18.005	18.87	18.785	18.816	18.873	18.887
AN SUM	30.995	31.016	31.058	31.045	31.009	31.034	30.985	36.483	31.027	31.023	31.104	31.136	31.045

Data for tourmaline from schist

99-10	59-1	59-2	59-3	59-4	59-5	59-6	59-7	59-8	59-9	59-10	59-11	59-12	59-13
F	1.2	0.15	0.49	0.97	0.48	0.36	1.31	0.03	0.68	1	0.77	0.31	0.28
NA2O	1.44	1.89	1.84	1.48	1.74	1.92	1.36	1.93	1.84	1.42	1.73	2.01	1.95
MGO	10.73	8.14	9.05	10.27	9.21	9.07	10.89	8.75	9.52	10.58	9.09	9.21	9.16
AL2O3	29.05	32.67	29.76	29.45	30.48	31.19	28.85	31.3	31.17	29.15	30.86	31.83	31.72
SIO2	35.98	35.74	35.11	35.18	35.48	35.39	35.2	35.89	35.89	35.68	35.23	35.31	35.7
K2O	0.03	0.02	0.01	0.02	0.01	0.02	0.04	0.04	0.02	0.02	0.03	0.01	0.02
CAO	2.88	0.93	2.02	2.65	1.98	1.67	3.05	1.5	1.66	2.91	1.98	1.56	1.66
TIO2	0.33	0.34	0.89	0.6	0.82	0.55	0.34	0.42	0.3	0.58	0.23	0.14	0.2
CR2O3	0.23	0.09	0.4	0.03	0.09	0.08	0.26	0.16	0.21	0.14	0	0.19	0.2
MNO	0.03	0.02	0	0.07	0.02	0.01	0.01	0.03	0.05	0.05	0.03	0.04	0.01
FEO	4.83	5.13	5.72	5.18	5.29	5.11	4.74	5.45	4.64	5.36	5.53	4.4	4.59
B2O3 *	10.51	10.55	10.36	10.44	10.46	10.48	10.41	10.53	10.56	10.53	10.43	10.49	10.53
H2O *	3.06	3.57	3.34	3.14	3.38	3.44	2.97	3.62	3.32	3.16	3.23	3.47	3.5
O=F	-0.51	-0.06	-0.21	-0.41	-0.2	-0.15	-0.55	-0.01	-0.29	-0.42	-0.32	-0.13	-0.12
TOTAL	99.79	99.17	98.79	99.07	99.24	99.14	98.88	99.63	99.57	100.16	98.81	98.84	99.4
F-	0.628	0.078	0.26	0.511	0.252	0.189	0.692	0.016	0.354	0.522	0.406	0.162	0.146
NA+	0.462	0.604	0.598	0.478	0.561	0.617	0.44	0.618	0.587	0.454	0.559	0.646	0.624
MG2+	2.645	2	2.263	2.55	2.282	2.243	2.71	2.154	2.336	2.603	2.259	2.275	2.253
AL3+	5.662	6.346	5.882	5.781	5.97	6.097	5.675	6.091	6.047	5.67	6.063	6.216	6.169
SI4+	5.95	5.89	5.888	5.859	5.896	5.87	5.875	5.926	5.907	5.889	5.873	5.851	5.891
K+	0.006	0.004	0.002	0.004	0.002	0.004	0.009	0.008	0.004	0.004	0.006	0.002	0.004
CA2+	0.51	0.164	0.363	0.473	0.353	0.297	0.545	0.265	0.293	0.515	0.354	0.277	0.294
TI4+	0.041	0.042	0.112	0.075	0.102	0.069	0.043	0.052	0.037	0.072	0.029	0.017	0.025
CR3+	0.03	0.012	0.053	0.004	0.012	0.01	0.034	0.021	0.027	0.018	0	0.025	0.026
MN2+	0.004	0.003	0	0.01	0.003	0.001	0.001	0.004	0.007	0.007	0.004	0.006	0.001
FE2+	0.668	0.707	0.802	0.721	0.735	0.709	0.662	0.753	0.639	0.74	0.771	0.61	0.633
B3+	3	3	3	3	3	3	3	3	3	3	3	3	3
H+	3.372	3.922	3.74	3.489	3.748	3.811	3.308	3.984	3.646	3.478	3.594	3.838	3.854
O2-	30.453	31.001	30.871	30.53	30.871	30.912	30.351	31.097	30.716	30.527	30.664	30.927	30.975
CATSUM	18.978	18.772	18.963	18.955	18.915	18.919	18.994	18.892	18.884	18.973	18.919	18.925	18.922
AN SUM	31.081	31.08	31.131	31.04	31.123	31.101	31.042	31.112	31.07	31.049	31.07	31.09	31.122

Data for tourmaline from schist

AD1-21.2	12-1	12-2	12-3	12-4	12-5	12-6	12-7	12-8	12-9	12-10	12-11	12-13	12-14
F	0.11	1.37	0.39	0.72	1.33	1.63	0	1.72	0	0	1.27	1.08	1.52
NA2O	1.87	1.72	1.71	1.96	1.68	1.65	1.98	1.9	1.95	1.81	1.84	2.11	1.66
MGO	8.19	9.59	8.27	7.63	9.44	9.45	8	8.73	7.81	8.26	8.41	7.13	9.13
AL2O3	31.8	29.79	31.67	31.59	29.98	29.82	32.28	30.09	32.99	31.99	30.64	32.1	30.17
SIO2	35.89	35.52	35.69	35.69	35.71	35.47	35.8	35.48	35.33	35.98	35.44	35.44	35.97
K2O	0.01	0.04	0	0.02	0	0.04	0.02	0.04	0.02	0.02	0.02	0.04	0.02
CAO	1.64	2.32	1.56	1.32	2.43	2.5	1.09	1.89	1.19	1.05	2	0.93	2.17
TIO2	0.38	0.15	0.57	0.24	0.19	0.19	0.21	0.2	0.18	0.13	0.22	0.12	0.27
CR2O3	0.03	0	0.02	0	0	0	0	0.02	0	0	0.02	0.01	0
MNO	0.05	0.09	0	0.03	0.06	0.11	0.06	0.09	0.04	0.05	0.11	0.09	0.13
FEO	6.43	5.84	6.13	7.06	5.71	6.09	5.73	6.19	5.61	5.75	6.41	6.97	5.87
B2O3 *	10.58	10.43	10.53	10.48	10.44	10.43	10.52	10.36	10.51	10.54	10.4	10.42	10.47
H2O *	3.6	2.95	3.45	3.27	2.97	2.83	3.63	2.76	3.63	3.64	2.98	3.08	2.89
O=F	-0.05	-0.58	-0.16	-0.3	-0.56	-0.69	0	-0.72	0	0	-0.53	-0.45	-0.64
TOTAL	100.53	99.23	99.83	99.7	99.38	99.52	99.32	98.74	99.26	99.21	99.23	99.06	99.63
F-	0.057	0.722	0.204	0.378	0.7	0.859	0	0.913	0	0	0.671	0.57	0.798
NA+	0.596	0.556	0.547	0.631	0.542	0.533	0.634	0.618	0.625	0.579	0.596	0.683	0.534
MG2+	2.006	2.383	2.034	1.887	2.343	2.347	1.971	2.184	1.925	2.031	2.096	1.773	2.259
AL3+	6.157	5.852	6.158	6.177	5.883	5.855	6.287	5.952	6.429	6.218	6.037	6.312	5.903
SI4+	5.896	5.92	5.888	5.922	5.946	5.91	5.916	5.955	5.842	5.934	5.925	5.913	5.971
K+	0.002	0.009	0	0.004	0	0.009	0.004	0.009	0.004	0.004	0.004	0.009	0.004
CA2+	0.289	0.414	0.276	0.235	0.434	0.446	0.193	0.34	0.211	0.186	0.358	0.166	0.386
TI4+	0.047	0.019	0.071	0.03	0.024	0.024	0.026	0.025	0.022	0.016	0.028	0.015	0.034
CR3+	0.004	0	0.003	0	0	0	0	0.003	0	0	0.003	0.001	0
MN2+	0.007	0.013	0	0.004	0.008	0.016	0.008	0.013	0.006	0.007	0.016	0.013	0.018
FE2+	0.883	0.814	0.846	0.98	0.795	0.849	0.792	0.869	0.776	0.793	0.896	0.973	0.815
B3+	3	3	3	3	3	3	3	3	3	3	3	3	3
H+	3.943	3.278	3.796	3.622	3.3	3.141	4	3.087	4	4	3.329	3.43	3.202
O2-	31.054	30.339	30.885	30.714	30.416	30.219	31.098	30.197	31.104	31.037	30.459	30.527	30.313
CATSUM	18.886	18.979	18.823	18.869	18.976	18.988	18.832	18.967	18.84	18.769	18.959	18.857	18.924
AN SUM	31.111	31.061	31.089	31.092	31.116	31.078	31.098	31.11	31.104	31.037	31.131	31.096	31.111

Data for tourmaline from schist

AD1-115.9	59-22	59-23	59-24	59-25	59-26	59-27	59-28	59-29
F	0.54	0.21	0	0.05	0	0.13	0	0.05
NA2O	1.84	1.88	1.86	1.76	1.9	1.89	1.81	1.83
MGO	8.99	9.27	8.43	8.69	8.49	8.53	8.64	8.31
AL2O3	30.89	31.17	32.98	31.5	31.78	31.89	31.51	30.83
SIO2	35.35	35.6	36.61	35.97	35.57	36.22	35.47	35.68
K2O	0.03	0.01	0.02	0	0.01	0.02	0.01	0.02
CAO	1.67	1.68	0.83	1.65	1.42	1.4	1.66	1.65
TIO2	0.58	0.54	0.22	0.7	0.5	0.34	0.68	1.01
CR2O3	0.02	0.03	0.06	0.07	0.26	0.12	0.15	0.18
MNO	0	0.04	0.01	0.06	0	0.03	0	0
FEO	5.01	5.09	4.52	5.56	5.35	5.31	5.72	6.23
B2O3 *	10.4	10.53	10.67	10.58	10.51	10.58	10.53	10.49
H2O *	3.33	3.53	3.68	3.63	3.63	3.59	3.63	3.59
O=F	-0.23	-0.09	0	-0.02	0	-0.05	0	-0.02
TOTAL	98.43	99.49	99.89	100.2	99.42	100	99.82	99.85
F-	0.285	0.11	0	0.026	0	0.068	0	0.026
NA+	0.596	0.602	0.588	0.56	0.609	0.602	0.579	0.588
MG2+	2.239	2.281	2.048	2.128	2.092	2.088	2.125	2.053
AL3+	6.081	6.064	6.334	6.097	6.192	6.172	6.128	6.021
SI4+	5.905	5.876	5.966	5.908	5.88	5.948	5.853	5.913
K+	0.006	0.002	0.004	0	0.002	0.004	0.002	0.004
CA2+	0.299	0.297	0.145	0.29	0.252	0.246	0.293	0.293
TI4+	0.073	0.067	0.027	0.086	0.062	0.042	0.084	0.126
CR3+	0.003	0.004	0.008	0.009	0.034	0.016	0.02	0.024
MN2+	0	0.006	0.001	0.008	0	0.004	0	0
FE2+	0.7	0.703	0.616	0.764	0.74	0.729	0.789	0.863
B3+	3	3	3	3	3	3	3	3
H+	3.715	3.89	4	3.974	4	3.932	4	3.974
O2-	30.834	30.966	31.105	31.092	31.112	31.066	31.095	31.124
CATSUM	18.901	18.901	18.737	18.851	18.863	18.852	18.875	18.885
AN SUM	31.12	31.076	31.105	31.118	31.112	31.134	31.095	31.15

Data for tourmaline from schist

HN-2-14	14-14	14-15	14-16	14-17	14-18	14-19	14-20	14-21	14-22	14-23	14-24
F	0	0	0	0.13	0	0	0.06	0.05	0	0.02	0.05
NA2O	1.88	1.92	1.88	1.99	1.82	1.96	1.93	1.95	1.81	1.95	1.96
MGO	9.3	9.44	9.27	9.43	9.57	9.63	9.5	9.42	8.69	8.28	8.7
AL2O3	32.19	31.83	32.26	32.29	31.36	31.56	31.66	32.06	30.72	33.07	32.17
SIO2	35.33	35.05	36.12	35.24	35.85	34.58	35.71	35.23	33.57	35.25	35.75
K2O	0	0.02	0	0.01	0.01	0.02	0.01	0.01	0.01	0.02	0.04
CAO	1.38	1.54	1.29	1.39	1.65	1.51	1.5	1.39	1.59	1.08	1.31
TIO2	0.6	0.6	0.52	0.48	0.6	0.71	0.48	0.61	0.98	0.44	0.32
CR2O3	0.22	0.2	0.18	0.13	0.12	0.25	0.12	0.37	0.25	0.14	0.28
MNO	0.01	0.04	0.03	0	0.03	0	0.03	0.01	0	0.02	0.02
FEO	3.75	3.7	3.98	4.03	3.85	3.85	4.09	3.73	6.03	4.81	5.15
B2O3 *	10.53	10.47	10.64	10.57	10.53	10.44	10.55	10.54	10.28	10.55	10.59
H2O *	3.63	3.61	3.67	3.58	3.63	3.6	3.61	3.61	3.55	3.63	3.63
O=F	0	0	0	-0.05	0	0	-0.03	-0.02	0	-0.01	-0.02
TOTAL	98.83	98.42	99.84	99.21	99.02	98.11	99.23	98.96	97.47	99.25	99.95
F-	0	0	0	0.068	0	0	0.031	0.026	0	0.01	0.026
NA+	0.601	0.618	0.595	0.635	0.583	0.633	0.616	0.624	0.593	0.623	0.624
MG2+	2.288	2.336	2.257	2.312	2.355	2.39	2.332	2.316	2.191	2.034	2.128
AL3+	6.26	6.226	6.209	6.26	6.101	6.194	6.145	6.233	6.122	6.421	6.221
SI4+	5.83	5.817	5.899	5.797	5.918	5.758	5.881	5.811	5.676	5.807	5.866
K+	0	0.004	0	0.002	0.002	0.004	0.002	0.002	0.002	0.004	0.008
CA2+	0.244	0.274	0.226	0.245	0.292	0.269	0.265	0.246	0.288	0.191	0.23
TI4+	0.074	0.075	0.064	0.059	0.074	0.089	0.059	0.076	0.125	0.055	0.039
CR3+	0.029	0.026	0.023	0.017	0.016	0.033	0.016	0.048	0.033	0.018	0.036
MN2+	0.001	0.006	0.004	0	0.004	0	0.004	0.001	0	0.003	0.003
FE2+	0.517	0.514	0.544	0.554	0.531	0.536	0.563	0.515	0.853	0.663	0.707
B3+	3	3	3	3	3	3	3	3	3	3	3
H+	4	4	4	3.932	4	4	3.969	3.974	4	3.99	3.974
O2-	31.094	31.104	31.102	30.99	31.135	31.048	31.063	31.06	30.965	31.075	31.054
CATSUM	18.845	18.896	18.821	18.882	18.876	18.906	18.883	18.871	18.884	18.818	18.862
AN SUM	31.094	31.104	31.102	31.058	31.135	31.048	31.094	31.086	30.965	31.086	31.08

Data for tourmaline from schist

HN-2-10	10-14	10-15	10-16
F	0.04	0	0
NA2O	1.93	1.8	1.74
MGO	8.79	8.47	8.8
AL2O3	31.96	31.5	31.33
SIO2	35.66	35.14	35.36
K2O	0.01	0.02	0.01
CAO	1.39	1.61	1.54
TIO2	0.39	0.26	0.52
CR2O3	0.11	0.24	0.21
MNO	0.02	0.03	0
FEO	5.26	6.19	5.9
B2O3 *	10.57	10.48	10.53
H2O *	3.63	3.62	3.63
O=F	-0.02	0	0
TOTAL	99.74	99.36	99.58
F-	0.021	0	0
NA+	0.615	0.579	0.557
MG2+	2.155	2.093	2.165
AL3+	6.193	6.155	6.094
SI4+	5.863	5.826	5.835
K+	0.002	0.004	0.002
CA2+	0.245	0.286	0.272
TI4+	0.048	0.032	0.065
CR3+	0.014	0.031	0.027
MN2+	0.003	0.004	0
FE2+	0.723	0.858	0.814
B3+	3	3	3
H+	3.979	4	4
O2-	31.048	31.029	31.012
CATSUM	18.862	18.869	18.831
AN SUM	31.069	31.029	31.012

Data for tourmaline from schist

99-10	59-14	59-15	59-16	59-17	59-18	59-19	59-20	59-21
F	0.75	0.65	0.37	1.13	0.49	0.56	0.32	0.66
NA2O	1.58	1.7	1.76	1.18	1.89	1.67	1.99	1.71
MGO	9.85	9.7	9.48	13.37	9.26	9.61	9.13	9.77
AL2O3	29.5	29.63	30.66	16.68	30.11	29.83	31.64	30.63
SIO2	35.44	35.11	35.83	44.86	35.44	35.09	35.71	35.79
K2O	0.02	0.02	0.03	0.07	0.02	0.02	0	0.01
CAO	2.48	2.25	1.98	7.51	1.91	2.16	1.62	2.07
TIO2	0.69	0.75	0.46	0.39	0.68	0.57	0.18	0.36
CR2O3	0.25	0.23	0.24	0.07	0.11	0.15	0.14	0.19
MNO	0	0	0	0.2	0	0.03	0.04	0.02
FEO	5.2	5.26	4.73	7.58	5.38	5.23	4.58	4.5
B2O3 *	10.42	10.39	10.5	10.58	10.41	10.37	10.51	10.5
H2O *	3.24	3.28	3.45	3.11	3.36	3.31	3.48	3.31
O=F	-0.32	-0.27	-0.16	-0.48	-0.21	-0.24	-0.13	-0.28
TOTAL	99.11	98.69	99.33	106.26	98.85	98.37	99.2	99.25
F-	0.396	0.344	0.194	0.587	0.259	0.297	0.167	0.345
NA+	0.511	0.552	0.565	0.376	0.612	0.543	0.638	0.549
MG2+	2.449	2.42	2.34	3.274	2.305	2.401	2.25	2.41
AL3+	5.797	5.844	5.983	3.23	5.926	5.891	6.166	5.973
SI4+	5.909	5.875	5.933	7.37	5.918	5.88	5.904	5.922
K+	0.004	0.004	0.006	0.015	0.004	0.004	0	0.002
CA2+	0.443	0.403	0.351	1.322	0.342	0.388	0.287	0.367
TI4+	0.087	0.094	0.057	0.048	0.085	0.072	0.022	0.045
CR3+	0.033	0.03	0.031	0.009	0.015	0.02	0.018	0.025
MN2+	0	0	0	0.028	0	0.004	0.006	0.003
FE2+	0.725	0.736	0.655	1.041	0.751	0.733	0.633	0.623
B3+	3	3	3	3	3	3	3	3
H+	3.604	3.656	3.806	3.413	3.741	3.703	3.833	3.655
O2-	30.716	30.744	30.941	31.467	30.864	30.771	30.957	30.763
CATSUM	18.958	18.959	18.923	19.712	18.958	18.935	18.925	18.918
AN SUM	31.112	31.088	31.134	32.054	31.123	31.068	31.125	31.108

Data for tourmaline from schist

AD1-21.2	12-15	12-16	12-17	12-18	12-19	12-20	12-21	12-22	12-23	12-24	12-25	12-26	12-27	12-28
F	0.81	0.89	1.13	1.35	0.89	1.04	1.15	0.09	0.5	0.17	0.16	0.09	1.23	0.58
NA2O	1.88	1.8	1.77	1.8	1.87	2.05	1.98	1.92	1.69	2.01	1.85	1.71	2.11	1.83
MGO	7.07	8.32	8.2	9.1	8.14	7.91	8.42	8.3	7.93	8.12	7.78	7.6	8.67	8.87
AL2O3	32.09	31.38	30.61	29.87	31.11	31.46	30.47	31.02	31.71	31.72	31.88	31.52	30.82	30.8
SIO2	35.74	35.77	35.71	35.34	35.77	35.98	35.41	35.68	34.25	35.59	35.04	35.66	35.11	35.39
K2O	0.01	0	0.01	0.03	0.04	0.02	0.04	0.01	0.02	0	0.03	0.04	0.02	0
CAO	0.96	1.49	1.68	2.15	1.44	1.2	1.79	1.39	1.88	1.4	1.58	1.62	1.63	1.52
TIO2	0.11	0.13	0.17	0.26	0.15	0.22	0.2	0.39	0.29	0.38	0.38	0.54	0.13	0.39
CR2O3	0	0	0.04	0.05	0.02	0	0	0	0	0.03	0.01	0	0.02	0
MNO	0.11	0.11	0.06	0.14	0.06	0.13	0.15	0.02	0.02	0.05	0	0.02	0.1	0
FEO	6.73	6.21	6.49	6.29	6.24	6.23	6.6	6.49	6.8	6.46	6.86	7.06	6.15	5.83
B2O3 *	10.42	10.49	10.39	10.4	10.42	10.47	10.39	10.47	10.35	10.52	10.46	10.48	10.39	10.44
H2O *	3.21	3.2	3.05	2.95	3.17	3.12	3.04	3.57	3.34	3.55	3.53	3.57	3	3.33
O=F	-0.34	-0.37	-0.48	-0.57	-0.37	-0.44	-0.48	-0.04	-0.21	-0.07	-0.07	-0.04	-0.52	-0.24
TOTAL	98.8	99.41	98.83	99.15	98.95	99.39	99.16	99.31	98.57	99.93	99.49	99.88	98.87	98.73
F-	0.427	0.466	0.598	0.714	0.469	0.546	0.608	0.047	0.265	0.089	0.084	0.047	0.651	0.305
NA+	0.608	0.578	0.574	0.583	0.604	0.66	0.642	0.618	0.55	0.644	0.596	0.55	0.684	0.591
MG2+	1.759	2.055	2.045	2.268	2.023	1.958	2.1	2.054	1.984	1.999	1.928	1.879	2.161	2.202
AL3+	6.31	6.127	6.036	5.885	6.113	6.157	6.007	6.07	6.273	6.174	6.245	6.16	6.074	6.044
SI4+	5.963	5.926	5.975	5.908	5.964	5.974	5.923	5.924	5.749	5.877	5.824	5.913	5.871	5.893
K+	0.002	0	0.002	0.006	0.009	0.004	0.009	0.002	0.004	0	0.006	0.008	0.004	0
CA2+	0.172	0.264	0.301	0.385	0.257	0.213	0.321	0.247	0.338	0.248	0.281	0.288	0.292	0.271
TI4+	0.014	0.016	0.021	0.033	0.019	0.027	0.025	0.049	0.037	0.047	0.047	0.067	0.016	0.049
CR3+	0	0	0.005	0.007	0.003	0	0	0	0	0.004	0.001	0	0.003	0
MN2+	0.016	0.015	0.009	0.02	0.008	0.018	0.021	0.003	0.003	0.007	0	0.003	0.014	0
FE2+	0.939	0.86	0.908	0.879	0.87	0.865	0.923	0.901	0.955	0.892	0.954	0.979	0.86	0.812
B3+	3	3	3	3	3	3	3	3	3	3	3	3	3	3
H+	3.573	3.534	3.402	3.286	3.531	3.454	3.392	3.953	3.735	3.911	3.916	3.953	3.349	3.695
O2-	30.681	30.593	30.509	30.353	30.635	30.58	30.49	31.017	30.772	30.994	30.994	31.08	30.412	30.725
CATSUM	18.782	18.843	18.878	18.975	18.87	18.878	18.972	18.867	18.892	18.891	18.884	18.846	18.98	18.862
AN SUM	31.109	31.059	31.107	31.067	31.104	31.126	31.098	31.064	31.037	31.083	31.078	31.127	31.062	31.031

Data for tourmaline from aplite

RR-02-30a	30-1	30-2	30-3	30-4	30-5	30-6	30-7	30-8	30-9	30-10	30-11	30-12
F	0	0.03	0	0.07	0.75	0.38	0.34	0.52	0.94	0.64	0.27	0.6
NA2O	1.82	1.73	1.77	1.78	1.27	1.71	1.86	1.8	2.08	2.15	1.93	2.09
MGO	8.89	8.71	8.76	8.74	11.84	9.27	8.82	8.87	6.32	5.72	4.04	4.78
AL2O3	30.9	30.62	31.21	31.07	20.52	30.51	31.72	31.24	32.18	32.83	34.4	33.74
SIO2	35.35	34.4	34.48	35.47	42.18	34.27	34.82	34.57	33.48	34.34	33.72	33.16
K2O	0.02	0.02	0.03	0	0.05	0.04	0	0	0.05	0.03	0.02	0.02
CAO	1.63	1.79	1.77	1.58	4.63	1.67	1.46	1.54	1.18	0.8	0.47	0.69
TIO2	0.69	0.83	0.79	0.88	0.41	0.5	0.46	0.44	0.24	0.18	0.18	0.26
CR2O3	0.09	0.19	0.07	0.01	0.11	0.08	0.07	0.14	0.02	0	0.05	0
MNO	0.02	0.03	0	0.03	0.15	0.06	0.01	0	0.16	0.25	0.15	0.17
FEO	5.3	5.6	5.25	5.01	6.9	5.25	4.93	5.27	8.09	8.24	9.42	9.02
B2O3 *	10.43	10.31	10.35	10.43	10.46	10.3	10.41	10.37	10.19	10.29	10.25	10.19
H2O *	3.6	3.54	3.57	3.56	3.25	3.37	3.43	3.33	3.07	3.25	3.41	3.23
O=F	0	-0.01	0	-0.03	-0.32	-0.16	-0.14	-0.22	-0.4	-0.27	-0.11	-0.25
TOTAL	98.75	97.79	98.06	98.6	102.21	97.26	98.19	97.87	97.6	98.45	98.2	97.7
F-	0	0.016	0	0.037	0.394	0.203	0.179	0.276	0.507	0.342	0.145	0.324
NA+	0.588	0.566	0.576	0.575	0.409	0.559	0.602	0.585	0.688	0.704	0.634	0.691
MG2+	2.207	2.19	2.192	2.172	2.932	2.331	2.194	2.217	1.607	1.44	1.021	1.216
AL3+	6.066	6.085	6.174	6.103	4.017	6.065	6.239	6.173	6.47	6.536	6.874	6.783
SI4+	5.888	5.801	5.788	5.912	7.006	5.781	5.811	5.796	5.712	5.801	5.717	5.657
K+	0.004	0.004	0.006	0	0.011	0.009	0	0	0.011	0.006	0.004	0.004
CA2+	0.291	0.323	0.318	0.282	0.824	0.302	0.261	0.277	0.216	0.145	0.085	0.126
TI4+	0.086	0.105	0.1	0.11	0.051	0.063	0.058	0.055	0.031	0.023	0.023	0.033
CR3+	0.012	0.025	0.009	0.001	0.014	0.011	0.009	0.019	0.003	0	0.007	0
MN2+	0.003	0.004	0	0.004	0.021	0.009	0.001	0	0.023	0.036	0.022	0.025
FE2+	0.738	0.79	0.737	0.698	0.958	0.741	0.688	0.739	1.154	1.164	1.336	1.287
B3+	3	3	3	3	3	3	3	3	3	3	3	3
H+	4	3.984	4	3.963	3.606	3.797	3.821	3.724	3.493	3.658	3.855	3.676
O2-	31.1	31.054	31.089	31.107	31.213	30.765	30.875	30.741	30.537	30.75	30.941	30.732
CATSUM	18.883	18.893	18.901	18.857	19.244	18.87	18.863	18.862	18.915	18.855	18.724	18.822
AN SUM	31.1	31.07	31.089	31.144	31.607	30.968	31.054	31.017	31.044	31.092	31.086	31.055

Data for tourmaline from aplite

HN-2-6	6-1	6-2	6-3	6-4	6-5	6-6	6-7	6-8	6-9	6-10	6-11	6-12
F	0.74	0.82	0.77	0.78	0.9	0.67	0.7	0.45	0.7	0.61	0.8	0.75
NA2O	2.41	2.52	2.54	2.42	2.37	2.23	2.13	2.43	2.47	2.45	2.55	2.39
MGO	7.73	8.12	8.03	7.81	8.73	8.93	9	7.97	9.02	8.21	8.02	8.85
AL2O3	31.46	30.47	31.16	31.19	31.09	29.53	29.37	31.97	30.31	30.84	30.82	30.34
SIO2	35.36	35	35.07	35.71	36.01	34.7	35.48	35.77	35.4	35.18	35.3	35.62
K2O	0.03	0.03	0.02	0	0.04	0	0.03	0.02	0.02	0.02	0.03	0.01
CAO	0.7	0.81	0.7	0.75	0.97	1.26	1.46	0.65	0.93	0.75	0.6	0.98
TIO2	0.16	0.22	0.14	0.17	0.14	0.26	0.26	0.1	0.16	0.13	0.14	0.17
CR2O3	0.16	0.24	0.1	0.02	0.02	0.03	0	0	0.06	0.04	0.08	0.13
MNO	0.21	0.24	0.23	0.25	0.16	0.18	0.21	0.29	0.15	0.22	0.22	0.22
FEO	6.16	5.94	6.21	6.24	5.37	6.07	6.18	5.04	5.95	5.78	6.32	5.61
B2O3 *	10.37	10.26	10.35	10.39	10.48	10.23	10.32	10.41	10.41	10.3	10.34	10.39
H2O *	3.23	3.15	3.21	3.22	3.19	3.21	3.23	3.38	3.26	3.27	3.19	3.23
O=F	-0.31	-0.35	-0.32	-0.33	-0.38	-0.28	-0.29	-0.19	-0.29	-0.26	-0.34	-0.32
TOTAL	98.41	97.47	98.2	98.62	99.08	97.02	98.07	98.29	98.54	97.54	98.07	98.37
F-	0.392	0.439	0.409	0.413	0.472	0.36	0.373	0.238	0.37	0.325	0.425	0.397
NA+	0.783	0.828	0.827	0.785	0.762	0.735	0.696	0.786	0.8	0.801	0.831	0.775
MG2+	1.931	2.051	2.01	1.947	2.159	2.262	2.26	1.983	2.245	2.065	2.01	2.207
AL3+	6.212	6.084	6.166	6.148	6.079	5.915	5.83	6.289	5.964	6.132	6.107	5.981
SI4+	5.924	5.929	5.888	5.972	5.974	5.897	5.976	5.971	5.911	5.935	5.935	5.958
K+	0.006	0.006	0.004	0	0.008	0	0.006	0.004	0.004	0.004	0.006	0.002
CA2+	0.126	0.147	0.126	0.134	0.172	0.229	0.263	0.116	0.166	0.136	0.108	0.176
TI4+	0.02	0.028	0.018	0.021	0.017	0.033	0.033	0.013	0.02	0.016	0.018	0.021
CR3+	0.021	0.032	0.013	0.003	0.003	0.004	0	0	0.008	0.005	0.011	0.017
MN2+	0.03	0.034	0.033	0.035	0.022	0.026	0.03	0.041	0.021	0.031	0.031	0.031
FE2+	0.863	0.842	0.872	0.873	0.745	0.863	0.871	0.704	0.831	0.815	0.889	0.785
B3+	3	3	3	3	3	3	3	3	3	3	3	3
H+	3.608	3.561	3.591	3.587	3.528	3.64	3.627	3.762	3.63	3.675	3.575	3.603
O2-	30.688	30.64	30.628	30.683	30.618	30.626	30.666	30.902	30.615	30.733	30.613	30.646
CATSUM	18.915	18.981	18.957	18.919	18.943	18.964	18.966	18.907	18.97	18.941	18.946	18.953
AN SUM	31.081	31.079	31.037	31.096	31.09	30.986	31.039	31.139	30.985	31.058	31.038	31.043

Data for tourmaline from aplite

HN-2-58B	58a-1	58a-2	58a-3	58a-4	58a-5	58a-6	58a-7	58a-8	58a-9	58a-10	58a-11	58a-12
F	0.99	0.48	0.63	0.96	0.36	0.95	0.87	1.01	0.9	0.86	0.75	1.05
NA2O	2.21	1.94	1.92	2.17	1.87	2.14	2.14	2.22	2.18	2.12	2.19	2.22
MGO	5.95	4.87	5.05	5.79	4.58	5.65	4.93	6	5.57	5.61	5.33	5.98
AL2O3	29.91	32.58	32.84	30.41	32.39	30.44	32.22	30.75	31.17	31.56	30.15	29.87
SIO2	34.72	35.33	35.24	34.8	35.53	34.72	35.08	34.53	35.2	35.13	34.7	34.66
K2O	0.08	0.02	0.04	0.04	0.03	0.06	0.06	0.05	0.04	0.04	0.03	0.04
CAO	0.89	0.29	0.34	0.94	0.28	0.92	0.5	0.72	0.68	0.61	0.82	0.89
TIO2	1.5	0.3	0.3	0.87	0.3	0.97	0.44	0.71	0.7	0.6	0.89	1.05
CR2O3	0	0.02	0	0	0	0	0	0	0	0.01	0	0.02
MNO	0.23	0.16	0.19	0.2	0.19	0.17	0.22	0.21	0.2	0.22	0.22	0.27
FEO	8.98	8.73	8.53	8.84	8.82	9.22	9.36	8.03	8.5	8.43	8.93	8.75
B2O3 *	10.16	10.27	10.31	10.14	10.23	10.15	10.28	10.1	10.2	10.24	10.02	10.1
H2O *	3.04	3.32	3.26	3.04	3.36	3.05	3.14	3	3.09	3.13	3.1	2.99
O=F	-0.42	-0.2	-0.27	-0.4	-0.15	-0.4	-0.37	-0.43	-0.38	-0.36	-0.32	-0.44
TOTAL	98.24	98.11	98.39	97.8	97.79	98.04	98.87	96.91	98.06	98.19	96.82	97.44
F-	0.536	0.257	0.336	0.521	0.193	0.514	0.465	0.55	0.485	0.462	0.411	0.572
NA+	0.733	0.636	0.627	0.721	0.616	0.71	0.701	0.741	0.72	0.698	0.736	0.741
MG2+	1.518	1.228	1.269	1.48	1.16	1.442	1.242	1.54	1.415	1.419	1.378	1.535
AL3+	6.031	6.496	6.524	6.145	6.485	6.143	6.418	6.238	6.259	6.313	6.162	6.061
SI4+	5.94	5.977	5.94	5.967	6.036	5.945	5.929	5.944	5.997	5.962	6.017	5.967
K+	0.017	0.004	0.009	0.009	0.007	0.013	0.013	0.011	0.009	0.009	0.007	0.009
CA2+	0.163	0.053	0.061	0.173	0.051	0.169	0.091	0.133	0.124	0.111	0.152	0.164
TI4+	0.193	0.038	0.038	0.112	0.038	0.125	0.056	0.092	0.09	0.077	0.116	0.136
CR3+	0	0.003	0	0	0	0	0	0	0	0.001	0	0.003
MN2+	0.033	0.023	0.027	0.029	0.027	0.025	0.031	0.031	0.029	0.032	0.032	0.039
FE2+	1.285	1.235	1.202	1.268	1.253	1.32	1.323	1.156	1.211	1.196	1.295	1.26
B3+	3	3	3	3	3	3	3	3	3	3	3	3
H+	3.464	3.743	3.664	3.479	3.807	3.486	3.535	3.45	3.515	3.538	3.589	3.428
O2-	30.651	30.88	30.783	30.668	30.986	30.657	30.677	30.614	30.72	30.698	30.827	30.602
CATSUM	18.914	18.693	18.697	18.903	18.673	18.892	18.805	18.885	18.853	18.817	18.895	18.914
AN SUM	31.187	31.137	31.119	31.189	31.179	31.172	31.142	31.163	31.205	31.16	31.238	31.174

Data for tourmaline from aplite

RR-02-30a	30-13	30-14	30-15	30-16	30-18	30-20	30-22	30-23	30-24	30-25
F	0.84	1.03	0.77	0.35	0.41	0.28	0.34	0.52	0.66	0.35
NA2O	2.13	2.05	1.65	1.93	1.86	2.02	1.89	1.81	1.84	1.98
MGO	5.44	6.29	9.98	9.13	9.02	9.1	9.38	9.52	9.41	9.28
AL2O3	31.53	31.51	29.76	30.48	30.75	30.75	30.22	30.32	30.01	30.93
SIO2	34.7	33.86	35.22	35.48	34.75	35.59	34.92	34.97	35.46	34.92
K2O	0.04	0.03	0.03	0.03	0.02	0.01	0.01	0.01	0.02	0.01
CAO	0.86	1.29	2.34	1.81	1.63	1.62	1.82	1.95	1.97	1.71
TIO2	0.52	0.21	0.79	0.76	0.61	0.52	0.57	0.7	0.63	0.47
CR2O3	0.04	0	0.04	0.13	0.07	0.1	0.05	0.17	0.13	0.08
MNO	0.23	0.13	0.05	0.01	0.03	0	0.02	0	0.03	0.01
FEO	9.47	8.47	5.42	5.57	5.31	5.19	5.28	5.44	5.41	5.41
B2O3 *	10.26	10.16	10.47	10.47	10.36	10.45	10.36	10.44	10.43	10.45
H2O *	3.14	3.02	3.25	3.45	3.38	3.47	3.41	3.36	3.28	3.44
O=F	-0.35	-0.43	-0.32	-0.15	-0.17	-0.12	-0.14	-0.22	-0.28	-0.15
TOTAL	98.84	97.62	99.44	99.45	98.03	98.99	98.13	98.99	99	98.89
F-	0.45	0.557	0.404	0.184	0.218	0.147	0.18	0.274	0.348	0.184
NA+	0.7	0.68	0.531	0.621	0.605	0.651	0.615	0.584	0.595	0.639
MG2+	1.374	1.603	2.469	2.26	2.256	2.256	2.346	2.363	2.338	2.302
AL3+	6.298	6.35	5.822	5.964	6.079	6.026	5.975	5.949	5.896	6.065
SI4+	5.881	5.79	5.846	5.89	5.829	5.918	5.858	5.821	5.911	5.81
K+	0.009	0.007	0.006	0.006	0.004	0.002	0.002	0.002	0.004	0.002
CA2+	0.156	0.236	0.416	0.322	0.293	0.289	0.327	0.348	0.352	0.305
TI4+	0.066	0.027	0.099	0.095	0.077	0.065	0.072	0.088	0.079	0.059
CR3+	0.005	0	0.005	0.017	0.009	0.013	0.007	0.022	0.017	0.011
MN2+	0.033	0.019	0.007	0.001	0.004	0	0.003	0	0.004	0.001
FE2+	1.342	1.211	0.752	0.773	0.745	0.722	0.741	0.757	0.754	0.753
B3+	3	3	3	3	3	3	3	3	3	3
H+	3.55	3.443	3.596	3.816	3.782	3.853	3.82	3.726	3.652	3.816
O2-	30.659	30.514	30.638	30.927	30.831	30.971	30.875	30.762	30.75	30.847
CATSUM	18.865	18.922	18.953	18.95	18.902	18.942	18.944	18.934	18.951	18.946
AN SUM	31.109	31.071	31.043	31.111	31.048	31.118	31.056	31.036	31.098	31.032

Data for tourmaline from aplite

HN-2-6	6-13	6-14	6-15	6-16	6-17	6-18	6-19	6-20	6-21	6-22	6-23	6-24
F	0.53	0.69	0.69	0.52	0.56	0.55	0.78	0.9	0.9	0.68	0.96	1.59
NA2O	2.28	2.31	2.29	2.41	2.39	2.44	2.39	2.26	2.44	2.35	2.19	2.21
MGO	8.44	8.78	8.23	8.19	8.05	8.49	8.55	9.07	8.71	8.59	9.33	10.21
AL2O3	31.89	30.38	31.23	31.56	32.13	30.54	30.79	29.77	30.04	30.89	29.21	29.47
SIO2	35.86	35.46	35.71	35.59	35.93	35.75	36	35.69	35.53	35.83	35.61	36.21
K2O	0.01	0	0.04	0.01	0.03	0.03	0.03	0.01	0.02	0.01	0.03	0.02
CAO	0.88	1.1	1.13	0.79	0.62	0.82	0.94	1.25	1.06	1.01	1.39	1.46
TIO2	0.13	0.17	0.21	0.12	0.1	0.17	0.16	0.25	0.15	0.18	0.21	0.25
CR2O3	0.07	0.07	0.06	0.03	0	0.09	0.08	0.12	0.17	0.13	0.1	0
MNO	0.16	0.2	0.27	0.26	0.25	0.2	0.21	0.19	0.18	0.21	0.21	0.16
FEO	4.72	5.51	5.14	5.03	4.95	5.85	5.69	5.5	5.64	5.17	6.09	4.52
B2O3 *	10.46	10.35	10.37	10.37	10.45	10.39	10.45	10.35	10.32	10.4	10.36	10.46
H2O *	3.36	3.24	3.25	3.33	3.34	3.32	3.23	3.14	3.13	3.27	3.12	2.85
O=F	-0.22	-0.29	-0.29	-0.22	-0.24	-0.23	-0.33	-0.38	-0.38	-0.29	-0.4	-0.67
TOTAL	98.56	97.97	98.33	98	98.57	98.41	98.97	98.13	97.91	98.43	98.41	98.74
F-	0.279	0.367	0.366	0.276	0.294	0.291	0.41	0.478	0.48	0.359	0.509	0.836
NA+	0.735	0.752	0.744	0.783	0.77	0.791	0.771	0.736	0.797	0.761	0.712	0.712
MG2+	2.091	2.198	2.056	2.045	1.995	2.117	2.121	2.27	2.188	2.139	2.332	2.529
AL3+	6.246	6.013	6.167	6.231	6.296	6.022	6.038	5.891	5.965	6.082	5.773	5.772
SI4+	5.959	5.955	5.984	5.962	5.973	5.981	5.99	5.992	5.986	5.986	5.971	6.017
K+	0.002	0	0.009	0.002	0.006	0.006	0.006	0.002	0.004	0.002	0.006	0.004
CA2+	0.157	0.198	0.203	0.142	0.11	0.147	0.168	0.225	0.191	0.181	0.25	0.26
TI4+	0.016	0.021	0.026	0.015	0.013	0.021	0.02	0.032	0.019	0.023	0.026	0.031
CR3+	0.009	0.009	0.008	0.004	0	0.012	0.011	0.016	0.023	0.017	0.013	0
MN2+	0.023	0.028	0.038	0.037	0.035	0.028	0.03	0.027	0.026	0.03	0.03	0.023
FE2+	0.656	0.774	0.72	0.705	0.688	0.818	0.792	0.772	0.795	0.722	0.854	0.628
B3+	3	3	3	3	3	3	3	3	3	3	3	3
H+	3.721	3.633	3.634	3.724	3.706	3.709	3.59	3.522	3.52	3.641	3.491	3.164
O2-	30.85	30.696	30.811	30.854	30.838	30.774	30.68	30.593	30.611	30.762	30.491	30.217
CATSUM	18.893	18.95	18.955	18.927	18.887	18.945	18.945	18.963	18.993	18.944	18.968	18.976
AN SUM	31.128	31.062	31.177	31.13	31.132	31.065	31.09	31.071	31.09	31.121	31	31.052

Data for tourmaline from aplite

HN-2-58B	58a-13	58a-14	58a-15
F	0.5	0.92	0.87
NA2O	2.01	2.19	2.25
MGO	5.05	6.16	6.05
AL2O3	32.51	30.8	30.65
SIO2	35.56	34.91	34.98
K2O	0.02	0.07	0.05
CAO	0.36	0.93	0.9
TIO2	0.34	0.79	0.84
CR2O3	0.02	0.03	0.01
MNO	0.18	0.18	0.2
FEO	8.69	8.13	8.3
B2O3 *	10.32	10.19	10.18
H2O *	3.32	3.08	3.1
O=F	-0.21	-0.39	-0.37
TOTAL	98.68	98	98.02
F-	0.266	0.496	0.47
NA+	0.656	0.724	0.745
MG2+	1.267	1.566	1.54
AL3+	6.451	6.19	6.166
SI4+	5.987	5.953	5.971
K+	0.004	0.015	0.011
CA2+	0.065	0.17	0.165
TI4+	0.043	0.101	0.108
CR3+	0.003	0.004	0.001
MN2+	0.026	0.026	0.029
FE2+	1.224	1.159	1.185
B3+	3	3	3
H+	3.734	3.504	3.53
O2-	30.886	30.695	30.735
CATSUM	18.725	18.909	18.92
AN SUM	31.152	31.191	31.205

Data for tourmaline from quartz vein

HN-2-58A	58b-1	58b-2	58b-3	58b-4	58b-5	58b-6	58b-7	58b-8	58b-9	58b-10	58b-11	58b-12
F	0.64	0.66	0.91	0.82	0.68	0.62	0.83	0.94	0.96	0.62	0.56	0.7
NA2O	1.91	2.1	2.2	2.15	2.17	1.96	2.27	2.33	2.34	1.95	2.13	2.1
MGO	0.98	3.16	5.6	3.15	5.37	2.77	3.72	3.56	3.87	3.28	3.03	3.5
AL2O3	32.41	31.61	30.97	31.45	31.16	31.82	31.06	30.83	30.8	32.4	31.69	30.98
SIO2	34.29	34.3	34.84	34.68	34.36	34.3	34.54	33.76	34.72	34.79	34.28	34.34
K2O	0.06	0.05	0.06	0.08	0.05	0.04	0.04	0.05	0.09	0.04	0.02	0.05
CAO	0.17	0.58	0.77	0.53	0.78	0.32	0.42	0.6	0.45	0.28	0.48	0.6
TIO2	0.75	1.25	0.9	1.05	0.76	0.8	0.81	1.11	0.58	0.45	1.09	1.13
CR2O3	0	0	0	0.02	0.04	0	0	0	0.02	0	0	0.01
MNO	0.84	0.26	0.24	0.31	0.19	0.17	0.32	0.2	0.23	0.21	0.32	0.19
FEO	13.31	11.76	8.83	11.79	9.06	12.03	10.99	11.57	11.57	10.92	12.06	11.75
B2O3 *	10.01	10.11	10.19	10.12	10.13	10.05	10.05	9.97	10.09	10.14	10.12	10.07
H2O *	3.15	3.18	3.08	3.1	3.17	3.17	3.08	3	3.03	3.2	3.23	3.14
O=F	-0.27	-0.28	-0.38	-0.35	-0.29	-0.26	-0.35	-0.4	-0.4	-0.26	-0.24	-0.29
TOTAL	98.24	98.74	98.21	98.91	97.64	97.79	97.78	97.52	98.35	98.02	98.77	98.27
F-	0.352	0.359	0.491	0.445	0.369	0.339	0.454	0.518	0.523	0.336	0.304	0.382
NA+	0.643	0.7	0.727	0.716	0.722	0.657	0.761	0.787	0.781	0.648	0.709	0.703
MG2+	0.254	0.81	1.424	0.806	1.373	0.714	0.959	0.925	0.993	0.838	0.776	0.9
AL3+	6.635	6.404	6.225	6.364	6.301	6.485	6.329	6.331	6.251	6.545	6.416	6.301
SI4+	5.956	5.896	5.942	5.954	5.895	5.932	5.971	5.883	5.979	5.963	5.889	5.926
K+	0.013	0.011	0.013	0.018	0.011	0.009	0.009	0.011	0.02	0.009	0.004	0.011
CA2+	0.032	0.107	0.141	0.097	0.143	0.059	0.078	0.112	0.083	0.051	0.088	0.111
TI4+	0.098	0.162	0.115	0.136	0.098	0.104	0.105	0.145	0.075	0.058	0.141	0.147
CR3+	0	0	0	0.003	0.005	0	0	0	0.003	0	0	0.001
MN2+	0.124	0.038	0.035	0.045	0.028	0.025	0.047	0.03	0.034	0.03	0.047	0.028
FE2+	1.933	1.691	1.259	1.693	1.3	1.74	1.589	1.686	1.666	1.565	1.732	1.696
B3+	3	3	3	3	3	3	3	3	3	3	3	3
H+	3.648	3.641	3.509	3.555	3.631	3.661	3.546	3.482	3.477	3.664	3.696	3.618
O2-	30.88	30.863	30.69	30.792	30.787	30.832	30.75	30.687	30.641	30.837	30.878	30.81
CATSUM	18.688	18.818	18.881	18.831	18.876	18.725	18.848	18.91	18.884	18.708	18.802	18.825
AN SUM	31.232	31.222	31.181	31.237	31.156	31.171	31.204	31.205	31.164	31.173	31.182	31.192

Data for tourmaline from quartz vein

HN-2-38	38-1	38-2	38-3	38-4	38-5	38-6	38-7	38-8	38-9	38-10	38-11	38-12
F	0.64	0.68	0.71	0.68	0.64	0.59	0.55	0.71	0.72	0.8	0.52	1.45
NA2O	2.37	2.28	2.32	2.14	2.13	2.11	2.05	2.16	2.17	2.31	2.24	0.27
MGO	4.41	4.67	4.93	0.38	0.36	0.57	0.68	0.69	0.79	4.37	4.09	3.1
AL2O3	31.17	31.07	31.5	32.29	32.47	32.12	31.76	31.87	31.8	31.09	31.23	29
SIO2	34.54	34.83	34.99	33.82	34.19	33.66	33.6	33.59	33.75	34.6	34.46	46.08
K2O	0.06	0.06	0.05	0.04	0.05	0.05	0.06	0.09	0.07	0.07	0.06	10.99
CAO	0.52	0.59	0.64	0.19	0.19	0.21	0.25	0.27	0.25	0.48	0.47	0.01
TIO2	1.04	1.12	0.68	0.71	0.62	0.56	0.55	0.64	0.52	0.9	0.98	0.71
CR2O3	0	0.01	0	0.01	0	0	0	0	0	0	0	0
MNO	0.17	0.17	0.21	0.75	0.78	0.69	0.48	0.53	0.46	0.19	0.25	0.15
FEO	10.45	10.03	10.1	14.79	14.38	14.38	14.85	15	15.01	11.22	10.84	2.28
B2O3 *	10.14	10.17	10.27	9.96	9.98	9.89	9.88	9.92	9.93	10.19	10.12	10.13
H2O *	3.2	3.19	3.21	3.12	3.14	3.13	3.15	3.09	3.09	3.14	3.25	2.81
O=F	-0.27	-0.29	-0.3	-0.29	-0.27	-0.25	-0.23	-0.3	-0.3	-0.34	-0.22	-0.61
TOTAL	98.44	98.58	99.3	98.59	98.66	97.72	97.63	98.26	98.26	99.02	98.29	106.37
F-	0.347	0.367	0.38	0.375	0.352	0.328	0.306	0.393	0.398	0.431	0.282	0.787
NA+	0.788	0.755	0.762	0.724	0.719	0.719	0.699	0.733	0.736	0.764	0.746	0.09
MG2+	1.127	1.189	1.244	0.099	0.093	0.149	0.178	0.18	0.206	1.111	1.047	0.793
AL3+	6.296	6.257	6.285	6.639	6.663	6.649	6.584	6.578	6.557	6.247	6.319	5.863
SI4+	5.92	5.951	5.924	5.9	5.953	5.912	5.91	5.882	5.904	5.899	5.916	7.904
K+	0.013	0.013	0.011	0.009	0.011	0.011	0.013	0.02	0.016	0.015	0.013	2.405
CA2+	0.095	0.108	0.116	0.036	0.035	0.04	0.047	0.051	0.047	0.088	0.086	0.002
TI4+	0.134	0.144	0.087	0.093	0.081	0.074	0.073	0.084	0.068	0.115	0.127	0.092
CR3+	0	0.001	0	0.001	0	0	0	0	0	0	0	0
MN2+	0.025	0.025	0.03	0.111	0.115	0.103	0.072	0.079	0.068	0.027	0.036	0.022
FE2+	1.498	1.433	1.43	2.158	2.094	2.112	2.184	2.197	2.196	1.6	1.556	0.327
B3+	3	3	3	3	3	3	3	3	3	3	3	3
H+	3.653	3.633	3.62	3.625	3.648	3.672	3.694	3.607	3.602	3.569	3.718	3.213
O2-	30.851	30.849	30.775	30.839	30.914	30.888	30.872	30.79	30.776	30.684	30.885	32.89
CATSUM	18.896	18.876	18.888	18.768	18.766	18.769	18.76	18.804	18.799	18.867	18.845	20.497
AN SUM	31.198	31.216	31.155	31.215	31.266	31.215	31.178	31.183	31.174	31.115	31.167	33.676

Data for tourmaline from quartz vein

RR-02-29	29-1	29-2	29-3	29-4	29-5	29-6	29-7	29-8	29-9	29-10	29-11	29-12
F	1.14	1.01	0.7	0.3	0.38	0.58	0.68	0.73	1.2	1.53	1.55	1.11
NA2O	2.24	2.18	2.07	1.87	1.71	1.98	2.17	2.08	1.77	1.42	1.45	2.08
MGO	7.46	6.72	5.29	4.38	3.06	4.4	4.76	4.49	8.21	10.09	12.04	6.96
AL2O3	31.38	32.19	33.21	35.24	35.46	33.42	32.81	33.31	30.71	29.69	29.04	31.7
SIO2	35.38	34.95	34.21	35.33	34.55	34.39	35.08	34.77	35.53	35.55	35.7	34.47
K2O	0.05	0.03	0.04	0.03	0	0.04	0.01	0.04	0.02	0.04	0.02	0.04
CAO	1.23	1.1	0.81	0.55	0.46	0.68	0.76	0.68	2.12	3.04	3.08	1.32
TIO2	0.19	0.22	0.24	0.15	0.2	0.28	0.34	0.29	0.29	0.26	0.19	0.2
CR2O3	0	0	0	0	0.02	0	0.07	0.01	0.08	0	0	0.01
MNO	0.2	0.11	0.25	0.11	0.27	0.27	0.22	0.23	0.16	0.09	0.05	0.22
FEO	7.04	7.35	8.87	8.69	9.83	9.33	9.19	9.57	6.49	4.91	3.12	7.57
B2O3 *	10.39	10.35	10.32	10.53	10.37	10.26	10.32	10.33	10.41	10.42	10.51	10.3
H2O *	3.04	3.09	3.23	3.49	3.4	3.27	3.24	3.22	3.02	2.87	2.89	3.03
O=F	-0.48	-0.43	-0.29	-0.13	-0.16	-0.24	-0.29	-0.31	-0.51	-0.64	-0.65	-0.47
TOTAL	99.27	98.87	98.94	100.54	99.55	98.66	99.36	99.44	99.5	99.27	98.98	98.54
F-	0.603	0.536	0.373	0.157	0.201	0.311	0.362	0.388	0.634	0.807	0.811	0.592
NA+	0.726	0.71	0.676	0.599	0.556	0.65	0.709	0.679	0.573	0.459	0.465	0.681
MG2+	1.86	1.683	1.328	1.078	0.764	1.111	1.196	1.126	2.044	2.508	2.969	1.751
AL3+	6.186	6.372	6.593	6.856	7.003	6.67	6.515	6.606	6.045	5.834	5.662	6.305
SI4+	5.917	5.87	5.763	5.832	5.789	5.824	5.911	5.851	5.934	5.928	5.906	5.817
K+	0.011	0.006	0.009	0.006	0	0.009	0.002	0.009	0.004	0.009	0.004	0.009
CA2+	0.22	0.198	0.146	0.097	0.083	0.123	0.137	0.123	0.379	0.543	0.546	0.239
TI4+	0.024	0.028	0.03	0.019	0.025	0.036	0.043	0.037	0.036	0.033	0.024	0.025
CR3+	0	0	0	0	0.003	0	0.009	0.001	0.011	0	0	0.001
MN2+	0.028	0.016	0.036	0.015	0.038	0.039	0.031	0.033	0.023	0.013	0.007	0.031
FE2+	0.985	1.032	1.25	1.2	1.377	1.321	1.295	1.347	0.907	0.685	0.432	1.068
B3+	3	3	3	3	3	3	3	3	3	3	3	3
H+	3.397	3.464	3.627	3.843	3.799	3.689	3.638	3.612	3.366	3.193	3.189	3.408
O2-	30.52	30.603	30.705	31.022	30.976	30.836	30.846	30.768	30.533	30.347	30.23	30.487
CATSUM	18.957	18.914	18.831	18.702	18.638	18.782	18.848	18.81	18.957	19.011	19.015	18.928
AN SUM	31.123	31.14	31.078	31.179	31.177	31.147	31.209	31.157	31.167	31.154	31.041	31.079

Data for tourmaline from quartz vein

RR-02-36	29-16	29-17	29-18	29-19	29-20	29-21	29-22	29-23	29-24	29-25	29-26	29-27
F	1.21	0.68	0.52	0.86	0.19	0.65	0.31	0.66	0.24	0.28	0.64	0.38
NA2O	2.03	2.15	1.78	2.21	1.66	2.18	1.73	1.99	1.7	1.72	2.09	1.73
MGO	7.19	2.9	2.31	3.82	2.59	3.6	2.22	2.93	2.23	2.34	3.06	2.38
AL2O3	31.32	31.11	33.12	31.33	33.26	31.48	33.48	31.71	33.65	33.41	31.91	33.43
SIO2	35.21	34.2	34.39	34.3	34.4	33.72	35	34.63	34.97	34.46	34.21	34.64
K2O	0.04	0.05	0.04	0.05	0.02	0.05	0.04	0.06	0.03	0.04	0.06	0.04
CAO	1.36	0.5	0.26	0.64	0.17	0.62	0.17	0.51	0.13	0.18	0.48	0.19
TIO2	0.21	1.16	0.4	1.08	0.27	1.04	0.32	1.22	0.28	0.29	1.12	0.32
CR2O3	0	0.01	0	0.02	0	0	0.03	0	0.02	0	0.04	0
MNO	0.11	0.3	0.28	0.23	0.25	0.21	0.28	0.27	0.32	0.33	0.25	0.26
FEO	7.39	13.33	12.59	11.75	12.1	11.82	12.34	12.34	12.75	12.37	12.4	12.18
B2O3 *	10.34	10.13	10.19	10.17	10.2	10.08	10.26	10.18	10.33	10.22	10.18	10.22
H2O *	3	3.17	3.27	3.1	3.43	3.17	3.39	3.2	3.45	3.39	3.21	3.35
O=F	-0.51	-0.29	-0.22	-0.36	-0.08	-0.27	-0.13	-0.28	-0.1	-0.12	-0.27	-0.16
TOTAL	98.9	99.41	98.93	99.2	98.45	98.35	99.45	99.42	99.99	98.91	99.38	98.96
F-	0.643	0.369	0.281	0.465	0.102	0.354	0.166	0.356	0.128	0.151	0.346	0.204
NA+	0.661	0.715	0.589	0.732	0.549	0.728	0.568	0.659	0.555	0.567	0.692	0.57
MG2+	1.801	0.741	0.587	0.973	0.658	0.925	0.56	0.746	0.56	0.593	0.779	0.603
AL3+	6.202	6.288	6.658	6.311	6.682	6.394	6.681	6.382	6.676	6.699	6.422	6.698
SI4+	5.916	5.865	5.866	5.862	5.864	5.812	5.926	5.914	5.886	5.863	5.842	5.889
K+	0.009	0.011	0.009	0.011	0.004	0.011	0.009	0.013	0.006	0.009	0.013	0.009
CA2+	0.245	0.092	0.048	0.117	0.031	0.114	0.031	0.093	0.023	0.033	0.088	0.035
TI4+	0.027	0.15	0.051	0.139	0.035	0.135	0.041	0.157	0.035	0.037	0.144	0.041
CR3+	0	0.001	0	0.003	0	0	0.004	0	0.003	0	0.005	0
MN2+	0.016	0.044	0.04	0.033	0.036	0.031	0.04	0.039	0.046	0.048	0.036	0.037
FE2+	1.038	1.912	1.796	1.679	1.725	1.704	1.747	1.762	1.795	1.76	1.771	1.732
B3+	3	3	3	3	3	3	3	3	3	3	3	3
H+	3.357	3.631	3.719	3.535	3.898	3.646	3.834	3.644	3.872	3.849	3.654	3.796
O2-	30.481	30.745	30.813	30.681	30.945	30.773	30.963	30.834	30.937	30.92	30.795	30.898
CATSUM	18.915	18.818	18.645	18.86	18.584	18.854	18.607	18.765	18.585	18.609	18.793	18.614
AN SUM	31.124	31.114	31.093	31.146	31.047	31.128	31.129	31.191	31.065	31.07	31.14	31.103

Data for tourmaline from quartz vein

RR-02-31c	12-30	12-31	12-32	12-33	12-34	12-35	12-36	12-37	12-38	12-41	12-43	12-44
F	1.52	1.17	1.17	0.39	1.15	1	1.23	0.88	1	1.08	0.67	0.78
NA2O	2.41	2.19	2.19	1.59	2.16	2.17	2.19	2.05	1.99	2.04	1.99	2.06
MGO	6.74	6.83	7.28	3.93	6.66	7.58	7.45	5.52	7.23	6.68	5.07	5.84
AL2O3	31.9	31.8	31.52	34.69	31.96	31.82	31.49	32.65	31.29	31.25	33.18	33.05
SIO2	34.73	34.13	34.57	34.72	34.84	34.94	35.18	34.89	34.25	34.69	34.56	34.74
K2O	0.05	0.03	0.05	0.04	0.04	0.04	0.03	0.02	0.03	0.02	0.02	0.03
CAO	0.7	0.99	1.27	0.29	1.13	1.24	1.24	0.89	1.54	1.36	0.79	0.94
TIO2	0.12	0.15	0.2	0.11	0.21	0.19	0.22	0.32	0.21	0.25	0.26	0.14
CR2O3	0.02	0	0	0.01	0.01	0.04	0	0	0.02	0	0.02	0
MNO	0.19	0.12	0.17	0.24	0.17	0.19	0.17	0.2	0.14	0.16	0.21	0.17
FEO	7.51	7.66	7.24	8.89	7.72	6.86	7.19	8.52	7.42	8.36	9.15	8.11
B2O3 *	10.3	10.24	10.3	10.33	10.34	10.41	10.4	10.33	10.24	10.29	10.34	10.36
H2O *	2.83	2.98	3	3.38	3.02	3.12	3	3.15	3.06	3.04	3.25	3.21
O=F	-0.64	-0.49	-0.49	-0.16	-0.48	-0.42	-0.52	-0.37	-0.42	-0.45	-0.28	-0.33
TOTAL	98.39	97.8	98.47	98.45	98.92	99.17	99.27	99.04	98	98.76	99.23	99.1
F-	0.811	0.628	0.624	0.207	0.612	0.528	0.65	0.468	0.537	0.577	0.356	0.414
NA+	0.788	0.72	0.716	0.518	0.704	0.703	0.71	0.669	0.655	0.668	0.648	0.67
MG2+	1.695	1.727	1.831	0.985	1.67	1.887	1.857	1.385	1.829	1.682	1.27	1.46
AL3+	6.342	6.359	6.267	6.876	6.334	6.263	6.205	6.476	6.257	6.222	6.571	6.533
SI4+	5.859	5.791	5.832	5.839	5.859	5.835	5.882	5.871	5.811	5.86	5.807	5.827
K+	0.011	0.006	0.011	0.009	0.009	0.009	0.006	0.004	0.006	0.004	0.004	0.006
CA2+	0.127	0.18	0.23	0.052	0.204	0.222	0.222	0.16	0.28	0.246	0.142	0.169
TI4+	0.015	0.019	0.025	0.014	0.027	0.024	0.028	0.04	0.027	0.032	0.033	0.018
CR3+	0.003	0	0	0.001	0.001	0.005	0	0	0.003	0	0.003	0
MN2+	0.027	0.017	0.024	0.034	0.024	0.027	0.024	0.029	0.02	0.023	0.03	0.024
FE2+	1.059	1.087	1.021	1.25	1.086	0.958	1.005	1.199	1.053	1.181	1.286	1.138
B3+	3	3	3	3	3	3	3	3	3	3	3	3
H+	3.189	3.372	3.376	3.793	3.388	3.472	3.35	3.532	3.463	3.423	3.644	3.586
O2-	30.261	30.405	30.459	30.9	30.501	30.543	30.441	30.678	30.542	30.508	30.74	30.705
CATSUM	18.925	18.907	18.957	18.579	18.916	18.933	18.938	18.834	18.941	18.919	18.795	18.845
AN SUM	31.072	31.032	31.083	31.107	31.113	31.071	31.092	31.147	31.079	31.085	31.096	31.118

Data for tourmaline from quartz vein

HN-2-64	T64-1	T64-2	T64-3	T64-4	T64-5	T64-6	T64-7	T64-8	T64-9	64-10	64-11	64-12
F	0.44	0.84	0.29	0.84	0.97	0.98	0.62	0.73	0.89	0.75	0.58	0.89
NA2O	1.72	2.13	1.84	2.12	2.13	2.14	2.19	2.14	2.3	2.23	2.19	2.22
MGO	5.43	6.61	5.48	4.64	6.72	6.77	4.39	4.5	6.93	6.65	5.42	5.8
AL2O3	33.91	32.98	34.29	32.91	31.58	32.72	32.63	32.61	32.4	32.83	32.77	32.63
SIO2	35.23	33.14	34.38	32.47	34.17	32.65	33.8	33.81	34	33.92	34.56	34.6
K2O	0.05	0.01	0.03	0.05	0.05	0.05	0.03	0.06	0.03	0.05	0.05	0.07
CAO	0.31	0.99	0.34	0.51	0.95	0.91	0.52	0.58	0.84	0.82	0.77	0.68
TIO2	0.13	0.49	0.15	0.82	0.75	0.37	1.09	1.05	0.36	0.49	0.64	0.55
CR2O3	0	0.01	0.05	0	0	0	0.01	0.03	0.02	0	0	0.01
MNO	0.2	0.12	0.18	0.22	0.18	0.11	0.25	0.21	0.14	0.15	0.22	0.19
FEO	7.68	7.6	7.46	9.64	7.81	7.34	10.19	10	7.31	7.41	8.79	8.44
B2O3 *	10.43	10.28	10.37	10.08	10.27	10.17	10.24	10.23	10.32	10.34	10.34	10.35
H2O *	3.39	3.15	3.44	3.08	3.08	3.05	3.24	3.18	3.14	3.21	3.29	3.15
O=F	-0.19	-0.35	-0.12	-0.35	-0.41	-0.41	-0.26	-0.31	-0.37	-0.32	-0.24	-0.37
TOTAL	98.73	97.99	98.18	97.03	98.26	96.85	98.94	98.83	98.3	98.53	99.38	99.21
F-	0.232	0.449	0.154	0.458	0.519	0.529	0.333	0.392	0.474	0.399	0.308	0.473
NA+	0.556	0.698	0.598	0.708	0.699	0.709	0.721	0.705	0.751	0.727	0.713	0.723
MG2+	1.349	1.666	1.369	1.192	1.695	1.724	1.111	1.14	1.741	1.667	1.358	1.452
AL3+	6.662	6.573	6.773	6.684	6.297	6.587	6.528	6.528	6.433	6.505	6.489	6.457
SI4+	5.873	5.604	5.762	5.596	5.781	5.577	5.738	5.743	5.728	5.703	5.806	5.809
K+	0.011	0.002	0.006	0.011	0.011	0.011	0.006	0.013	0.006	0.011	0.011	0.015
CA2+	0.055	0.179	0.061	0.094	0.172	0.167	0.095	0.106	0.152	0.148	0.139	0.122
TI4+	0.016	0.062	0.019	0.106	0.095	0.048	0.139	0.134	0.046	0.062	0.081	0.069
CR3+	0	0.001	0.007	0	0	0	0.001	0.004	0.003	0	0	0.001
MN2+	0.028	0.017	0.026	0.032	0.026	0.016	0.036	0.03	0.02	0.021	0.031	0.027
FE2+	1.071	1.075	1.046	1.389	1.105	1.049	1.447	1.421	1.03	1.042	1.235	1.185
B3+	3	3	3	3	3	3	3	3	3	3	3	3
H+	3.768	3.551	3.846	3.542	3.481	3.471	3.667	3.608	3.526	3.601	3.692	3.527
O2-	30.827	30.535	30.88	30.54	30.533	30.415	30.767	30.716	30.548	30.635	30.824	30.626
CATSUM	18.622	18.88	18.665	18.814	18.882	18.886	18.822	18.823	18.909	18.885	18.863	18.86
AN SUM	31.059	30.984	31.033	30.998	31.052	30.944	31.1	31.108	31.022	31.034	31.132	31.099

Data for tourmaline from quartz vein

HN-2-8	T8-1	T8-2	T8-3	T8-4	T8-5	T8-6	T8-7	T8-8	T8-9	T8-10	T8-11	T8-12
F	0.76	0.42	1.07	0.56	0.96	0.03	0.72	0.64	0.74	0.93	0.72	0.62
NA2O	2.34	2.35	2.2	2.17	2.36	2.05	2.43	2.46	1.97	2.17	2.11	2.38
MGO	7.55	7.6	8.62	5.63	7.13	6.61	6.88	8.05	9.21	8.9	6.44	6.46
AL2O3	31.78	32.43	31.06	32.9	32.32	33.44	33.01	32.43	31.93	30.8	32.87	33.38
SIO2	35.31	34.94	34.44	34.49	33.71	35.05	34.72	34.78	35.26	35.06	34.46	35.27
K2O	0.02	0.02	0.03	0.03	0.03	0.02	0.02	0.03	0.02	0.02	0	0.04
CAO	0.9	0.76	1.39	0.6	0.81	0.26	0.63	0.79	1.63	1.29	0.75	0.54
TIO2	0.12	0.16	0.2	0.17	0.15	0.05	0.13	0.15	0.12	0.26	0.14	0.12
CR2O3	0	0	0	0.01	0	0.01	0.02	0	0.02	0	0	0.04
MNO	0.22	0.32	0.26	0.39	0.29	0.26	0.31	0.26	0.04	0.24	0.28	0.26
FEO	6.38	6.16	6.33	8.69	6.88	6.45	6.46	5.96	4.98	5.97	7.45	7.17
B2O3 *	10.39	10.43	10.38	10.36	10.26	10.43	10.39	10.46	10.54	10.43	10.36	10.5
H2O *	3.22	3.4	3.07	3.31	3.08	3.58	3.24	3.31	3.28	3.16	3.23	3.33
O=F	-0.32	-0.18	-0.45	-0.24	-0.4	-0.01	-0.3	-0.27	-0.31	-0.39	-0.3	-0.26
TOTAL	98.67	98.82	98.6	99.07	97.58	98.23	98.66	99.05	99.43	98.84	98.5	99.84
F-	0.402	0.221	0.567	0.297	0.514	0.016	0.381	0.336	0.386	0.49	0.382	0.325
NA+	0.759	0.759	0.714	0.706	0.775	0.663	0.788	0.792	0.63	0.701	0.687	0.764
MG2+	1.884	1.888	2.152	1.408	1.801	1.643	1.716	1.993	2.265	2.211	1.611	1.595
AL3+	6.268	6.368	6.131	6.506	6.453	6.57	6.509	6.348	6.208	6.049	6.502	6.515
SI4+	5.909	5.821	5.768	5.787	5.711	5.843	5.809	5.776	5.817	5.842	5.784	5.841
K+	0.004	0.004	0.006	0.006	0.006	0.004	0.004	0.006	0.004	0.004	0	0.008
CA2+	0.161	0.136	0.249	0.108	0.147	0.046	0.113	0.141	0.288	0.23	0.135	0.096
TI4+	0.015	0.02	0.025	0.021	0.019	0.006	0.016	0.019	0.015	0.033	0.018	0.015
CR3+	0	0	0	0.001	0	0.001	0.003	0	0.003	0	0	0.005
MN2+	0.031	0.045	0.037	0.055	0.042	0.037	0.044	0.037	0.006	0.034	0.04	0.036
FE2+	0.893	0.858	0.887	1.219	0.975	0.899	0.904	0.828	0.687	0.832	1.046	0.993
B3+	3	3	3	3	3	3	3	3	3	3	3	3
H+	3.598	3.779	3.433	3.703	3.486	3.984	3.619	3.664	3.614	3.51	3.618	3.675
O2-	30.699	30.821	30.402	30.73	30.48	31	30.709	30.672	30.656	30.492	30.648	30.773
CATSUM	18.925	18.899	18.97	18.82	18.929	18.713	18.905	18.939	18.922	18.936	18.821	18.868
AN SUM	31.101	31.042	30.969	31.027	30.994	31.015	31.09	31.009	31.042	30.982	31.03	31.098

Data for tourmaline from quartz vein

RR-02-40	40-1	40-2	40-3	40-4	40-5	40-6	40-7	40-8	40-9	40-10	40-11	40-12
F	1.06	0.84	1.15	0.67	0.44	1.09	0.53	0.9	1.3	0.95	1.28	0.82
NA2O	1.87	2.04	2.16	2.04	1.66	2.11	1.98	2.1	1.85	1.91	1.89	2.02
MGO	7.9	7.32	7.47	6.9	6.03	7.29	7.01	7.13	7.97	8.02	7.92	5.64
AL2O3	30.75	32.31	32.3	34.28	34.53	31.6	34.06	33.16	30.69	30.54	30.83	32.93
SIO2	35.66	34.4	33.69	33.93	34.7	33.92	34.84	34.29	34.21	34.69	34.44	34.3
K2O	0.03	0.02	0.03	0.01	0.02	0.03	0.03	0.03	0.02	0.02	0.03	0.04
CAO	1.8	1.34	1.23	0.84	0.68	1.33	0.95	1.15	1.8	1.79	1.71	0.6
TIO2	0.25	0.19	0.16	0.12	0.1	0.21	0.13	0.18	0.25	0.26	0.2	0.06
CR2O3	0.01	0.04	0	0	0	0.02	0.03	0	0	0	0.02	0.01
MNO	0.13	0.1	0.12	0.11	0.12	0.16	0.1	0.2	0.1	0.1	0.12	0.14
FEO	7.11	6.18	6.12	5.52	6.28	7.31	5.49	6.56	7.14	6.88	7.28	8.3
B2O3 *	10.42	10.29	10.22	10.36	10.41	10.25	10.45	10.4	10.25	10.27	10.3	10.27
H2O *	3.09	3.15	2.98	3.26	3.38	3.02	3.36	3.16	2.92	3.09	2.95	3.15
O=F	-0.45	-0.35	-0.48	-0.28	-0.19	-0.46	-0.22	-0.38	-0.55	-0.4	-0.54	-0.35
TOTAL	99.64	97.87	97.15	97.76	98.16	97.88	98.74	98.89	97.96	98.13	98.43	97.94
F-	0.559	0.449	0.618	0.355	0.232	0.585	0.279	0.476	0.697	0.508	0.683	0.439
NA+	0.605	0.668	0.712	0.664	0.538	0.694	0.638	0.68	0.608	0.626	0.618	0.663
MG2+	1.964	1.843	1.893	1.726	1.501	1.843	1.737	1.776	2.014	2.022	1.991	1.423
AL3+	6.045	6.431	6.472	6.777	6.797	6.316	6.673	6.529	6.13	6.089	6.128	6.568
SI4+	5.948	5.81	5.727	5.692	5.795	5.752	5.792	5.728	5.798	5.868	5.809	5.805
K+	0.006	0.004	0.007	0.002	0.004	0.006	0.006	0.006	0.004	0.004	0.006	0.009
CA2+	0.322	0.242	0.224	0.151	0.122	0.242	0.169	0.206	0.327	0.324	0.309	0.109
TI4+	0.031	0.024	0.02	0.015	0.013	0.027	0.016	0.023	0.032	0.033	0.025	0.008
CR3+	0.001	0.005	0	0	0	0.003	0.004	0	0	0	0.003	0.001
MN2+	0.018	0.014	0.017	0.016	0.017	0.023	0.014	0.028	0.014	0.014	0.017	0.02
FE2+	0.992	0.873	0.87	0.774	0.877	1.037	0.763	0.916	1.012	0.973	1.027	1.175
B3+	3	3	3	3	3	3	3	3	3	3	3	3
H+	3.441	3.551	3.382	3.645	3.768	3.415	3.721	3.524	3.303	3.492	3.317	3.561
O2-	30.57	30.682	30.449	30.724	30.866	30.445	30.86	30.589	30.331	30.577	30.338	30.603
CATSUM	18.933	18.915	18.943	18.817	18.663	18.942	18.814	18.892	18.939	18.955	18.933	18.78
AN SUM	31.13	31.13	31.067	31.079	31.099	31.03	31.138	31.064	31.028	31.085	31.021	31.042

Data for tourmaline from quartz vein

HN-2-58A	58b-13	58b-14	58b-15
F	0.65	0.57	0.47
NA2O	2.17	2.27	2.25
MGO	3.52	3.03	3.46
AL2O3	30.93	31.59	31.39
SIO2	34.02	34.58	34.73
K2O	0.05	0.06	0.06
CAO	0.62	0.36	0.38
TIO2	1.14	0.9	0.72
CR2O3	0	0	0
MNO	0.25	0.34	0.3
FEO	11.83	11.89	11.02
B2O3 *	10.04	10.11	10.07
H2O *	3.16	3.22	3.25
O=F	-0.27	-0.24	-0.2
TOTAL	98.11	98.67	97.9
F-	0.356	0.31	0.257
NA+	0.728	0.757	0.753
MG2+	0.908	0.777	0.89
AL3+	6.308	6.402	6.386
SI4+	5.887	5.946	5.995
K+	0.011	0.013	0.013
CA2+	0.115	0.066	0.07
TI4+	0.148	0.116	0.093
CR3+	0	0	0
MN2+	0.037	0.05	0.044
FE2+	1.712	1.71	1.591
B3+	3	3	3
H+	3.644	3.69	3.743
O2-	30.818	30.904	30.979
CATSUM	18.854	18.836	18.837
AN SUM	31.174	31.214	31.235

Data for tourmaline from quartz vein

HN-2-38	38-13	38-14
F	1	1.4
NA2O	2.23	0.28
MGO	4.46	2.61
AL2O3	31.28	29.27
SIO2	33.86	46.45
K2O	0.06	10.89
CAO	0.48	0.01
TIO2	0.92	0.93
CR2O3	0.06	0
MNO	0.19	0.14
FEO	10.43	1.89
B2O3 *	10.08	10.11
H2O *	3	2.82
O=F	-0.42	-0.59
TOTAL	97.63	106.21
F-	0.545	0.761
NA+	0.745	0.093
MG2+	1.146	0.669
AL3+	6.356	5.932
SI4+	5.838	7.987
K+	0.013	2.389
CA2+	0.089	0.002
TI4+	0.119	0.12
CR3+	0.008	0
MN2+	0.028	0.02
FE2+	1.504	0.272
B3+	3	3
H+	3.455	3.239
O2-	30.562	33.055
CATSUM	18.847	20.484
AN SUM	31.108	33.816

Data for tourmaline from quartz vein

RR-02-29	29-13	29-14	29-15
F	0.56	0.47	0.69
NA2O	1.79	2.04	2.02
MGO	2.81	5.87	4.62
AL2O3	32.63	33.41	33.4
SIO2	34.41	33.79	34
K2O	0.02	0	0.02
CAO	0.45	0.98	0.84
TIO2	0.6	0.28	0.25
CR2O3	0.01	0	0
MNO	0.3	0.13	0.2
FEO	12.11	7.77	9.28
B2O3 *	10.18	10.28	10.24
H2O *	3.25	3.32	3.21
O=F	-0.24	-0.2	-0.29
TOTAL	98.89	98.15	98.47
F-	0.302	0.251	0.37
NA+	0.592	0.669	0.665
MG2+	0.715	1.479	1.169
AL3+	6.563	6.656	6.682
SI4+	5.872	5.712	5.771
K+	0.004	0	0.004
CA2+	0.082	0.177	0.153
TI4+	0.077	0.036	0.032
CR3+	0.001	0	0
MN2+	0.043	0.019	0.029
FE2+	1.728	1.098	1.317
B3+	3	3	3
H+	3.698	3.749	3.63
O2-	30.81	30.836	30.761
CATSUM	18.679	18.846	18.822
AN SUM	31.112	31.087	31.131

Data for tourmaline from quartz vein

RR-02-36	29-28	29-29	29-30
F	0.66	0.44	0.58
NA2O	2.28	1.91	2.11
MGO	3.82	2.45	2.76
AL2O3	32.02	33.37	32.64
SIO2	34.02	34.97	33.72
K2O	0.08	0.04	0.06
CAO	0.65	0.24	0.44
TIO2	1.06	0.66	0.91
CR2O3	0.01	0.04	0
MNO	0.21	0.35	0.31
FEO	11.7	12.3	12.7
B2O3 *	10.22	10.32	10.18
H2O *	3.21	3.35	3.24
O=F	-0.28	-0.19	-0.24
TOTAL	99.67	100.26	99.4
F-	0.355	0.234	0.313
NA+	0.752	0.624	0.698
MG2+	0.968	0.615	0.702
AL3+	6.417	6.624	6.567
SI4+	5.784	5.89	5.756
K+	0.017	0.009	0.013
CA2+	0.118	0.043	0.08
TI4+	0.136	0.084	0.117
CR3+	0.001	0.005	0
MN2+	0.03	0.05	0.045
FE2+	1.664	1.732	1.813
B3+	3	3	3
H+	3.645	3.766	3.687
O2-	30.777	30.913	30.779
CATSUM	18.887	18.676	18.792
AN SUM	31.132	31.147	31.093

Data for tourmaline from quartz vein

RR-02-31c	12-45	12-46	12-47	12-48	12-49	12-50	12-51
F	0.83	0.58	0.54	0.78	0.81	0.99	0.68
NA2O	2.07	1.78	1.91	2.05	2.01	2.14	1.68
MGO	5.88	4.03	4.53	5.3	6.02	5.86	4.34
AL2O3	33.35	34.01	33.45	32.34	33.32	32.82	33.75
SIO2	34.69	34.97	34.49	35.11	34.63	34.57	34.78
K2O	0.03	0.02	0.02	0.03	0.01	0.02	0.08
CAO	0.93	0.43	0.76	0.98	1	0.97	0.53
TIO2	0.19	0.19	0.23	0.36	0.21	0.22	0.15
CR2O3	0	0.03	0.03	0	0.01	0	0.01
MNO	0.16	0.23	0.11	0.24	0.1	0.2	0.23
FEO	8.03	9.58	9.33	9.17	8.05	8.32	9.26
B2O3 *	10.4	10.36	10.28	10.34	10.41	10.34	10.32
H2O *	3.19	3.3	3.29	3.2	3.21	3.1	3.24
O=F	-0.35	-0.24	-0.23	-0.33	-0.34	-0.42	-0.29
TOTAL	99.4	99.27	98.75	99.57	99.45	99.14	98.76
F-	0.439	0.308	0.289	0.415	0.428	0.526	0.362
NA+	0.671	0.579	0.626	0.668	0.651	0.697	0.548
MG2+	1.465	1.008	1.141	1.328	1.498	1.468	1.089
AL3+	6.569	6.723	6.662	6.405	6.555	6.499	6.697
SI4+	5.797	5.865	5.829	5.9	5.781	5.808	5.856
K+	0.006	0.004	0.004	0.006	0.002	0.004	0.017
CA2+	0.167	0.077	0.138	0.176	0.179	0.175	0.096
TI4+	0.024	0.024	0.029	0.045	0.026	0.028	0.019
CR3+	0	0.004	0.004	0	0.001	0	0.001
MN2+	0.023	0.033	0.016	0.034	0.014	0.028	0.033
FE2+	1.122	1.344	1.319	1.289	1.124	1.169	1.304
B3+	3	3	3	3	3	3	3
H+	3.561	3.692	3.711	3.585	3.572	3.474	3.638
O2-	30.672	30.814	30.855	30.746	30.663	30.585	30.741
CATSUM	18.844	18.66	18.768	18.851	18.832	18.876	18.661
AN SUM	31.111	31.121	31.144	31.161	31.091	31.111	31.103

Data for tourmaline from quartz vein

HN-2-64	64-13	64-14	64-15	64-16	64-17	64-18	64-19	64-20	64-21
F	0.57	0.65	0.35	0.55	0.87	0.3	0.64	0.58	0.55
NA2O	1.78	2.18	1.9	2.16	2.13	1.8	2.18	1.97	2.05
MGO	5.86	4.51	5.59	4.78	6.38	5.47	4.67	5.51	4.03
AL2O3	34.12	32.81	33.45	32.37	31.77	34.29	32.68	33.49	33.09
SIO2	35.13	32.84	34.43	33.2	33.89	34.48	34.76	35.19	33.55
K2O	0.03	0.03	0.04	0.07	0.04	0.02	0.04	0.04	0.05
CAO	0.31	0.51	0.38	0.54	1.07	0.3	0.54	0.43	0.59
TIO2	0.16	0.98	0.17	0.93	0.59	0.14	0.98	0.32	0.99
CR2O3	0.01	0.01	0	0	0	0	0	0	0.04
MNO	0.1	0.23	0.1	0.18	0.14	0.1	0.22	0.12	0.21
FEO	7.51	10.41	7.78	9.75	8.5	7.82	9.74	8.06	10.28
B2O3 *	10.49	10.18	10.3	10.14	10.26	10.4	10.35	10.42	10.21
H2O *	3.35	3.2	3.39	3.24	3.13	3.45	3.27	3.32	3.26
O=F	-0.24	-0.27	-0.15	-0.23	-0.37	-0.13	-0.27	-0.24	-0.23
TOTAL	99.18	98.27	97.73	97.67	98.4	98.44	99.79	99.21	98.67
F-	0.299	0.351	0.187	0.298	0.466	0.159	0.34	0.306	0.296
NA+	0.572	0.721	0.622	0.718	0.7	0.583	0.71	0.637	0.677
MG2+	1.447	1.148	1.406	1.222	1.612	1.362	1.169	1.37	1.023
AL3+	6.66	6.6	6.651	6.541	6.345	6.752	6.469	6.582	6.639
SI4+	5.818	5.606	5.809	5.693	5.743	5.761	5.838	5.868	5.712
K+	0.006	0.007	0.009	0.015	0.009	0.004	0.009	0.009	0.011
CA2+	0.055	0.093	0.069	0.099	0.194	0.054	0.097	0.077	0.108
TI4+	0.02	0.126	0.022	0.12	0.075	0.018	0.124	0.04	0.127
CR3+	0.001	0.001	0	0	0	0	0	0	0.005
MN2+	0.014	0.033	0.014	0.026	0.02	0.014	0.031	0.017	0.03
FE2+	1.04	1.486	1.098	1.398	1.205	1.093	1.368	1.124	1.464
B3+	3	3	3	3	3	3	3	3	3
H+	3.701	3.649	3.813	3.702	3.534	3.841	3.66	3.694	3.704
O2-	30.714	30.639	30.853	30.751	30.573	30.843	30.813	30.792	30.816
CATSUM	18.633	18.821	18.699	18.833	18.903	18.641	18.816	18.722	18.795
AN SUM	31.012	30.989	31.04	31.049	31.039	31.002	31.153	31.098	31.112

Data for tourmaline from quartz vein

HN-2-8	T8-13	T8-14	T8-15	T8-16	T8-17	T8-18	T8-19	T8-20	T8-21	T8-22	T8-23
F	0.97	0.23	0.54	0.8	0.97	0.76	0.99	0.97	0.18	0.46	0.96
NA2O	2.28	5.7	2.22	2.23	2.25	2.31	2.32	2.18	1.89	2.02	1.74
MGO	6.66	2.32	6.42	7.3	6.82	6.38	8.87	8.46	5.12	6.42	10.06
AL2O3	32.05	21.61	33.56	32.24	31.92	32.35	31.23	31.62	34.93	33.36	30.59
SIO2	35.09	60.18	34.8	33.97	35.54	34.06	35.31	35.04	34.79	34.92	35.35
K2O	0.04	0.05	0.01	0.03	0.02	0.01	0.02	0.03	0.01	0.02	0.02
CAO	0.87	2.88	0.49	0.94	0.92	0.78	1.19	1.26	0.19	0.47	2.13
TIO2	0.32	0.02	0.14	0.19	0.21	0.3	0.14	0.16	0.07	0.04	0.15
CR2O3	0	0.03	0	0	0	0.02	0.03	0.02	0.03	0	0.02
MNO	0.3	0.03	0.24	0.26	0.28	0.32	0.22	0.2	0.35	0.16	0.06
FEO	7.97	1.99	6.81	6.55	7.84	8.04	5.81	5.72	7.38	7.24	4.87
B2O3 *	10.42	10.52	10.42	10.28	10.46	10.3	10.49	10.43	10.44	10.43	10.5
H2O *	3.14	3.52	3.34	3.17	3.15	3.2	3.15	3.14	3.52	3.38	3.17
O=F	-0.41	-0.1	-0.23	-0.34	-0.41	-0.32	-0.42	-0.41	-0.08	-0.19	-0.4
TOTAL	99.7	108.99	98.76	97.62	99.97	98.51	99.35	98.82	98.83	98.73	99.22
F-	0.512	0.12	0.285	0.428	0.51	0.405	0.519	0.511	0.095	0.242	0.502
NA+	0.737	1.825	0.718	0.731	0.725	0.755	0.745	0.704	0.61	0.653	0.558
MG2+	1.656	0.571	1.596	1.841	1.689	1.604	2.191	2.102	1.27	1.595	2.482
AL3+	6.299	4.206	6.597	6.426	6.251	6.431	6.1	6.211	6.851	6.551	5.966
SI4+	5.851	9.938	5.805	5.745	5.905	5.745	5.852	5.84	5.79	5.818	5.849
K+	0.009	0.011	0.002	0.006	0.004	0.002	0.004	0.006	0.002	0.004	0.004
CA2+	0.155	0.51	0.088	0.17	0.164	0.141	0.211	0.225	0.034	0.084	0.378
TI4+	0.04	0.002	0.018	0.024	0.026	0.038	0.017	0.02	0.009	0.005	0.019
CR3+	0	0.004	0	0	0	0.003	0.004	0.003	0.004	0	0.003
MN2+	0.042	0.004	0.034	0.037	0.039	0.046	0.031	0.028	0.049	0.023	0.008
FE2+	1.111	0.275	0.95	0.926	1.089	1.134	0.805	0.797	1.027	1.009	0.674
B3+	3	3	3	3	3	3	3	3	3	3	3
H+	3.488	3.88	3.715	3.572	3.49	3.595	3.481	3.489	3.905	3.758	3.498
O2-	30.558	34.852	30.784	30.594	30.575	30.614	30.488	30.535	30.971	30.768	30.508
CATSUM	18.901	20.345	18.808	18.908	18.893	18.899	18.961	18.936	18.646	18.741	18.94
AN SUM	31.069	34.972	31.069	31.022	31.085	31.019	31.007	31.047	31.066	31.011	31.011

Data for tourmaline from quartz vein

RR-02-40	40-13	40-14	40-15	40-16	40-17	40-18	40-19	40-20	40-21	40-22	40-23	40-24
F	0.65	1.1	0.55	0.55	1.17	1.09	0.74	0.85	0.98	0.96	0.82	1.07
NA2O	1.7	2	1.96	1.87	1.96	1.67	1.97	2.05	2.03	2.01	2	1.93
MGO	5.46	7.56	6.87	5.73	7.76	8.14	5.84	6.13	7.22	6.99	7.26	7.39
AL2O3	32.65	31.19	34.4	33.46	31.03	30.12	32.87	32.03	32.68	32.95	33.56	33.18
SIO2	33.68	34.81	34.95	34.21	34.76	35.07	34.14	34.51	33.41	34.8	33.77	34.04
K2O	0.02	0.03	0.01	0.02	0.01	0.02	0.04	0.03	0.04	0.02	0.03	0.03
CAO	0.66	1.4	0.93	0.5	1.54	2.26	0.61	0.82	1.28	1.29	1.25	1.41
TIO2	0.09	0.22	0.15	0.08	0.23	0.31	0.14	0.15	0.19	0.23	0.17	0.22
CR2O3	0	0	0.03	0	0.02	0.01	0	0.02	0.01	0.03	0.01	0.04
MNO	0.14	0.09	0.13	0.14	0.11	0.1	0.06	0.1	0.12	0.16	0.07	0.17
FEO	8.05	7.19	5.7	7.72	7.08	7.52	8.06	7.91	6.89	6.26	5.47	5.34
B2O3 *	10.11	10.32	10.51	10.29	10.32	10.35	10.25	10.22	10.28	10.38	10.3	10.31
H2O *	3.18	3.04	3.37	3.29	3.01	3.05	3.19	3.12	3.08	3.13	3.17	3.05
O=F	-0.27	-0.46	-0.23	-0.23	-0.49	-0.46	-0.31	-0.36	-0.41	-0.4	-0.35	-0.45
TOTAL	96.11	98.49	99.33	97.63	98.51	99.25	97.6	97.59	97.8	98.81	97.53	97.73
F-	0.354	0.586	0.288	0.294	0.623	0.579	0.397	0.457	0.524	0.508	0.438	0.571
NA+	0.567	0.653	0.628	0.612	0.64	0.544	0.648	0.676	0.666	0.652	0.654	0.631
MG2+	1.4	1.897	1.693	1.443	1.947	2.038	1.476	1.554	1.82	1.744	1.826	1.857
AL3+	6.618	6.189	6.701	6.66	6.157	5.962	6.567	6.418	6.513	6.5	6.673	6.593
SI4+	5.792	5.861	5.777	5.777	5.852	5.89	5.788	5.867	5.65	5.824	5.697	5.739
K+	0.004	0.006	0.002	0.004	0.002	0.004	0.009	0.007	0.009	0.004	0.006	0.006
CA2+	0.122	0.253	0.165	0.09	0.278	0.407	0.111	0.149	0.232	0.231	0.226	0.255
TI4+	0.012	0.028	0.019	0.01	0.029	0.039	0.018	0.019	0.024	0.029	0.022	0.028
CR3+	0	0	0.004	0	0.003	0.001	0	0.003	0.001	0.004	0.001	0.005
MN2+	0.02	0.013	0.018	0.02	0.016	0.014	0.009	0.014	0.017	0.023	0.01	0.024
FE2+	1.158	1.012	0.788	1.09	0.997	1.056	1.143	1.125	0.974	0.876	0.772	0.753
B3+	3	3	3	3	3	3	3	3	3	3	3	3
H+	3.646	3.414	3.712	3.706	3.377	3.421	3.603	3.543	3.476	3.492	3.562	3.429
O2-	30.667	30.479	30.841	30.722	30.436	30.512	30.631	30.63	30.476	30.657	30.674	30.569
CATSUM	18.693	18.912	18.795	18.707	18.92	18.955	18.767	18.832	18.906	18.888	18.887	18.892
AN SUM	31.02	31.065	31.128	31.016	31.059	31.091	31.028	31.087	31	31.165	31.112	31.14

Data for tourmaline from quartz vein

RR-02-40	40-25	40-26	40-27	40-28	40-29	40-30	40-31	40-32	40-33	40-34	40-35	40-36
F	0.67	0.81	1.24	1.03	0.95	0.86	0.9	0.64	1.32	1.17	1.01	1
NA2O	1.89	1.94	1.88	1.99	1.85	2.02	2.07	1.97	1.87	2.1	1.92	2.01
MGO	6.79	7.31	8.1	7.3	7.46	6.91	7.05	6.92	7.27	7.4	7.09	7.85
AL2O3	34.13	33.4	30.27	31.89	32.84	32.66	32.35	33.97	30.54	31.78	31.89	31.18
SIO2	34.36	35.23	33.68	34.08	34.06	34.53	33.95	33.47	33.66	35.25	34.15	33.95
K2O	0.03	0	0.03	0.02	0	0.02	0.02	0.03	0.03	0.03	0.01	0
CAO	0.98	1.26	1.88	1.5	1.44	1.1	1.25	1.05	1.93	1.36	1.43	1.64
TIO2	0.13	0.25	0.23	0.2	0.24	0.14	0.17	0.14	0.38	0.21	0.27	0.24
CR2O3	0	0.06	0	0	0.04	0.01	0.01	0	0	0	0.05	0
MNO	0.12	0.1	0.05	0.11	0.07	0.17	0.1	0.11	0.18	0.09	0.17	0.1
FEO	5.48	5.59	7.09	7.07	5.96	6.44	6.78	5.65	7.77	6.98	7.24	7.24
B2O3 *	10.37	10.48	10.15	10.28	10.33	10.31	10.25	10.28	10.13	10.41	10.28	10.28
H2O *	3.26	3.23	2.91	3.06	3.11	3.15	3.11	3.24	2.87	3.04	3.07	3.07
O=F	-0.28	-0.34	-0.52	-0.43	-0.4	-0.36	-0.38	-0.27	-0.56	-0.49	-0.43	-0.42
TOTAL	97.93	99.33	96.99	98.09	97.95	97.95	97.63	97.21	97.39	99.32	98.16	98.14
F-	0.355	0.425	0.672	0.551	0.506	0.459	0.483	0.342	0.716	0.618	0.54	0.535
NA+	0.614	0.624	0.624	0.652	0.604	0.66	0.68	0.646	0.622	0.68	0.629	0.659
MG2+	1.697	1.806	2.068	1.84	1.871	1.737	1.782	1.744	1.859	1.843	1.787	1.979
AL3+	6.742	6.525	6.111	6.356	6.513	6.49	6.464	6.767	6.175	6.256	6.353	6.213
SI4+	5.759	5.84	5.769	5.763	5.731	5.822	5.756	5.657	5.775	5.888	5.772	5.74
K+	0.006	0	0.007	0.004	0	0.004	0.004	0.006	0.007	0.006	0.002	0
CA2+	0.176	0.224	0.345	0.272	0.26	0.199	0.227	0.19	0.355	0.243	0.259	0.297
TI4+	0.016	0.031	0.03	0.025	0.03	0.018	0.022	0.018	0.049	0.026	0.034	0.031
CR3+	0	0.008	0	0	0.005	0.001	0.001	0	0	0	0.007	0
MN2+	0.017	0.014	0.007	0.016	0.01	0.024	0.014	0.016	0.026	0.013	0.024	0.014
FE2+	0.768	0.775	1.016	1	0.839	0.908	0.961	0.799	1.115	0.975	1.023	1.024
B3+	3	3	3	3	3	3	3	3	3	3	3	3
H+	3.645	3.575	3.328	3.449	3.494	3.541	3.517	3.658	3.284	3.382	3.46	3.465
O2-	30.778	30.749	30.342	30.516	30.577	30.658	30.597	30.733	30.365	30.51	30.521	30.469
CATSUM	18.797	18.847	18.976	18.929	18.863	18.863	18.912	18.842	18.983	18.93	18.89	18.956
AN SUM	31.133	31.173	31.014	31.066	31.082	31.116	31.079	31.075	31.081	31.128	31.061	31.003

Data for tourmaline from quartz vein

RR-02-40	40-37	40-38	40-39	40-40	40-41	40-42	40-43	40-44	40-45	40-46	40-47	40-48
F	0.68	1.01	1.02	0.82	0.72	0.92	0.98	0.92	0.79	1.07	0.39	0.82
NA2O	1.99	1.99	2.06	2.09	1.98	1.86	1.85	2.13	2.01	2.04	1.7	2.1
MGO	6.84	7.78	7.82	7.14	6.36	7.68	7.8	5.51	6.18	6.74	5.69	7.16
AL2O3	32.55	30.87	31.1	32.07	31.81	31.45	31.41	32.5	32.57	32.12	35.34	32.44
SIO2	35.23	34.65	34.66	33.9	33.99	35.34	34.88	34.03	34.94	34.06	33.98	33.84
K2O	0.02	0.03	0.03	0.04	0.06	0.03	0.03	0.04	0.01	0.05	0.01	0.01
CAO	1.31	1.64	1.55	1.2	1.14	1.57	1.69	0.6	0.76	0.96	0.47	1.19
TIO2	0.18	0.2	0.23	0.16	0.22	0.58	0.29	0.15	0.09	0.09	0.08	0.18
CR2O3	0.02	0.04	0	0	0.03	0	0.03	0.03	0.02	0	0	0.05
MNO	0.17	0.14	0.1	0.13	0.18	0.15	0.11	0.23	0.11	0.1	0.12	0.16
FEO	7	7.28	7.18	7.11	8.37	6.78	7.16	8.48	8.1	7.78	5.98	6.6
B2O3 *	10.42	10.31	10.34	10.26	10.23	10.44	10.41	10.19	10.37	10.27	10.34	10.26
H2O *	3.27	3.08	3.08	3.15	3.19	3.17	3.13	3.08	3.2	3.04	3.38	3.15
O=F	-0.29	-0.43	-0.43	-0.35	-0.3	-0.39	-0.41	-0.39	-0.33	-0.45	-0.16	-0.35
TOTAL	99.4	98.6	98.74	97.72	97.98	99.58	99.36	97.51	98.82	97.86	97.32	97.62
F-	0.359	0.538	0.542	0.439	0.387	0.484	0.517	0.496	0.419	0.573	0.207	0.439
NA+	0.643	0.65	0.671	0.687	0.652	0.6	0.599	0.704	0.653	0.669	0.554	0.69
MG2+	1.701	1.954	1.96	1.804	1.611	1.906	1.941	1.401	1.544	1.701	1.425	1.808
AL3+	6.398	6.131	6.161	6.405	6.368	6.172	6.18	6.531	6.434	6.407	6.998	6.475
SI4+	5.876	5.839	5.826	5.745	5.774	5.884	5.823	5.802	5.857	5.765	5.709	5.731
K+	0.004	0.006	0.006	0.009	0.013	0.006	0.006	0.009	0.002	0.011	0.002	0.002
CA2+	0.234	0.296	0.279	0.218	0.207	0.28	0.302	0.11	0.136	0.174	0.085	0.216
TI4+	0.023	0.025	0.029	0.02	0.028	0.073	0.036	0.019	0.011	0.011	0.01	0.023
CR3+	0.003	0.005	0	0	0.004	0	0.004	0.004	0.003	0	0	0.007
MN2+	0.024	0.02	0.014	0.019	0.026	0.021	0.016	0.033	0.016	0.014	0.017	0.023
FE2+	0.976	1.026	1.009	1.008	1.189	0.944	1	1.209	1.135	1.101	0.84	0.935
B3+	3	3	3	3	3	3	3	3	3	3	3	3
H+	3.641	3.462	3.458	3.561	3.613	3.516	3.483	3.504	3.581	3.427	3.793	3.561
O2-	30.798	30.518	30.512	30.594	30.641	30.642	30.539	30.559	30.632	30.421	30.874	30.617
CATSUM	18.882	18.953	18.957	18.913	18.873	18.887	18.907	18.822	18.792	18.854	18.641	18.908
AN SUM	31.157	31.056	31.054	31.033	31.028	31.126	31.056	31.055	31.05	30.994	31.081	31.056

Data for tourmaline from quartz vein

RR-02-40	40-49	40-50	40-51	40-52	40-53	40-54	40-55	40-56	40-57	40-58	40-59	40-60
F	1.29	0.83	1.28	0.8	1.17	0.66	1.25	1.24	0.48	1.05	1.07	0.7
NA2O	1.86	1.92	1.95	2.11	2.08	1.9	2.07	1.63	1.95	2.04	1.83	2
MGO	8.63	7.01	8.06	7	7.26	6.72	7.64	8.35	6.62	8.08	6.75	7.12
AL2O3	30.9	33.41	30.78	32.57	31.81	34.28	30.89	29.58	34.88	30.48	32.31	33.07
SIO2	33.81	33.11	33.17	34.08	33.12	32.78	34.82	33.89	35.02	34.89	33.97	33.3
K2O	0.03	0.04	0.03	0.02	0.03	0.01	0.04	0.03	0.03	0.03	0.03	0.03
CAO	2	1.23	1.89	1.13	1.36	1.04	1.66	2.33	0.73	1.71	1.47	1.01
TIO2	0.22	0.16	0.26	0.21	0.25	0.11	0.2	0.54	0.12	0.26	0.23	0.12
CR2O3	0.02	0	0	0	0	0	0	0	0	0.02	0	0
MNO	0.11	0.17	0.1	0.13	0.13	0.16	0.16	0.11	0.1	0.13	0.15	0.12
FEO	6.2	5.97	6.71	6.5	7.23	5.3	7.33	7.31	5.29	7.21	7.51	5.28
B2O3 *	10.26	10.22	10.12	10.27	10.17	10.18	10.32	10.17	10.5	10.34	10.28	10.14
H2O *	2.93	3.13	2.89	3.16	2.95	3.2	2.97	2.92	3.39	3.07	3.04	3.17
O=F	-0.54	-0.35	-0.54	-0.34	-0.49	-0.28	-0.53	-0.52	-0.2	-0.44	-0.45	-0.29
TOTAL	97.72	96.85	96.7	97.64	97.07	96.06	98.82	97.58	98.91	98.86	98.18	95.76
F-	0.691	0.446	0.695	0.428	0.632	0.356	0.666	0.67	0.251	0.558	0.572	0.38
NA+	0.611	0.633	0.649	0.693	0.689	0.629	0.676	0.54	0.626	0.665	0.6	0.665
MG2+	2.179	1.777	2.063	1.767	1.85	1.711	1.919	2.126	1.634	2.025	1.702	1.82
AL3+	6.169	6.697	6.229	6.498	6.407	6.898	6.134	5.955	6.806	6.04	6.44	6.682
SI4+	5.727	5.631	5.696	5.769	5.66	5.597	5.866	5.789	5.798	5.867	5.745	5.709
K+	0.006	0.009	0.007	0.004	0.007	0.002	0.009	0.007	0.006	0.006	0.006	0.007
CA2+	0.363	0.224	0.348	0.205	0.249	0.19	0.3	0.426	0.129	0.308	0.266	0.186
TI4+	0.028	0.02	0.034	0.027	0.032	0.014	0.025	0.069	0.015	0.033	0.029	0.015
CR3+	0.003	0	0	0	0	0	0	0	0	0.003	0	0
MN2+	0.016	0.024	0.015	0.019	0.019	0.023	0.023	0.016	0.014	0.019	0.021	0.017
FE2+	0.878	0.849	0.964	0.92	1.033	0.757	1.033	1.044	0.732	1.014	1.062	0.757
B3+	3	3	3	3	3	3	3	3	3	3	3	3
H+	3.309	3.554	3.305	3.572	3.368	3.644	3.334	3.33	3.749	3.442	3.428	3.62
O2-	30.321	30.599	30.324	30.67	30.36	30.71	30.435	30.366	30.911	30.506	30.492	30.707
CATSUM	18.98	18.866	19.004	18.902	18.945	18.821	18.984	18.973	18.762	18.98	18.873	18.857
AN SUM	31.013	31.045	31.02	31.099	30.992	31.066	31.101	31.036	31.162	31.065	31.064	31.086

Sample	Point	c-axis	elongate	zoned	light	dark	core	rim
RR-02-29	29-1	y		y		y		y
RR-02-29	29-2	y		y		y		y
RR-02-29	29-3	y		y	y		y	
RR-02-29	29-4	y		y		y	y	
RR-02-29	29-5	y		y	y		y	
RR-02-29	29-6		y	y	y		y	
RR-02-29	29-7		y	y	y		y	
RR-02-29	29-8		y	y	y		y	
RR-02-29	29-9		y	y		y	y	
RR-02-29	29-10		y	n			y	
RR-02-29	29-11	y		y		y	y	
RR-02-29	29-12	y		y	y			y
RR-02-29	29-13	y		y	y		y	
RR-02-29	29-14	y		y		y	y	
RR-02-29	29-15	y		y	y			y
RR-02-29	29-16	y		y		y		y
RR-02-36	29-17	y		n		y	y	
RR-02-36	29-18	y?		y	y		y	
RR-02-36	29-19	y?		y		y		y
RR-02-36	29-20	y		y	y		y	
RR-02-36	29-21	y		y		y		y
RR-02-36	29-22		y	sw	y		y	
RR-02-36	29-23		y	sw	y			y
RR-02-36	29-24		y	sw		y	y	
RR-02-36	29-25		y	sw		y	y	
RR-02-36	29-26		y	sw	y			y
RR-02-36	29-27	y		y	y		y	
RR-02-36	29-28	y		y		y		y
RR-02-36	29-29	y?		sw	y		y	
RR-02-36	29-30	y?		sw		y		y
AD1-21.2	212-1	y		y	y		y?	
AD1-21.2	212-2		y	y		y		y
AD1-21.2	212-3		y	y	y		y	
AD1-21.2	212-4		y	y		y		y
AD1-21.2	212-5	y		n		y		
AD1-21.2	212-6		y	y	y		y	
AD1-21.2	212-7		y	y		y	y	
AD1-21.2	212-8		y	y	y			y?
AD1-21.2	212-9	y		n	y		y	
AD1-21.2	212-10		y?	n	y		y	
AD1-21.2	212-11		y?	n	y			
AD1-21.2	212-12		y?	n	y			
AD1-21.2	212-13		y?	n	y			y?
AD1-21.2	212-14		y	n?	y		y	
AD1-21.2	212-15		y	n?	y		y	
AD1-21.2	212-16		y	n?	y		y	
AD1-21.2	212-17		y	n?	y			
AD1-21.2	212-18		y	n?	y			y
AD1-21.2	212-19		y	n?	y		y	
AD1-21.2	212-20		y	n?	y			y
AD1-21.2	212-21	y?		y	y			
AD1-21.2	212-22	y?		y		y		
AD1-21.2	212-23	y?		y	y			
AD1-21.2	212-24		y	y	y			y
AD1-21.2	212-25		y	y		y	y	

Sample	Point	c-axis	elongate	zoned	light	dark	core	rim
AD1-21.2	212-26		y	y	y			y
AD1-21.2	212-27	y?		y	y			y
AD1-21.2	212-28	y?		y		y	y	
AD1-21.2	212-29	y?		y	y			y
RR-02-31c	212-30		y		y			
RR-02-31c	212-31		y		y			
RR-02-31c	212-32		y		y			
RR-02-31c	212-33							
RR-02-31c	212-34	y		n			y	
RR-02-31c	212-35	y		n				y
RR-02-31c	212-36		y	y		y		y
RR-02-31c	212-37		y	y	y		y	
RR-02-31c	212-38		y	y		y		y
RR-02-31c	212-39							
RR-02-31c	212-40		y		y		y	
RR-02-31c	212-41	y		y	y			y
RR-02-31c	212-42	y		y		y	y	
RR-02-31c	212-43	y		y	y		y	
RR-02-31c	212-44	y		y		y		y
RR-02-31c	212-45	y		y		y		y
RR-02-31c	212-46	y		y	y		y	
RR-02-31c	212-47			y		y		
RR-02-31c	212-48			y	y			
RR-02-31c	212-49			y		y		
RR-02-31c	212-50							
RR-02-31c	212-51							
99-10	1159-1	y		y		y		y
99-10	1159-2	y		y	y		y	
99-10	1159-3		y	sw	y?			y?
99-10	1159-4		y	sw	y?			y?
99-10	1159-5		y	sw	y?			y?
99-10	1159-6		y	sw	y?		y	
99-10	1159-7		y	sw		y		y
99-10	1159-8	y				y		y
99-10	1159-9	y		y	y		y	
99-10	1159-10	y		y		y		y
99-10	1159-11	y		n?		y?		y?
99-10	1159-12		y	sw	y		y	
99-10	1159-13		y	sw	y		y	
99-10	1159-14		y	sw	y		y	
99-10	1159-15		y	sw		y		y?
99-10	1159-16		y	sw		y		y?
99-10	1159-17	y		y	y		y	
99-10	1159-18	y		y		y		y
99-10	1159-19	y		y				
99-10	1159-20	y		y				
99-10	1159-21	y				y		
99-10	1159-22	y		sw		y	y	
AD1-115.9	1159-23		y					y
AD1-115.9	1159-24		y				y	
AD1-115.9	1159-25		y				y	
AD1-115.9	1159-26							
AD1-115.9	1159-27							
AD1-115.9	1159-28							
AD1-115.9	1159-29							

Sample	Point	c-axis	elongate	zoned	light	dark	core	rim
AD1-115.9	1159-30							
RR-02-40	40-1	y?						y
RR-02-40	40-2	y?					y	
RR-02-40	40-3		y				y	
RR-02-40	40-4		y				y	
RR-02-40	40-5		y				y	
RR-02-40	40-6	y		y				y
RR-02-40	40-7	y					y	
RR-02-40	40-8	y						y
RR-02-40	40-9	y?						y?
RR-02-40	40-10		y				y	
RR-02-40	40-11		y				y	
RR-02-40	40-12	y						y
RR-02-40	40-13	y					y	
RR-02-40	40-14		y?					y?
RR-02-40	40-15		y?				y	
RR-02-40	40-16		y				y	
RR-02-40	40-17		y				y	
RR-02-40	40-18	y					y	
RR-02-40	40-19	y					y	
RR-02-40	40-20	y?					y?	
RR-02-40	40-21	y?					y?	
RR-02-40	40-22	y?					y?	
RR-02-40	40-23	y?					y?	
RR-02-40	40-24	y?					y?	
RR-02-40	40-25	y?					y?	
RR-02-40	40-26	y?					y?	
RR-02-40	40-27		y				y	
RR-02-40	40-28		y				y	
RR-02-40	40-29		y				y	
RR-02-40	40-30	y				y	y	
RR-02-40	40-31	y			y			y
RR-02-40	40-32	y				y	y	
RR-02-40	40-33	y			y			y
RR-02-40	40-34	y?						
RR-02-40	40-35	y?		y				y
RR-02-40	40-36	y?		y				y
RR-02-40	40-37		y				y	
RR-02-40	40-38		y				y	
RR-02-40	40-39		y				y	
RR-02-40	40-40		y				y	
RR-02-40	40-41		y				y	
RR-02-40	40-42	y				y	y	
RR-02-40	40-43	y			y			y
RR-02-40	40-44		y				y	
RR-02-40	40-45		y				y	
RR-02-40	40-46		y				y	
RR-02-40	40-47	y					y	
RR-02-40	40-48	y						y
RR-02-40	40-49	y?		y			y	
RR-02-40	40-50	y?		y			y	
RR-02-40	40-51	y?		y				y
RR-02-40	40-52		y	n			y	
RR-02-40	40-53		y				y	
RR-02-40	40-54					y		

Sample	Point	c-axis	elongate	zoned	light	dark	core	rim
RR-02-40	40-55					y		
RR-02-40	40-56					y		
RR-02-40	40-57	y		y			y	
RR-02-40	40-58	y		y				y
RR-02-40	40-59	y					y	
RR-02-40	40-60	y						y
RR-02-30a	30-1							
RR-02-30a	30-2							
RR-02-30a	30-3							
RR-02-30a	30-4							
RR-02-30a	30-5						y	
RR-02-30a	30-6						y	
RR-02-30a	30-7							y
RR-02-30a	30-8							y
RR-02-30a	30-9			y	y			
RR-02-30a	30-10			y		y		
RR-02-30a	30-11			y	y			
RR-02-30a	30-12			y		y	y	
RR-02-30a	30-13			y	y		y	
RR-02-30a	30-14			y				
HN-2-8	T8-1	y		y	y			y
HN-2-8	T8-2					y	y	
HN-2-8	T8-3		y		?			
HN-2-8	T8-4		y		?			
HN-2-8	T8-5	y		y	y			y
HN-2-8	T8-6	y		y		y	y	
HN-2-8	T8-7		y	y	y			y
HN-2-8	T8-8		y	y		y	y	
HN-2-8	T8-9		y	y		y		y
HN-2-8	T8-10		y	y	y		y	
HN-2-8	T8-11		y	y	y			y
HN-2-8	T8-12		y	y		y	y	
HN-2-8	T8-13	y		y	y		y	
HN-2-8	T8-15		y	y		y	y	
HN-2-8	T8-16		y	y				y
HN-2-8	T8-17	y			y			
HN-2-8	T8-18	y		y	y		y	
HN-2-8	T8-19	y		y		y		y
HN-2-8	T8-20	y		y	y			y
HN-2-8	T8-21	y		y		y	y	
HN-2-8	T8-22		y				y	
HN-2-8	T8-23		y				y	
HN-2-64	T64-1	y					y	
HN-2-64	T64-2	y						y
HN-2-64	T64-3	y					y	
HN-2-64	T64-4	y		y	y			y
HN-2-64	T64-5	y		y		y	y	
HN-2-64	T64-6		y			y	y	
HN-2-64	T64-7		y		y			y
HN-2-64	T64-8	y		y	y			y
HN-2-64	T64-9	y		y		y	y	
HN-2-64	64-10	y		y		y	y	
HN-2-64	64-11	y		y	y			y
HN-2-64	64-12	y		y	y			y
HN-2-64	64-13		y	y		y	y	

Sample	Point	c-axis	elongate	zoned	light	dark	core	rim
HN-2-64	64-14		y	y	y			y
HN-2-64	64-15	y		y		y	y	
HN-2-64	64-16	y		y	y			y
HN-2-64	64-17		y					
HN-2-64	64-18		y	y		y	y	
HN-2-64	64-19		y	y	y			y
HN-2-64	64-20	y		y		y	y	
HN-2-64	64-21	y		y	y			y
HN-2-14	T14-1		y	y				y
HN-2-14	T14-2		y	y				y
HN-2-14	T14-3		y	y			y	
HN-2-14	T14-4		y	y				y
HN-2-14	T14-5		y	y			y	
HN-2-14	T14-6		y	y				y
HN-2-14	T14-7		y	y				y
HN-2-14	T14-8		y	y			y	
HN-2-14	T14-9	y					y	
HN-2-14	T14-11	y		y				y
HN-2-14	T14-12	y		y				y
HN-2-14	14-13		y	y				y
HN-2-14	14-14		y	y				y
HN-2-14	14-15		y	y				y
HN-2-14	14-16		y	y			y	
HN-2-14	14-17		y	y			y	
HN-2-14	14-18		y	y			y	
HN-2-14	14-19	y		y				y
HN-2-14	14-20	y		y			y	
HN-2-14	14-21	y						
HN-2-14	14-22	y						
HN-2-14	14-23	y						
HN-2-14	14-24	y						
HN-2-10	T10-1							
HN-2-10	T10-2							
HN-2-10	T10-3							
HN-2-10	T10-4							
HN-2-10	T10-5							
HN-2-10	T10-6							
HN-2-10	T10-7							
HN-2-10	T10-9							
HN-2-10	10-10							
HN-2-10	10-11							
HN-2-10	10-12							
HN-2-38	T38-1	y		n				y
HN-2-38	T38-2	y		n			y	
HN-2-38	T38-3	y		n				y
HN-2-38	T38-4		y	n				y
HN-2-38	T38-5		y	n			y	
HN-2-38	T38-6		y	n			y	
HN-2-38	T38-7		y	n				y
HN-2-38	T38-8		y	n			y	
HN-2-38	T38-9			n				
HN-2-38	T3810			n				
HN-2-38	T3811			n				
HN-2-38	T3813			n				
HN-2-6	T6-1							

Sample	Point	c-axis	elongate	zoned	light	dark	core	rim
HN-2-6	T6-2							
HN-2-6	T6-3							
HN-2-6	T6-4							
HN-2-6	T6-5							
HN-2-6	T6-6							
HN-2-6	T6-7							
HN-2-6	T6-8			sw		y		
HN-2-6	T6-9			sw	y			
HN-2-6	T6-10							
HN-2-6	T6-11							
HN-2-6	T6-12							
HN-2-6	T6-13							
HN-2-6	T6-14							
HN-2-6	T6-15		y					
HN-2-6	T6-16		y					
HN-2-6	T6-17		y					
HN-2-6	T6-18		y					
HN-2-6	T6-19		y					
HN-2-6	T6-20							
HN-2-6	T6-21							
HN-2-6	T6-22							
HN-2-6	T6-23							
HN-2-6	T6-24							
HN-2-58A	58a-1							
HN-2-58A	58a-2	y						
HN-2-58A	58a-3	y						
HN-2-58A	58a-4	y						
HN-2-58A	58a-5							
HN-2-58A	58a-6							
HN-2-58A	58a-7							
HN-2-58A	58a-8							
HN-2-58A	58a-9							
HN-2-58A	58a10							
HN-2-58A	58a11	y						
HN-2-58A	58a12							
HN-2-58A	58a13							
HN-2-58A	58a14							
HN-2-58A	58a15							
HN-2-58B	58b-1	y					y	
HN-2-58B	58b-2		y					y
HN-2-58B	58b-3		y	sw		y		y
HN-2-58B	58b-4		y	y	y		y	
HN-2-58B	58b-5	y		sw		y		y
HN-2-58B	58b-6							
HN-2-58B	58b-7	y		n			y	
HN-2-58B	58b-8							
HN-2-58B	58b-9							
HN-2-58B	58b10	y						
HN-2-58B	58b11							
HN-2-58B	58b12							
HN-2-58B	58b13							
HN-2-58B	58b14		y					y
HN-2-58B	58b15							
HN-2-58B	58a16							
HN-2-58B	58a17							